Tyrosine Kinase and Protein Kinase A Modulation of α7 Nicotinic Acetylcholine Receptor Function on Layer 1 Cortical Interneurons

by

Pragya Komal
BSc, Vellore Institute of Technology, India, 2005

A Dissertation Submitted in Partial Fulfillment
of the Requirements for the Degree of

DOCTOR OF PHILOSOPHY

in the Department of Biology (Neuroscience)

Supervisory Committee

Tyrosine Kinase and Protein Kinase A Modulation of α7 Nicotinic Acetylcholine Receptor Function on Layer 1 Cortical Interneurons

by

Pragya Komal
BSc, Vellore Institute of Technology, India, 2005

Supervisory Committee

Dr. Raad Nashmi (Department of Biology)
Supervisor

Dr. Kerry Delaney (Department of Biology)
Departmental Member

Dr. Brian R. Christie (Divison of Medical Sciences, Department of Biology)
Departmental Member

Dr. Christopher J. Nelson (Department of Biochemistry and Microbiology)
Outside Member

Abstract

Supervisory Committee
Dr. Raad Nashmi (Department of Biology)
Supervisor
Dr. Kerry Delaney (Department of Biology)
Departmental Member
Dr. Brian R Christie (Division of Medical Sciences, Department of Biology)
Departmental Member
Dr. Christopher J. Nelson (Department of Biochemistry and Microbiology)
Outside Member

Nicotinic acetylcholine receptors (nAChRs) are a major class of ligand-gated ion channels in the brain, with the α7 subtype of nAChRs playing an important role in attention, working memory and synaptic plasticity. Alterations in expression of α7 nAChRs are observed in neurological disorders including schizophrenia and Alzheimer's disease. Therefore, understanding the fundamentals of how α7 nAChRs are regulated will increase our comprehension of how α7 nAChRs influence neuronal excitability, cognition and the pathophysiology of various neurological disorders. The purpose of this thesis was to investigate how protein kinases modulate the function and trafficking of α7 nAChRs in CNS neurons.

In chapter 2, I describe a novel fast agonist applicator that I developed to reliably elicit α7 nAChR currents in both brain slices and cultured cells. In chapter 3, I examined whether an immune protein in the brain, the T-cell receptor (TCR), can modulate α7 nAChR activity. Activation of TCRs decreased α7 nAChR whole-cell recorded currents from layer 1 prefrontal cortical (PFC) neurons. TCR attenuated α7 nAChR currents through the activation of Fyn and Lck tyrosine kinases, which targeted tyrosine 442 in the M3-M4 cytoplasmic loop of α7. The mechanisms of the attenuated α7 current were

contributed by a TCR mediated decrease in surface receptor expression and an attenuation of the α7 single-channel conductance. TCR stimulation also resulted in a decrease in neuronal excitability by negatively modulating α7 activity.

In chapter 4, I tested whether PKA can modulate α7 nAChR function in CNS neurons. The pharmacological agents PKA agonist 8-Br-cAMP and PKA inhibitor KT-5720, as well as over-expressing dominant negative PKA and the catalytic subunit of PKA, demonstrated that activation of PKA leads to a reduction of α7 nAChR currents in HEK 293T cells and layer 1 cortical interneurons. Serine 365 of the M3-M4 cytoplasmic domain of α7 was necessary for the PKA modulation of α7. The mechanism of down-regulation in α7 receptor function was due to decreased surface receptor expression but not alterations in single-channel conductance nor gating kinetics.

The results of this thesis demonstrate that α7 nAChRs constitute a major substrate for modulation via TCR activated tyrosine kinases and the cyclic AMP/PKA pathway.

Table of Contents

List of Figures

List of Abbreviations

ACh	Acetylcholine
AC	Adenylyl cyclase
AD	Alzheimer's disease
ADHD	Attention deficit hyperactivity disorder
ATP	Adenosine triphosphate
α7 KO	alpha7 nicotinic receptor knockout
AMPA	α-amino-3-hydroxy-5-methyl-4-isoxazolepropoionic acid
8-Br-cAMP	8-bromo-3' 5'-cyclic adenosine monophosphate
BDNF	Brain derived neurotrophic factor
BF	Basal forebrain
α-BTX	α-bungarotoxin
C_α	Catalytic subunit of PKA
cAMP	3'-5'-cyclic adenosine monophosphate
cGMP	3'-5'-cyclic guanosine monophosphate
cys	Cysteine
CaMK	Calcium/calmodulin-dependent protein kinase
CNS	Central nervous system
CRE	cAMP response element
CREB	cAMP response element binding protein
Ctx	Cortex
5-CSRTT	5-choice serial reaction time task
CNQX	6-cyano-7-nitroquinoxaline-2,3-dione
DA	Dopamine
DhβE	Dihydro-β-erythrodine
DG	Dentate gyrus
dLGN	Dorsolateral geniculate nucleus
ECS	Extracellular solution
EC_{50}	Half maximum effective concentration
ERK	Extracellular signal-regulated kinase
EPSP	Excitatory Postsynaptic potential
EPSC	Excitatory Postsynaptic current
FI-α-Btx	Alexa 647 conjugated α-bungarotoxin
FKD	Fyn kinase dead
FKA	Fyn kinase active
GABA	Gamma aminobutyric acid
GPCR	G-protein coupled receptor
HEK 293 Tcells	Human embronic kidney cell line
IC_{50}	Half maximum inhibitory concentration
ITAM	Immunoreceptor tyrosine-based activation motif
KO	Knockout
LAT	Linker for activated T cells
LTD	Long-term depression
LTP	Long-term potentiation

LGIC	Ligand gated ion-channel
MAP-2	Microtubule associated protein-2
MHC-I	Major histocompatibility complex I
mPFC	Medial prefrontal cortex
MLA	Methyllycaconitine
MAPK	Mitogen-activated protein kinase
NA	Noradrenaline
nAChR	Nicotinic acetylcholine receptor
NaCl	Sodium chloride
NAcc	Nucleus accumbens
NMDA	N-methyl-D-aspartate receptor
NFκB	Nuclear factor kappa
NGF	Nerve growth factor
PKA	Protein kinase A
PKC	Protein kinase C
PI3K-Akt	Phosphoinositide 3-kinase-protein kinase B
P I3K	Phosphatidyl inositol-3-kinase
PNS	Peripheral nervous system
RMP	Resting membrane potential
PrL	Prelimbic area
R_2	Regulatory subunit of protein kinase A
SFKs	Src family kinases
SH	Src homology domain
Ser	Serine
STP	Short term potentiation
STD	Short term depression
STDP	Spike time dependent plasticity
TCR	T cell receptor
TCR β KO	T cell receptor beta subunit knock out
TTX	Tetrodotoxin
Tyr	Tyrosine
VTA	Ventral tegmental area
WT	Wild type
***(e.g. α4* nAChR)**	Containing (e.g. nAChR containing other subtypes of nicotinic receptor subunits in addition to α4)

Acknowledgments

The person whom I would like to acknowledge the first for all my research, is my supervisor, Dr. Raad Nashmi. Raad, you believed in me and your indispensable support, patience, guidance, advice and influence throughout these years cannot be put in words. I cannot thank you enough for the opportunity you gave me in this field of research. Thank you for surviving the multiple cardiac episodes I have undoubtedly caused over the years, and more specifically, giving me the opportunity to work under you and be a part of such a stimulating and fascinating line of work. I never imagined I would have someone so co-operative like you in a new place and environment. I would also like to convey my heartfelt appreciation to Dr. Kerry Delaney, whose sharp mind has kept me on my scientific toes. I have such deep respect for your intelligence. I am also sincerely grateful to my thesis committee members, Dr. Christpher J. Nelson for providing countless thoughts and advices for experimental design and project development and Dr. Brian Christie, for consistently pointing me in the right direction. Geoff Gudavicius deserves great thanks for his help with Western blotting experiment. My project would never have been completed without Geoff's expertize.

Secondly, a big thank you to my life partner, Dr. Anurag Gautam, whose immense support and understanding took me where I am today. Anu, your presence completed my life and my graduation would not have been possible if you were not here with me. You scarificed other post-doctorate opportunities just to accompany me here and your presence gave immence mental support. I love you so much. Thanks alot for the late night dinner you prepared for me while I struggled through my electrophysiology experiments at midnight. Next, I would especially like to acknowledge beyond words to

the building blocks of my life, my parents, without whom it would be impossible to pursue research. Additional thanks to my sisters, relatives and friends. Beyond that I would like to thank all the members of the neuroscience program, animal care staff and Department of Biology at the University of Victoria. It is truly an incredible group of individuals and place to work.

Lastly and importantly, thank you to Anna Patten for her help and to all the members of the Delaney lab and Nashmi lab, Stephanie, Waleed, Alex, Heather, Tony, Adam, Kevin, Dave, Nora, and all my colleagues and friends who provided fun and meaning to this chapter of my life. Its been a trip.

Dedication

I would like to dedicate this thesis to my parents for all their love and support.

Chapter 1 - Introduction

1.1 Overview and rationale

Neurons communicate with each other through the release of neurotransmitters at chemical synapses. The first neurotransmitter discovered was acetylcholine by Otto Loewi, who called it "vagusstoff" since the discovery was made from a preparation involving the vagus nerve and the heart (Loewi, 1924). Acetylcholine forms the endogenous ligand for nicotinic acetylcholine receptors (nAChRs). These receptors belong to the family of ligand-gated ion channels and play an important role in learning and memory (Couey et al., 2007; Dani and Bertrand, 2007; Ge and Dani, 2005; McGehee and Role, 1995). Neuronal nicotinic receptors are expressed at the pre- or postsynaptic sites of neurons in the central nervous and peripheral nervous system (CNS and PNS) (Bibevski et al., 2000; Flores et al., 1996; Jones and Yakel, 1997; Mansvelder and McGehee, 2002; Pidoplichko et al., 2013). Nicotinic receptor activation at the presynaptic terminals of neurons facilitates neurotransmitter release (Lambe et al., 2003; Mansvelder and McGehee, 2000), whereas postsynaptic receptor activation depolarizes the membrane potential to increase the frequency of action potential firing (Frazier et al., 2003; Ge and Dani, 2005; Pidoplichko et al., 2013). Thus, regulation of nAChR function can modify the strength of chemically mediated neurotransmission and neuronal excitability. Post-translational modification by protein phosphorylation of ion channels including nAChRs is a common mechanism for the regulation of receptor function (Chen et al., 2004; Esteban et al., 2003; Swope et al., 1992). Protein kinases catalyse the transfer of a highly charged phosphate moiety from adenosine triphosphate (ATP) to a

serine, threonine or tyrosine residues of target proteins, thereby altering the charge of those residues, which may potentially alter the conformation or function of the target protein. Phosphorylation of target proteins, including neurotransmitter receptors, is reversible, and may result in changes in the receptor function thereby affecting the strength of synaptic transmission. There is a diverse set of neuronal nAChR subtypes, each with their unique pharmacological and biophysical properties. For vertebrates there exist 12 different neuronal nAChR subunits (α2-α10, β2-β4), which may combine to form either heteropentamers or homopentamers. α4β2 containing nAChRs form the major heteromeric nAChR subtype in the brain. The major homomeric neuronal nicotinic receptor subtype is the α7 nAChR which is unique among the nicotinic receptor family, owing to a high Ca^{2+} permeability of the ion-channel (Berg and Conroy, 2002; Dajas-Bailador et al., 2002a; Wallace and Porter, 2011). These receptors are multimeric proteins composed of homologous subunits. Each subunit spans the membrane four times and contains a large cytoplasmic loop that includes many regulatory motifs like consensus sites for protein phosphorylation. The best characterized group of protein kinases are serine-threonine kinases and tyrosine kinases (Kalia et al., 2004; Wagner et al., 1991). These kinases exhibit a widespread distribution in the brain and are highly expressed in neurons (Hirano et al., 1988; Naira et al., 1985). Thus, α7 nAChRs are likely to be phosphorylated and functionally modulated by these protein kinases in neurons.

In the mammalian brain, α7 nAChRs are widely expressed in the prefrontal cortex (PFC) (Dickinson et al., 2008; Parikh et al., 2010; Thomsen et al., 2010; Yang et al., 2013), a brain region where these receptors are implicated in cognitive function and in

the pathophysiology of neurodegenerative diseases like schizophrenia (Martin and Freedman, 2007; Severance and Yolken, 2008). In the PFC α7 nAChR activation promotes the release of neurotransmitters like acetylcholine and dopamine suggesting the involvement of cholinergic and dopaminergic pathways in the modulation of PFC circuits (Livingstone et al., 2009; Thomsen et al., 2010). Postsynaptic α7 mediated nicotinic currents have also been reliably recorded from the majority of layer 1 interneurons of the neocortex (Christophe et al., 2002).

These receptors play a role in higher brain function including enhanced learning and cognition (Bloem et al., 2014; Lendvai et al., 2013; Russo and Taly, 2012; Yang et al., 2013; Young et al., 2007a). α7 nAChR specific agonists improve attention deficits in patients with schizophrenia (AhnAllen, 2012). Altered function and expression of α7 nAChRs are also observed in other neurobiological diseases such as Alzheimer's, Parkinson and autism (Russo and Taly, 2012; Wang et al., 2000). Therefore, post-translational modification of α7 nAChRs by phosphorylation through protein kinases may serve an important role in normal neurobiological function.

A large number of immune proteins have been shown to be expressed in the brain (Boulanger, 2009). One of these proteins, in particular, the T cell receptor (TCR) is highly expressed throughout the cerebral cortex (Syken and Shatz, 2003). T cell receptor receptors (TCRs) are expressed on T lymphocytes where they play a critical role in adaptive immunity (Germain, 2001). Once activated T cell receptors signal intracellularly through the activation of Src family of tyrosine kinases (Brownlie and Zamoyska, 2013). Therefore, I hypothesized that in addition to an immune function, TCRs may have a neuronal function, which may include the downstream phosphorylation

and modification of neuronal proteins including α7 nAChRs. In this thesis I examined how T cell receptors can modulate α7 nAChR activity and in turn modify neuronal excitability. I also examined how cAMP-dependent protein kinase (PKA) activation can regulate α7 nAChR function.

1.2 Research objective and hypothesis

1.2.1 Research objective

A variety of biochemical studies show that the M3-M4 cytoplasmic loop of nicotinic receptors is directly phosphorylated at key amino acid residues namely, serine (S), threonine (T) and tyrosine (Y) by a range of protein kinases (Séguéla et al., 1993) (Swope et al., 1992). These sites are commonly referred to as consensus sequence phosphorylation sites (Pearson and Kemp, 1991). These protein kinase recognition motifs in the major cytoplasmic loop play an important role in the regulation of nicotinic receptors. The large cytoplasmic segment of the α7 nicotinic receptor contains the consensus sequences for putative phosphorylation sites for the following major protein kinases: protein kinase A, Src tyrosine kinase, casein kinase and calcium/calmodulin-dependent kinase. In this study, from the plethora of protein kinases being expressed in the brain, we concentrated on two specific families of protein kinases, namely protein kinase A and Src family of tyrosine kinases. In the first part of this study, we examined how Src family tyrosine kinase activation via T cell receptor stimulation affects α7 nicotinic receptor function and neuronal excitability. In the latter part we explored the impact of second messenger, 8-Br-cAMP mediated activation of PKA and its modulation on α7 nicotinic receptor function. The main rationale for brain slice electrophysiology

from layer 1 interneurons of the prefrontal and frontal cortices are that the cerebral cortex shows abundant expression of functional α7 nicotinic receptors in the majority of neurons in layer 1 which are mostly inhibitory neurons (Christophe et al., 2002). Furthermore, in the brain T cell receptors are found exclusively in the cerebral cortex (Syken and Shatz, 2003) while PKA is found ubiquitously in all the cells. In order to examine α7 nicotinic currents, I developed a novel and high performance rapid agonist application system that is flexible enough to elicit nicotinic currents in both cultured cell lines and brain slices.

1.2.2 Hypothesis and specific aims

I hypothesize that TCRs by stimulating Src family kinases and PKA enzymes directly phosphorylate distinct amino acid residues in the M3–M4 cytoplasmic loop of α7 nicotinic receptors, in order to modulate receptor activity and ultimately modify neuronal excitability in the CNS.

My specific aims are as follows:

1) To examine whether T cell receptor activation modulates the function and trafficking of α7 nAChRs in CNS neurons.

2) Likewise, we determined whether PKA affects the function, expression and trafficking of α7 nAChRs in CNS neurons.

1.3 Background

1.3.1 Nicotinic acetylcholine receptors

The cholinergic neurons of the central nervous system produces the neurotransmitter, acetylcholine (ACh) (Karczmar, 1993). ACh binds to two types of acetylcholine receptors in the brain, the G protein coupled muscarinic acetylcholine receptors and the

ionotropic nicotinic acetylcholine receptors (nAChRs), which are ligand-gated ion channels (Dani and Bertrand, 2007). Acetylcholine (ACh) is produced by the enzyme choline acetyltransferase (ChAT) from the substrates choline and acetyl-coenzyme A. The excess ACh in the cholinergic synaptic cleft is hydrolyzed into choline and acetylcoA, by the enzyme acetylcholinesterase. The byproduct choline can uniquely activate only the α7 nAChR subtype in the CNS (Alkondon et al., 1997). In addition to binding to the endogenous ligand ACh, nAChRs also bind to the exogenous ligand nicotine, the alkaloid found in tobacco (Picciotto, 1998). Nicotinic receptors belong to the cys-loop super family of ligand-gated ion channels (Dani, 2001), because all families of subunits contain in their amino-terminal region a unique pair of disulphide-bonded cysteines. Other members of the cys-loop family of ligand-gated ion channels include 5-hydroxytryptamine type 3 (5-HT3), γ-aminobutyric acid type A ($GABA_A$) and glycine receptors. Nicotinic receptors form non-selective cation channels, where binding of ACh or nicotine causes a conformational change resulting in the flux of Na^+, K^+ and Ca^{2+} down their electrochemical gradients (Dani and Bertrand, 2007). Since nicotinic receptors can flux intracellular calcium, which functions as an important second messenger, nAChR activation can stimulate a number of signal transduction cascades. These may influence nicotinic receptor function and subcellular distribution (Fayuk and Yakel, 2005; Fucile, 2004; Gotti and Clementi, 2004).

1.3.1.1 Nicotinic receptor structure

Nicotinic acetylcholine receptors represent a large and well-characterized family of ligand-gated ion channels that are expressed throughout the central and peripheral nervous system. They are also found in non-neuronal cells (Dani, 2001). nAChRs can be

classified broadly into two main categories: muscle or neuronal nAChRs. Muscle nAChRs are expressed primarily in skeletal neuromuscular junctions and are composed of the α1, β1, δ, and ε or γ subunits (Huganir, 1987). In contrast, in the vertebrate nervous system there are 12 different neuronal nicotinic receptor subunits including α2-α10 and β2-β4 (Lindstrom, 1996). As already mentioned, all nicotinic receptor subunits contain the signature cys-loop structure, which consists of a cys-cys disulphide bond to a loop of the extracellular N-terminal region that is situated close to the outer cellular membrane of the cell. Not to be confused with the cys-loop, another disulphide bonded pair of cysteines located in the N-terminal extracellular region of the receptor, known as the double cys is essential for agonist binding. On the contrary β subunits, which lack the double cys structure of adjacent cysteine residues, must combine with α subunits to form functional receptors. α2-α6 combine with β subunits to form heteromeric channels. α7 subunits form homomeric receptors, while α9 combine with α10 to form heteromeric receptors not requiring a β subunit. A combination of five receptor subunits forms a functional ion-channel. Early structural information on nAChRs was derived from cryo-electronmicroscopy studies of Torpedo muscle nAChR which revealed the dimensions and shape of the molecule, the location of the ligand-binding sites, and the organization of the ion channel (Unwin, 1995). Each nAChR gene encodes a protein subunit consisting of a ~ 200 residue extracellular N-terminus which forms the ligand binding domain, four transmembrane segments (M1-M4), a variable long cytoplasmic intracellular loop (~83 to ~265 residues) between M3 and M4, and a short (2-22 residues) extracellular C-terminus (Corringer et al., 2000) **(Fig. 1.1)**. The M2 transmembrane segment of all five subunits forms the conducting pore of the channel, with regions in the

M1-M2 intracellular loop and key residues in M2 contributing to ion selectivity (Bertrand et al., 1993; Tapia et al., 2007). The subunit composition of each channel determines its electrophysiological properties, cation selectivity and pharmacological profile of agonist and antagonist binding affinities (Corringer et al., 2000; McGehee and Role, 1995). The majority of neuronal nicotinic receptor subtypes fall into two major categories: receptors that bind nicotine with high affinity (nM concentrations); and those that bind with lower affinity (μM concentrations). Most of the nAChRs in the CNS, which have high affinity to nicotine, are the α4β2 containing receptors (denoted α4β2*, where the asterisk represents other subunits that may also be present in the receptor) while nAChRs with low affinity to nicotine are mainly the homopentameric α7 receptors, which have high affinity to the competitive antagonist α-bungarotoxin (Nashmi and Lester, 2006).

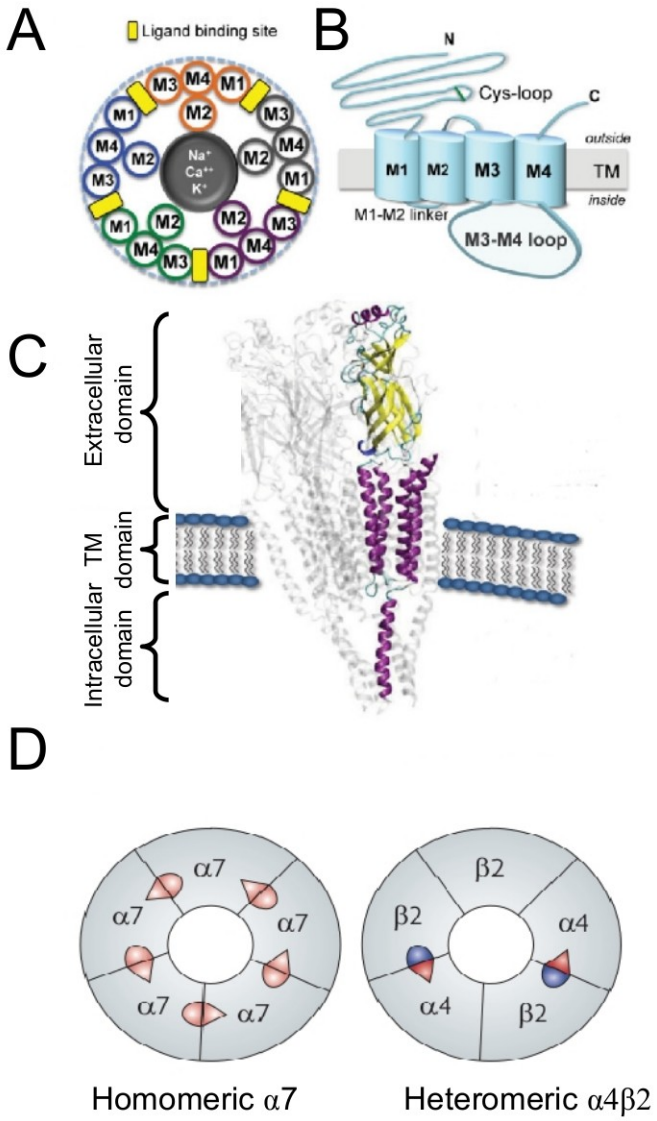

Figure 1.1 Structural representation of a functional nicotonic acetylcholine receptor. **(A)** Nicotinic acetylcholine receptors (nAChRs) are transmembrane oligomers that consist of five subunits. **(B)** Membrane topology of the receptor showing that each subunit comprises a large extracellular amino terminal adopting a twisted β-sandwich structure that precedes four α-helical transmembrane segments (M1–M4). The M3-M4 cytoplasmic domain contains the amphipathic helix close to M4 that forms the inner lining of the channel pore. M4 is followed by a short extracellular C terminus. **(C)** Cryo-electron microscopy structure of the Torpedo muscle nAChR at 4 Å resolution depicts the extracellular domain (ECD), which binds to ACh or nicotine (shown in

yellow). The ECD of receptor contains the double cys, required for ligand binding, while there is also the Cys-loop struction found in all Cys-loop receptors. The M3–M4 intracellular domain of each receptor subunit contains putative phosphorylation sites for protein kinases and is important for cell signalling pathways. Non-alpha subunits (β subunits) lacks the double cys essential for ligand binding and thus acts as complementary subunits in the formation of functional receptor. **(D)** The number of agonist binding sites per pentamer ranges from two to five, depending on its composition, from two (in muscle nAChRs or brain α4β2 heteromeric nAChRs) to five (in the α7 homopentamer). Modified from (Changeux et al., 1998; Kabbani et al., 2013; Karlin, 2002; Unwin, 2005)

1.3.1.2 Nicotinic acetylcholine receptors: substrates for protein kinases

A variety of biochemical studies show that the M3-M4 cytoplasmic loop of nicotinic receptors is directly phosphorylated at key amino acid residues namely, serine (S), threonine (T) and tyrosine (Y) by a range of protein kinases (Séguéla et al., 1993) (Swope et al., 1992). These sites are commonly referred to as consensus sequence phosphorylation sites (Pearson and Kemp, 1991). These protein kinase recognition motifs in the major cytoplasmic loop play an important role in the regulation of nicotinic receptors **(Fig. 1.2)**. With the advent of cloning and determination of the primary sequences of the nAChR subunits, it has been possible to predict potential sites of phosphorylation in nicotinic receptors based on consensus sequence motifs of a variety of protein kinases (Pearson and Kemp, 1991). Early evidence for modification by phosphorylation came from the studies performed on muscle nAChRs from the Torpedo electric organ (Huganir, 1987; Huganir et al., 1984). Three endogenous protein kinases were identified to phosphorylate specific subunits of the Torpedo muscle nicotinic acetylcholine receptor: cyclic AMP dependent protein kinase (protein kinase A, PKA), protein kinase C (PKC), and a tyrosine-specific protein kinase (Poulter et al., 1989).

Early insight into neuronal nicotinic receptor modulation by phosphorylation came from the studies of cultured embryonic chicken sympathetic ganglion neurons which express α3, α4, α5, α7, α2, β3 and β4 nicotinic receptor subunits (Swope et al., 1992). The evidence for kinase modulation of neuronal nicotinic receptor function and trafficking has been indirect and inferred from the use of kinase and phosphatase inhibitors. Since α4β2 nicotinic receptors constitute the predominant heteromeric, high-affinity nicotinic receptor subtype in the brain and play a major role in nicotine addiction, most of the studies done with this receptor subtype have demonstrated that activators and inhibitors of PKA and PKC modified both the surface expression of the receptors and their recovery from desensitization (Fenster et al., 1999; Gopalakrishnan et al., 1997; Nashmi et al., 2003). The major cytoplasmic loop between the third (M3) and fourth (M4) transmembrane domain of α4 contains more than 20 putative phosphorylation motifs for serine/threonine protein kinases, many of which are highly conserved among human, rat and mouse (Blom et al., 1999). Recently, Wecker and group have shown that the fusion protein containing α4 subunits with the serine and threonine residues in the M3-M4 cytoplasmic domain are phosphorylated by both PKA and PKC, using two-dimensional (2D) phosphopeptide mapping and site-directed mutagenesis (Wecker et al., 2001).

Evidence for phosphorylation mediated regulation of α7 nicotinic receptors come from the in vitro studies performed on recombinant chick and rat α7 receptors which showed PKA specifically phosphorylated only the evolutionary conserved single serine residue (S342) in the major intracellular cytoplasmic loop of the channel (Moss et al., 1996). This serine was not phosphorylated by other protein kinases like protein kinase C and cGMP-dependent protein kinase, or calcium/calmodulin-dependent protein kinases.

Studies conducted on cultured chick ciliary ganglionic neurons showed α3 and α5 nicotinic receptors mediated whole-cell current potentiation upon PKA activation following cyclic AMP incubation for 6-48 hours (Margiotta et al., 1987). Thus, based on amino acid sequence, structure and phosphorylation prediction algorithms, the large cytoplasmic domain of the nicotinic receptor forms an important substrate of site specific phosphorylation by protein kinases. This post-translational modification of ligand-gated ion channels could potentially influence synaptic plasticity and synaptic transmission.

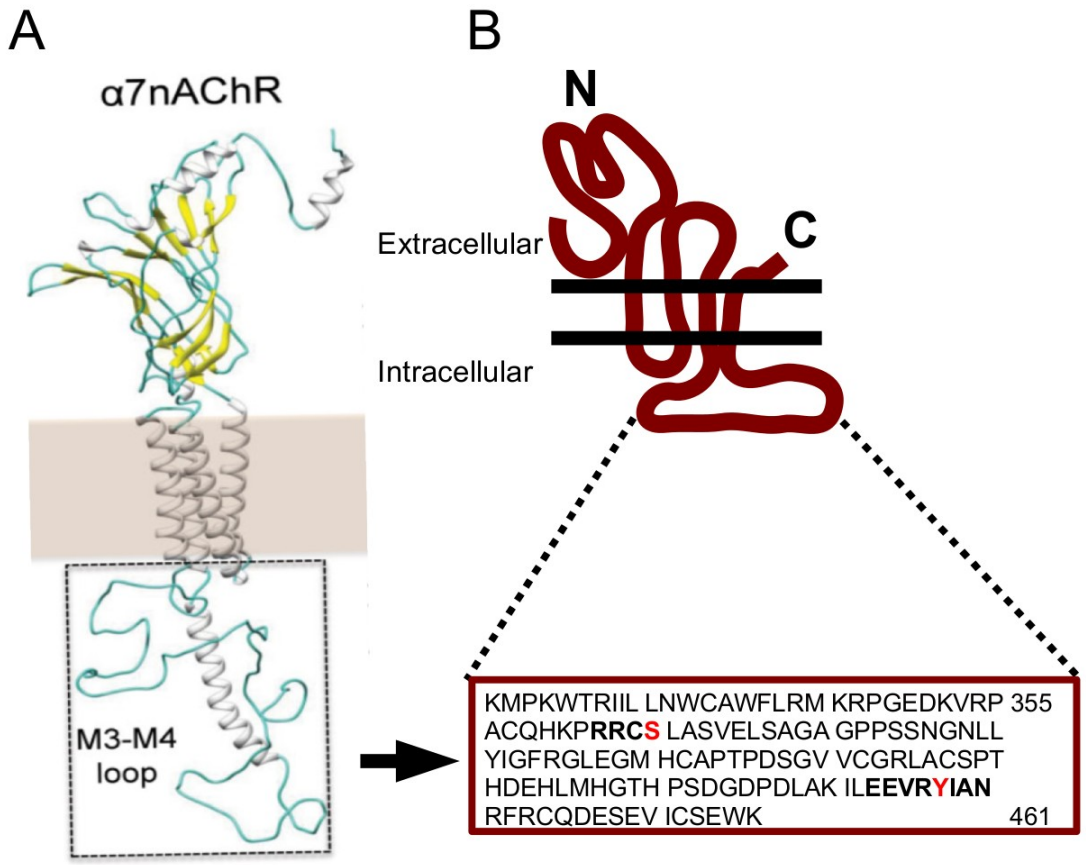

Figure 1.2 α7 nicotinic acetylcholine receptor M3-M4 cytoplasmic loop.
(A) Ribbon structural diagram of one subunit of the α7 nAChR depicting the intracellular cytoplasmic loop which lies between the transmembrane 3 (M3) and 4 (M4) domain of the channel. **(B)** Membrane topology of one subunit of α7 showing a blow-up of the

sequence of the M3-M4 cytoplasmic domain with the putatitive tyrosine kinase and protein kinase A phosphorylation sites highlightened in red (Kabbani et al., 2013).

1.3.1.3 Role of nAChRs in the physiology of neurons and behaviour

The physiological role of nicotinic receptors in neurotransmission and behaviour depends upon the precise neuroanatomical location of specific subtypes of nAChRs expressed in neuronal circuits of the brain (Nashmi and Lester, 2006). The majority of neuronal nAChRs fall into two categories: those that bind acetylcholine/nicotine with high affinity (EC50 = 2.4 μM, nicotine EC50 = 1.6 μM) (Buisson and Bertrand, 1998; Dani and Bertrand, 2007) and those that bind with lower affinity (EC50 = 150 μM, nicotine EC50 = 40 μM) (Komal et al., 2011a). Homopentameric α7 receptors, which are α-bungarotoxin sensitive, form the low-affinity receptors whereas α4β2 nAChRs account for greater than 70% of the high-affinity nicotinic receptors in the brain (Perry et al., 2002a; Whiting and Lindstrom, 1988). Nicotinic receptors transition between three principal conformational states: closed unbound, open bound and desensitized bound states (Hille B, 2001). In the closed unbound state, the channel is non-conducting due to obstruction of the channel pore. Upon agonist binding the channel transitions to an open state, in which the barrier to the pore is removed and thereby conducting cations, namely Ca^{2+}, Na^{+} and K^{+}. In the desensitized state the channel is non-conducting even during the presence of agonist (Pearson and Kemp, 1991). The ion selectivity of a channel, particularly with respect to the permeability of calcium ions, depends on the type of nAChR subunit composition (Vernino et al., 1992). The homomeric α7 nicotinic receptors have the highest permeability to calcium among all nAChRs, making it unique among the nicotinic receptor family (Seguela et al., 1993), though the addition of the α5

subunit to α4β2 can make this receptor also highly permeable to calcium (Tapia et al., 2007).

The major long-range cholinergic projections within the brain arise from four distinct brain regions (the basal forebrain, medial habenula, pontomesencephalic nuclei and the medullary nuclei) providing broad, diffuse and generally sparse innervation to wide areas of the brain to activate nicotinic receptors, except for some of the cholinergic medullary nuclei that innervate motor targets (Woolf, 1991). nAChR subtypes are diverse and are distributed presynaptically and postsynaptically on neuronal subcompartments, which include dendrites, soma, presynaptic terminals and sometimes axons of neurons (Jones and Wonnacott, 2004; Jones and Yakel, 1997; McKay et al., 2007). Receptors expressed on dendrites and soma mediate fast synaptic transmission and contribute to neuronal excitability through generation of excitatory postsynaptic potentials (EPSPs) (Alkondon et al., 1998) while nicotinic receptor activation expressed at presynaptic terminals enhances neurotransmitter release through calcium influx and/or depolarization of the presynaptic terminal (Shen and Yakel, 2009). Considerable evidence has shown that activation of presynaptically localized nicotinic receptors facilitates the release of ACh (Wilkie et al., 1993), noradrenaline (NA), (Clarke and Reuben, 1996), dopamine (DA), (Grady et al., 1992) (Rapier et al., 1990) glutamate (McGehee and Role, 1995) and γ-amino butyric acid (GABA) (Yang et al., 1996).

The most extensively studied neuronal nicotinic receptor subtype is the α4β2 nAChR, which plays a key role in nicotine addiction (Maskos et al., 2005; Picciotto et al., 1998; Tapper et al., 2004). α4* nAChR (asterisk denotes that other subunits are incorporated in the receptor in addition to α4) upregulation on GABAergic neurons in the

ventral tegmental area (VTA), a mid brain region associated with reward and motivation, is known to be involved in the mechanism of nicotine tolerance by dampening the neuronal firing of dopaminergic neurons (Nashmi et al., 2007). The normal function of α4* nAChRs on GABAergic and dopaminergic neurons in the VTA is similar to that in the substantia nigra, where activation of α4* nAChRs by endogenous release of ACh increases the action potential firing frequency of these spontaneously firing neurons (Nashmi et al., 2007; Pidoplichko et al., 1997; Xiao et al., 2009). The activation of presynaptically localized α7 receptors on glutamatergic terminals in the VTA enhances glutamatergic inputs to DA neurons and induces long term potentiation (LTP), a cellular mechansim underlying memory formation (Mansvelder and McGehee, 2000). In the hippocampus the cellular location of activated nAChRs can modulate the valence of synaptic plasticity. Electrical stimulation of the Schaffer collaterals in conjunction with activation of nAChRs localized postsynaptically on CA1 pyramidal neurons by puffing on ACh stimulated long-term potentiation of glutamatergic responses. While the activation of nAChRs localized on GABAergic interneurons during tetanic stimulation of the Schaffer collaterals can inhibit long-term potentiation of glutamatergic responses (Ji et al., 2001).

More specifically the physiological role of nicotinic receptors in the prefrontal cortex has also been examined. In the prefrontal cortex, the contribution of nicotinic receptors to synaptic plasticity has also been well documented. Nicotinic receptor activation on GABAergic interneurons in the PFC caused increased inhibition of pyramidal neurons and increased the threshold for spike timing dependent potentiation (STDP) of excitatory transmission with accompanying strong reduction in the dendritic

calcium signaling (Couey et al., 2007). Nicotine mediated activation of high affinity α4β2 receptors on thalamocortical terminals enhances glutamate release onto layer V pyramidal neurons of the PFC as measured by spontaneous excitatory postsynaptic currents (sEPSCs), an effect which was not observed in β2 knockout mice (Lambe et al., 2003). Another study showed that activation of α7 and β2* nAChRs on layer 1 interneurons of the PFC results in increased excitability of pyramidal neurons via disinhibition as layer 1 neurons inhibit layer 2 interneurons, which synapse onto pyramidal neurons (Christophe et al., 2002). Also, the activation of channelrhodopsin expressing basal forebrain cholinergic terminals in the cerebral cortex generated spikes in nicotinic receptor expressing interneurons which in turn specifically inhibited either layer 2/3 pyramidal neurons or fast spiking interneurons, and therefore, resulted in disynaptic inhibition of neighboring cortical neurons (Arroyo et al., 2012). The latter study was consistent with another finding where the authors showed that layer 1 interneurons in auditory cortex exhibited α7 and β2 nAChR dependent increase in spiking after foot shock and inhibited spiking specifically in layer 2 and 3 parvalbumin positive interneurons (Letzkus et al., 2011). Thus, the activation of α7 and β2 nAChRs on layer 1 interneurons was sufficient to produce disinhibition of the cortical circuit and was argued to be an important mechanism for learning and synaptic plasticity (Christophe et al., 2002a; Jiang et al., 2013; Letzkus et al., 2011).

Other nAChR subunits though expressed at much lower levels than the two major subtypes, α4β2 and α7, also plays a significant role in exerting their influence in cholinergic mediated behaviours. α3β4 nicotinic receptors in the medial habenula, a brain region involved in stress and anxiety (Murphy et al., 1996), is hypothesized to play

a role in mediating nicotine consumption (Frahm et al., 2011). α6 nAChRs is expressed in midbrain dopamine (DA) neurons of the substantia nigra pars compacta (SNc) , VTA and norepinephrine neurons of the locus coeruleus (Cohen, 2002; Léna et al., 1999). The role of α6 nAChRs has been hypothesized to enhance locomotor activity (Drenan et al., 2008). α5 subtype expression in prefrontal cortex, represent its importance in the modulation corticothalamic circuitary and is essential for normal attention performance (Bailey et al., 2010). α5 is an auxiliary nicotinic receptor subunit that cannot function without the presence of different alpha and beta subunits. However, α5 can modify the function of other nicotinic receptor through its enhanced calcium permeability (Tapia et al., 2007) (Bailey et al., 2010) (Gotti et al., 2009). Nicotinic receptor containing β2 and α7 subunits are critical for attention behaviour. Mice deficient of either of these two nicotinic receptor subunits showed impaired attention performance on the 5-choice serial reaction time task (5-CSRTT) (Robbins, 2002), an attentional task for rodents in which the animals have to respond to 5 different light cues by making a nosepoke in the corresponding hole in order to obtain food rewards (Bailey et al., 2010; Guillem et al., 2011; Young et al., 2007). Furthermore, both β2 and α7 subunits are critical for performance in spatial memory learning tasks (Levin et al., 2009).

Thus, the different effects of nicotine on different neurons in the brain is influenced by the multitude of nicotinic receptor subtypes, each with their distinct functional properties and pharmacological profile, and their distinct localization in specific neuronal circuits of the brain. Furthermore, nicotine exerts its behavioural effects by targeting receptors expressed in key neuronal circuits responsible for those specific behaviours.

1.3.1.4 Functional properties of α7 nicotinic receptor

α7 nAChRs are unique in the nicotinic receptor family in that they can be activated not only by the neurotransmitter ACh but also by choline, the breakdown product of ACh (Khiroug et al., 2002). These receptors display low affinity to nicotine, unlike α4β2, the dominant heteromeric nAChR subtype in the brain. α-Bungarotoxin (α-BTX) is a neurotoxin, found in the venom of the cobra snake, *Bungagus Fasciatus* which binds reversibly with high affinity (1 nM) to neuronal α7 nAChRs (Moise et al., 2002). Neuronal nicotinic receptors are also classified as the α-BTX sensitive versus α-BTX insensitive ones. Although α7 nAChR subunits form primarily homopentameric receptors in the brain, α7 nicotinic receptor subunits can also form functional channels assembled with other subunits of the α-BTX insensitive subfamily namely α5, β3 and β2 (Girod et al., 1999; Gotti and Clementi, 2004; Khiroug et al., 2002; Liu et al., 2009). Functional α7 receptor expression in cell lines requires the presence of the chaperone protein, RIC-3 (Dau et al., 2013). RIC-3, first discovered in *Caenorhabditis elegans*, is an endoplasmic reticulum resident protein that is required for the assembly of α7 subunits into receptors and the trafficking of α7 receptors to the cell surface (Dau et al., 2013; Williams et al., 2005).

The Ca^{2+} /Na^{+} permeability ratio of α7 receptors is five fold more than α4β2 nAChRs and equal to that of NMDA receptors (Seguela et al., 1993; Tapia et al., 2007; Vernino et al., 1992). This extraordinary calcium-permeability makes α7 distinct from other nAChRs in that the opening of α7 nAChR channels alone can impact several Ca^{2+}dependent signaling pathways, including kinase activation and regulation of gene transcription, in addition to its role in fast excitatory synaptic neurotransmission **(Fig.**

1.3) (Fayuk and Yakel, 2005). α7 nAChRs display rapid activation kinetics upon agonist binding, reaching peak current in less than 20 ms. The rapid inward current is followed by a rapid decay in current, due to receptor desensitization (Komal et al., 2011). Similar to other nAChR subtypes, the α7 nAChR displays strong inward rectification, caused by Mg^{2+} or polyamine blockade of the intracellular mouth of the channel (Forster and Bertrand, 1995; Haghighi and Cooper, 1998). Hence, α7 nAChRs pass current at negative membrane potentials, which provide a strong driving force for inward cationic current (Dani and Bertrand, 2007). This is in contrast to ionotropic N-methyl-D-aspartate glutamate receptors (NMDA) which require the membrane potential to be depolarized to relieve channel block to allow inward current upon agonist binding. Thus, nAChRs are well suited to modulate the probability of receptor opening of other ion channels at negative membrane potential, e.g. the NMDA receptor (Castro and Albuquerque, 1995).

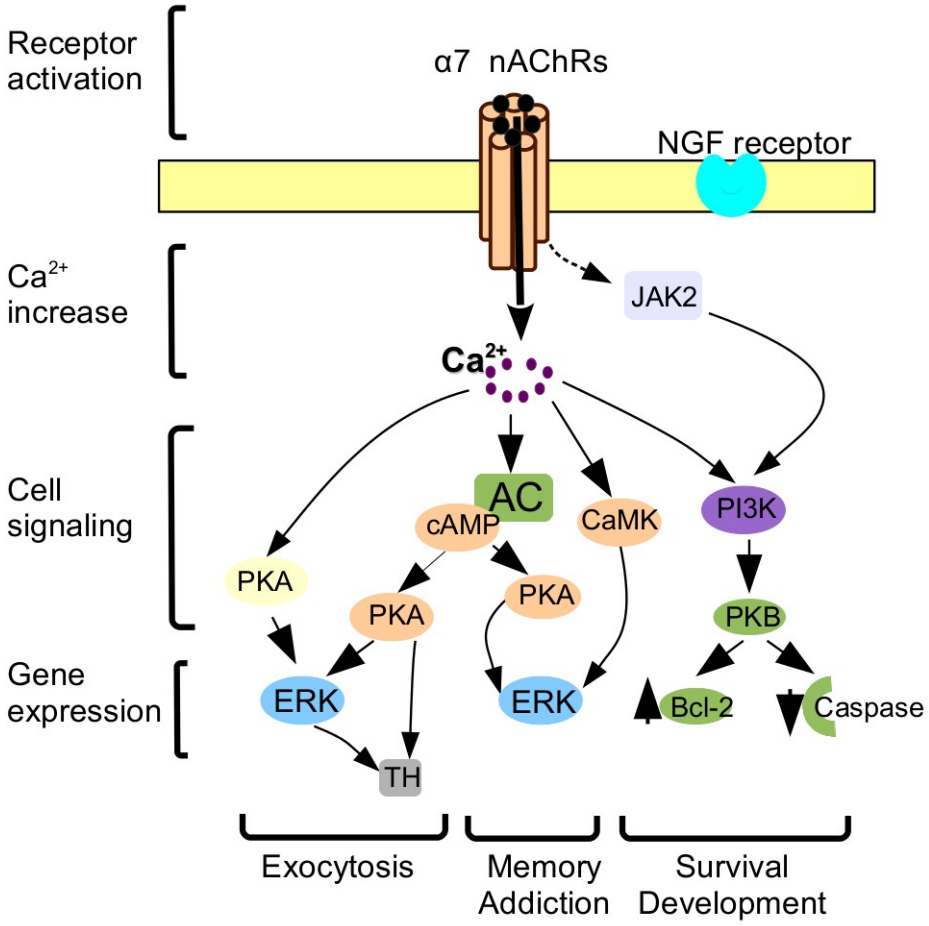

Figure 1.3 Nicotinic acetylcholine receptor (nAChR) activation increases intracellular Ca^{2+}levels which activates key signaling molecules in Ca^{2+} dependent manner.

The increase in intracellular Ca^{2+} that arises from nAChR activation can activate adenylyl cyclase (AC), protein kinase A (PKA), PKC, Ca^{2+}-calmodulin-dependent protein kinase (CaMK) and phosphatidylinositol 3-kinase (PI3K). In turn, these phosphorylate downstream targets, such as extracellular signal-regulated mitogen-activated protein kinase (ERK), which leads to the activation of transcription factors such as the cAMP response element-binding protein (CREB), which increases gene transcription of specific genes, for example, tyrosine hydroxylase (TH) or nerve growth factor (NGF) receptors. The lipid signaling cascade that is initiated by PI3K, through phosphorylation of protein kinase B (Akt), is credited with modulating the relative activities of neuroprotective and apoptotic factors, such as Bcl-2 and caspases, respectively. Thus, α7 nAChRs can exert a wide range of influences through Ca^{2+}signals, from changes in synaptic plasticity, which is pertinent to many situations including cognition, memory and addiction, to the life-and-death events involved in development and neuroprotection. Modified from (Dajas-Bailador and Wonnacott, 2004).

1.3.1.5 α7 Nicotinic receptor localization and function

α7 receptor expression in the brain is non-uniform and autoradiographic labeling using (^{125}I)-α-bungarotoxin (BTX) binding in rats demonstrated that α7 nAChRs are concentrated in areas of brain important for learning, memory and cognition, namely the cerebral cortex, hippocampus, midbrain, pons and medulla (Clarke et al., 1985; Gotti et al., 2009). A high density of binding are present in layers I, V, and VI of the cerebral cortex, basal forebrain as well as in the hippocampus (Tribollet et al., 2004). Non-neuronal expression of α7 receptor is found in peripheral tissue including the endothelium, bone marrow and macrophages (Koval et al., 2008; Li and Wang, 2006). α7 receptor expression in macrophages constitute an important role of these receptors in the cholinergic anti-inflammatory pathways (Wang et al., 2003). Much evidence suggests a role for α7 receptor in cognitive function, sensory information processes, attention, working memory, and reward pathways (Castner et al., 2011; Chan et al., 2007; Hoyle et al., 2006; Mansvelder and McGehee, 2000; Thomsen et al., 2010b; Yang et al., 2013). α7 nAChRs has also emerged as a novel therapeutic drug target owing to the alterations of α7 receptor mediated cholinergic signaling found in neurological disorders like epilepsy, autism, Alzheimer's disease (AD), schizophrenia and addiction (Wallace and Bertrand, 2013; Wallace and Porter, 2011).

Neuronal α7 nAChRs are expressed at somatic, pre-terminal, pre-synaptic, peri-synaptic, and extra-synaptic sites where they mediate fast synaptic transmission, neurotransmitter release and synaptic plasticity upon activation (Jones and Wonnacott, 2004; Mansvelder and McGehee, 2000; Wonnacott, 1997). In VTA and PFC, the presynaptic activation of α7 directly controls glutamate release, independent of

membrane depolarization, leading to presynaptic facilitation and synaptic plasticity (Livingstone et al., 2010). Microdialysis studies have shown that systemic administration of α7 nAChR agonists promotes the release of acetylcholine and dopamine in PFC of rats (Biton et al., 2007; Livingstone et al., 2009). In hippocampus, presynaptic α7 activation leads to LTP and enhances glutamatergic transmission via PKA activation (Cheng and Yakel, 2014; Jones and Yakel, 1997). Interestingly, it has also been shown in cortical culture that axonal α7 expression drives presynaptic NMDA glutamate receptor expression and modulates both presynaptic and postsynaptic maturation of glutamatergic synapses, further indicating presynaptic α7 nAChR/NMDAR interactions in synaptic development and plasticity (Lin et al., 2010). Recently, α7 nAChR mediated modulation of NMDARs has been shown to enhance cognition in the prefrontal cortex (Yang et al., 2013).

The desensitization kinetics of α7 nicotinic receptors serve an important role in shaping neurotransmitter release at the central nervous system synapses. For example, a relatively low dose of nicotine (as delivered by tobacco smoking ~ 100-200 nM) stimulates the midbrain dopaminergic neurons to release dopamine into the nucleus accumbens (NAc) (Mansvelder and McGehee, 2002; Wooltorton et al., 2003). This in turn preferentially desensitizes the non-α7 nAChRs of dopaminergic and GABAergic neurons and activates α7 receptors present on the glutamatergic terminals from PFC to enable glutamate mediated excitatory inputs to the dopaminergic neurons, thus facilitating the release of dopamine onto the nucleus accumbens (NAcc) neurons. Studies investigating the somatodendritic localization of α7 receptor in CA1 interneuron of hippocampus have shown modulation of neurotransmission via activation of α7 receptors

on inhibitory interneurons. (Frazier et al., 1998a; Jones and Yakel, 1997). Electron microscopy findings done in PFC of rodents provide evidence of α7 nAChRs distribution on dendrites and spines supporting a functional importance of postsynaptic α7 nAChRs in the PFC circuit (Duffy et al., 2009). Interestingly, membrane localization studies done on α7 nAChRs have shown that unlike α4β2 subunits, α7 receptors are localized in lipid rafts of the plasma membrane, which are areas highly enriched in cholesterol and sphingolipids (Kihara et al., 2001). These specialized microdomains, in which α7 receptors are localized, serve a role as an organizational structural platform for signal transduction pathways (Brusés et al., 2001; Oshikawa et al., 2003).

1.3.1.6 Tyrosine kinase and protein kinase A mediated modulation of α7 nicotinic receptors

Early evidence on Src family of tyrosine kinases (SFKs) mediated modulation comes from the studies performed on peripheral nicotinic receptors. For example, in adrenal medulla chromaffin cells it was shown that Src potentiated ganglionic type heteromeric nAChR responses and regulated the secretion of catecholamines. SFKs were shown to play a key role in the clustering of muscle nAChRs (Mittaud et al., 2004; Smith et al., 2001). SFKs are also widely expressed and abundant in neurons as well (Kalia et al., 2004). Neuronal α7 nicotinic receptors constitute an important substrate for phosphorylation by Src family kinases and modulate neuronal network activity in the CNS (Charpantier et al., 2005; Cho et al., 2005). Studies have shown that α7 nicotinic receptors are prone to undergo rapid phosphorylation and dephosphorylation by SFKs. Charpantier et al showed that Src kinase inhibition resulted in profound potentiation in α7 mediated whole-cell current responses in neuroblastoma cells, hippocampal CA1

interneurons, and supraoptic magnocellular neurons. Cho et al (2005) found rapid upregulation in the number of functional cell surface α7 nAChRs upon tyrosine dephosphorylation unlike the previous study. They showed that brief exposure to a broad-spectrum protein tyrosine kinase inhibitor, genistein, specifically and reversibly potentiated α7 nAChR mediated responses, whereas tyrosine phosphatase inhibitor, pervanadate, caused depression. Thus, the physiological impact of SFKs modulation on neuronal α7 nAChRs function depends on the cell type and subcellular location of receptor expression.

In addition to SFKs, protein kinase A activation via G-protein receptor family (GPCRs) stimulation are also known to regulate neuronal nicotinic receptor function (Liu et al., 2000). In one study it was shown that G-protein subunits directly interact with the intracellular cytoplasmic domain of α3 and α5 nAChR subunits (Fischer et al., 2005). PKA activation via second messenger cAMP stimulation directly phosphorylated the αlpha subunit of nicotinic receptors (Dajas-Bailador and Wonnacott, 2004; Vijayaraghavan et al., 1990). One study specifically showed that protein kinase A phosphorylated only a single serine residue located in the cytoplasmic loop of the rat and chick α7 nicotinic receptor (Moss et al., 1996). Thus, considerable evidence suggests that the functional properties of neuronal α7 nAChRs are subject to control by GPCRs that modulate cAMP levels within neurons (Kabbani et al., 2013). One of the physiological activators of PKA is the dopamine D1 receptor (Snyder et al., 1998). These GPCRs are routinely considered to stimulate cAMP production within neurons and the intracellular signaling cascades mediated upon D1 receptor activation are important in a number of cognitive functions (Beaulieu and Gainetdinov, 2011; Wang et al., 2005) .

1.3.1.7 Role of α7 nAChR in neurological disorders

Nicotinic receptors are targeted to improve cognitive deficits observed in many neurological and neuropsychiatric diseases such as Alzheimer's disease and schizophrenia (AhnAllen, 2012; Kem, 2000). Traditionally recognized drugs known to improve cognition have focused on enhancing cholinergic neurotransmission in brain especially targeting α7 nicotinic receptors (Thomsen et al., 2010; Wallace and Porter, 2011). A significant reduction in the expression of α7 nicotinic receptor was observed in the postmortem brains of Alzheimer's patients (Guan et al., 1999). It was also found that Alzheimer's disease progression was positively correlated with the loss of α7 nAChRs expression in the cortex (Kadir et al., 2006). In such cognitive deficit disorders, α7 nicotinic receptor activation promotes signal pathways mediating neuroprotection and neuronal survival (Kihara et al., 2001). Substantially low α7 receptor expression was also observed in schizophrenic patients (AhnAllen, 2012). There is evidence supporting a link between α7 nAChRs and deficits observed in schizophrenia, showing that α7 nAChRs subunit gene *CHRNA7* is linked to schizophrenia (Leonard et al., 2002). Furthermore, greater than 90% of schizophrenics smoke, likely as a means of self-medication to treat their cognitive disabilities (Leonard et al., 2002).

1.3.1.8 Role of α7 nicotinic receptors in the prefrontal cortex

The prefrontal cortex (PFC) is one of the brain areas responsible for integrating cortical and subcortical inputs to execute essential cognitive functions such as attention, working memory planning and decision making (Miller and Cohen, 2001). Patients with schizophrenia, Tourette syndrome, Parkinson's disease, and attention deficit and hyperactivity disorder (ADHD) exhibit many symptoms implicating prefrontal cortex

dysfunction. The basal forebrain (BF) cholinergic system and its projections to the PFC, represent an integral and necessary component for execution of vital cognitive functions (Everitt and Robbins, 1997). Also, dopamine (DA) projections from the midbrain provide a key modulatory input to the PFC that is essential for cognitive performance (Brozoski et al., 1979). The cell bodies of cortically projecting cholinergic neurons are situated in the nucleus basalis of Meynert and the substantia innominata in the basal forebrain shows high expression of α7 nAChRs and project strongly to PFC **(Fig. 1.4)** (Breese et al., 1997; Rye et al., 1984). Furthermore, the activation of α7 nAChRs promotes the release of acetylcholine and dopamine, suggesting the importance of cholinergic and dopaminergic pathways in PFC circuitary (Biton et al., 2007; Tietje et al., 2008). These cholinergic afferents innervate both pyramidal and non-pyramidal neurons of the PFC (Zhou and Hablitz, 1996). The pyramidal neurons are projection cells that send axons out of the cortex or to distant targets within cortex, whereas the non-pyramidal neurons are local-circuit GABAergic interneurons (Kawaguchi and Kubota, 1997). In contrast to the rest of the cellular layer, layer I neurons of cortex are only GABAergic and show robust modulation by cholinergic basal forebrain input (Alitto and Dan, 2013). Layer 1 interneurons in the visual cortex are preferentially activated through α7 nAChRs during strong cortical desynchronization and the cholinergic input from the BF causes a significant shift in the relative activity levels of different subtypes of cortical neurons at increasing levels of cortical desynchronization (Alitto and Dan, 2013). Also, layer 1 of the neocortex is one of the areas of brain which have high expression of α7 receptors in a majority of its neurons (Christophe et al., 2002). Thus, α7 nicotinic receptor contribute a significant role in PFC network function and influences the release

of dopamine and acetylcholine presynaptically and modulate neuronal firing postsynaptically (Simon Sydserff, 2009; Thomsen et al., 2010a). The ability of α7 receptors to facilitate neurotransmitter release in the PFC thus can fine tune neuronal function of the PFC, which would likely modulate executive function (Livingstone et al., 2009b).

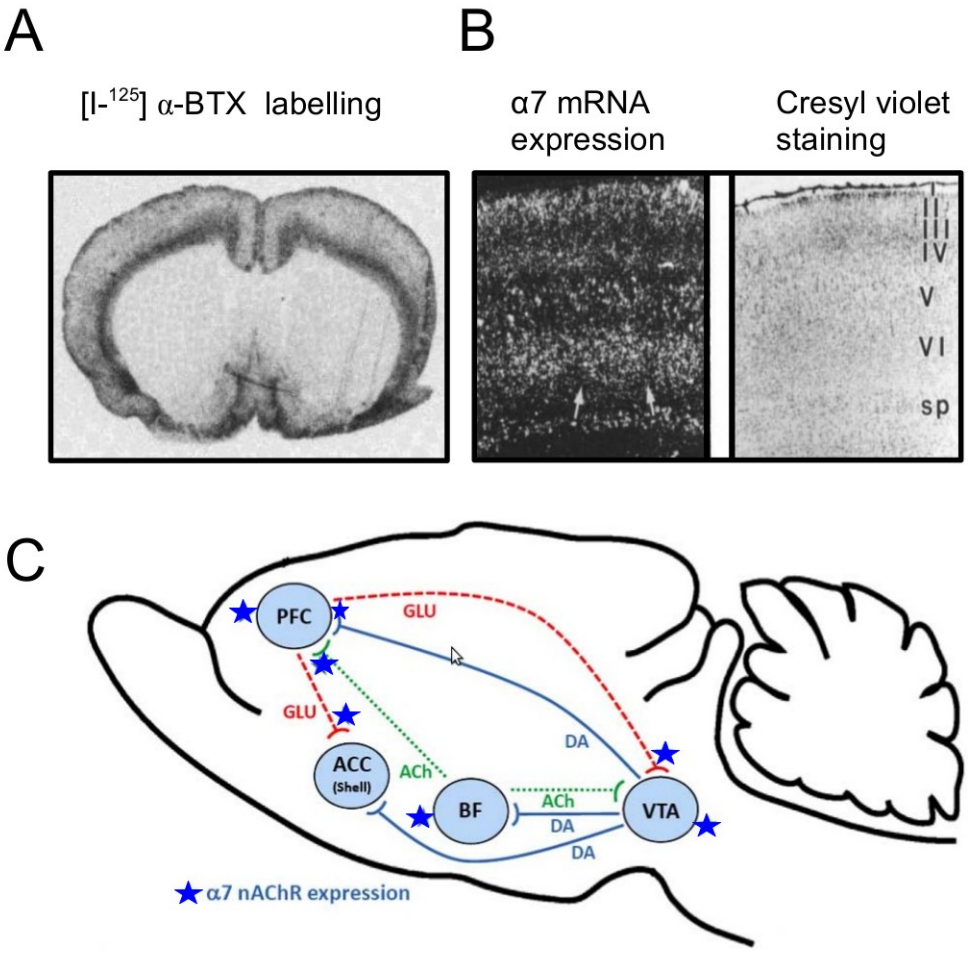

Figure 1.4 α7 nicotinic receptor expression in the rat cortex and its involvement in neurotransmission in the prefrontal cortex.

(A) Autoradiographic image of coronal mouse brain section showing [I-125] α-bungarotoxin (α7 antagonist) labelling for α7 nAChRs in rat brain. Highest labelling is observed in the layer 1 and deeper pyramidal neurons of the cortex. **(B)** Dark field photomicrograph image of coronal rat brain section showing α7 mRNA expression, post

natal day 7 (left image). The arrows label the deeper layer VI pyramidal neurons. Bright-field photomicrograph of an adjacent brain section stained with cresyl violet (right image). **(C)** Critical pathways showing α7 nAChRs expression and its involvement in neurotransmission. Cholinergic fibres which arise from the basal forebrain (BF) contain functional α7 nicotinic receptors whose activation facilitate neurotransmitter, acetylcholine release in the prefrontal cortex (PFC) (green). Two major dopamine (DA) pathways originate in the ventral tegmental area (VTA) of the midbrain. The mesolimbic pathway (blue) that originates in the VTA and terminates in the nucleus accumbens (ACC) and the mesocortical pathway (blue) that project from the VTA to the prefrontal cortex. Both pathways express presynaptic α7 nAChRs. Dopaminergic projections from VTA contain α7 receptors which contributes towards dopamine mediated activation of the PFC circuitry. Modified from (Broide et al., 1995; Clarke et al., 1985; Thomsen et al., 2010a).

1.3.2 Immune proteins in the brain

A number of studies have shown that immune proteins, previously thought to be restricted in expression to the immune system, are also found in the central nervous system with neuronal function (Boulanger et al., 2001). Shatz and colleagues (Boulanger and Shatz, 2004; Corriveau et al., 1998; Goddard et al., 2007; Shatz, 2009; Syken and Shatz, 2003a) have demonstrated the expression of a number of immune proteins in the brain with unique neuronal functions. One such class of immune proteins in the CNS are major histocompatibility complex I (MHC I) molecules. The study conducted by Shatz group (Corriveau et al., 1998) suggested that the widespread network of MHC I receptor – ligand systems in electrically active neuron are used at times when they are undergoing remodeling and synaptic plasticity. Immune related genes are also found to be dynamically regulated in human cerebral cortex (Sterner et al., 2012). These findings further raise the question of whether under physiological conditions neurons use this system of immune proteins for higher brain function?

1.3.2.1 T cell receptor: structure and function

T cell receptors (TCRs) are antigen receptors natively found on T lymphocytes. A functional TCR is an octameric complex that contains two primary α and β subunits that confer antigen specificity. MHC class I proteins are a set of cell surface proteins found on virtually all nucleated cells (Natarajan et al., 1999). The physiologic function of MHC I molecules is the presentation of peptide antigen derived from endogenous cytosolic proteins to the TCR found on T lymphocytes. The accessory molecule of TCRs is known as the CD3 zeta complex which contains γ, δ, ε and the ζ chain (Janeway, 1992). The CD3 zeta complex has a long cytoplasmic domain and an associated enzymatic function that contains one or more tyrosine phosphorylation sites within an 'immunoreceptor tyrosine-based activation motif' (ITAM). Upon T cell receptor ligand recognition, the paired tyrosines within the ITAMs are rapidly phosphorylated by the Src-family of tyrosine kinases namely Lck and/or Fyn kinase **(Fig. 1.5)**. Each of these components is required for efficient TCR signal transduction. T cell receptor activation occurs when the TCR recognizes an antigen in the form of peptide fragments bound to the polymorphic cleft at the outer end of the major histocompatibility complex (Latour and Veillette, 2001). The Src family tyrosine kinase (SFK) members Lck (also known as p56-Lck) and Fyn (also known as p59-Fyn) are the first molecules to be activated following TCR-peptide engagement (Brownlie and Zamoyska, 2013). SFKs are essential for providing the tonic signaling which is required for sustained TCR activation. The TCR αβ has no intrinsic enzymatic activity and instead depends on the kinase activity of the SFKs, particularly Lck and Fyn, to initiate signaling. Lck kinases bind to the cytoplasmic domains of the TCR co-receptors CD4 and CD8 (Veillette et al., 1988). TCR interaction

with a peptide–MHC complex are important for targeting the delivery of Lck into close proximity to the TCR-associated CD3 ζ-chain immunoreceptor tyrosine-based activation motifs (ITAMs) (Artyomov et al., 2010). Though the native function of TCR is antigen clearance by T lymphocytes, a growing body of evidence suggests that most of the TCR signaling components are also expressed in the brain and have a neuronal function **(Fig. 1.6)**

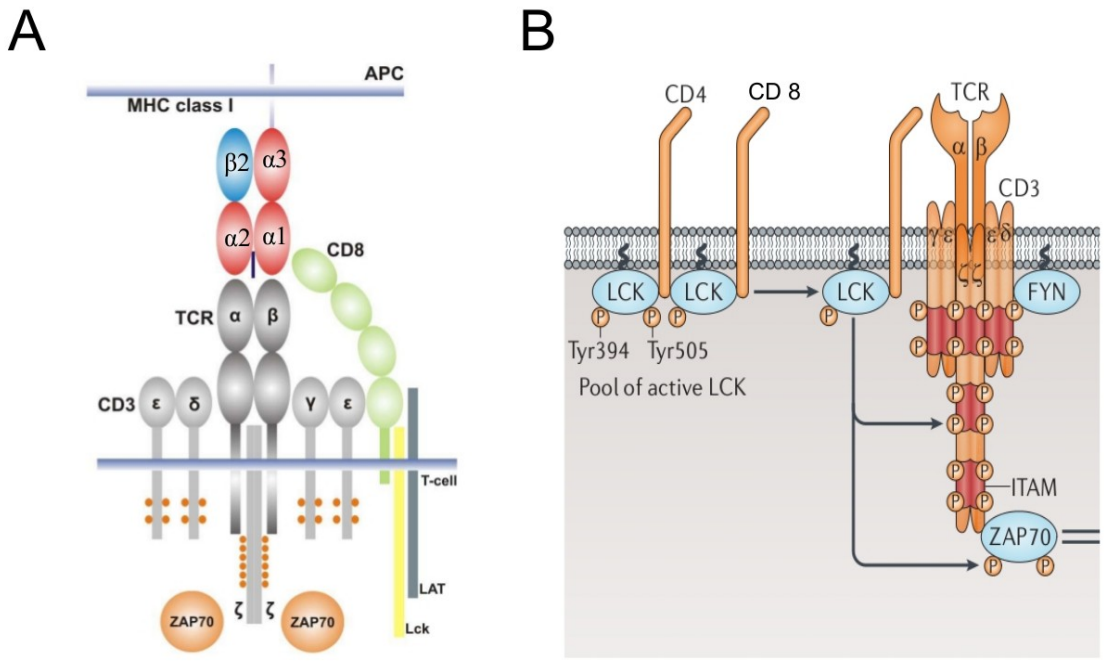

Figure 1.5 Overview of TCR signaling.
(A) T cell receptor (TCR) subunit stoichiometry and its recognition of cognate peptide–MHC molecules. The TCR complex contains the highly variable α and β chains, which bind to the peptide presented by the MHC I complex. The accessory moecules of the TCR complex contains six subunits referred to as the CD3 complex. It contains γ, δ, ε and ζ chain. The MHC I complex is a tetrameric complex of α1, α2, α3 and β2 microglobulin subunits and presents a peptide to the TCR. **(B)** TCR signaling pathway. The first molecule to be recruited to the TCR–CD3 complex upon binding to the peptide is the Src family of tyrosine kinase (SFK) members Fyn and Lck. Lck kinase phosphorylates the immunoreceptor tyrosine-based activation motifs (ITAMs) of the CD3γ chain, CD3δ chain, CD3ε chains and the ζ-chains. Phosphorylation of the ITAMs enables the recruitment of ZAP70 (ζ-chain associated protein kinase), its phosphorylation

by Lck and its activation. Activated ZAP70 phosphorylates four key tyrosine residues on the linker for activation of T cells (LAT), which recruits numerous downstream signaling molecules to form a multiprotein complex. Lck is found in T cells in three forms: phosphorylated only on tyrosine 505 (Y505, inactive form), phosphorylated only on tyrosine 394 (Y394, active form) or phosphorylated on both tyrosine 394 and tyrosine505 (Y505 + Y394, active form). The negatively regulating tyrosine 505 of Lck is phosphorylated by CSK kinase and dephosphorylated by CD45 (a phosphatase). The activating Y394 is autophosphorylated by Lck or phosphorylated by Fyn kinase. Modified from (Brownlie and Zamoyska, 2013).

1.3.2.2 Major histocompatibilty class I molecules: neuronal expression and function

The major histocompatibility complex (MHC class I) is a set of cell surface proteins found on virtually all nucleated cells and are the most polymorphic molecules expressed in all vertebrates (Natarajan et al., 1999). The physiologic function of MHC I molecules is the presentation of a peptide antigen derived from endogenous cytosolic proteins to T cells. MHC I is a tripeptide complex, consisting of a heavy chain with a peptide binding groove, β2 microglobulin (β2 M) and a peptide fragment (8–11 amino acid residues) from a degraded cytosolic protein **(Fig. 1.6)** (Natarajan et al., 1999). The neuronal function of MHC I comes from the studies done on mouse dorsolateral geniculate nucleus and visual cortex, where the majority of MHC class I molecules were found associated with the glutamatergic synapses, localized to dendrites, dendritic spines, and axon terminals (Needleman et al., 2010). These authors found MHC I expression at both pre and post-synaptic compartments. Another study showed MHC I localization with synapses which undergo activity dependent remodeling (Boulanger and Shatz, 2004). The two classical endogenous partners of MHC I molecules are Pir B receptors, found on natural killer cells, and T cell receptors found on white blood cells, the T lymphocytes (Davis and

Bjorkman, 1988). The role of Pir B receptors in synaptic plasticity in the visual cortex is well documented (Syken et al., 2006) but the neuronal function of TCR is still unknown.

The physiological role of MHC I function in neurons also comes from the studies conducted on β2 microglobulin knockout mice. These mice displayed ectopic clusters of retinal inputs in their dorsal lateral geniculate nucleus, increased synapsin levels in the hippocampus, enhanced long-term potentiation (LTP) and reduced long-term depression (LTD) in the hippocampus, and altered motor learning (Goddard et al., 2007). Neuronal MHC I was determined to be an essential modulator of glutamate receptors, affecting both NMDA receptor function and AMPA receptor trafficking. MHC I deficient synapses showed enhanced NMDAR-mediated responses with no significant changes in NMDA receptor levels, distribution, or subunit composition. A key finding from these data also showed MHC I mediated regulation of NMDA receptor dependent synaptic plasticity in the hippocampus (Fourgeaud et al., 2010). Another study showed the role of neuronal MHC I proteins in mediating excitatory neurotransmission at mossy fiber–CA3 synapses in the *Marmoset* hippocampus (Ribic et al., 2010). Altogether, these finding suggests that MHC I molecules are expressed on the neuronal cell surface, where they function to modulate synaptic transmission within the CNS.

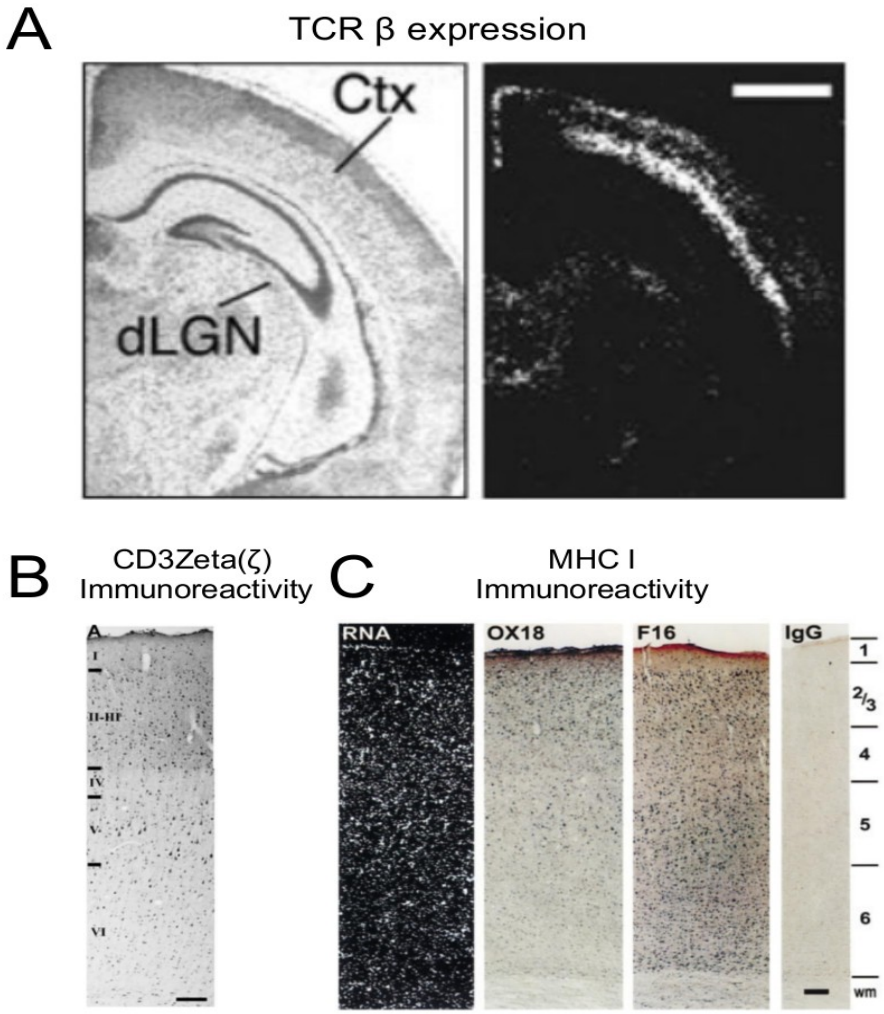

Figure 1.6 Expression of T cell receptor and its signaling component in the mammalian cortex.

(A) TCR β mRNA expression in the mouse cortex. Coronal section of mouse cortex (Ctx) from postnatal day 7 (P7), depicting TCR β mRNA expression in cerebral cortex and dorsal lateral geniculate nucleus (dLGN) conducted via in-situ hybridization, scale bar 1mm (right image) and the adjacent section with cresyl violet staining (left image) (modified from Syken et al 2003). **(B)** CD3ζ immunoreactivity in the rat parietal cortex, **s**cale bar 300 μm (modified from Baudouin et al 2008). **(C)** MHC I expresssion in rat somatosensory cortex. In situ hybridization (left) and immunohistochemistry (right) of rat somatosensory cortex brain sections. In situ hybridization (left) was carried out by using a rat class I MHC probe (panel RNA, darkfield optics) and immunohistochemistry was carried out using either of two mouse anti rat monoclonal antibodies, OX-18 or F16–4–4, and mouse IgG as a negative control. Cortical layers (I-VI) are indicated on left, scale bar, 100 μm. Image adapted from (Corriveau et al., 1998)**.**

1.3.2.3 TCR and MHCI expression in the brain

The first evidence about neuronal expression of TCR subunits was demonstrated by Syken and Shatz, 2003. They showed neuronal expression of T cell receptor beta (TCR β) mRNA in neurons of the murine central nervous system (Syken and Shatz, 2003). A major finding of this study was the expression of TCRβ locus restricted only to the cerebral cortex of the murine CNS **(Fig. 1.6)**. TCRβ requires CD3ζ for efficient downstream signaling upon TCR activation and CD3ζ chain is also expressed in the mammalian cerebral cortex (Baudouin et al., 2008) (Corriveau et al., 1998).

The current assumption of TCR-CD3ζ complex signaling is that the ITAM phosphorylation of CD3ζ triggers the docking of SH2-containing signaling molecules such as the protein tyrosine kinases of the SFKs (Germain, 1997). In accordance with this notion, the above evidence showed the expression of CD3 ζ and TCR β subunits in the rodent cerebral cortex. The main downstream Src kinases activated upon TCR-MHC interaction are Src family of tyrosine kinases, namely Fyn and Lck kinases, which are also found in neurons (Thomas and Brugge, 1997). These findings indicate that class I MHC molecules, TCR and CD3 complex classically thought to mediate cell-cell interactions exclusively in immune function, may also play a novel role in neuronal signaling and activity-dependent changes in synaptic connectivity.

1.3.3 Protein kinases

The mammalian brain comprises a rich repetoire of proteins of the phosphorylation system including diverse protein kinases, phosphoprotein substrates and neuromodulators (Walaas and Greengard, 1991). A comparison between endogenous protein phosphorylation activity in rat forebrain and peripheral tissues showed that neurons

possesses a greater number of endogenous protein kinases and respective substrates (Nestler and Greengard 1989). Neuronal specific phosphoproteins found in the nervous system indicate the importance that protein phosphorylation plays in neuronal function (Nestler et al., 1984). On the basis of the amino acids targeted for phosphorylation, protein kinases are broadly classified as either protein serine/threonine kinases or protein tyrosine kinases (Naira et al., 1985). Protein tyrosine kinases were originally identified as retroviral oncogene products and were subsequently shown to have normal cellular function (Brugge and Erikson, 1977; Wagner et al., 1991).

In late 1950s, Sutherland and colleagues discovered that the generation of the second messenger cyclic AMP (cAMP) by showing that binding of hormones like adrenaline and glucagon to their receptors enhanced the breakdown of glycogen into glucose in the mammalian liver, for which they received the Nobel Prize (Sutherland and Rall, 1958). Hence, phosphorylation of proteins by multiple kinases was accepted as a general mechanism of protein modulation via activation of many hormones, neurotrasmitters and other extracellular signals to regulate cellular function. The mammalian brain contains two distinct cyclic-nucleotide dependent kinases, namely cAMP-dependent protein kinases (PKA) and cGMP-dependent protein kinases (PKG) (Scott, 1991). These protein kinases differ from each other in several aspects like substrate specificities, sensitivities, mechanisms of activation by cyclic nucleotides and tissue distribution (Hemmings et al., 1989). The variation between these two groups of protein kinases suggest their distinct roles in the regulation of physiological processes.

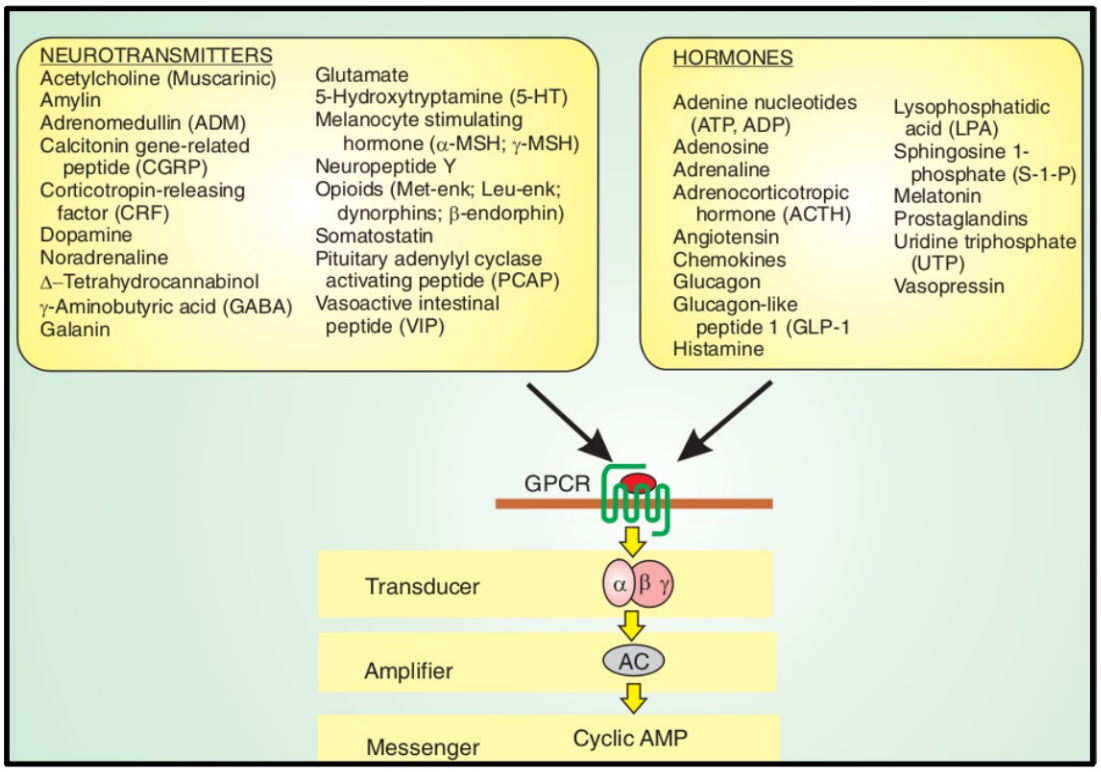

Figure 1.7 Cyclic AMP signaling pathway.
A large number of neurotransmitters and hormones act through G protein-coupled receptors (GPCRs) to engage the cyclic AMP signaling pathway. The GPCR acts through a heterotrimeric G protein complex, composed of α and βγ subunits, to stimulate the amplifier adenylyl cyclase (AC) to generate the second messenger cyclic AMP. Image adapted from (Berridge, 2012).

1.3.3.1 Cyclic AMP-dependent protein kinase (PKA)

Cyclic-AMP mediated protein kinase A pathway activation commences with the binding of an extracellular ligand (eg. hormones or neurotransmitters) to its G protein-coupled receptor (GPCR). The GPCR is attached to its stimulatory G protein subunit Gαs and two other G proteins (Gβγ). Upon binding of the GPCR to its agonist, Gαs separates from the GPCR and Gβγ. Gαs then targets the membrane bound adenylyl cyclases (ACs), which catalyze the conversion of ATP to cAMP **(Fig. 1.7)** (Walaas and Greengard, 1991). The principal intracellular receptor for cAMP is protein kinase A (PKA), found

highly enriched in the brain as compared to peripheral tissues (Nestler and Greengard 1989). In the absence of cAMP, PKA exists as a heterotetramer inactive form (R_2C_2), comprised of two regulatory subunits (R) and two catalytic subunits (C) joined by a disulfide bond. Each regulatory subunit contains two cAMP binding sites and exhibits cooperative binding of the nucleotides **(Fig. 1.8)**. This process lowers the affinity of the regulatory subunits for the catalytic subunits and induces the release of catalytic subunits to form a catalytically active enzyme (Nestler and Greengard, 1983). Cyclic nucleotide phosphodiesterases, which hydrolyze cAMP, lead to the regeneration and reassociation of the inactive PKA heterotetramer (Edelman et al., 1987). The mouse genome encodes four R subunit genes (RIα, RIβ, RIIα, RIIβ) and two C subunit genes (Cα and Cβ) (Naira et al., 1985). These two isozymes of cAMP-dependent protein kinase contain identical C subunits but differ in their R subunits. Cβ isoforms comprise the major PKA catalytic component in the brain (Uhler et al., 1986). Though type I/II regulatory subunits of PKA greatly differ in several of their biochemical properties, both isoforms are widely distributed throughout brain and differ in their regional distribution. PKA I is cytosolic and ubiquitous while PKAII is tethered to specific membrane compartments through interation with several cytoplasmic brain proteins including the cytoskeletal protein, microtubule associated protein (MAP-2), calcineurin (Ca^{2+} and calmodulin dependent protein phosphatase) as well as other unknown proteins (Soderling and Beavo, 2000). In addition to the unique expression pattern of PKA isoforms, PKA RII subunits show preferential binding to A-kinase anchoring proteins (AKAPs), which act as molecular scaffolds and direct PKA to subcellular compartments like neuronal dendrites, golgi apparatus or the nuclear envelope (Taskén and Aandahl, 2004). With the help of AKAP

scaffolds, cAMP-mediated PKA signaling supports the formation of multiprotein complexes that could also include other kinases and phosphatases **(Fig. 1.9)**.

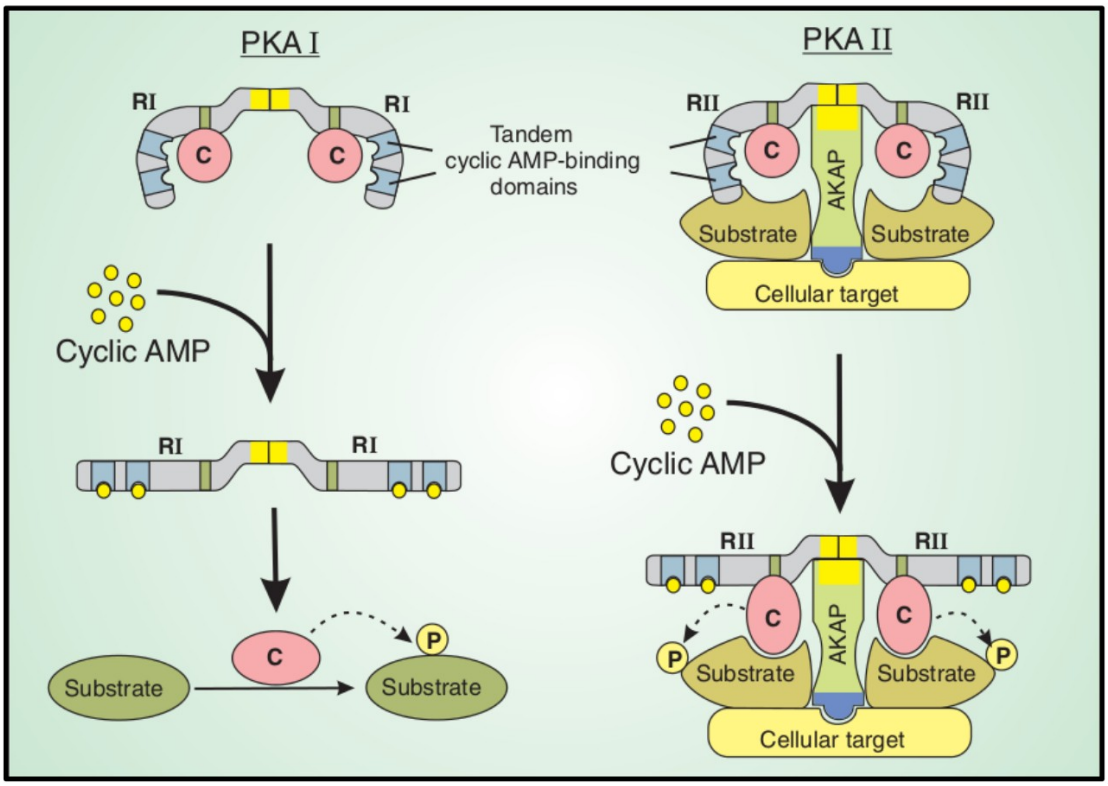

Figure 1.8 The structural and functional organization of protein kinase A isoforms (PKA).
There are two types of PKA isoforms found in neurons, type I PKA (PKA I) and type II PKA (PKA II), which differ primarily in the type of regulatory (R) subunits that associate with the catalytic (C) subunits. There are four R subunit isoforms (RIα, RIβ, RIIα and RIIβ), which have somewhat different properties with regard to their affinity for cyclic AMP and their ability to associate with the A-kinase-anchoring proteins (AKAPs). It is these different R subunits that define the properties of the two types of PKA. Image taken from (Berridge, 2012).

1.3.3.2 Neurobiological function of PKA

The cAMP-PKA system represents a critical signaling pathway for learning and memory in organisms ranging from invetebrates such as *Aplysia* to mammels (Abel et al., 1997; Byrne and Kandel, 1996). PKA is highly enriched in neurons where its activation

contributes to synaptic plasticity in the hippocampus of the brain, leading to long term potentiation (LTP) and long-term depression (LTD) (Abel et al., 1997). In the mossy fibre pathway of the hippocampus, one study showed that elevation of cAMP interfered with the tetanus induced mossy fibre LTP (Weisskopf et al., 1994). Moreover, blockers of the cAMP dependent signal transduction pathway blocked mossy fibre activated LTP (Weisskopf et al., 1994). In the cerebral cortex, layer 2/3 pyramidal neurons showed PKA type II isoform restricted localization in the dendritic shafts as compared to the dendritic spines (Zhong et al., 2009). Upon cAMP stimulation MAP2-tethered PKA type II regulatory subunits redistributed from dendritic shafts to spines. In the same study it was shown that the spatial gradient of type II PKA between the dendritic shafts and spines was critical for the regulation of synaptic strength and long term potentiation. Thus, the translocation of type II PKA can influence PKA function in neurons.

The PKA system also contributes to the plasticity that underlies sensitization to noxious stimuli (Taiwo and Levine, 1991). Furthermore, there is elevated activity of cAMP and PKA in smokers' brains potentially implicating dysfunctional PKA signaling in nicotine addiction (Hope et al., 2007). A functional role of PKA in neurons comes from studies performed on mutant mice lacking the expression of the PKA catalytic or regulatory subunit (Kirschner et al., 2009). Transgene disruption of regulatory isoform, RI α/β, resulted in long-term memory impairments which was not observed in RII β mutant mice (Brandon et al., 1995). This study indicated that type I R subunits are more critical in the earliest phase of activation of the cAMP-PKA pathway and necessary for memory consolidation. Also RI type isoforms are more sensitive to cAMP activation than type RII-PKA isoforms (Woodford et al., 1989). However, in neurons RII β

expression is region specific. For example RII β subunits are found highly expressed in the striatum and RII β knockout mice showed significantly reduced PKA activity in the same region of the brain (Brandon et al., 1997). Since dopaminergic neurotransmission in the striatum is critical for motor output (Centonze et al., 2001), alterations in PKA subunits could disrupt dopaminergic signaling (Brandon et al., 1998). At a molecular level, RII β was shown critical for striatal gene expression, as amphetamine induction of c-fos mRNA, and constitutive prodynorphin mRNA expression were reduced in the RII β knockout mice (Brandon et al., 1998). Together, these evidence indicate that the temporal and spatial expression of PKA isoforms greatly determine the net activation and downstream effect of cAMP-PKA mediated physiological processes.

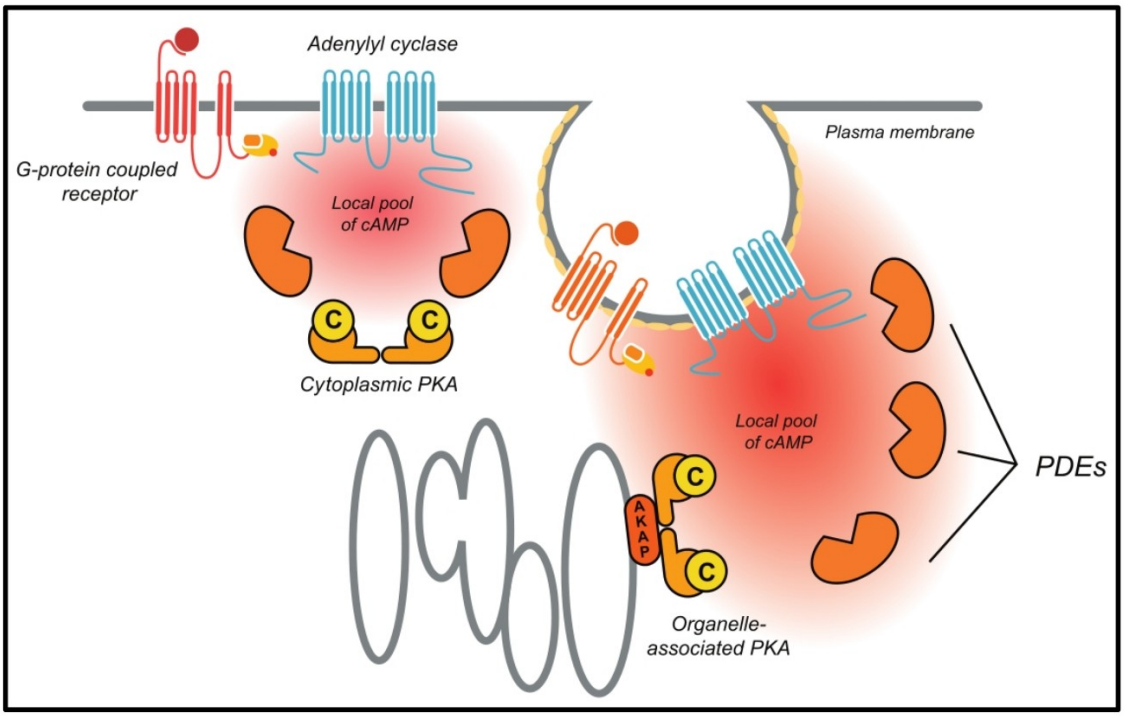

Figure 1.9 G protein-coupled receptors (GPCR) regulate activation of different isoforms of adenylyl cyclase leading to generation of cAMP.
Ligand bound GPCRs activate adenylyl cyclases (ACs) in their proximity and generate pools of cAMP. The local concentration and distribution of the cAMP gradient is limited by the enzyme phosphodiesterase (PDE), which cleaves cAMP. The subcellular

structures harbor specific isozymes of PKA that are anchored via A kinase anchoring proteins (AKAPs) which in turn are responsible for defined localization of PKA in the vicinity of the GPCRs and the ACs. These mechanisms serve to localize and limit the assembly of the PKA pathway to a defined subdomains of cells. Image taken from (Taskén and Aandahl, 2004).

1.3.3.3 Structure and function of Src family of tyrosine kinases

Tyrosine phosphorylation of cellular substrates has been implicated in the regulation of a variety of cellular processes, including cell growth, cell differentiation and neuronal signaling (Thomas and Brugge, 1997). In this regard, members of non-receptor tyrosine kinase family (Src family of tyrosine kinases) have been recognized in the CNS to regulate ion-channel activity, synaptic potentiation and synaptic plasticity, thereby regulating learning and memory processes (Kalia et al., 2004). Src family of tyrosine kinases are classified into eight subfamilies based on the structural differences, namely Src, Fyn, Yes, Fgr, Lyn, Hck, Lck, Blk and Yrk respectively (Brown and Cooper, 1996). All the members of the Src family have a common structure as shown in **Fig. 1.10**. Only five members of the Src family kinases are expressed in the mammalian brain which are Src, Fyn, Yes, Lck and Lyn kinases (Salter and Kalia, 2004). Src kinases are typically 52-62 kDa proteins, comprised of six functional regions. Src homology 4 (SH4) domain, the unique region, the SH3 domain, the SH2 domain, the catalytic kinase domain and a short negative regulatory tail present in the carboxyl terminus (Thomas and Brugge, 1997). The SH4 domain contains a 15 amino acid sequence that includes signals for lipid modification of Src family kinases and targets it to cellular membrane upon myristoylation. The unique domain is distinct within the member of Src kinases (Roskoski, 2004). The SH3 and SH2 domains are protein-binding domains and are important for intra as well as intermolecular interactions that regulate Src catalytic

activity, Src localization, and recruitment of substrates (Weng et al., 1994). All SH3 domain ligands contain a core consensus sequence of P-X-X-P (P = proline) and the amino acids surrounding the prolines confer affinity and specificity for individual SH3 domains. The SH2 domain is involved in regulating the catalytic activity of Src kinases, localization of Src and this domain binds to specific short contiguous amino acid sequences containing phosphotyrosine (Songyang et al., 1993). The catalytic activity of Src kinases is dynamically regulated through phosphorylation and dephosphorylation of the kinases at the key tyrosine (Y) residues Y416 and Y527 **(Fig. 1.10)**. Dephosphorylation of Y527 by protein tyrosine phosphatases prevents the intramolecular interaction with SH2 domain and activates the kinase (Xu et al., 1999).

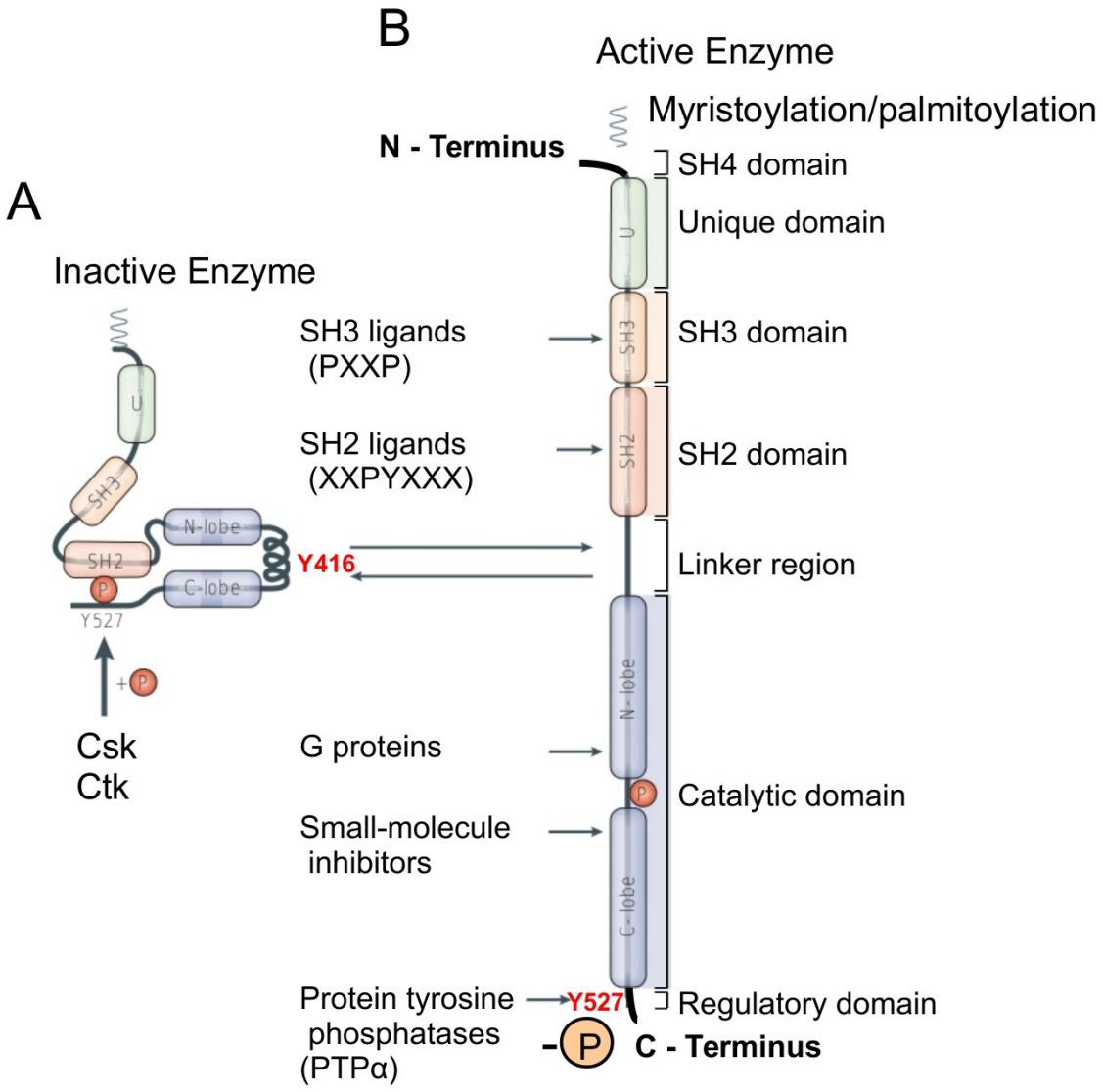

Figure 1.10 Structure and regulation of Src family kinases.
All members of Src family non-receptor tyrosine kinases share a common domain structure which includes Src homology (SH4) domain, unique (U) domain, SH3 domain, SH2 domain, linker region and catalytic domain. The regulation of catalytic activity is mediated by intramolecular interactions and tyrosine phosphorylation and dephosphorylation of the kinase itself. **(A)** Inactive conformation of the Src family of tyrosine kinase. The inactive conformation occurs upon phosphorylation of the terminal tyrosine (Y527) by kinases such as Csk or Ctk. **(B)** Active conformation of Src family of tyrosine kinases. Upon dephosphorylation by phosphatases of terminal Y527, intramolecular displacement occurs between SH3 and SH2, which results in an open and active conformation of Src kinase. Autophosphorylation of Y416 results in a conformational change of the activation loop, which renders the kinase fully active. Small-molecule inhibitors (such as PP2 (4-amino-5-(4-chlorophenyl)-7-(t-

butyl)pyrazolo[3,4-d]pyrimidine)) bind to the ATP-binding site in the catalytic domain and blocks phosphate transfer to target proteins. Some G proteins (such as Gαs, Gαi and H-Ras) interact with the catalytic domain and alter kinase activity by unknown mechanisms. Modified from (Salter and Kalia, 2004).

1.3.3.4 Neurobiological function of Src kinases

Src kinases are expressed ~ 200 fold more in neurons as compared to peripheral tissues (Thomas and Brugge, 1997). The role of Src kinase activation on neuronal function comes from the study conducted by Kalia et al (2004). The authors showed that Src kinase activation upregulated the activity of NMDA receptors and other ion channels (Kalia et al., 2004). NMDA receptors (NMDARs) constitute one subtype of glutamate receptors that mediate excitatory transmission at most central synapses (Cull-Candy et al., 2001). Kalia and colleagues showed that Src kinase modulated the function of NMDA receptors through phosphorylation, which led to changes in synaptic plasticity. Specific members of Src kinases like Fyn, Lck and Src kinases are highly expressed in the post-synaptic density (PSD) of neurons, the main postsynaptic structural component of glutamatergic synapses (Takagi et al., 1999). Src mediated upregulation of NMDA receptor function resulted in NMDAR-dependent synaptic potentiation and plasticity. Thus, Src kinases are required for cellular processes of learning and memory, and pathological plasticity, such as pain and epilepsy.

Recent studies have also shown the regulation of α7 nicotinic receptor by tyrosine phosphorylation mediated via Src kinases. Tyrosine dephosphorylation unlike NMDARs resulted in robust potentiation of whole-cell responses of α7 currents in cultured hippocampal neurons and in neuroblastoma cells (Charpantier et al., 2005a). A similar study also showed that the number of functional cell surface α7 nAChRs was controlled

indirectly via tyrosine phosphorylation (Cho et al., 2005). In the former study it was hypothesized that Src mediated inhibition of α7 nAChRs on inhibitory interneurons could be one mechansim of disinhibition of pyramidal cells in the hippocampus. Thus, these experimental studies showed that Src kinases are versatile enzymes that play key roles in modulation of the neuronal circuit through phosphorylation of ion channels. These results also suggest that Src kinases have a broad range of substrates. The net signaling outcome of the Src kinase pathway depends on the specific isoform of Src kinase expression, its cellular localization and its cross talk with other receptor signaling pathways. Interestingly, Src kinases are highly concentrated in the lipid microenvironment on the cell surface known as lipid rafts. The precise localization of Src signaling in these lipid raft regions protects the target phosphosubstrate from non-raft enzymes such as membrane phosphatases that otherwise could affect the signaling process (Simons and Toomre, 2000). This in turn favours specific protein–protein interactions, resulting in the activation of diverse signaling cascades.

Chapter 2 - A Rapid Agonist Application System for Fast Activation of Ligand-Gated Ion Channels

Abstract

The synaptic delay between neurotransmitter release across the synaptic cleft and activation of neurotransmitter gated ion channels is less than a msec. Nicotinic acetylcholine receptors (nAChRs), like many other classes of ligand-gated ion channels, are comprised of different protein subunits forming a variety of receptors with different activation and desensitization kinetics and pharmacological sensitivities. To measure and fully characterize ligand-gated ion channel currents accurately, one must apply agonists in a fraction of a msec and repeatedly at various concentrations without any prior desensitization of the receptors. In this paper, we describe an economical, easy to assemble and operate, rapid drug application system. The drug applicator system consists of a parallel array of three pinch valves, which allow either agonist or wash solution into a theta tube. Solution exchanges of 0.16 ms can be achieved. In transfected cells, ACh elicited α4β2 nicotinic currents with mean rise times of 55 ± 13 msec. We recorded α7 nAChRs, which desensitize very rapidly, and obtained very fast rise times of 19 ± 2 msec. With this novel drug applicator, agonists can be applied repeatedly at intervals of 30 sec without any loss of current. Hence, complete dose-response relations can be obtained for even α7 nAChRs, which are very sensitive to desensitization caused by agonist exposure on a msec time scale. The drug application system can also be extended to the study of ligand-gated ion channels in brain slices. The theta tube valve-driven drug applicator

system can be applied to study other ligand-gated ion channels including glutamate and GABA receptors.

Publication Information

This chapter has previously been published as **Komal P,** Evans G and Nashmi R. A rapid agonist application system for fast activation of ligand-gated ion channels. *J Neurosci Methods* 198: 246-254 (2012). All experiments were performed and analyzed by PK and were designed by PK and RN. The paper was written by PK and RN.

2.1 Introduction

The major form of communication between neurons in the brain is governed by the release of neurotransmitters, which bind to receptors on the surface of postsynaptic neurons, called chemical synaptic transmission. The delay between neurotranmitter release from the presynaptic terminal and initiation of a postsynaptic response occurs in less than one msec. Ligand-gated ion channels mediate fast neurotransmission by their transition from the closed unbound state to the ligand-bound open state on a msec time scale. Upon prolonged agonist exposure ligand-gated ion channels transition to the ligand bound desensitized state. Nicotinic acetylcholine receptors (nAChRs) are one such class of ligand-gated ion channels. They are pentameric cation channels that are activated by ACh or nicotine permitting an influx of sodium and calcium and an efflux of potassium. Heteromeric α4β2* (* indicates that the receptor may contain additional subunits other than α4 and β2) and homomeric α7 form the two most abundant receptor subtypes of a total of 12 different neuronal subunits (α2-α10 and β2-β4) that exist in the vertebrate CNS (Whiting et al., 1987; Dani and Bertrand, 2006; Gotti et al.,

2006; Millar and Gotti, 2009). Hence, many different subunit combinations of nicotinic receptors can form with a great variety of desensitization kinetics and pharmacological profiles. To study accurately the activation of nicotinic receptors or any other class of ligand-gated ion channels and their physiological role in neuronal signaling one must deliver agonists rapidly on a msec time scale and eliminate leakage of agonist to prevent receptor desensitization. Furthermore, to accurately characterize different subtypes of nicotinic receptors one must deliver various concentrations of agonist for a dose-response profile of the receptors.

Many different agonist application systems have been developed over the years for the electrophysiological study of ligand-gated ion channels, all with their strengths and limitations. One of the drug applicators used routinely to examine ligand-gated ion channel currents is a picospritzer, which requires a high air pressure source and delivers regulated air pressure through tubing to the back of agonist filled glass micropipette to eject the drug (Ji et al., 2001; Klink et al., 2001; Nashmi et al., 2007). An improved modification of the puffer technique of drug application employs a daisywheel solution changer so that dose-response relations can be obtained in slice recordings (Pidoplichko 2005). Another device is a U-tube, which draws solution into a hole in the U-tubing until the valve is shut, after which solution is ejected from the hole in the U-tubing (Alkondon and Albuquerque, 2005; Nivalda O Rodrigues-Pinguet, 2005; Zhao et al., 2003). Piezoelectric driven theta tubes use two continuously flowing streams in which the recorded cell is bathed in the wash solution stream until high voltage is applied to the piezoelectric device, expanding and rapidly moving the drug solution stream onto the recorded cell. This achieves submillisecond solution exchange with no desensitization of

receptors (Buisson and Bertrand, 1998; Nashmi et al., 2003; Nashmi et al., 2007). Even more sophisticated and rapid techniques of drug applications have been developed using UV-uncaging of agonists (Dahan et al., 2004; Lester and Nerbonne, 1982) which can achieve not only rapid but also more localized delivery of agonists with the use of two-photon microscopes (Khiroug et al., 2003) .

In this chapter, we describe a simple and inexpensive drug application system operated by valves and a theta tube that can reliably and very rapidly apply agonist within 0.16 msec as measured by the 10-90% open tip rise response of change in the junction potential. The applicator did not leak agonist onto the recorded cell and therefore receptor desensitization is nonexistent. Accurate and complete dose-response relations can be attained using the valve-driven drug applicator. Furthermore, this application system is well suited to elicit ligand-gated ion channel currents in brain slices.

2.2 Materials and methods

2.2.1 Construction of the valve driven theta tube drug applicator to record nicotinic responses

A simple and inexpensive drug application system is developed in our lab that reliably and very rapidly applied agonist within 0.16 msec as measured by the 10-90% open tip rise response of change in junction potential. **Fig. 2.11 A** diagrammatically depicts the valve driven theta tube drug applicator system. Theta borosilicate glass tubing (cat# BT-150-10; Sutter Instruments) were partway pulled on a P-97 Flaming-Brown Micropipette Puller (Sutter Instruments). To separate the two ends of the theta tubing, the adjoining narrowed portion of the theta tube was scored with a file under microscopic observation

and the ends bent until there was a clean break. The outer diameter of the theta tubes ranged between 300-400 μm. Two separate polyethylene tubes (PE-50) with I.D, 0.28mm (0.011") and O.D 0.61mm (0.024") (cat# 427400; Becton Dickinson and Company) were inserted into the two parallel barrels of the theta glass tubing. The ends of the theta tubing were sealed with epoxy glue to produce an air-tight seal between the theta tube and PE-50 tubing. Through a series of connections to larger PE tubings, each of the two PE-50 tubings, which emanated from the theta glass tube eventually connected to platinum silicone tubings with I.D. of 1/16" and O.D. of 1/8" (cat# R-KT-5720-02; Cole-Parmer), which fed into a solenoid operated two channel pinch valve of 12 V and 2.6 Watts (cat# R-98302-42, Cole-Parmer) or 12 V and 2.8 Watts (cat# 075P3MP12-02S, Bio-Chem Fluidics). One of the two channels of the pinch valve is normally open while the other channel is normally closed. Application of 12V to the solenoid valve switches the flow path from one channel to the other by pinching one platinum silicon tubing while releasing the previously closed channel. A "Y" connector is attached to each of the two platinum silicone tubes entering the two channel pinch valve. Upstream to the two channel pinch valve were two sets of different solution reservoirs (60 ml syringe tubes), each of which could be selected through an 8-way manual valve (cat# 001103, Omnifit). The other port of each of the two "Y" connectors led to platinum silicon tubing with I.D. of 1/16" and O.D. of 1/8" (cat# R-KT-5720-02; Cole-Parmer) that fed to a normally closed one channel pinch valve (12 V, 2.6 Watts, cat# R-98302-02, Cole-Parmer) or 12 V and 2.8 Watts (cat# 075P3NC12-02SQ, Bio-Chem Fluidics) that led to waste. The purpose of the one channel pinch valve is to prime the solution before opening the channel of the two channel valve producing faster ejection of the solution onto the cell.

The three valves were attached to an 18” long aluminum rod with magnetic base. The same aluminum rod supported a manual micromanipulator, which held a 7” long probe holder (MXP-150, Siskiyou) to which the theta tube was fastened **(Fig. 2.11 B, C)**. The valves were driven by a three channel valve controller, with each channel supplying 12 V of DC power supply to each of the valves. Each of the channels was triggered by a voltage supplied by one of the digital output channels of the 1440A Digidata analog-to-digital converter (Molecular Devices).

The sequence of events to operate the valve-driven theta tube drug applicator are **(Fig. 2.12)**: **(1)** the drug solution channel is closed while the extracellular solution (ECS) channel is open for the two channel valve; **(2)** the one channel valve for the agonist is opened to prime agonist into the tube before drug application; **(3)** the two channel valve is activated so that the drug solution channel is opened and the ECS solution channel is closed; **(4)** the one channel valve for ECS solution is opened to prime the ECS tube before washing off the drug with ECS and returning to step **(1)**. The priming duration can be adjusted for optimal solution exchange. For a 1 sec drug application we found that 300 ms of priming of agonist and wash solutions produced optimal results.

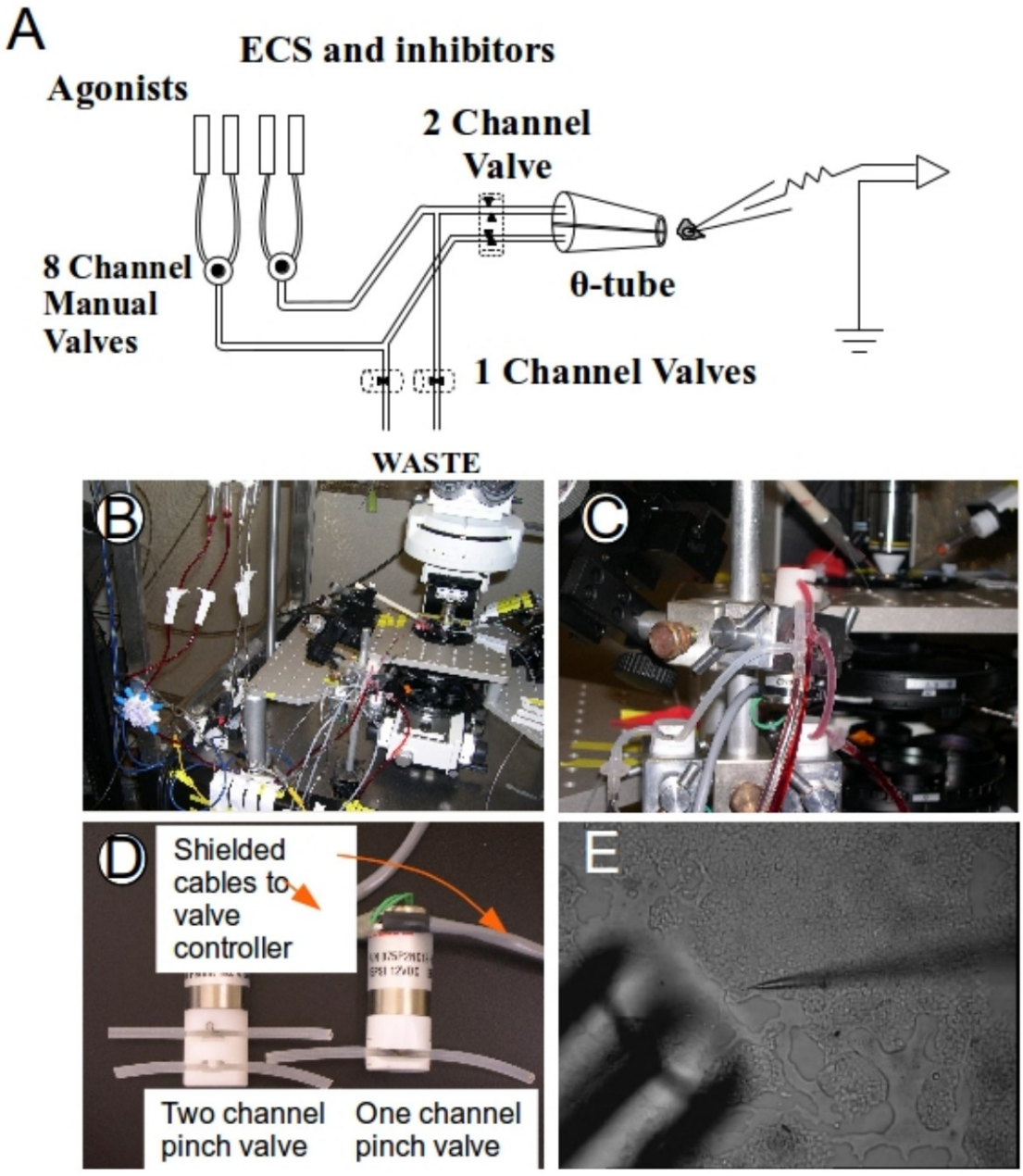

Figure 2.11 Construction of the valve driven theta tube drug applicator.
(A) Schematic diagram of the valve driven theta tube drug applicator. Flow through each of two tubings leading to the barrels of the theta tube is regulated by a two channel valve, one open and the other closed, which can be reversed with voltage. A pair of one channel valves were each used to prime the solution for faster flow down the two channel valve. **(B)** Photo of the setup. **(C)** A zoomed image of the setup showing the three valve system. **(D)** The two channel and the one channel pinch valves. **(E)** An image of the theta tube on the bottom left and the patch pipette recording electrode.

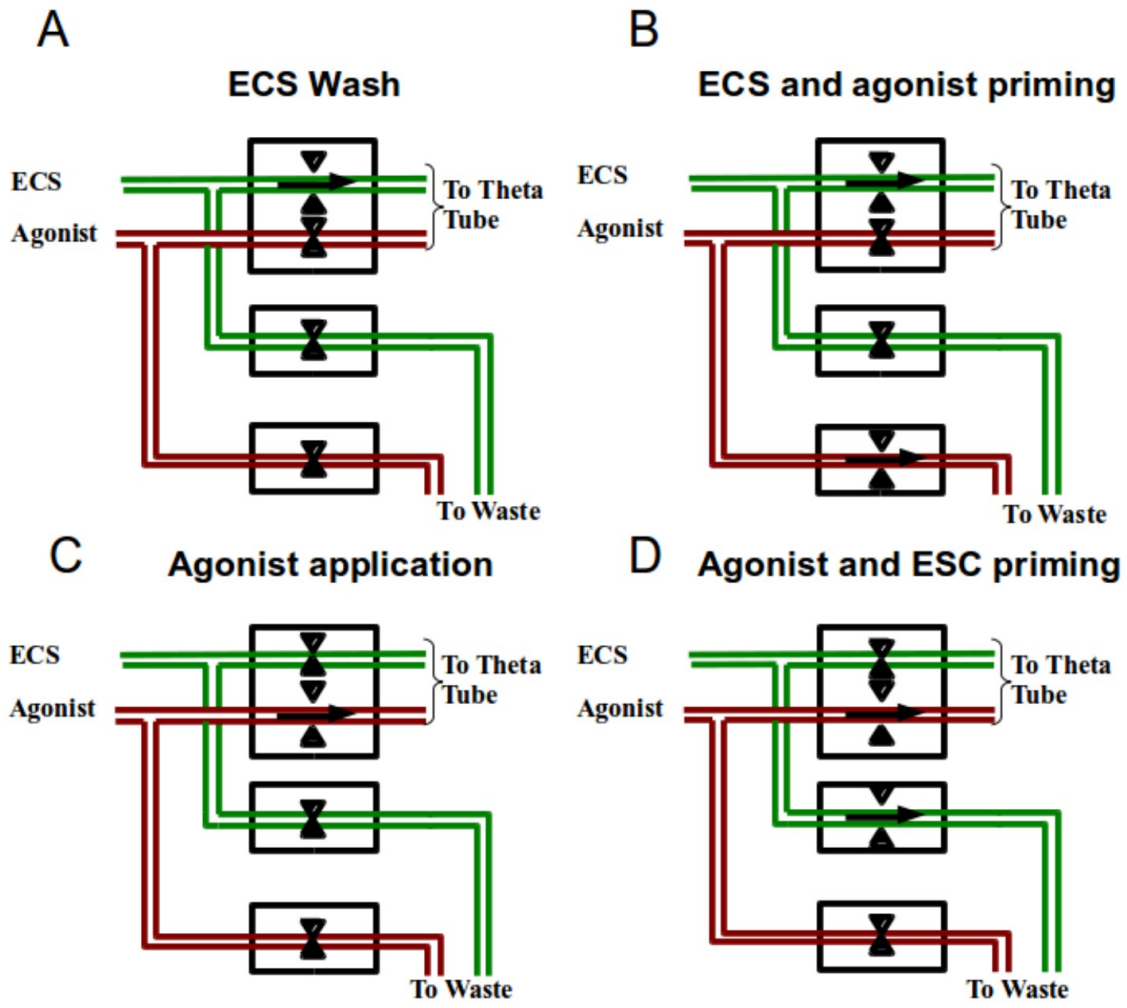

Figure 2.12 Schematic operation of the valve driven drug applicator.
The sequence of events to operate the valve driven theta tube drug applicator are as follows: **(A)** the agonist solution channel is closed while the extracellular solution (ECS) channel is open for the two channel pinch valve; **(B)** the one channel pinch valve for agonist is opened to give a 300 msec priming before agonist application; **(C)** the two channel valve is activated so that the agonist solution channel is opened and the ECS solution channel is closed; **(D)** the one channel valve for the ECS solution is opened to give a 300 msec priming before washing out the agonist with ECS and returning to step **(A).**

2.2.2 Culture and transfection of HEK 293T cells

Human RIC-3 cDNA was kindly provided by Neil Millar from the University College London. RIC-3 is a chaperone protein that is a requirement for the functional expression

of α7 nAChRs in many mammalian cell lines (Lansdell et al., 2005). The α4YFP β2CFP nAChR cDNA encoded mouse α4 and β2 nAChR subunits in which fluorescent proteins were inserted into the M3-M4 cytoplasmic loop and functioned normally in every respect as described previously (Nashmi et al., 2003). cDNA encoding mouse α7 nAChRs cloned into pcDNA3.1 was kindly provided by Jerry Stitzel from the University of Colorado Boulder. HEK293T cells (ATCC) were maintained in DMEM high glucose medium supplemented with 10% fetal calf serum, 2 mM L-glutamine, 100 U/ml penicillin, and 100 µg/ml streptomycin (DMEM complete medium). DMEM incomplete medium was identical to DMEM complete medium except that fetal calf serum was omitted. Three to six days before electrophysiological recordings, the cells were incubated with trypsin for 3 min, mechanically dissociated, and seeded on poly-DL-lysine (1 mg/ml, cat # P9011, Sigma) coated 5 mm glass coverslips (cat # 64-0700, Warner) placed inside 35 mm diameter petri dishes. Cells were transfected at 60 –70% confluency using Fugene Transfection Reagent (cat # PRE2311, Promega). To each dish was added either solution 1 (2 µg of α4YFP and 2 µg of β2CFP cDNA mixed with 3 µl of Fugene transfection reagent and 250 µl of incomplete DMEM medium) or solution 2 (2 µg of α7, 2 µg of RIC-3 and 0.2 µg of Venus mixed with 3 µl of Fugene transfection reagent and 250 µl of incomplete DMEM medium). Transfection was performed according to the manufacturer's protocol. Electrophysiological recordings were performed 2–3 d post-transfection.

2.2.3 Whole-cell electrophysiology in cultured cells

Cells were visualized with differential interference contrast illumination using an upright microscope (Nikon FN1) equipped with a CFI APO 40X W NIR objective (0.80

numerical aperture, 3.5 mm working distance). Transfected cells were identified with Venus fluorescent protein or fluorescently tagged nicotinic receptors under fluorescence illumination (Hg lamp). Standard whole-cell recordings were made using a Multiclamp 700B amplifier (Molecular Devices) filtered at 4 kHz, digitized at 10 kHz with a Digidata 1440A data acquisition system (Molecular Devices), and stored on a personal computer.. Whole-cell patch-clamp recordings were made 48 h post transfection. The culture medium was exchanged for extracellular solution (ECS) containing (in mM): 150 NaCl, 4 KCl, 2 $CaCl_2$, 2 $MgCl_2$, 10 HEPES, and 10 D-glucose adjusted to pH 7.4 (with NaOH) (osmolarity = 300 mosmol l^{-1}) . Micropipette recording electrodes were pulled from borosilicate glass of 1.5 mm O.D. and 1.0 mm I.D. (cat 1B150F-4, WPI) on a P-97 Flaming/Brown micropipette puller (Sutter Instrument). Patch electrodes (5-7 MΩ) were filled with pipette solution containing (in mM): 108 KH_2PO_4, 4.5 $MgCl_2$, 0.9 EGTA, 9 HEPES, 0.4 $CaCl_2$, 14 creatine phosphate (Tris salt), 4 Mg-ATP, 0.3 GTP (Tris salt), pH 7.4 with KOH. Series resistance was compensated 50%, and the membrane potential was held at -60 mV. Recorded potentials were corrected for the liquid junction potential. ACh was delivered using the two-barrel glass theta tube valve driven drug applicator, which was positioned ~300 μm from the recorded cell (Fig.. 1E). Agonists were applied for 1 second. The timing of agonist delivery and recordings were controlled using pCLAMP 10 acquisition software (Molecular Devices).

2.2.4 Whole-cell electrophysiology in brain slices

Whole-cell patch-clamp recordings in brain slices were performed on mice 10-11 days postnatal. Procedures on mice were performed in accordance to protocols approved by the University of Victoria Animal Care Committee and in accordance with the Canadian

Council on Animal Care. Mice were anesthetized with isofluorane, decapitated and the brains were removed and sectioned coronally into 320 μm thick slices in regular brain slice ECS with a vibratome (Leica 1000S). The ECS for brain slice recordings and slicing were identical and were comprised of (in mM): 125 NaCl, 2.5 KCl, 1.2 NaH_2PO_4, 1.3 $MgCl_2$, 2.4 $CaCl_2$, 26 $NaHCO_3$ and 11 D-glucose.

Neurons were visualized with an upright microscope (Nikon FN1) equipped with a CFI APO 40X W NIR objective (0.80 numerical aperture, 3.5 mm working distance) using infra-red differential interference contrast and a video camera (IR-1000, Dage MTI). The patch electrodes had resistances between 6 - 9 M when filled with pipette solution containing (in mM): 130 potassium gluconate, 5 EGTA, 0.5 $CaCl_2$, 2 $MgCl_2$, 10 HEPES, 3 Mg-ATP, 0.2 GTP and 5 phosphocreatine tris, pH adjusted to 7.4 with KOH, osmolarity adjusted to 300 mOsm with sucrose. Whole-cell voltage-clamp recordings were performed at room temperature with a MultiClamp 700B amplifier (Molecular Devices) and pCLAMP 10 software (Molecular Devices). Data were filtered at 4 kHz and sampled at 10 kHz with a Digidata 1440A data acquisition system (Molecular Devices). The membrane potential was corrected for liquid junction potential and series resistance was corrected 50%. Neurons were held at -60 mV. The theta tube of the valve driven drug applicator was positioned ~600 μm from the recorded cell and agonists were applied for 1 second.

2.2.5 Statistical analysis

Values are reported as mean ± standard error. Significant difference ($p < 0.05$) between two groups of data were determined using a *t* test for continuous data meeting parametric

assumptions of equal variances and normality. Otherwise, a Wilcoxon rank sum test was performed for nonparametric data.

2.3 Results

2.3.1 Testing the speed of solution delivery with the valve driven theta tube

To characterize the kinetic properties of ligand-gated ion channels accurately agonists must be delivered within a fraction of a msec without leakage of agonists to the cells to prevent desensitization of receptors. To precisely measure the rate of solution exchange we measured the open tip response of the change in the liquid junction potential of 10% ECS applied from the drug barrel of the theta tube. We visually inspected drug delivery and leakage by introducing phenol red dye in the 10% ECS and subsequent drug mixtures. Any test solution leakage would have also been identified by any slow changes in baseline current, which was never observed.

When 10% ECS was applied for a 1 sec duration every 15 sec, we obtained a consistent and repeatable rise to a steady state maximum during the 1 sec application, which quickly returned to baseline levels **(Fig. 2.13 A)**. We obtained sub-millisecond (mean = 0.68 ± 0.06 msec) 10-90% rise times of the open tip responses consistently over every day of recording **(Fig. 2.13 B, D)**, with our fastest time of 0.16 msec. The washout time of the 10% ECS was slower as measured from the 90-10% decay time with a mean time of 9.8 ± 1.9 msec **(Fig. 2.13 C, E)**. Our fastest open tip decay time was 0.12 msec, indicating that relatively fast washes could be achieved with optimal positioning of the theta tube in relation to the bath washout flow.

The submillisecond rise time performance approximates the kinetics of neurotransmitters reaching their target. The absence of any detected leakage of test solution should lead to consistently repeatable nicotinic responses devoid of receptor desensitization between drug applications.

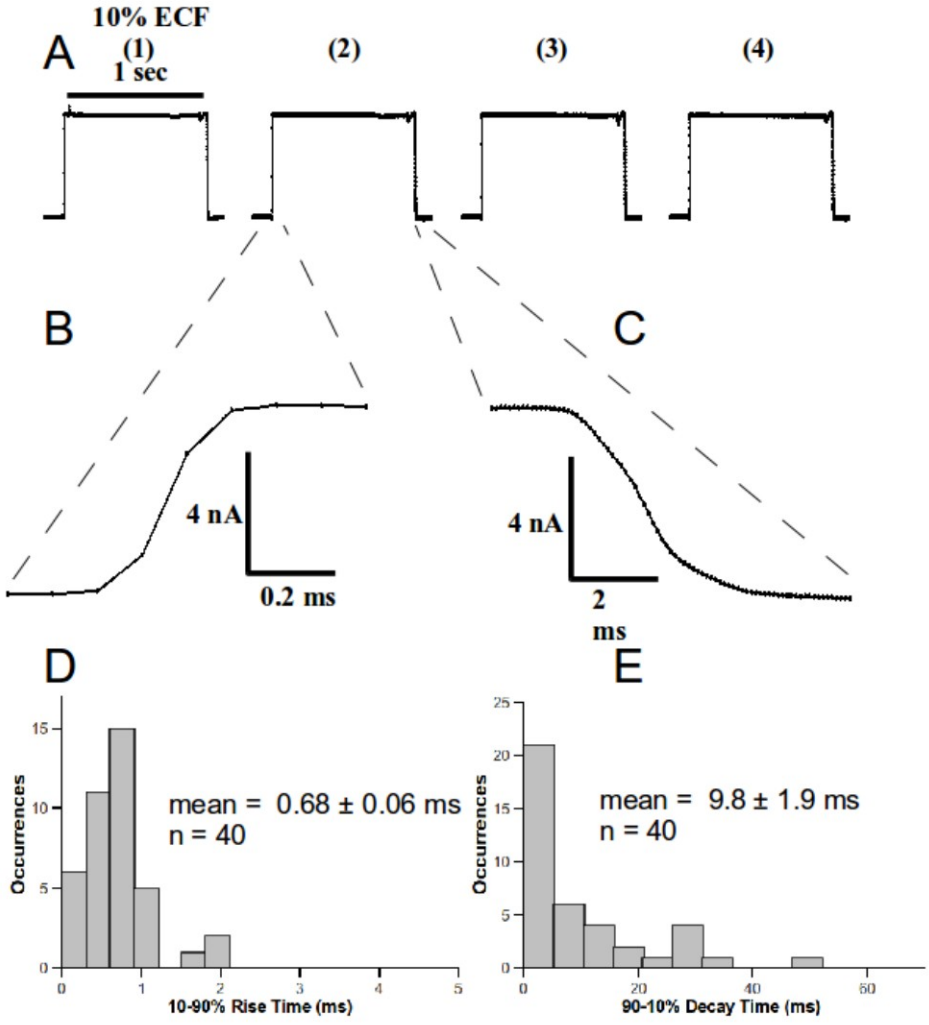

Figure 2.13 Testing speed of solution exchange using the valve driven drug applicator on open tip response.
To monitor the rate of solution exchange accurately, the open tip responses of the change in the liquid junction potential of 10% ECF applied from the agonist barrel of the theta tube were measured. The theta tube was positioned 300 μm from the recording pipette. The agonist delivery and leakage were visually inspected after introducing phenol red dye in the 10% ECF and subsequent drug mixtures. Solution exchanges as fast as 0.16 msec with an average of 0.68 ± 0.06 msec were achieved **(A, B, D).** The off time kinetics of

the drug applicator system was slower with a mean 90-10% decay time of 9.8 ± 1.9 msec. The fastest open tip decay time was measured at 0.12 msec.

2.3.2 Testing α4β2 nicotinic acetylcholine receptor activity in cultured HEK293T cells

The α4β2* nAChRs are the most prevalent nicotinic receptor subtype in the CNS (Whiting et al., 1987). These receptors are sensitive to agonist induced desensitization and therefore fast agonist application devoid of leakage between applications are critical requirements to induce robust nicotinic responses. Typical ACh (300 μM, 1 sec) elicited α4β2 nicotinic current responses in HEK293T cells transiently transfected with α4β2 mouse receptors are shown in **Fig. 2.14 A, B**. Dihydro-β-erythroidine (DHβE) is a well known competitive antagonist of α4β2* nAChRs (Nashmi et al., 2003). Stable repeated α4β2 nicotinic current responses elicited with 300 μM ACh (1 sec application every 30 sec) were completely inhibited with 1 μM DHβE, and recovered fully upon washing.

We obtained a mean α4β2 mediated nicotinic response of 310 ± 65 pA with a maximal response of 870 pA with 300 μM ACh **(Fig. 2.14 E)**. The 10-90% rise to peak time of the α4β2 nicotinic responses was 55 ± 13 msec **(Fig. 2.14 C)**. Desensitization occured relatively slowly with a desensitization time constant of 1093 ± 87 ms and **(Fig. 2.14 D).** Furthermore, the α4β2 mediated nicotinic current desensitized by 50 ± 4% of its original peak current value at the end of the 1 sec ACh application.

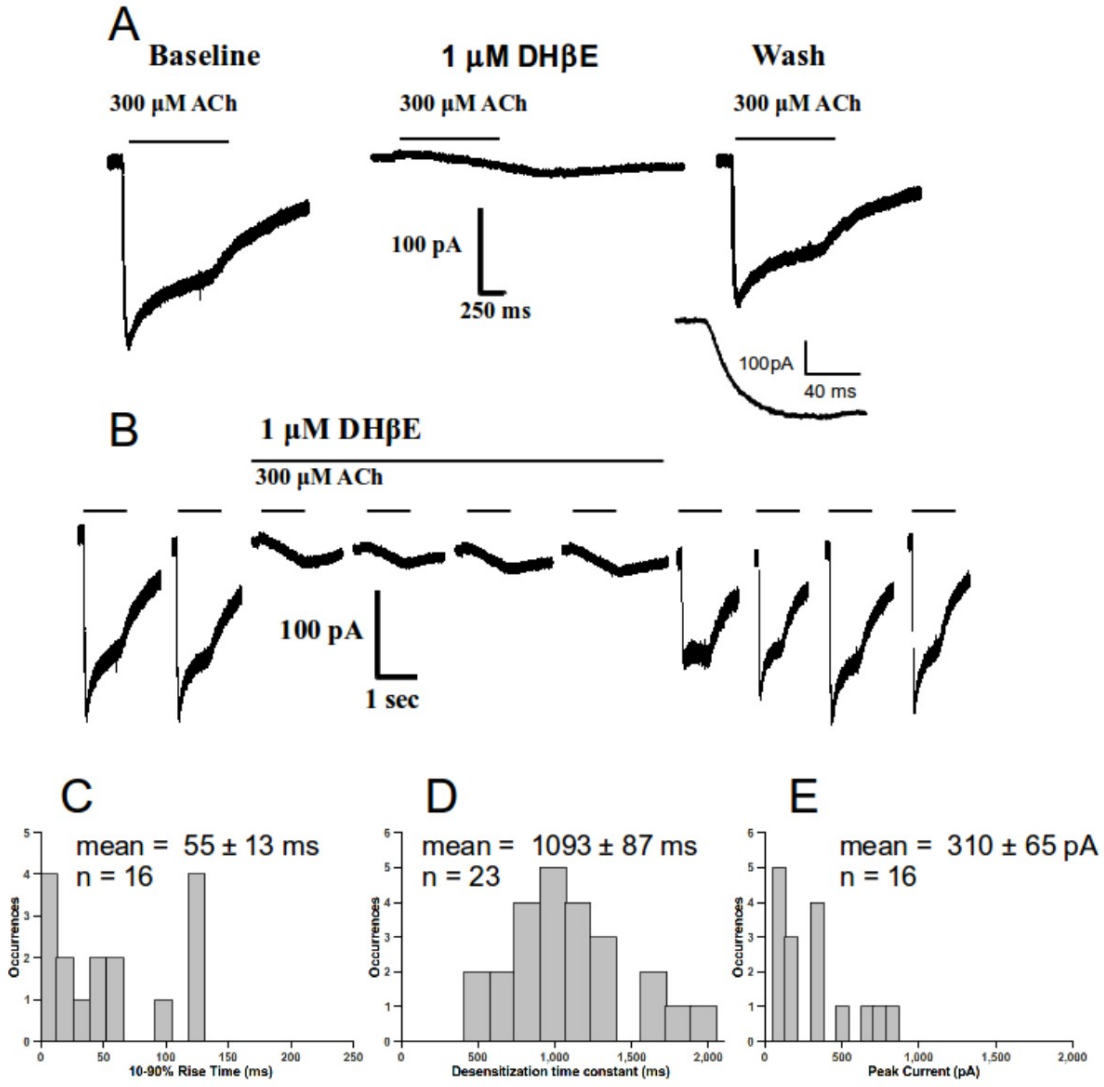

Figure 2.14 Testing α4β2 nicotinic receptor activity in HEK293T cells.
(A, B) α4β2 mediated nicotinic currents elicited by 1 sec application of 300 µM ACh every 30 sec. The competitive antagonist DHβE (1 µM) reversibly inhibited the nicotinic response. The first nicotinic response is shown at an expanded time scale. **(C, D)** The valve driven theta tube drug applicator elicited α4β2 mediated nicotinic responses with a mean 10-90% rise time of 55 ± 13 msec and a desensitization time constant of 1093 ± 87 msec. (E) The valve driven theta tube drug applicator was successful in activating robust nicotinic receptor responses (mean peak amplitude of 310 ± 65 pA). Repeated agonist applications resulted in stable nicotinic responses with no desensitization or rundown of the response.

2.3.3 Testing α7 nicotinic acetylcholine receptor activity in cultured HEK293T cells

α7 nAChRs are the second most prevalent receptors in the CNS (Millar and Gotti, 2009) and are also present in the PNS such as the cilliary ganglion (Triana-Baltzer et al., 2008). α7 nAChRs are characterized by fast activation kinetics and have the most rapid desensitization kinetics of all the nicotinic receptor subtypes. Rapid agonist application is an even more critical requirement to elicit α7 nAChR responses as compared to α4β2 receptors. Therefore we tested the performance of the drug applicator by examining ACh elicited α7 responses in HEK293T cells. We observed sharp fast rising α7 nicotinic currents that desensitized rapidly during application of 1 mM ACh (1 sec every 30 sec) **(Fig. 2.15 A).** Methyllycaconitine (MLA) at nM concentration is a specific competitive antagonist of α7 nicotinic receptors (Murray et al., 2009). We were consistently able to elicit stable α7 nicotinic responses with repeated ACh applications that were completely inhibited by 1 nM MLA and recovered upon washout of the inhibitor **(Fig. 2.15 A, B).** We routinely obtained robust α7 nicotinic responses (mean amplitude = 495 ± 32 pA; **Fig. 2.15 E)**. The α7 nicotinic responses have significantly faster activation kinetics than α4β2 receptors ($p = 0.028$, Wilcoxon rank sum test) as the mean 10-90% rise time of the α7 nicotinic currents was 19 ± 2 msec **(Fig. 2.15 C)**. Desensitization kinetics of α7 nicotinic receptor currents were significantly faster than α4β2 mediated nicotinic responses ($p < 0.001$, Wilcoxon rank sum test) with a mean desensitization time constant of 489 ± 19 ms **(Fig. 2.15 D)**. Moreover, the α7 mediated nicotinic responses showed greater levels of desensitization than α4β2 nicotinic responses as the α7 nicotinic currents desensitized by 78 ± 2% of its peak response at the end of 1 sec ACh application.

Concentration–response experiments performed on HEK293T cells transfected with α7 nicotinic receptor cDNA yielded robust α7 nicotinic responses that were stable with repetitive drug applications over a wide range of concentrations **(Fig. 2.16 A, B)**. The concentration-response relationship was fitted to a single Hill equation generating an EC50 of 168 ± 40 μM and a Hill coefficient (nH) of 0.77 ± 0.11. Because α7 nicotinic receptor desensitization is very rapid and therefore confounding accurate dose-response measurements based on current amplitudes, it has been suggested that area under the curve of nicotinic responses provide a more reliable measure (Papke and Porter, 2002; Papke and Thinschmidt, 1998) . The concentration-response relationship using area under the curve was fitted to a Hill equation with an EC50 of 5.6 ± 0.4 μM and a Hill coefficient of 1.7 ± 0.2.

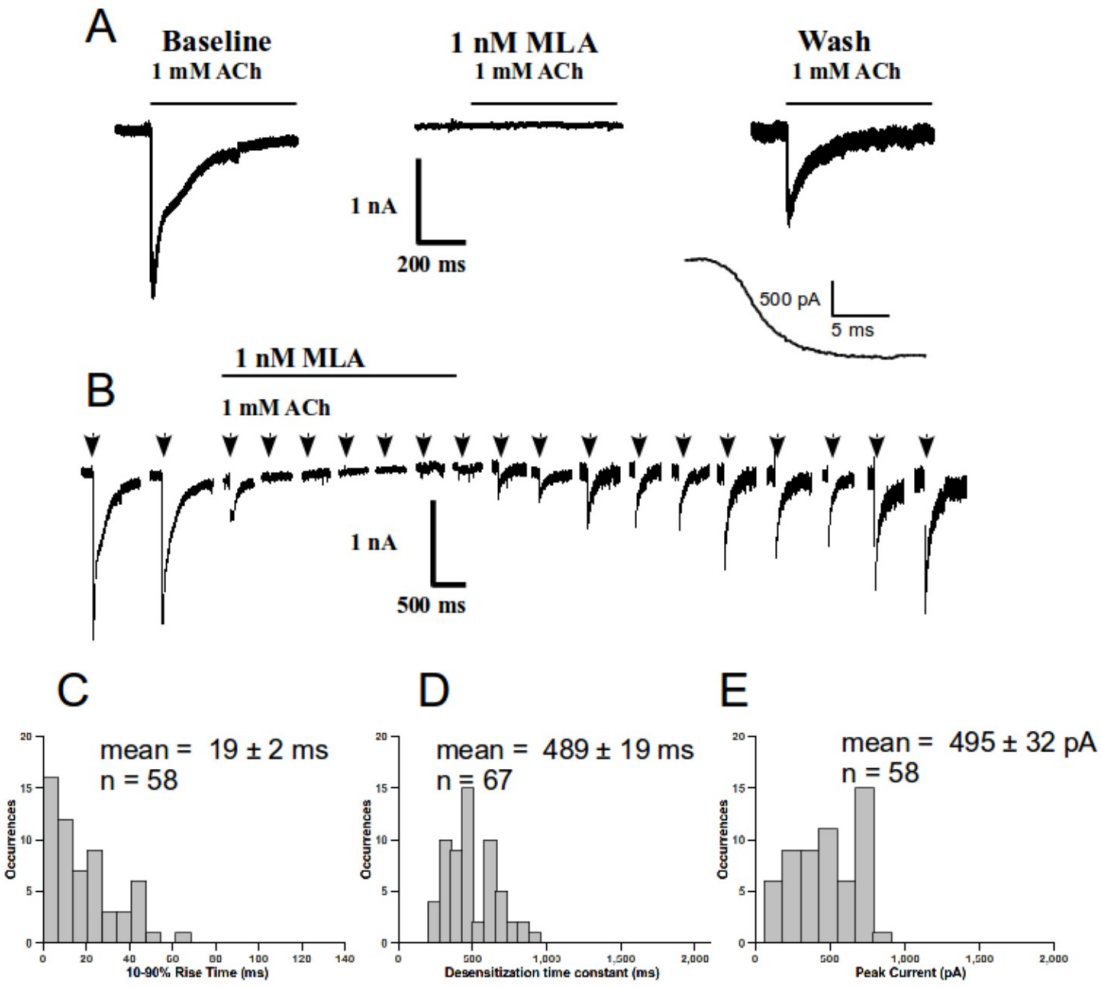

Figure 2.15 High efficiency of rapid drug applicator demonstrating α7 nicotinic receptor activity in HEK293T cells.

(A, B) The α7 mediated nicotinic currents elicited by a 1 sec application of 1 mM ACh every 30 sec. The competitive antagonist MLA (1 nM) reversibly inhibited the nicotinic response. The first α7 mediated nicotinic response is shown at an expanded time scale and has a 10-90% rise time of 5.8 ms. **(C, D)** The valve driven theta tube drug applicator elicited sharp rising and rapidly desensitizing α7 mediated nicotinic currents with a mean 10-90% rise time of 19 ± 2 msec and a mean desensitization time constant of 489 ± 19 msec. **(E)** Robust and stable α7 nicotinic responses (mean peak amplitude of 495 ± 32 pA) can be elicited with repeated ACh application using the valve driven drug applicator.

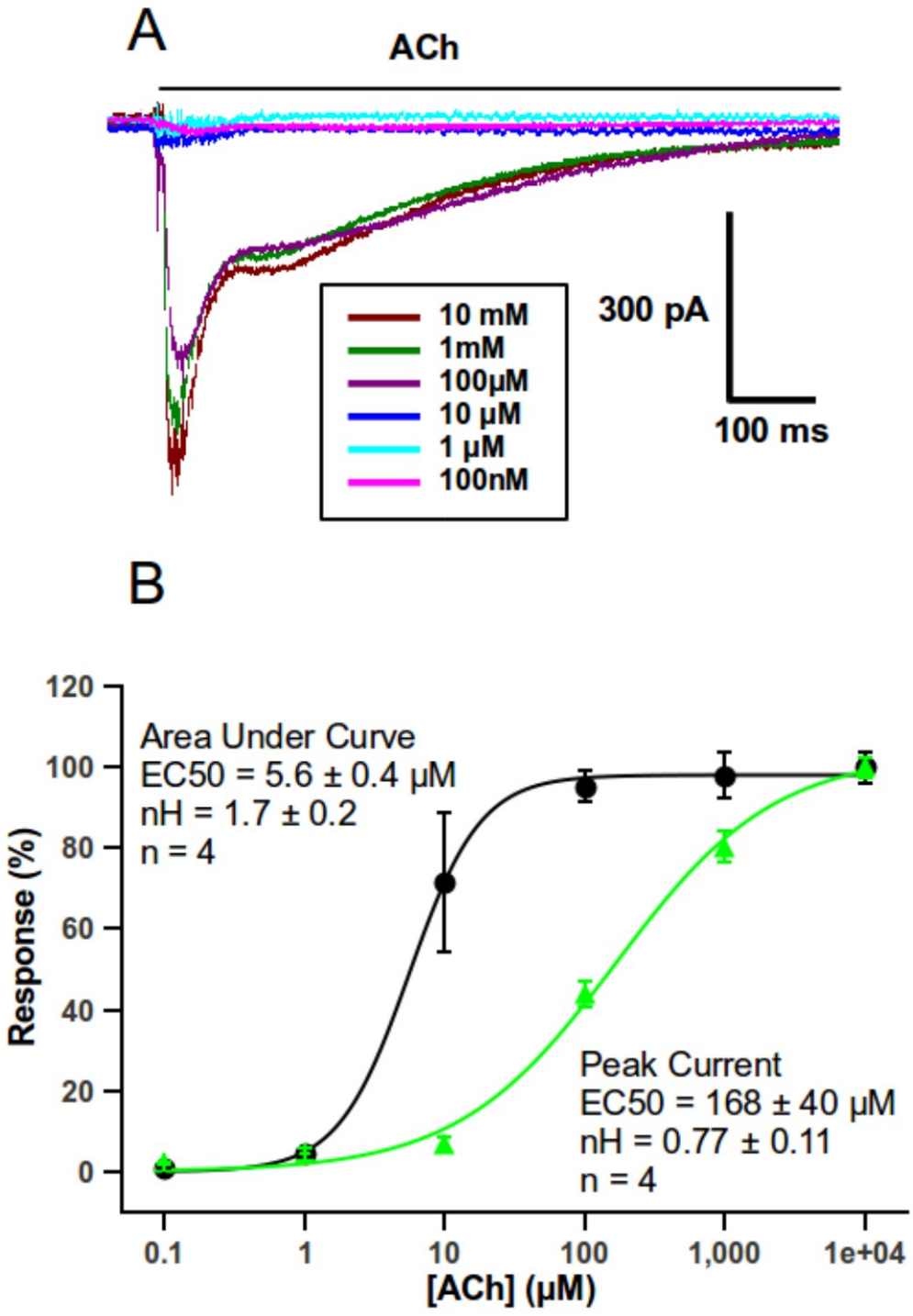

Figure 2.16 Dose-response relations of α7 nicotinic receptor responses.
(A) Dose-response relations of α7 mediated nicotinic receptor responses with varying concentrations of ACh applied for 1 sec every 30 sec. Maximal responses are elicited with 10 mM ACh. **(B)** Normalized dose-response relations of α7 nicotinic receptor currents determined for both peak amplitudes (green triangles) and area under the curve (black circles). The EC50 and Hill coefficient of α7 nicotinic receptor pea**k current**

amplitudes are 168 ± 40 μM and 0.77 ± 0.11, respectively, while those for area under the current curves are 5.6 ± 0.4 μM and 1.7 ± 0.2, respectively. Thus, repeated fast drug administration can be applied to obtain accurate dose-response relations on α7 nicotinic receptors, which are highly sensitive to agonist induced desensitization.

2.3.4 Testing ionotropic glutamate receptor activity in brain slices

We tested whether the valve driven theta tube drug applicator can also apply agonists rapidly in brain slices. In addition, we examined whether the drug applicator system's utility can be extended to study ligand-gated ion channels other than nicotinic receptors. We investigated ionotropic glutamate receptor activity since these receptors are the most prevalent of all excitatory ligand-gated ion channels in the CNS. Whole-cell patch-clamp recordings were performed in dentate granule neurons from hippocampal brain slices from 10-11 days old postnatal mice. We consistently elicited robust (mean amplitude = 213 ± 56 pA) fast rising (mean 10-90% rise time = 30 ± 2 ms, n = 6 neurons from 4 brain slices) non-NMDA ionotropic glutamate currents with 1 mM glutamate (1 sec) that was competitively and reversibly inhibited by the AMPA/kainate receptor antagonist, CNQX (10 μM) **(Fig. 2.17 A)** when the holding potential was at -60 mV.

We further characterized the rapid ionotropic glutamatergic currents by stepping the membrane potential from -80 to +20 mV at 20 mV increments and recording the resultant glutamatergic currents elicited with 1 mM glutamate (1 sec) **(Fig. 2.17 B)**. The current traces show rapidly activating and desensitizing currents that was maximally inward at -80 mV and progressively decreased in inward peak current amplitude with incrementally less hyperpolarized steps of membrane potential and reversed to an outward current at +20 mV. An I-V plot shows a reversal potential of -5.6 mV **(Fig. 2.17 C).**

This demonstrates that the valve-driven theta tube drug application system performs well in brain slice recordings since it was able to reliably elicit rapidly rising ionotropic glutamate receptor currents with no loss in function with repeated agonist application.

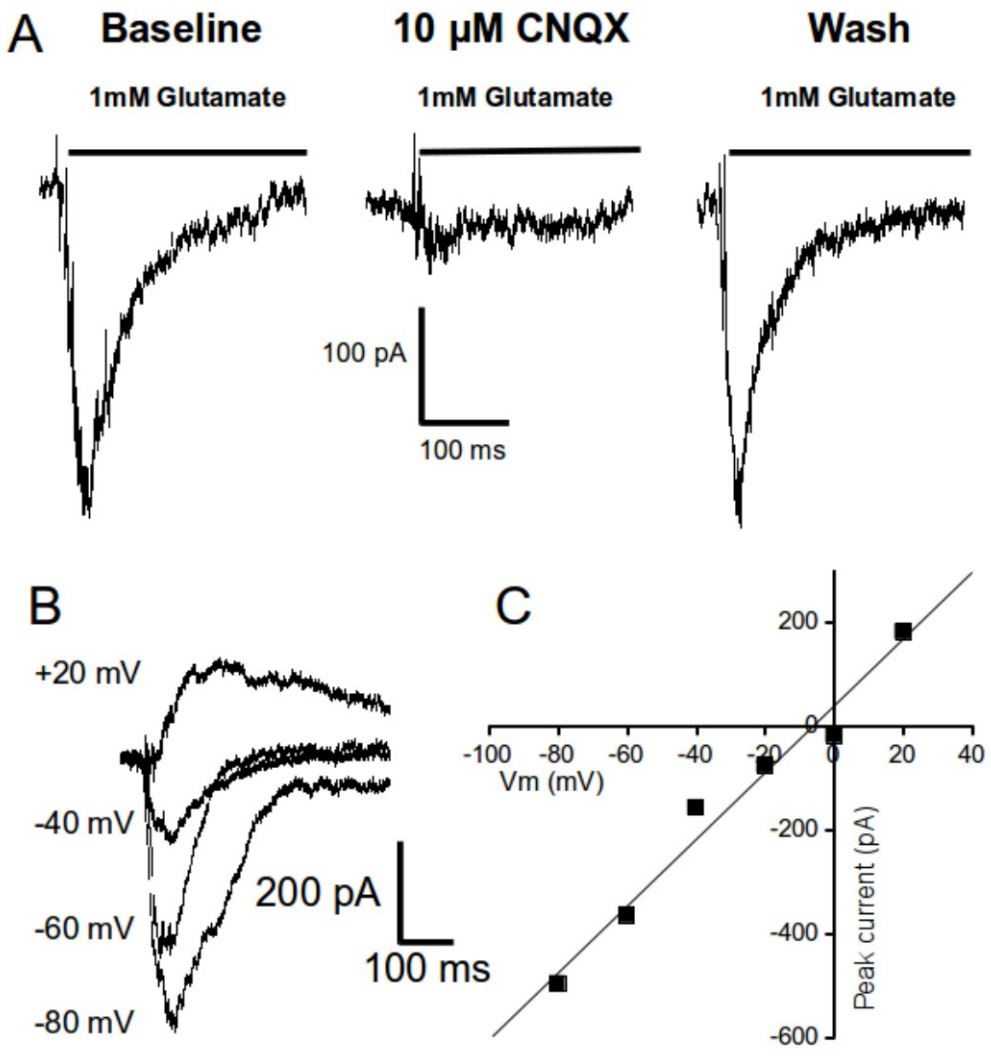

Figure 2.17 Eliciting glutamate receptor activity in hippocampal brain slices with the rapid agonist applicator system.
(A) Ionotropic glutamatergic currents elicited by a 1 sec application of 1 mM L-glutamate every min. The competitive AMPA/kainate receptor antagonist CNQX (10 µM) reversibly inhibited the glutamate mediated current. **(B)** Currents evoked by 1 sec application of L-glutamate at different membrane potentials of dentate granule neurons. **(C)** I-V relationship of peak amplitude of L-glutamate (1 mM) elicited whole-cell

currents recorded when potentials were stepped from -80 mV to +20 mV (20 mV intervals) showing a reversal potential at -5.6 mV.

2.4 Discussion

We have developed a valve driven theta tube agonist application system that satisfactorily delivers agonists rapidly enough to mimic the rates of neurotransmitter release at synapses. The drug applicator achieves all the necessary requirements to accurately characterize the fast current responses of ligand-gated ion channels. Very rapid mean open tip solution exchanges of 0.66 ± 0.07 ms were achieved with the theta tube drug applicator, with a maximal rate of 0.08 ms. Stable and robust α4β2 and α7 nicotinic currents could be elicited by repetitive ACh application. A full dose-response relation of α7 nicotinic currents could be obtained over repetitive ACh applications to the same cell. Furthermore, the agonist applicator could work reliably in brain slices, eliciting rapidly rising glutamate mediated AMPA currents in the hippocampus.

There are additional strong features of the theta tube valve driven drug applicator system. First the performance of the system in achieving sub-millisecond solution exchange approaches that of the liquid filament and piezoelectric driven theta tube systems (Nashmi et al., 2003; Buisson and Bertrand, 1998; Jonas, 1995; Franke et al., 1987) Second, the cost is low for construction of the system which involves the minimal cost of the three valves and a custom made 3-channel valve controller. Third, another strength in the system is the ease of operation. The drug application system does not require laminar flow of solution and does not produce oscillation artifact due to a moving theta tube since the valve driven theta tube is stationary and only one of the barrels of the theta tube delivers either drug or wash solution at any point in time. This perfusion

apparatus is a modification of the one used by Dilger and colleagues (Liu and Dilger, 1991). However, an advantage of the valve driven driven theta tube agonist applicator is that by attaching the theta tube to a course manipulator it is feasible to rapidly apply agonists to attached cultured cells in addition to patches and lifted cells. The Dilger drug applicator also achieves submillisecond solution exchanges but can only work with patches and lifted cells that must be moved by the recording pipette to the drug application tubing. Furthermore, the theta tube allowed the valve-driven drug application system to reliably elicit rapidly rising fast ligand-gated ion channel currents, such as AMPA glutamate receptor activity, in brain slices.

A limitation of our drug application system is the relatively large size of the theta tube tip (300-400 μm). This precludes very focal drug application that may be advantageous in examining the function of receptors in subcellular regions, for example receptor activity spatially distributed from distal dendrites to soma in neurons which can be achieved using a picospritzer system (Ji et al., 2001b) or uncaging of caged agonists (Poisik et al., 2008; Khiroug et al., 2003).

Although we have tested the drug applicator with two subtypes of neuronal nicotinic receptors with different activation and desensitization kinetics and AMPA glutamate receptors, we are confident that the utility of present drug applicator can be extended to the detailed study of other fast ligand-gated ion channels including but not limited to other ionotropic glutamate receptors, $GABA_A$ receptors, 5-HT3 receptors and P2X receptors.

Chapter 3 - T Cell Receptor Activation Decreases Excitability of Cortical Interneurons by Inhibiting α7 Nicotinic Receptors

Abstract

Many proteins in the immune system are also expressed in the brain. One such class of immune proteins are T cell receptors (TCRs), whose functions in T lymphocytes in adaptive immunity are well characterized. In the brain, TCRs are confined to neocortical neurons but their functional role has not been determined. In mouse layer 1 neocortical neurons, TCR activation inhibited α7 nicotinic currents. TCRs modulated α7 currents via tyrosine phosphorylation of α7 nicotinic receptors (nAChRs) through Src tyrosine kinases because eliminating Lck kinase expression, coexpressing Fyn kinase dead or mutating tyrosine to alanine in α7 blocked the effect of TCR activation. We found that TCR stimulation decreased surface α7 nAChRs and reduced single-channel conductance. These results reveal that TCRs play a major role in the modulation of cholinergic neurotransmission in the brain mediated by α7 nAChRs and that this has a profound effect on regulating neuronal excitability.

Publication Information

This chapter has previously been published as **Komal P,** Geoff Gudavicius, Christopher J. Nelson and Raad Nashmi. T cell receptor activation decreases excitability of cortical interneurons by inhibiting α7 nicotinic receptors. *J Neurosci* 34(1): 22-35 (2014) **(Featured article)**. P.K., C.J.N. and R.N. designed the research; P.K. and G.G. performed the experiments; P.K., G.G. and R.N. analyzed the data; P.K., G.G., C.J.N. and R.N. wrote the paper.

3.1 Introduction

The central nervous system has been regarded as an immune privileged organ, owing to the blood brain barrier and an immunosuppressive microenvironment (Sallusto et al., 2012). However, there is evidence that immune proteins such as major histocompatibility complex (MHC), cytokines, and T cell receptor (TCR) subunits, originally thought to have only immune function are also expressed in CNS neurons (Boulanger et al., 2001b) (Syken and Shatz, 2003a). TCRs are known for their role in adaptive immunity on T lymphocytes (Irvine et al., 2002) but this restrictive role in only immune system function has recently been challenged. TCR expression in the adult brain is restricted to the neocortex (Syken and Shatz, 2003a). The TCR is an octameric complex of subunits where the αβ subunits bind to the peptide/MHC complex (Huang and Wange, 2004). T cell antigen receptor β (TCRβ) along with MHC class I and CD3ζ are expressed in neurons, with the latter two proteins known to play a role in the induction of synaptic plasticity (Baudouin et al., 2008; Escande-Beillard et al., 2010). However, there is no reported evidence that TCRs can modify activity of any ligand-gated ion channel in the CNS. The earliest activated kinases following TCR stimulation are downstream Src family kinases (Weiss and Littman, 1994).

α7 nicotinic acetylcholine receptors (nAChRs) are members of the pentameric cys loop family of ligand-gated ion channels. These receptors constitute the high affinity α-bungarotoxin (α-BTX) binding sites in the CNS and are the second most prevalent nAChR subtype in the CNS after α4β2 (Chen and Patrick, 1997). α7 nAChRs play an important role in cognition such as attention and memory (Levin et al., 2006; Young et al., 2007) These receptors are expressed most abundantly in the hippocampus and

neocortex (Freedman et al., 1993; Christophe et al., 2002). The long intracellular loop between the third and fourth membrane spanning regions of each α7 subunit contains putative protein kinase phosphorylation sites including at least one tyrosine phosphorylation site (Charpantier et al., 2005). Tyrosine phosphorylation of α7 nicotinic receptors is known to modulate their activity (Charpantier et al., 2005; Cho et al., 2005).

Since α7 nAChRs and TCRs are both highly expressed in the cerebral cortex and TCRs can signal via tyrosine kinases, this opens the possibility that TCRs can have downstream effects on α7 nAChRs. We examined whether TCR activation can modulate α7 nAChRs in CNS neurons. We provide evidence that TCR activation inhibits α7 currents in cortical neurons. The negative modulatory effect of TCRs on α7 nAChR activity is mediated through activation of Fyn and Lck tyrosine kinases and the subsequent tyrosine phosphorylation of the cytoplasmic loop of α7. The TCR negative regulation of α7 receptors was due to a loss of surface α7 receptors and a decrease in α7 single-channel conductance. Furthermore, we found that TCR activation decreased the excitability of neurons. Taken together our results reveal a novel mechanism of modulation of neuronal excitability by altering ion channel function through phosphorylation mediated by activation of an immune receptor.

3.2 Materials and methods

3.2.1 cDNA constructs

Mouse α7 nAChR and human RIC-3 cDNA plasmids were kindly provided by Dr. Jerry Stitzel (University of Colorado Boulder) and Dr. Neil Millar (University of London), respectively. RIC-3 is a chaperone protein that is a requirement for the

functional expression of α7 nAChRs in many mammalian cell lines (Lansdell et al., 2005). Venus fluorescent protein was generously provided by Atsushi Miyawaki (Riken Brain Science Institute, Tokyo, Japan) (Nagai et al., 2002). We constructed a cDNA construct in which Venus fluorescent protein and hemagglutinin epitope tag were fused to α7 nAChR in the M3-M4 cytoplasmic loop (α7-Venus) and functions normally in every respect (Dau et al., 2013)

According to ProSite analysis, there is a single putative tyrosine kinase phosphorylation site in the M3-M4 cytoplasmic region of α7 at Y442. Using gene synthesis approach (Bioscience Ltd, Toronto) the wildtype tyrosine 442 codon (**TAC**) was mutated to the alanine codon (**GCT**) in both α7 (α7(Y442A)) and α7-Venus (α7(Y442A)Venus).

Expression vectors for constitutively active Fyn kinase (FKA) and Fyn kinase dead construct (FKD) were kindly provided by Dr. Todd Holmes (New York University, New York, NY) (Nitabach et al., 2002)

3.2.2 Cell culture and transfection

In this study we cultured Jurkat cells (clone E6-1, cat# TIB-152, ATCC). Jurkat cells are a clonal T lymphocyte cell line, which natively expresses T cell receptors. Other Jurkat cells used in the study include the Jurkat TCR β subunit knockout, in which there is loss of expression of the β subunit of the T cell receptor (clone J.RT3-T3.5, cat# TIB-153, ATCC) and the Jurkat Lck knockout cells, in which the cells are deficient in Lck tyrosine kinase activity (JCaM 1.6, cat# CRL-2063, ATCC). Jurkat cells were maintained in RPMI 1640 medium supplemented with 10% FBS, penicillin (100 U/ml), streptomycin (100 μg/ml), and 5% glutamine in a humidified CO_2 incubator at 37°C.

We transiently transfected Jurkat cells using electroporation. On the day of electroporation, inside 35 mm petri dishes we coated 5 mm diameter round glass coverslips (cat # 64-0700, Warner) with rat collagen type 1 (0.05 mg/ml, cat # 92590, Millipore) for 3 hours and washed twice with PBS (pH 7.4). In an electroporation cuvette (cat # 165-2088, Bio-Rad) 1 x 10^7 Jurkat cells were incubated with 6 μg of α7 nAChR cDNA, 6 μg of RIC-3 cDNA and 0.6 μg of soluble Venus fluorescent protein cDNA, in 300 μl of incomplete RPMI 1640 medium and subjected to electroporation with a Gene Pulser Xcell (Bio-Rad) at 250 V and 960 μF. RPMI-1640 incomplete medium was identical to RPMI-1640 complete medium except that fetal bovine serum was omitted. Electroporated cells were then plated into the 35 mm dishes each containing 2.5 ml complete RPMI media. Whole-cell patch-clamp recordings were performed two days post electroporation. For experiments involving confocal imaging of cells, the Jurkat cells were plated onto collagen type 1 coated coverslip bottom 35 mm dishes (cat # P35G-0-14-C, MatTek Corp).

HEK293T cells were also used in the study. They were grown in DMEM high glucose medium supplemented with 10% FBS, 2 mM L-glutamine, 100 U/ml penicillin, and 100 μg/ml streptomycin (DMEM complete medium) and maintained in a CO_2 incubator at 37 °C. Three to six days before electrophysiological recordings, the cells were incubated with trypsin for 3 min, mechanically dissociated, and seeded onto poly-DL-lysine (1 mg/ml, cat # P9011, Sigma) coated 5 mm glass coverslips (cat # 64-0700, Warner) placed inside 35 mm diameter petri dishes. Cells were transfected at 60-70% confluency using Fugene Transfection Reagent (cat # PRE2311, Promega). To each dish 2 μg of α7 nAChR cDNA, 2 μg of RIC-3 cDNA and 0.2 μg of soluble Venus fluorescent

protein cDNA were mixed with 3 µl of Fugene transfection reagent and 250 µl of incomplete DMEM medium, which was identical to the complete DMEM except lacking FBS. Transfection was performed according to the manufacturer's protocol. Electrophysiological recordings were performed 2–3 d post-transfection.

3.2.3 Whole-cell patch-clamp recordings from cultured cells

Cells were visualized with differential interference contrast illumination using an upright microscope (Nikon FN1) equipped with a CFI APO 40X W NIR objective (0.80 numerical aperture, 3.5 mm working distance). Transfected cells were identified with Venus fluorescent protein under fluorescence illumination with a mercury lamp. Standard whole-cell recordings were performed using a Multiclamp 700B amplifier (Molecular Devices) low pass filtered at 4 kHz and digitized at 10 kHz with a Digidata 1440A (Molecular Devices). Whole-cell patch-clamp recordings were performed using extracellular solution (ECS) containing (in mM): 150 NaCl, 4 KCl, 2 $CaCl_2$, 2 $MgCl_2$, 10 HEPES, and 10 D-glucose adjusted to pH 7.4. Micropipette recording electrodes were pulled from borosilicate glass of 1.5 mm O.D. and 1.0 mm I.D. (cat 1B150F-4, WPI) on a P-97 Flaming/Brown micropipette puller (Sutter Instrument). Patch electrodes (7-9 MΩ) were filled with pipette solution containing (in mM): 108 KH_2PO_4, 4.5 $MgCl_2$, 0.9 EGTA, 9 HEPES, 0.4 $CaCl_2$, 14 creatine phosphate (Tris salt), 4 Mg-ATP, 0.3 GTP (Tris salt), pH 7.4 with KOH. Atropine (100 nM) was present in the bath throughout all recordings to block muscarinic acetylcholine receptor responses. Series resistance was compensated 50%, and the membrane potential was held at -60 mV. Holding potentials were corrected for the liquid junction potential. ACh was delivered for 1 sec duration using the two-

barrel glass theta tube valve driven drug applicator, which was positioned ~300 μm from the recorded cell (Komal et al., 2011). Solution exchange rates measured from open tip junction potential changes during application with 10% ECS were typically <500 μsec (10–90% peak time). The timing of agonist delivery and recordings were controlled using pCLAMP 10.2 acquisition software (Molecular Devices).

3.2.4 Whole-cell patch-clamp recordings from brain slices

All experiments on mice were performed in accordance of the Canadian Council of Animal Care and approved by the Animal Care Committee of the University of Victoria. 10-15 day post-natal day wild type C57BL/6J mice, TCR β subunit knockout mice (strain: B6.129P2-Tcrb^{tm1Mom}/J, stock # 002118, The Jackson Laboratory) or α7 nAChR knockout mice (strain: B6.129S7-*Chrna7*^{tm1Bay}/J, stock # 003232, The Jackson Laboratory) of either sex were anesthetized with isofluorane and decapitated. Subsequently, the brain was rapidly removed, kept for a minute in slicing solution and sectioned coronally into 320 μm thick slices in oxygenated slicing solution with a vibratome (Leica 1000S). Slicing solution comprised of (in mM): 250 sucrose, 2.5 KCl, 1.2 NaH_2PO_4, 1.3 $MgCl_2$, 2.4 $CaCl_2$, 26 $NaHCO_3$ and 11 D-glucose. Slices were transferred and incubated in a 37°C water bath for one hr. ConA (75 μg/ml) incubation time of 30 min was used for all our experiments. Slices were continuously bubbled in 95% O_2 and 5% CO_2 during incubation and recording.

Using infra-red video assisted differential interference contrast illumination in combination with an upright microscope (Nikon FN1) equipped with a CFI APO 40X W NIR objective (0.80 numerical aperture, 3.5 mm working distance), whole-cell patch-

clamp recordings were performed on layer 1 medial prefrontal cortical neurons from C57BL/6J mice (wildtype, WT) and TCR β KO mice. Data were acquired using a Multiclamp 700B amplifier (Molecular Devices), low-pass filtered at 4 kHz and digitized at 10 kHz with a Digidata 1440A A/D converter. Brain slices were perfused continuously with extracellular solution comprised of (in mM): 125 NaCl, 2.5 KCl, 1.2 NaH_2PO_4, 1.3 $MgCl_2$, 2.4 $CaCl_2$, 26 $NaHCO_3$ and 11 D-glucose. Neurons were visualized with an upright microscope (Nikon FN1) equipped with a CFI APO 40X W NIR objective (0.80 numerical aperture, 3.5 mm working distance) using infra-red differential interference contrast and a video camera (IR-1000, Dage MTI). The patch electrodes had resistances between 9-11 MΩ when filled with pipette solution containing (in mM): 130 potassium gluconate, 5 EGTA, 0.5 $CaCl_2$, 2 $MgCl_2$, 10 HEPES, 3 Mg-ATP, 0.2 GTP and 5 phosphocreatine tris, pH adjusted to 7.4 with KOH, osmolarity adjusted to 300 mOsm with sucrose. Whole-cell voltage-clamp recordings were performed at room temperature with a MultiClamp 700B amplifier (Molecular Devices) and pCLAMP 10.2 software (Molecular Devices). Data were filtered at 4 kHz and sampled at 10 kHz with a Digidata 1440A data acquisition system (Molecular Devices). The membrane potential was corrected for liquid junction potential and series resistance was corrected 50%. Neurons were held at -60 mV. The theta tube of the valve driven drug applicator was positioned ~600 μm from the recorded cell and 100 μM PHA543613 hydrochloride (cat # 3092, Tocris), a specific agonist for α7 nicotinic receptor, was applied for 1 sec.

The firing frequency of layer 1 cortical neurons from brain slices of WT mice and TCR β KO mice for untreated and ConA treatment (75 μg/ml, 30 min) were measured in current-clamp mode of whole-cell configuration, with bridge balance correction.

Methylycaconitine (MLA, 10 nM) was used in control experiments to identify the contribution by α7 nicotinic receptors towards the firing rate of layer 1 neurons. Current-clamp steps ranging from 0 pA to 200 pA (500 ms duration) in 20 pA increments were used to induce action potentials in cortical neurons. Firing frequency was calculated by dividing the number of action potentials by the 500 ms duration of each depolarizing step current. All data acquisition and analysis was performed using pClamp 10.2 software. Cells were not used for analysis if resting membrane potential (V_m) was more depolarized than -40 mV, access resistance (R_a) > 35 MΩ or input resistance (R_{input}) < 100 MΩ.

3.2.5 Current fluctuation analysis to estimate single-channel conductance

Estimation of single-channel conductance of α7 nicotinic receptor was done by fluctuation analysis as previously described (Sigworth, 1980; Lambert et al., 1989; Gill et al., 1995; Brown et al., 1998). We used Clampfit 10.2 software (Molecular Devices) to conduct fluctuation analysis on the whole-cell current traces. Briefly, repeated whole-cell α7 currents evoked using 100 μM PHA543613 hydrochloride from brain slices of mice held at -60 mV were obtained. The variance of the current at each sample point of each trace was plotted against the mean current of the averaged traces at the same sample point in time. Then a linear fit was performed through the sampled points. The slope of the fit estimated the unitary current, i, of the nicotinic ion channel. The single-channel conductance was calculated using the equation $\gamma = i / (V_h - E_{rev})$ where, V_h is the holding potential (-60 mV) and E_{rev} is the reversal potential for α7 receptors, determined experimentally as (-0.7 mV).

3.2.6 Single-channel recordings

Single-channel recordings in the cell-attached patch-clamp configuration were performed at room temperature on wildtype Jurkat cells electroporated with mouse α7 nAChR receptor and RIC-3 cDNA. The bath and pipette solutions contained (in mM): 150 NaCl, 4 KCl, 2 $CaCl_2$, 2 $MgCl_2$, 10 HEPES, 10 D-glucose and 10^{-4} atropine adjusted to pH 7.4, with 100 μM ACh dissolved in the pipette solution. Micropipette recording electrodes were 1.5 mm O.D. and 1.0 mm I.D. borosilicate glass (cat 1B150F-4, WPI) that were pulled on a P-97 Flaming/Brown micropipette puller (Sutter Instrument). The pulled pipettes were coated with Sylgard #184 (Dow Corning) and fire polished. Recording micropipettes had resistances between 6-15 MΩ. A pipette holding potential (V_p) of +60 mV was used throughout the recordings. Because recordings were made in the cell-attached configuration this meant that the membrane potential underneath the patch of membrane was hyperpolarized by -60 mV in addition to the resting membrane potential. Single-channel currents were acquired using a Multiclamp 700B amplifier (Molecular Devices), low-pass filtered at 4 kHz, digitized at 50 kHz with a Digidata 1440A A/D converter (Molecular Devices) and collected with pClamp 10.2 software.

Clampfit 10.2 software (Molecular Device) was used to analyze single-channel recordings to determine single-channel amplitudes and gating kinetics. Single-channel recordings were notch-filtered at 60 Hz followed by 4 kHz Gaussian filter. The "Event Detection – Single-Channel Search" feature in Clampfit was used to detect the open and closed channel events and analyzed for single-channel amplitudes and closed and open durations. Single-channel current amplitudes were analyzed by plotting an amplitude histogram fitted with two Gaussian functions, one Gaussian corresponded to the closed

channel current level, and the other corresponded to the open channel current level. Single-channel conductance was calculated in two ways. One way was dividing the single-channel amplitude by the driving force $\gamma = i / (V_h - E_{rev})$ where, V_h was estimated to be -108 mV by taking an average of the resting membrane potentials recorded from whole-cell recordings from Jurkat cells (-48 mV) minus the pipette potential (+60 mV) ($V_h = V_m - V_p$). Single-channel conductance was also verified by calculating the slopes of current-voltage relationships of single-channel recordings stepped at various pipette potentials. To assess gating kinetics, open and closed duration histograms of single-channel events were graphed on a semi-log plot and fit with functions with multiple.

3.2.7 Immunoprecipitation and Western blot analysis

Jurkat cells (1 x 10^7 cells/ml) were electroporated with 6 μg of α7-Venus, 6 μg of mouse RIC-3 in 300 μl of incomplete RPMI media. α7-Venus contains both a Venus fluorescent protein and an upstream HA epitope tag inserted into the M3-M4 cytoplasmic loop of the α7 nAChR subunit. Electroporated cells were then plated onto 35 mm dishes each containing 2.5 ml complete RPMI media. On the second day of post-transfection, WT α7-Venus receptor containing Jurkat cells were treated with control solution (RPMI solution) or ConA for 30 min at 37°C. Prior to immunoprecipitation cells were washed with ice cold PBS (pH7.4) at 4°C and resuspended in 1 ml freshly prepared immunoprecipitation buffer (IP) containing 50 mM Tris-HCl pH 8, 150 mM NaCl, 0.5% NP40, 0.5% Triton X-100, 0.5% sodium deoxycholate, 0.1% SDS, 1 mM EDTA, 2 mM sodium orthovanadate, 1 μg/mL pepstatin, 1 μg/mL leupeptin, 1 μg/mL aprotinin). The cells were lysed on ice for 10 min and clarified by centrifugation at 18,000 x g for 5 min. α7 receptors were immunoprecipitated using 2 μL of anti-HA antibody (clone 12ca5, gift

from Ivan Sadowski, University of British Columbia) and incubated with lysate for 1 hr prior to addition of 20 µl of BSA blocked protein A/G agarose beads (200 µg BSA in 1 ml IP buffer with beads) (cat# 20422, Pierce) for an additional hour with rotation. Beads were washed 3 times in 1 ml IP buffer and immune complexes were released by briefly boiling in 25 µl SDS loading buffer. Proteins were resolved by SDS-PAGE and transferred to nitrocellulose membrane. Western blotting was performed using anti-HA antibody (clone 12ca5) at 1:5000 dilution to detect total cellular α7 nicotinic receptors. Tyrosine phosphorylation of α7 receptors was detected with anti-phosphotyrosine antibodies (1:2000 dilution, Clone 4G10, Millipore). Horseradish peroxidase conjugated anti-mouse secondary antibody (cat# NXA931, GE) was used at 1:5000. Proteins were detected by chemiluminescence (Amersham Biosciences).

3.2.8 Surface α-bungarotoxin labeling and spectral confocal microscopy

Jurkat cells were transfected with 6 µg of mouse α7-Venus or α7(Y442A)-Venus nAChR cDNA and 6 µg of mouse RIC-3. For cell surface receptor expression assays, 48 hr post-transfection cells were incubated on ice for 1 hr to ensure that the temperature was below 4°C. ConA was incubated (75 µg/ml) for 30 min at 37ºC. Cells were then fixed with 4% paraformaldehyde in PBS for 10 min on ice and washed twice with ice cold PBS. Surface α7 receptors were then labeled with Alexa Fluor 647 α-bungarotoxin (1:200, Fl-BTx, cat# B35450, Invitrogen) under nonpermeabilized conditions for 30 min and washed twice with ice cold PBS. Then the cells were plated on rat tail collagen type I coated dishes prior to imaging (0.05 mg/ml, cat # 92590, Millipore). Surface expression of Fl-BTx labeled WT α7-Venus receptors vs mutant α7(Y442A)-Venus receptors was examined with a Nikon C1si spectral confocal microscope system using a Plan Apo VC

60X 1.4 NA oil immersion objective (0.13 mm working distance). A lambda stack of X-Y images were collected simultaneously with one laser sweep onto an array of 32 photomultiplier tubes. Jurkat cells containing α7-Venus were imaged from 496.5 – 696.5 nm at 5 nm wavelength separation. Images were acquired at 512 pixels x 512 pixels, at 25 μm x 25 μm field of view and 12 bit intensity resolution. The pixel dwell time was set at 5.52 μsec and the pinhole was set to medium (60 μm diameter). Fl-BTx was excited with a 638 nm laser line at 15 % maximum intensity, and emission was measured at the emission peak channel (665 nm). Images were analyzed for mean signal intensity using ImageJ v1.43r software. Using JACoP (just another colocalization plugin) in Image J, we also calculated the Mander's coefficients, M1 and M2, which quantify the degree of overlap between α7-Venus and FI-Bgt (Manders et al., 1993). M1 measures the percentage of pixels in the red channel that overlaps with the signal in the green channel, while M2 measures the percentage of pixels in the green channel that overlaps with signal in the red channel. M1 and M2 coefficient were calculated for both control and ConA treated Jurkat cells.

3.2.9 Statistical analysis

Values are reported as mean ± standard error. Significant difference ($p < 0.05$) between two groups of data were determined using a *t*-test for continuous data meeting parametric assumptions of equal variances and normality. Otherwise, a Wilcoxon rank sum test was performed for nonparametric data. Comparison between three or more groups were analyzed using an analysis of variance (ANOVA) for parametric data followed by *post hoc* multiple pairwise analysis using a Tukey's HSD tests. For nonparametric data involving comparison of three or more groups of data a Kruskal-Wallis rank sum test was

performed followed by pairwise analyses using Wilcoxon rank sum tests. All statistical analyses were performed using the R statistical computing language (www.R-project.org).

3.3 Results

3.3.1 TCR activation decreases α7 nAChR responses in Jurkat cells

Since the TCR complex is involved in downstream transmembrane signaling through Src family tyrosine kinases, and α7 nicotinic receptors are negatively regulated by tyrosine kinases, we examined whether TCR activation could modulate the function of α7 receptors.

To test our hypothesis we used Jurkat cells, which are a human clonal T lymphocyte cell line that natively expresses TCRs. We activated endogenously expressed TCRs with 75 μg/ml concanavilin A (ConA), a lectin and exogenous agonist of TCRs (Palacios, 1982). We found that Jurkat cells transiently transfected with α7 nicotinic receptors and incubated for 30 min with ConA resulted in a decrease in nicotinic current responses elicited by rapid application of ACh (1 mM for 1 sec) as compared to Jurkat cells incubated with control solution **(Fig. 3.18 A)**. There was a significant decrease in the mean α7 peak current response in ConA treated Jurkat cells (185 ± 34 pA, n = 14) as compared to control (720 ± 113 pA, n = 14) ($p < 0.0001$, Wilcoxon rank sum test) **(Fig. 3.18 B)**.

To verify the role of TCR mediated decrease in α7 nicotinic responses we used a TCR β subunit knockout Jurkat cell line. In this cell line, the absence of the β subunit renders the TCR receptor complex nonfunctional (Ohashi et al., 1985) . Accordingly, the

exogenous ligand ConA should not be able to activate the incomplete TCR complex. Indeed we found no significant difference in the ACh mediated α7 nicotinic currents between control (590 ± 147 pA, n = 12) and ConA (470 ± 128 pA, n = 12) treated TCR β subunit knockout Jurkat cells (p = 0.4, Wilcoxon rank sum test) **(Fig. 3.18 D)**.

To further rule out the possibility that the effect of ConA was due to a direct interaction with α7 nicotinic receptors, we used HEK293T cells, which are devoid of TCRs (Shaw et al., 2002). Similarly, we found no significant difference in α7 nicotinic currents in HEK293T cells treated with ConA (606 ± 114 pA, n = 6) as compared to control treatment (407 ± 77 pA, n = 6) (p = 0.1, *t*-test) **(Fig. 3.18 F).** Together, these results demonstrate that the decrease in α7 nicotinic current responses in Jurkat cells is a TCR activation dependent event.

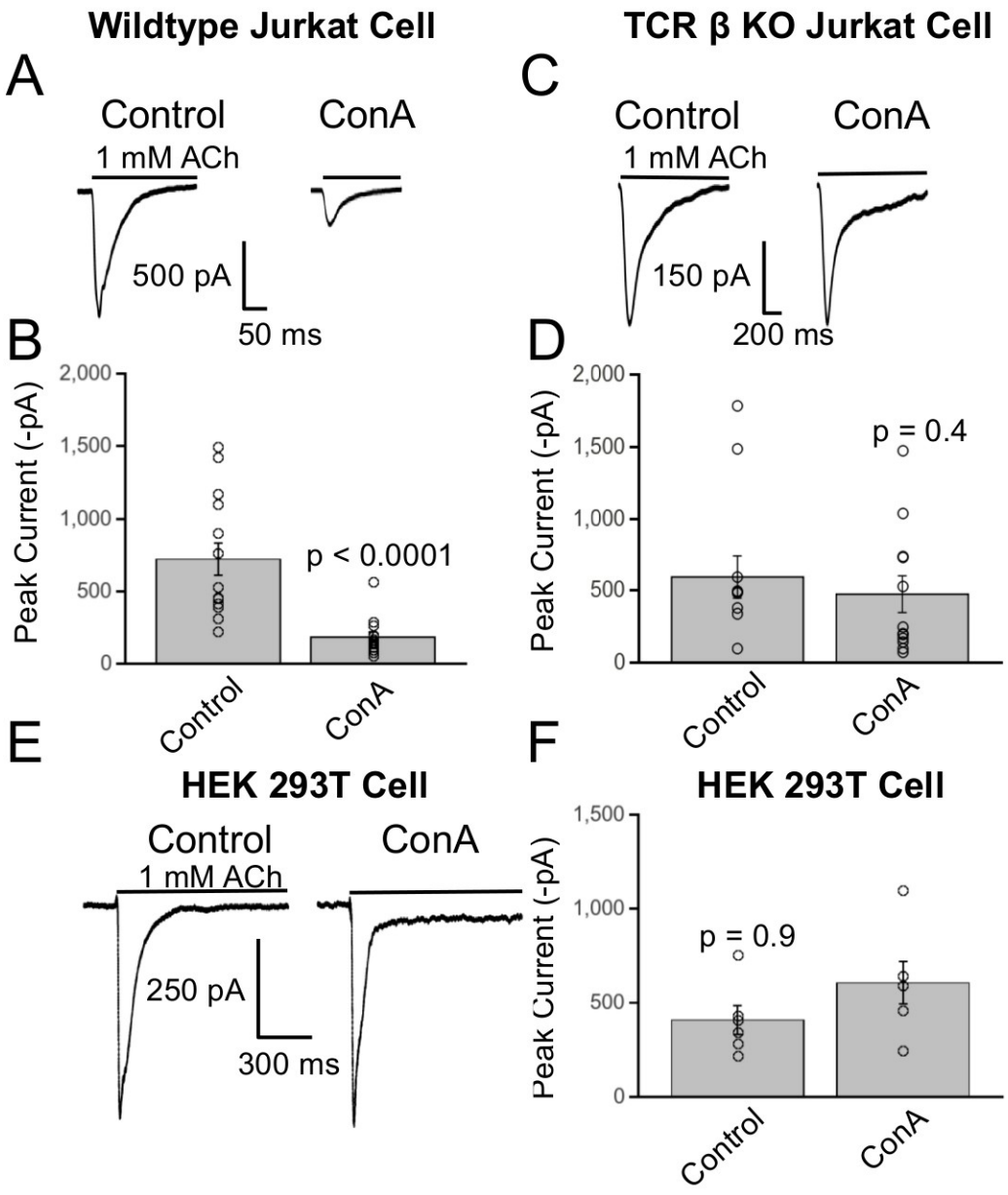

Figure 3.18 TCR activation decreases α7 nAChR responses in Jurkat cells.
Whole-cell recordings showing representative traces of ACh (1mM, 1 sec) induced α7 receptor currents in WT Jurkat cells **(A)** and TCR β KO Jurkat cells **(C)**. ConA incubation (75 μg/ml, 30 min) significantly decreased α7 nAChR currents in WT Jurkat cells (n = 14) as compared to control treatment (n = 14) ($p < 0.0001$, Wilcoxon rank sum test) **(A, B)** while ConA (n = 12) had no effect in TCR β KO Jurkat cells as compared to control treatment (n = 12) ($p = 0.4$, Wilcoxon rank sum test) **(C, D)**. **(E, F)** Whole-cell recordings done in HEK293T cells transfected with α7 nicotinic receptor shows that ConA incubation (75 μg/ml for 30 min) (n = 6) has no affect on ACh mediated current responses as compared to control treatment (n = 6) ($p = 0.1$, t-test). Each circle superimposed on bar chart represent the average α7 nicotinic receptor response from each

individual cell and bars represent mean ± SE of responses averaged across all measured cells.

3.3.2 TCR activation decreases α7 nicotinic currents in layer 1 prefrontal cortical neurons

We next asked if the phenomenon of TCR regulation of α7 receptors we observed in Jurkat cells could be found in CNS neurons. TCR β subunits are localized throughout all layers of the neocortex (Syken and Shatz, 2003) and α7 nicotinic receptors are present in layer 1 neocortical interneurons (Christophe et al., 2002) in addition to neurons in other cortical layers (Poorthuis et al., 2012). Thus, there is a high probability that TCRs and α7 nicotinic receptors are localized on the same neurons. We restricted our experiments to layer 1 of the medial frontal and prefrontal cortex, which is a simplified cortical layer essentially consisting almost entirely of GABAergic interneurons (Winer and Larue, 1989) and therefore is less heterogeneous than other layers, that contain pyramidal neurons and many subtypes of interneurons. To examine the functional interaction between TCRs and α7 receptors we performed whole-cell patch-clamp electrophysiology on layer 1 cortical neurons of the medial prefrontal cortex

In wildtype mouse brain slices incubated in ConA, using the α7 selective agonist PHA543613 (100 μM for 1 sec) we found that TCR activation significantly reduced α7 mediated currents (36 ± 6 pA, n = 10) as compared to control treated brain slices (80 ± 14 pA, n = 12) ($p = 0.003$, Wilcoxon rank sum test) **(Fig. 3.19 A)**. In order to isolate nicotinic responses recordings were voltage-clamped at -60 mV and performed in the presence of TTX, CNQX and atropine to inhibit action potential firing, glutamateric and muscarinic neurotransmission, respectively.

To confirm that the ConA mediated reduction in peak α7 nicotinic currents in brain slices was a TCR mediated event, we repeated the recordings in brain slices from TCR β subunit knock-out mice (TCR β KO). We found no significant difference in α7 nAChR peak current responses recorded from layer 1 prefrontal cortical interneurons between ConA (156 ± 50 pA, n = 10) and control treatments (136 ± 41 pA, n = 10) (p = 0.7, Wilcoxon rank sum test) **(Fig. 3.19 B)**. These findings are consistent with our results in wildtype and TCR β subunit knock-out Jurkat cells **(Fig. 3.18)**. Interestingly, we also found a significant elevation in the baseline α7 nicotinic responses from layer 1 cortical neurons in brain slices from TCR β KO mice (136 ± 41 pA, n = 12) as compared to wildtype mice (80 ± 14 pA, n = 12) (p = 0.0004, Kruskal-Wallis rank sum test) (p = 0.02, Wilcoxon rank sum test *post hoc* analysis) **(Fig. 3.19 C)**. This result confirmed that TCRs even in the absence of the exogenous compound ConA had a basal activity that was sufficient to reduce α7 nicotinic currents in wildtype mice.

These data show that TCRs, which have traditionally been known to play an important role in adaptive immunity, also have a neuronal function in the CNS, which involves the negative regulation of function of α7 nicotinic receptors.

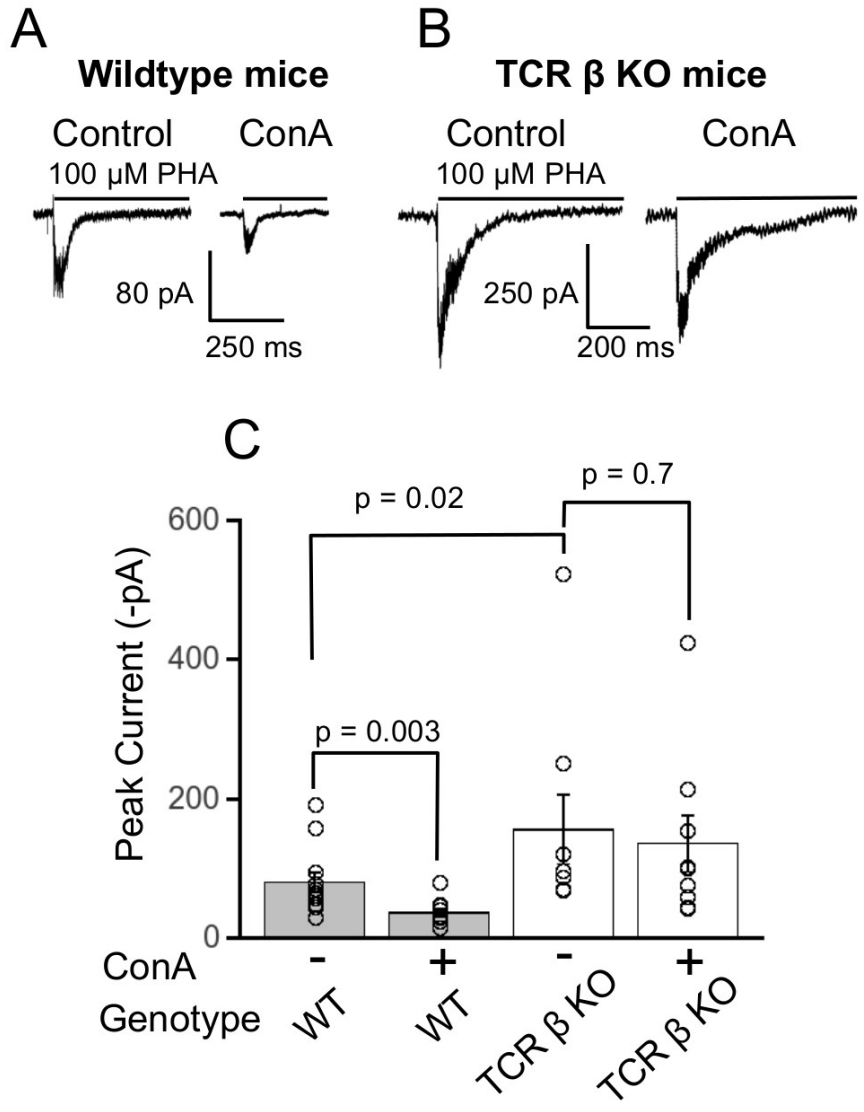

Figure 3.19 Activating TCRs decreases α7 nicotinic currents in layer 1 prefrontal cortical interneurons.

(A, C) Whole-cell recorded α7 nicotinic current traces elicited by the α7 specific agonist PHA543613 (PHA, 100 μM for 1 sec) showed a significantly diminished α7 nicotinic current in brain slices from WT C57BL/6J mice treated with ConA (75 μg/ml for 30 min) (n = 10) as compared to control treatment (n = 12) (p = 0.003, Wilcoxon rank sum test). Recordings were performed in the presence of TTX (200 nM) and CNQX (10 μM) to isolate nicotinic currents. **(B, C)** No difference was observed in the amplitude of α7 nicotinic currents in brain slices of TCR β knockout mice treated with ConA (n = 10) as compared to control treatment (n = 10) (p = 0.7, Wilcoxon rank sum test). **(C)** There was a significant increase in the mean baseline α7 nicotinic current amplitudes from neurons of TCR β subunit null mice as compared to α7 nicotinic currents from neurons of WT mice (p = 0.02, Wilcoxon rank sum test).

3.3.3 TCR activation inhibits α7 nicotinic currents via Src family tyrosine kinases

The earliest signaling events downstream of TCR stimulation are the activation of protein tyrosine kinases (PTKs) and the subsequent tyrosine phosphorylation of multiple intracellular proteins (Zhang et al., 1998). One of the earliest activated kinases upon TCR activation are the Src family tyrosine kinases (Parsons and Parsons, 2004a). Previous work done by Charpantier et al (Charpantier et al., 2005)and Cho et al (2005) have shown that α7 nicotinic receptors are prone to modulation by tyrosine kinases. Therefore, we asked whether two Src family kinases involved in TCR signaling, Fyn and Lck, play a role in the modulation of α7 nicotinic responses following TCR activation.

To investigate if TCR regulation of α7 nicotinic receptors involves tyrosine kinase action we compared α7 peak current responses to ConA in the presence and absence of the broad spectrum tyrosine kinase inhibitor genistein. Jurkat cells were transfected with α7 nAChRs and whole-cell electrophysiology was performed to compare the peak current responses between four different treatment groups: (1) control treatment, (2) ConA treatment (75 μg/ml, 30 min), (3) genistein preincubation (10 μM, 20 min) followed by ConA (75 μg/ml, 30 min) and (4) genistein treated cells (10 μM, 20 min) **(Fig. 3.20 A)**. When we inhibited tyrosine kinases with genistein alone α7 nicotinic currents increased significantly (2128 ± 335 pA, n = 14) as compared to control (882 ± 149 pA, n = 20) (p = 0.0005, Wilcoxon rank sum test *post hoc* analysis) **(Fig. 3.20 B)**. Genistein when preincubated for 20 min prior to ConA stimulation significantly decreased the ACh mediated responses (902 ± 175 pA, n = 15) relative to genistein alone (2128 ± 335 pA, n = 14) (p = 0.0009, Wilcoxon rank sum test). However, with genistein plus ConA stimulation α7 nicotinic responses (902 ± 175 pA, n = 15) were not significantly different

from α7 responses for control treatment (882 ± 149 pA, n = 20) (p = 0.8, Wilcoxon rank sum test *post hoc* analysis). ConA alone (398 ± 62 pA, n = 14) had significantly attenuated α7 responses (p < 0.0001, Kruskal-Wallis rank sum test) (p = 0.02, Wilcoxon rank sum test *post hoc* analysis) relative to control treatment (882 ± 149 pA, n = 20). These results are consistent with previously published work showing genistein mediated potentiation of α7 nicotinic receptor currents (Charpantier et al., 2005; Cho et al., 2005).

Since the Lck and Fyn kinases are the primary kinases activated upon TCR stimulation (Parsons and Parsons, 2004) we next asked if these tyrosine kinases regulate the activity of α7 nicotinic receptors. To examine the role of Fyn kinase signaling in TCR modulation of α7 receptors we cotransfected Jurkat cells with α7 nAChRs and either the gain of function (FKA) or the loss of function (FKD) Fyn kinase expression vector. Whole-cell recordings were then performed to monitor ACh-induced α7 nicotinic currents **(Fig. 3.20 C)**. We observed that α7 peak currents increased robustly and significantly in Jurkat cells cotransfected with FKD (2286 ± 241 pA, n = 34) as compared to that of control (970 ± 163 pA, n = 39) (p < 0.0001, Kruskal-Wallis rank sum test) (p < 0.0001, Wilcoxon rank sum test *post hoc* analysis) while ConA treatment alone reduced α7 current responses (501 ± 87 pA, n = 22) relative to control (p = 0.02, Wilcoxon rank sum test *post hoc* analysis) (Fig. 3D). However, in cells cotransfected with FKD, ConA stimulation in cells expressing FKD (2706 ± 631 pA, n = 7) did not lead to a significant change in the peak α7 current amplitude as compared to control treated FKD cotransfected cells (2286 ± 241 pA, n = 34) (p = 0.4, Wilcoxon rank sum test *post hoc* analysis). The abolition in TCR mediated α7 current inhibition, implicates the active role of Fyn kinase in negatively modulating α7 nicotinic responses following TCR activation

(Fig. 3.20 C, D). When we cotransfected Jurkat cells with FKA and control treatment, it led to a significant decrease in the ACh mediated α7 nicotinic responses (235 ± 39 pA, n = 16) as compared to control treatment alone ($p < 0.0001$, Wilcoxon rank sum test *post hoc* analysis) **(Fig. 3.20 C, D)**. The reciprocal effect of FKA and FKD suggest that Fyn kinase modulates α7 nicotinic receptor regulation and that Fyn kinase is one key downstream effector following TCR activation.

Because Lck kinase also plays a critical role in mediating phosphorylation of ITAM residues and downstream TCR mediated signaling (Weiss et al., 1992), we tested the possibility for the involvement of Lck kinase in TCR mediated α7 nicotinic receptor regulation. We used Jurkat cells devoid of Lck kinase (Lck KO). There were four experimental groups of cells transfected with α7 nAChRs: (1) wildtype Jurkat cells control treatment, (2) wildtype Jurkat cells ConA treated, (3) Lck KO Jurkat cells control treatment and (4) Lck KO Jurkat cells ConA treated. Whole-cell recorded ACh evoked α7 nicotinic receptor responses showed significant reduction in wildtype Jurkat cells upon ConA stimulation (261 ± 76 pA, n = 13) as compared to control (1036 ± 308 pA, n = 10) ($p < 0.001$, Kruskal-Wallis rank sum test) ($p = 0.002$, Wilcoxon rank sum test *post hoc* analysis), consistent with previous data **(Figs. 3.18, 3.19)**. However, we observed no significant difference in α7 nicotinic currents between Lck KO controls (1628 ± 420 pA, n = 13) and ConA treated Lck KO cells (842 ± 179 pA, n = 12) ($p = 0.2$, Wilcoxon rank sum test *post hoc* analysis) **(Fig. 3.20 F)**. Furthermore, neither Lck KO control treated cells (1628 ± 420 pA, n = 13) ($p = 0.4$, Wilcoxon rank sum test *post hoc* analysis) nor Lck KO ConA treated cells (842 ± 179 pA, n = 12) differed significantly ($p = 0.8$,

Wilcoxon rank sum test *post hoc* analysis) in α7 nicotinic currents as compared to control treated wildtype Jurkat cells (1036 ± 308 pA, n = 10).

Together, these data strongly suggest that both Lck and Fyn kinases are required for TCR-mediated negative regulation of α7 nicotinic receptor function. Furthermore, these data suggest that Fyn and Lck are lined up in series and are not in parallel in the same TCR signaling pathway, either TCR-Lck-Fyn-α7 or TCR-Fyn-Lck-α7. Therefore, Fyn and Lck are each not redundant in function. However, there is one potentially confounding result in **Fig. 3.20 B**. How can ConA still have an effect on inhibiting α7 nicotinic currents by activating Fyn and Lck when genistein preincubation, a general tyrosine kinase inhibitor, should inhibit these enzymes; i.e. should it not be the case that ConA with genistein incubation show the same level of potentiated α7 nicotinic currents as with genistein alone? The reason could be explained by the fact that genistein reversibly binds to src family of tyrosine kinases (Cho et al., 2005). Furthermore, unlike genistein which must diffuse to its target and can also diffuse away, TCRs are structurally closely associated with Fyn and Lck kinases. Fyn coimmunoprecipitates with the TCR complex (Samelson et al., 1990), while Lck physically interacts with the TCR co-receptor CD4. This may explain why TCR activation with ConA still attenuated α7 responses even with preincubation with genistein because the TCR has tighter association to Fyn and Lck than genistein.

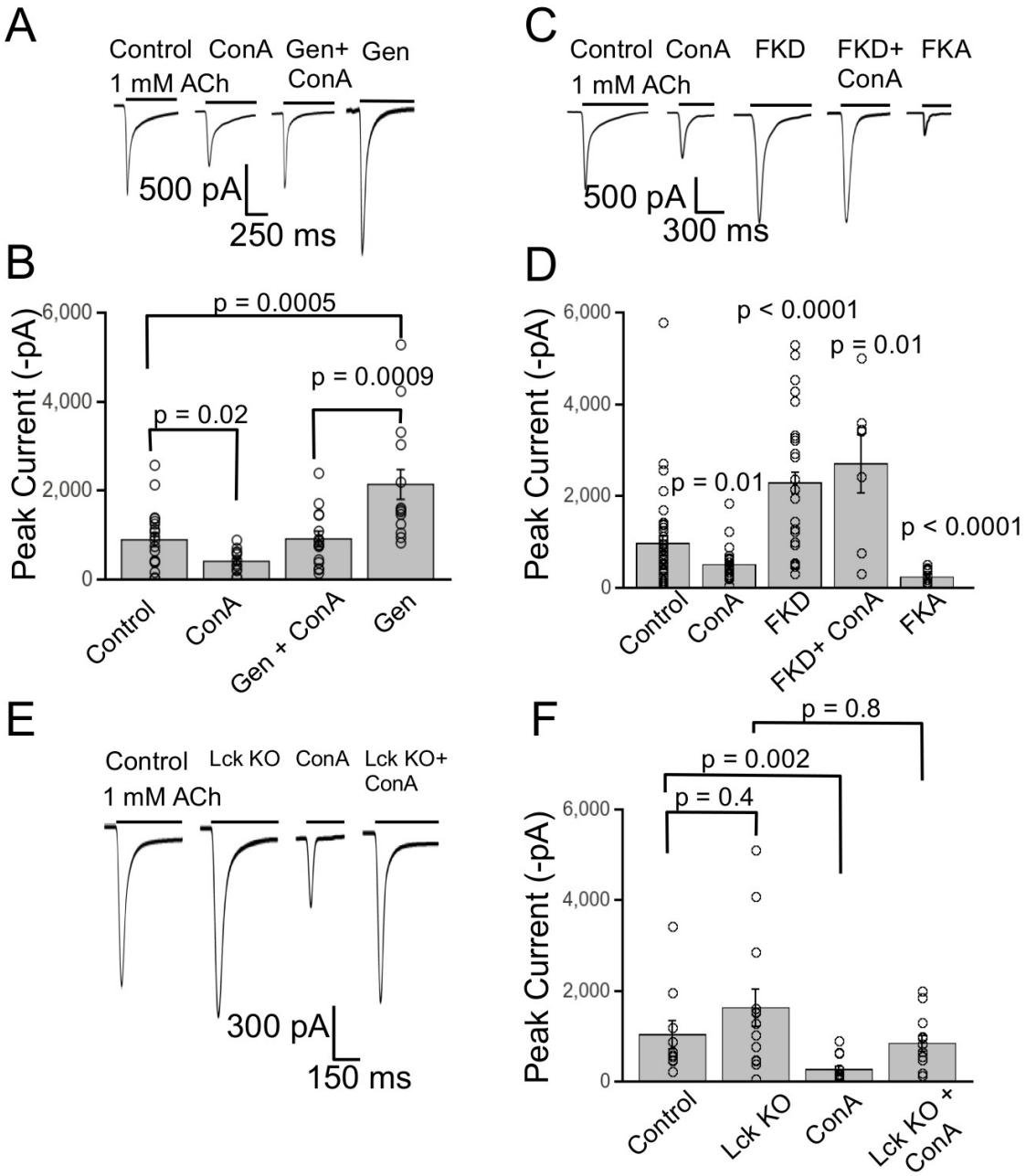

Figure 3.20 TCRs inhibit α7 nicotinic responses through activation of Src family tyrosine kinases.

Whole-cell patch-clamp recordings from Jurkat cells transfected with α7 nAChRs. **(A, B)** ACh (1 mM for 1 sec) induced α7 nAChR currents in Jurkat cells show that TCR activation by ConA (75 μg/ml for 30 min) (n = 14) significantly decreased α7 nAChRs responses as compared to control treatment (n = 20) (p = 0.02, Wilcoxon rank sum test). Preincubation with the tyrosine kinase inhibitor genistein (10 μM for 20 min) (n = 15) prior to ConA stimulation blocked the effect of ConA mediated decrease in α7 nicotinic current. Genistein alone (n = 14) resulted in a significant enhancement of α7 nicotinic

currents as compared to control treatment (n = 20) (p = 0.0005, Wilcoxon rank sum test). The genistein alone treatment had significantly enhanced α7 nicotinic currents as compared to ConA preincubated with genistein (p = 0.0009, Wilcoxon rank sum test). **(C, D)** ConA stimulation (n = 22) significantly reduced α7 nicotinic currents as compared to control treatment (n = 39) (p = 0.01, Wilcoxon rank sum test). α7 receptor mediated currents were significantly enhanced in cells co-transfected with a kinase dead form of Fyn kinase (FKD) (n = 34) as compared to control cells without FKD (n = 39) (p < 0.0001, Wilcoxon rank sum test), while cells co-transfected with FKD and treated with ConA (n = 7) still had augmented α7 currents as compared to control (p = 0.01, Wilcoxon rank sum test). Cells co-transfected with a constitutively active Fyn kinase (FKA) (n = 16) expressed significantly reduced α7 nicotinic responses as compared to control cells (p < 0.0001, Wilcoxon rank sum test). **(E, F)** α7 nAChR current traces from WT Jurkat cells and Lck knockout Jurkat cells. A significant decrease in α7 nAChR currents was observed between control treated (n = 10) and ConA (n = 13) treated WT Jurkat cells (p = 0.002, Wilcoxon rank sum test). However, there was no significant difference in α7 nAChR currents between control treated (n = 13) and ConA treated (n = 12) (p = 0.8 , Wilcoxon rank sum test). These results suggest that both Fyn and Lck contribute to TCR mediated decrease in α7 nAChR currents.

3.3.4 Tyrosine 442 in the M3-M4 cytoplasmic loop of α7 nicotinic receptor is targeted by TCR activation

One mode by which TCR activation and Fyn/Lck kinases could affect α7 nAChRs is via receptor tyrosine phosphorylation. To test this we monitored total tyrosine phosphorylation of α7 by immunoprecipitation and Western blots. Whole cell extracts from Jurkat cells expressing α7-Venus-HA nictonic receptors, which have both a Venus fluorescent protein and an HA epitope tag were generated (Dau et al., 2013) and α7 receptors were captured with anti-HA epitope antibody coated beads. Total α7 and tyrosine-phosphorylated α7 levels were monitored by Western blots using anti-HA and anti-4G10 antibodies, respectively **(Fig. 3.21 A).** Activation of TCRs with ConA (30 min) showed immunoprecipitated α7 nAChRs with higher tyrosine phosphorylation signal as compared to that of the control treated cells **(Fig. 3.21 A, B)**. Similarly, α7 nAChRs in cells cotransfected with constitutively active Fyn kinase showed greater

tyrosine phosphorylation than control cells **(Fig. 3.21 A)**. We calculated a tyrosine phosphorylation index by dividing the α7 tyrosine phosphorylation signal by the total α7 nicotinic receptor expression and found that there was a significant increase in tyrosine phosphorylation of α7 nAChRs in ConA treated cells as compared to control treatment **(Fig. 3.21 B)** ($p = 0.02$, Wilcoxon rank sum test). The bands analyzed were specific for α7 nAChRs as control IPs with IgG coated sepharose beads were devoid of signal with either anti-HA or anti-phosphotyrosine antibodies **(Fig. 3.21 A)**. Thus, both TCR activation and Fyn can potentiate tyrosine phosphorylation of α7 nAChRs.

Using Prosite analysis of the amino acid sequence of the M3-M4 cytoplasmic loop of the α7 nicotinic receptor we identified a putative tyrosine phosphorylation site at Tyr 442 of the receptor (EEVR**Y**IANR). There are two other tyrosines (Y317 and Y386) in the α7 M3-M4 loop (IVLR**Y**HHHD and GNLL**Y**IGFR, respectively), which were not recognized as consensus sites for tyrosine kinase phosphorylation by Prosite. Furthermore, Y442 is conserved over all 11 mouse neuronal nicotinic receptor subunits while neither Y317 nor Y386 is conserved in any other neuronal nicotinic receptor subunit. Thus we focused our attention to investigate whether the effects of TCR activation and Fyn tyrosine kinase was directed against the consensus tyrosine phosphorylation site at Y442 of the α7 nicotinic receptor.

To study the role of phosphorylation of α7 Tyr 442 on TCR regulation of α7 nicotinic receptor function we mutated α7 Tyr 442 into alanine (Y442A). Whole-cell recordings were performed on wildtype Jurkat cells expressing mutant α7 nictonic receptors **(Fig. 3.21 E, F)**. TCR activation with ConA stimulation for 30 min (300 ± 54 pA, n = 6) resulted in no significant difference in the ACh evoked α7 nicotinic current

responses as compared to control treatment (255 ± 56 pA, n = 6) (p = 0.7, *t*-test) **(Fig. 3.21 E, F)**. However, TCR activation with ConA in the Jurkat cells expressing WT α7 nictonic receptors showed a significant decrease in peak response (107 ± 35 pA, n = 10) as compared to that of control treatment (502 ± 119 pA, n = 9) (p = 0.0004, Wilcoxon rank sum test) **(Fig. 3.21 C, D)**. These data strongly suggest that Fyn/Lck kinases modulate α7 nicotinic receptor function by directly targeting Y442 of α7 nAChRs.

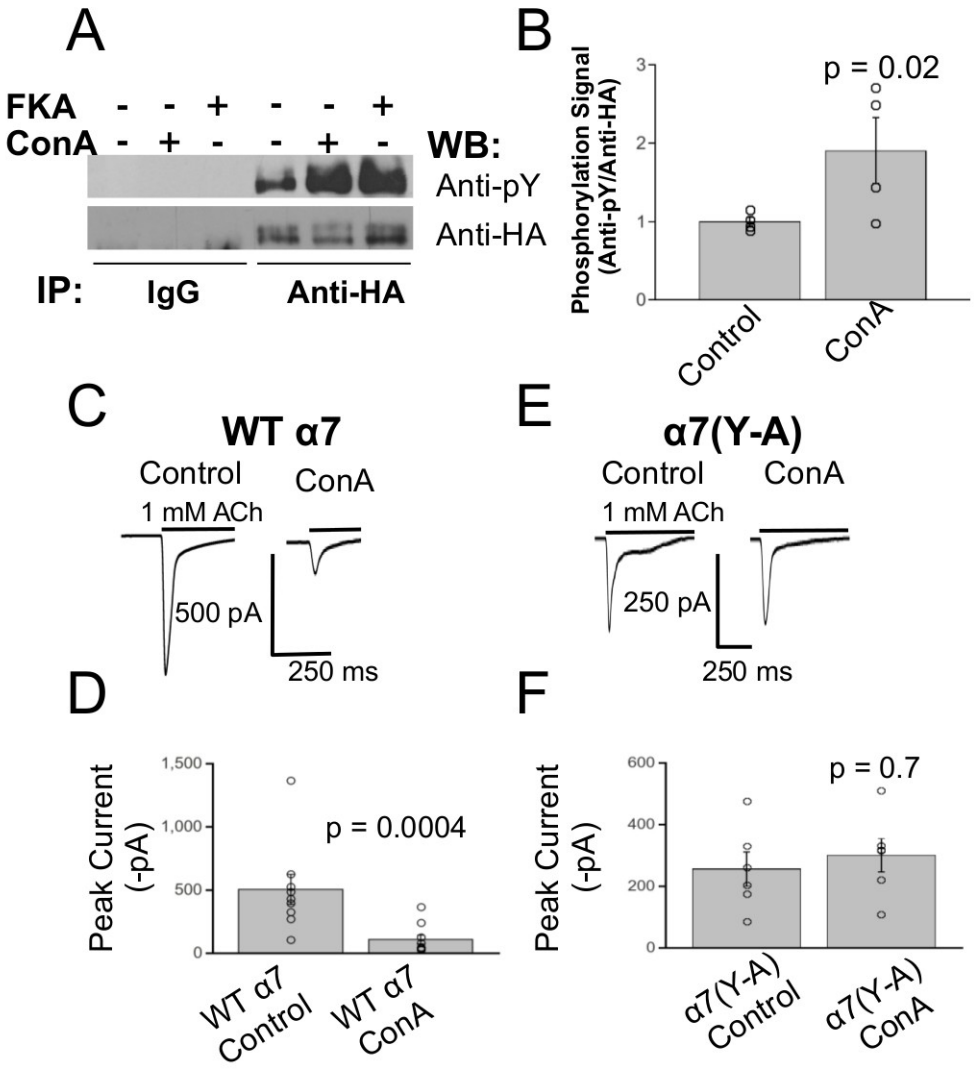

Figure 3.21 TCR activation phosphorylates tyrosine 442 of α7 nicotinic receptors to decrease nAChR function.

(A) An immunoprecipitation and Western blot experiment demonstrates that TCR activation results in an increase in tyrosine phosphorylation of α7-Venus nAChRs, which

also include an HA epitope tag. Anti-HA antibody coated sepharose beads are used to immunoprecipitate α7-Venus nAChRs and then probed on Western blots with either anti-phospho-tyrosine antibody to determine phosphorylated α7-Venus nAChRs or probed on a parallel blot with anti-HA antibody to determine total α7-Venus nAChRs. The first three lanes are negative controls of Jurkat cell samples expressing α7-Venus nAChRs and immunoprecipitated using IgG antibody. The next three lanes are samples immunoprecipitated with anti-HA antibody for Jurkat cells expressing α7-Venus nAChRs that had undergone control treatment, ConA treatment and coexpressing a constitutively active form of Fyn kinase (FKA). **(B)** Quantitative analysis of the density of the bands of control vs ConA treatment in which the phospho-tyrosine signal is normalized to the anti-HA signal shows that ConA treatment (n = 4) significantly enhanced tyrosine phosphorylation of α7-Venus nAChRs as compared to control treatment (n = 4) ($p = 0.02$, Wilcoxon rank sum test). **(C)** Whole-cell α7 nicotinic current traces elicited with 1 mM ACh (1 sec) and recorded from transfected Jurkat cells decreases in peak current amplitude following TCR activation with 30 min of ConA (75 μg/ml) incubation. **(D)** Averaged data shows a significant reduction in the mean current response between control (n = 10) and ConA (n = 9) ($p = 0.0004$, Wilcoxon rank sum test) treated Jurkat cells. **(E)** In Jurkat cells transfected with the mutant α7(Y-A) nicotinic receptors, in which Y442 in the M3-M4 cytoplasmic loop, was mutated to alanine, no difference was observed in peak nicotinic current responses between control and ConA treated Jurkat cells. **(F)** Bar charts illustrating no significant difference ($p = 0.7$, student t-test) in ACh mediated mutant α7(Y442A) nAChRs responses between control (n = 6) and ConA (n = 6) stimulated Jurkat cells.

3.3.5 TCR activation decreases the number of surface α7 nicotinic receptors

There is conflicting evidence regarding whether tyrosine kinases affect trafficking of α7 nicotinic receptors (Charpantier et al., 2005; Cho et al., 2005). Since we found that TCRs signal through Fyn and Lck kinases to decrease α7 receptor function, we examined whether the effect of TCR activation in Jurkat cells could be attributed to a decrease in the number of surface receptors. To test this, we imaged Alexa 647 conjugated α-bungarotoxin (Fl-BTx) binding on the surface of Jurkat cells transfected with α7-Venus under non-permeablized conditions and normalized the surface bound Fl-BTx to the total cellular fluorescence from α7-Venus. ConA incubation (75 μg/ml for 30 min) significantly decreased the number of surface Fl-BTx bound α7 nAChRs (0.29 ± 0.05, n = 58) as compared to that of the control treated cells (0.50 ± 0.07, n = 58) ($p = 0.0003$, Wilcoxon rank sum test) **(Fig. 3.22)**. However, the total cellular α7-Venus intensity remained same for both treated and untreated cells (data not shown), implicating no change in the total level of protein.

In Jurkat cells transfected with mutant α7-Venus in which the putative tyrosine phosphorylation site, Tyr 442, is mutated to alanine (α7(Y-A)Venus) ConA activation of TCRs did not show any significant change in surface Fl-BTx bound α7 nAChRs (0.30 ± 0.03, n = 63) as compared to control treatment (0.22 ± 0.02, n = 58) ($p = 0.09$, Wilcoxon signed rank test) **(Fig. 3.22 H-N)**. We demonstrated the specificity of Fl-BTx labeling of α7-Venus receptors since preincubation of wildtype α7-Venus transfected Jurkat cells with 10 nM MLA (0.26 ± 0.05, n = 26) was successful in competing for binding sites and significantly lowered ($p < 0.0001$, Wilcoxon rank sum test) Fl-BTx signal as compared to cells without MLA (0.79 ± 0.11, n = 26) **(Fig. 3.22 O)**.

Furthermore, we analyzed the specificity of Fl-BTx labeling of α7-Venus receptors by performing quantitative analysis of colocalization via calculation of the Mander's coefficients, M1 and M2, the proportion of colocalized α7-Venus pixels to Fl-BTx pixels and vice versa, respectively. We compared these Mander's coefficients to those calculated when the Fl-BTx was rotated 90° counter clockwise relative to the α7-Venus image, which should have less colocalization. We found that the Mander's coefficient of Fl-BTx colocalized to α7-Venus for both control (0.44 ± 0.03) and ConA (0.44 ± 0.03) treatment was significantly greater ($p = 0.002$, and $p = 0.0005$, Wilcoxon rank sum tests, respectively) than colocalization in the 90° rotated images for control (0.30 ± 0.03) and ConA treatments (0.28 ± 0.02). Thus, these measurements of Mander's colocalization coefficients validated the specificity of Fl-BTx labeling of α7 receptors and confirmed that TCR activation decreases the surface expression of α7 nAChRs without changing the amount of total cellular receptors through phosphorylation of Tyr 442.

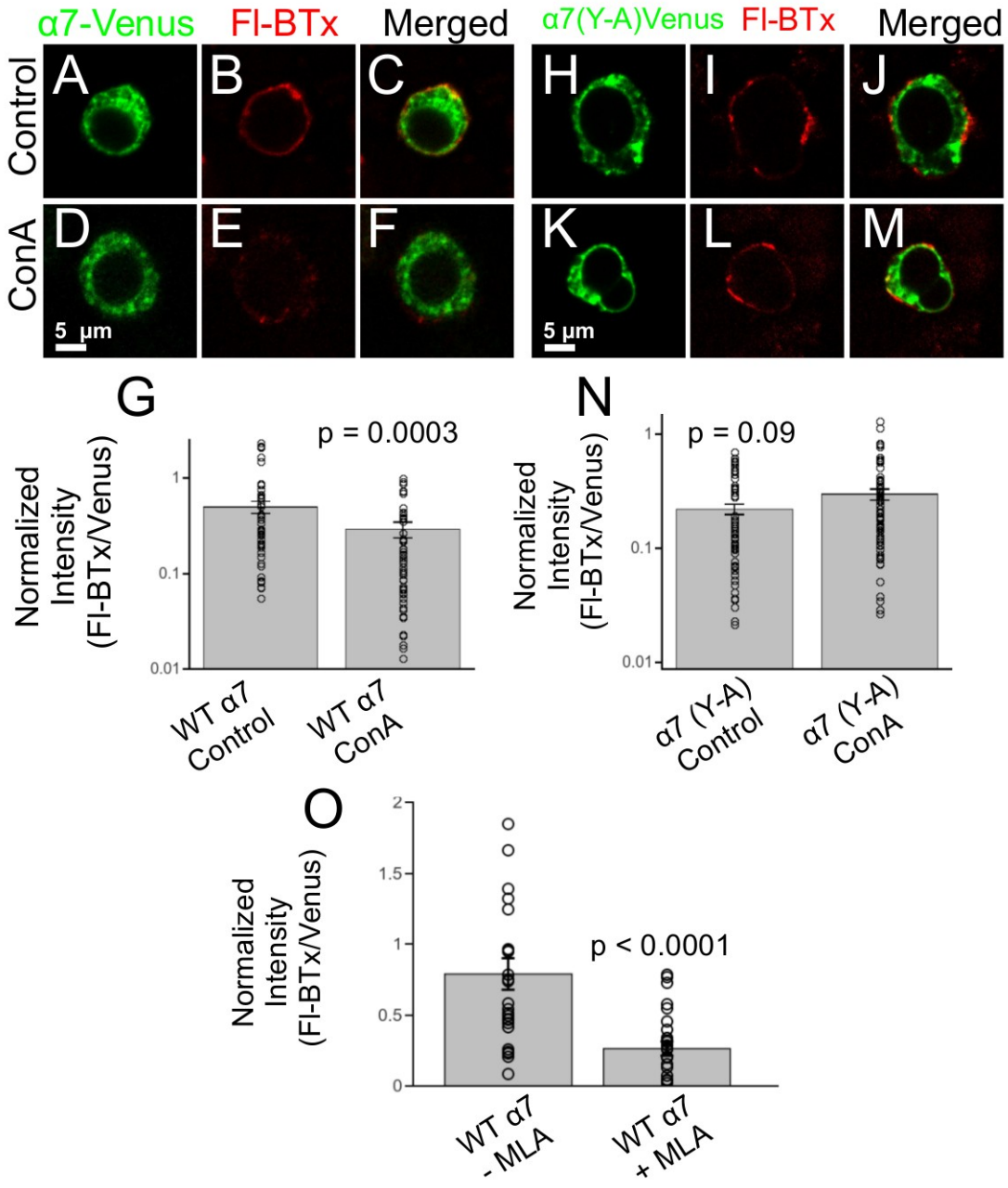

Figure 3.22 TCR activation decreases the number of α7 nAChRs expressed at the cell surface.

(A-F) Confocal images of Jurkat cells transfected with α7-Venus. Surface labeling of α7-Venus is performed with Alexa 647 conjugated α-bungarotoxin (Fl-BTx) under nonpermeabilizing conditions. ConA (75μg/ml for 30 min) stimulation (n = 58) resulted in a significant decrease in the amount of surface α7-Venus receptors as determined with Fl-BTx labeling as compared to control treatment (n = 58) (p = 0.0003, Wilcoxon rank sum test) **(G).** **(H-M)** Confocal images of Jurkat cells transfected with a mutant α7-

Venus in which the putative tyrosine phophorylated site (Y442) was mutated to alanine (α7(Y-A)Venus). **(N)** Upon incubation with ConA (75 μg/ml for 30 min) (n = 63) there was no significant change in Fl-BTx bound surface α7-Venus nAChRs as compared to control treatment (n = 58) (p = 0.09, Wilcoxon rank sum test). Note that both bar charts are displayed in logarithmic scale and represent the means ± SE with each circle showing the measure from each individual cell. **(O)** Control experiment demonstrating the specificity of Fl-BTx. Preincubation with 10 nM MLA (n = 26) is able to compete with and significantly lower Fl-BTx labeling as compared to control treatment (n = 26) ($p < 0.0001$, Wilcoxon rank sum test).

3.3.6 TCR activation decreases single-channel conductance of α7 nicotinic receptors

A second potential mechanism for the inhibition of nicotinic current following TCR activation is a decrease in intrinsic channel function. Since Y442 is located in the amphipathic helix of α7, which lines the ion permeation pathway, the addition of a phosphate group here could hinder ion conductance because of added steric hindrance. Hence, we used ionic current fluctuation analysis of whole-cell recorded nicotinic currents in brain slices to calculate single-channel conductance. Ionic current fluctuation analysis is a reliable tool to estimate single-channel conductance of ion channels (Sigworth, 1980; 1981; Gill et al., 1995). Using this method we aimed to determine whether a decrease in single-channel conductance of α7 nicotinic receptors contributed to the mechanism of TCR mediated decrease in α7 whole-cell current responses. Examples of whole-cell recorded α7 nicotinic currents elicited with PHA543613 and the corresponding AC filtered α7 nicotinic current (showing current fluctuation) are shown for each experimental condition **(Fig. 3.23)**. Current fluctuations are maximal during the peak of the nicotinic current response and represent maximal number of channel openings. PHA543613 is applied repeatedly and the variance of the current fluctuations of each trace is plotted against the mean current of the whole-cell current at each time

point. The slope of the relationship gives the unitary current and when divided by the driving force ($V_h - E_{rev}$) equals the single-channel conductance (γ).

The α7 receptor mediated inward currents recorded from layer 1 prefrontal cortical interneurons of control treated brain slices from WT mice (118 ± 34 pS, n = 12) was accompanied by a significantly greater calculated single-channel conductance than those of ConA treated WT brain slices (30 ± 12 pS, n = 8) (p = 0.02, Wilcoxon rank sum test) **(Fig. 3.23 A-C)**. Exemplary graphs of current variance versus current mean were plotted and shown for α7 nicotinic receptor single-channel conductances showing 61 pS and 22 pS, respectively, for control and ConA incubated brain slices **(Fig. 3.23 A, B)**. To verify that TCR activation with ConA is responsible for the change in single-channel conductance we performed fluctuation analysis of whole-cell recorded α7 nicotinic currents from TCR β KO mice **(Fig. 3.23 D-F)**. We calculated the single-channel conductance and observed no significant difference between brain slices treated with ConA (130 ± 68 pS, n = 4) as compared to brain slices with control treatment (118 ± 23 pS n = 8) from TCR β KO mice (p = 0.5, Wilcoxon rank sum test) **(Fig. 3.23 F)**. Plots of exemplary data of current fluctuation analyses are shown for control treated and ConA treated brain slices of TCR β KO mice exhibiting single-channel conductances of 101 pS and 67 pS, respectively **(Fig. 3.23 D,E).**

We further investigated the effects of TCR activation on modulating α7 channel gating kinetics recorded from layer 1 interneurons from WT brain slices. To examine the activation rate we fitted the rise to peak of the α7 current with a single exponential and showed that there was no significant difference between the activation time constant for control treatment (6.4 ± 0.8 ms, n = 11) and ConA treatment (5.6 ± 0.7 ms, n = 7) (p =

0.8, Wilcoxon rank sum test) **(Fig. 3.24)**. The time course of the α7 decay kinetics during PHA543613 application was well fit by the sum of two exponentials. Similarly, ConA application did not result in any significant change in either the slow (control: 57.0 ± 7.4 ms, n = 11 vs ConA: 62.1 ± 16.4 ms, n = 7) nor fast time constants (control: 15.0 ± 2.5 ms, n = 11 vs ConA: 14.3 ± 2.2 ms, n = 7) (p = 0.9, Wilcoxon rank sum test, for both slow and fast time constants).

These data demonstrate that TCR activation inhibits α7 mediated whole-cell currents by decreasing their single-channel conductance but does not alter their gating kinetics.

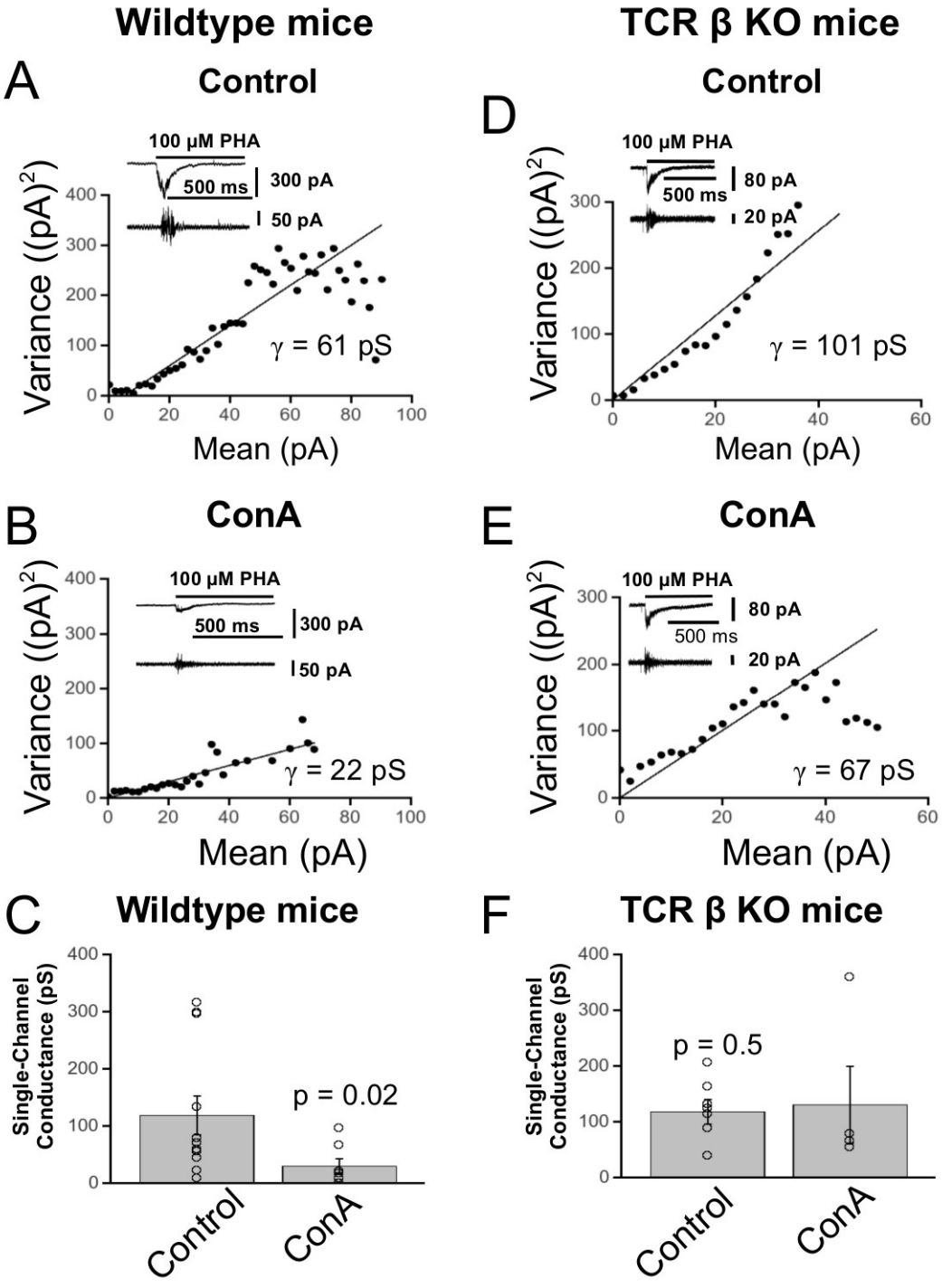

Figure 3.23 TCR activation attenuates single-channel conductance of α7 nAChRs. Current variance-current relations for fluctuations of PHA543613 (100 µM, 1 sec) elicited α7 nicotinic whole-cell currents recorded for both control **(A)** and ConA treatments **(B)** from layer 1 interneurons from WT mice. Single-channel conductances (γ) were calculated from the slope of current variance vs mean current response. Inset shows whole-cell α7 nicotinic current waveforms and their respective AC filtered

waveforms for control (A) and ConA treatments **(B). (C)** The mean single-channel conductance of α7 responses for ConA treated slices (n = 8) was significantly lower than that of control (n = 12) (p = 0.02, Wilcoxon rank sum test). Current variance vs mean current relations for α7 nicotinic whole-cell currents recorded for both control **(D)** and ConA treatments **(E)** from layer 1 interneurons from TCR β KO mice. **(F)** There was no significant difference in the mean single-channel conductance for α7 receptors between control (n = 7) and ConA (n = 5) treated slices of TCR β KO mice (p = 0.5, Wilcoxon rank sum test).

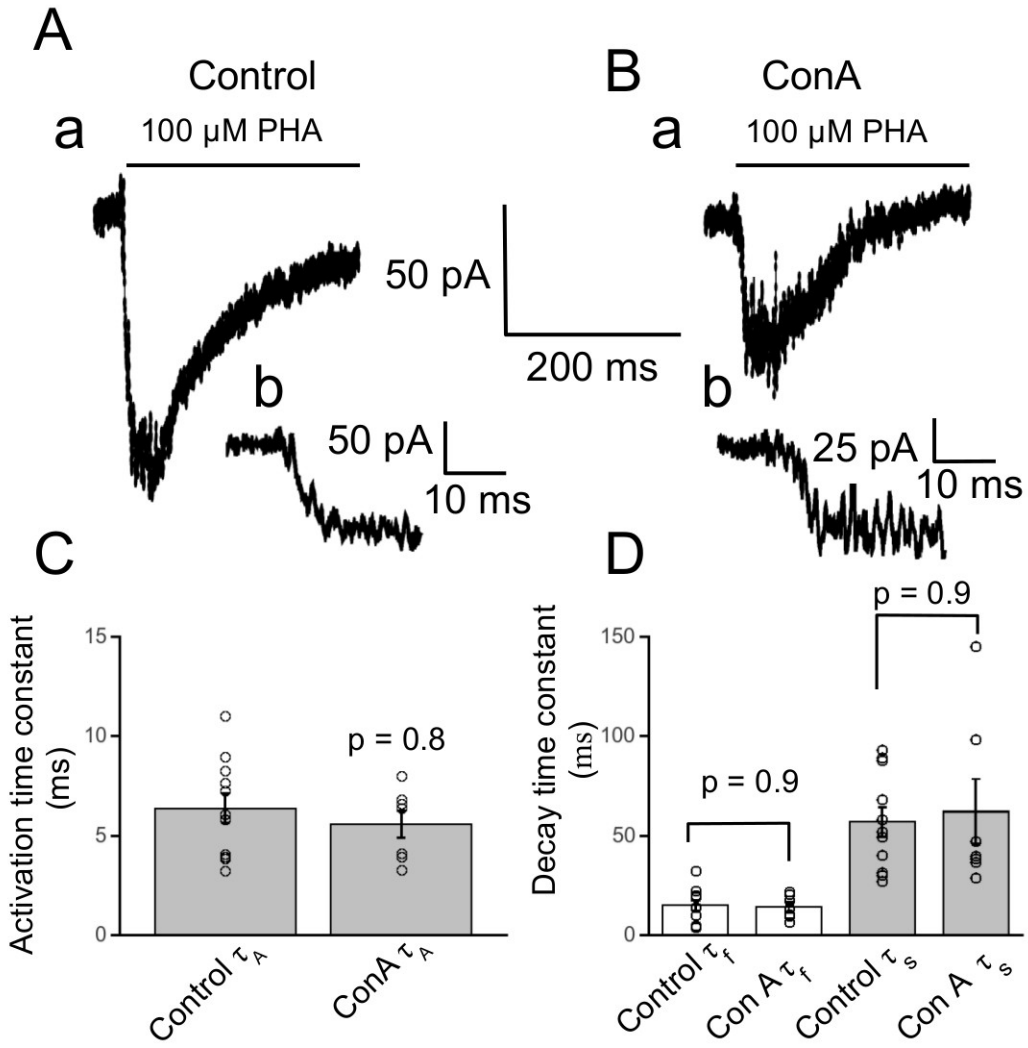

Figure 3.24 TCR activation does not alter gating kinetics of α7 nAChRs.
Whole-cell recorded PHA-543613 (100 µM, 1 sec) activated α7 nicotinic current traces from control treated **(Aa)** and ConA treated **(Ba)** layer 1 interneurons of medial prefrontal cortical brain slices. Insets show at higher time resolution comparable rates of activation rise times of α7 nicotinic currents for both control **(Ab)** and ConA treatments **(Bb). (C)** There was no significant difference in the activation time constant between control (n = 11) and ConA (n = 7) treatments (p = 0.8, Wilcoxon rank sum test). Futhermore, ConA

treatment did not result in a significant change in either the fast (control: 15.0 ± 2.5 ms, n = 11 vs ConA: 14.3 ± 2.2 ms, n = 7) nor the slow (control: 57.0 ± 7.4 ms, n = 11 vs ConA: 62.1 ± 16.4 ms, n = 7) decay time constants (p = 0.9, Wilcoxon rank sum test, for both fast and slow time constants).

3.3.7 Single-channel recordings verify that TCR activation reduces α7 nicotinic receptor single-channel conductance

In order to verify the whole-cell fluctuation analysis data that TCR activation decreases single-channel conductances of α7 nicotinic receptors, we performed single-channel recordings in cell-attached configuration from WT Jurkat cells exposed to either control or ConA (75 μg/ml for 30min) solutions. Single-channel α7 nicotinic receptor mediated currents were activated by having ACh (100 μM) in the patch pipette electrode solution. The extracellular solution was identical to the patch pipette recording solution minus ACh. The patch of membrane in cell-attached mode was voltage-clamped at a pipette potential of +60 mV. This would equal to a transmembrane potential of -60 mV plus the resting membrane potential of the cell, which was on average -48 mV. Thus, the estimated transmembrane potential was -108 mV. When plotting histograms of the current amplitudes of the fitted open single-channel events there was a significant reduction ($p < 0.0001$, Wilcoxon rank sum test) in α7 single-channel amplitudes of ConA treated cells (2.4 ± 0.0 pA, n = 13902 open channel events over 4 cells) as compared to control treatment (6.0 ± 0.1 pA, n = 1471 open channel events over 4 cells) **(Fig. 3.25 A-D)**. This corresponds to single-channel conductances of 22.0 ± 0.1 pS for ConA treated cells and 55.5 ± 0.6 pS for control treated cells. We also verified the conductance change by measuring the slope conductance of single-channel currents measured over various holding pipette potentials. Using this paradigm, we examined a control treated

cell with cell-attached single-channel currents having a higher slope conductance (41.4 pS) than a ConA treated cell (14.6 pS) (data not shown).

To determine the effects of TCR activation on the gating kinetics of α7 nicotinic receptors we plotted histograms of durations of single-channel open events and closed events for both control and ConA treatments **(Fig. 3.25 E-H)** and then fitted the histograms to multiple exponential functions. Each histogram represents the combined data from four separate cell-attached patch-clamp recordings. We report the fitted time constants and the standard errors of fit. For control treated cells the open channel duration histogram was fitted to a sum of two exponentials with time constants: $\tau 1 = 0.12 \pm 0.32$ ms and $\tau 2 = 0.66 \pm 0.49$ ms. For ConA treated cells the open channel duration histogram was fitted with a sum of two exponentials with $\tau 1 = 0.07 \pm 0.10$ ms and $\tau 2 = 0.42 \pm 0.21$ ms. Therefore, for the duration of the single-channel open events there was no observable differences in the distributions of the histograms between control and ConA treatments. Similarly, the durations of the closed single-channel events did not differ greatly between control and ConA treatments. Closed single-channel duration events for control treated cells were fit with the sum of four exponentials with $\tau 1 = 0.20 \pm 0.12$ ms, $\tau 2 = 1.95 \pm 0.13$ ms, $\tau 3 = 33.7 \pm 0.2$ ms and $\tau 4 = 1311.8 \pm 0.2$ ms. For ConA treated cells the closed single-channel durations were well fit with the sum of five exponentials: $\tau 1 = 0.10 \pm 0.10$ ms, $\tau 2 = 0.47 \pm 0.13$ ms, $\tau 3 = 3.42 \pm 0.09$ ms, $\tau 4 = 29.1 \pm 0.1$ ms and $\tau 5 = 227.0 \pm 0.1$ ms.

Thus, our single-channel data corroborates the whole-cell recorded current fluctuation analysis that TCR activation attenuates α7 mediated single-channel conductance while having little effect on gating kinetics.

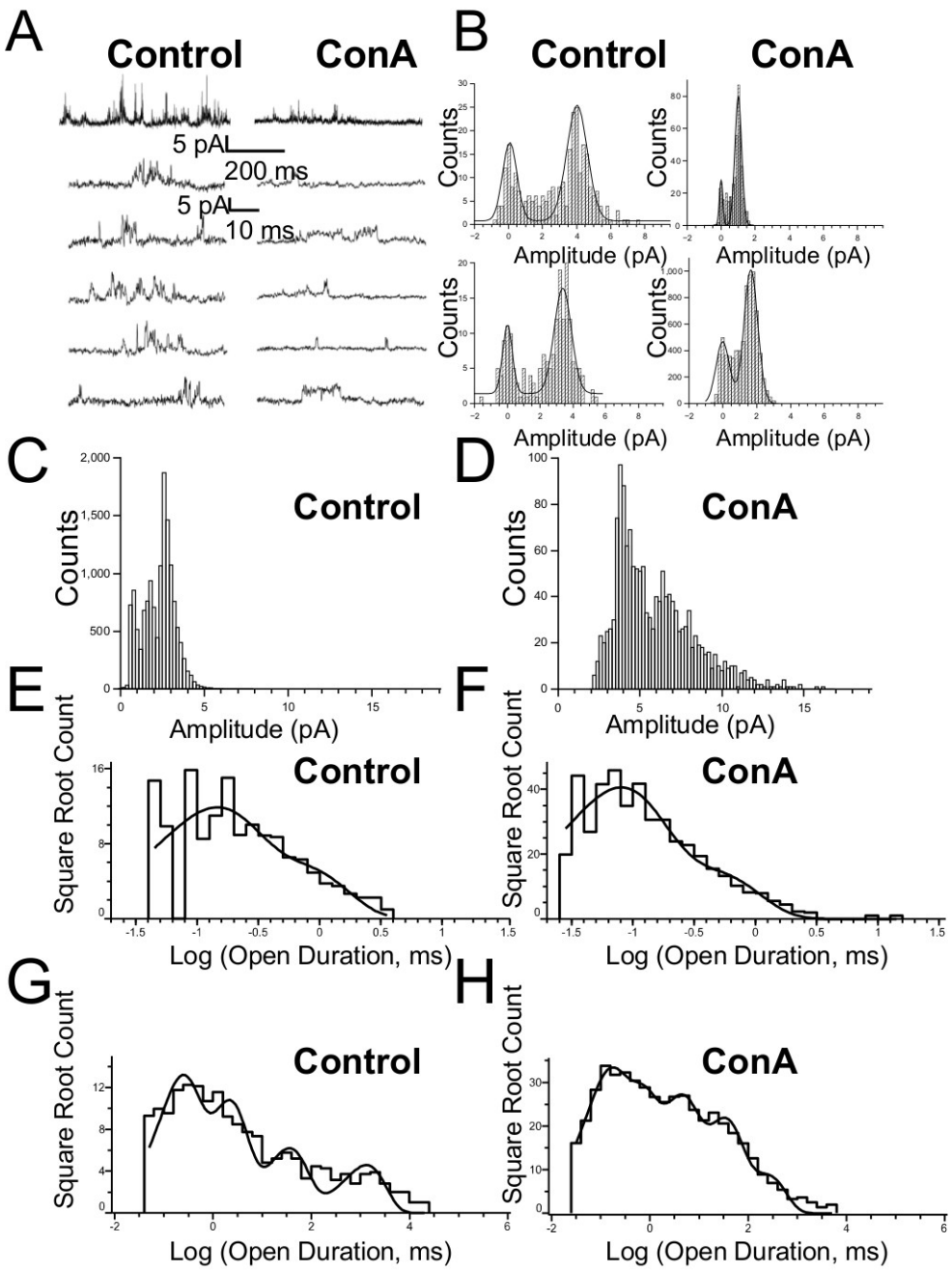

Figure 3.25 Single-channel recordings show that TCR activation decreases single-channel conductance of α7 nAChRs.

(A) Examples of Jurkat cell-attached single-channel traces for control and ConA treatment. The ConA treated single-channel responses have smaller single-channel current amplitudes than control treatment. The patch electrode solution contained 100 μM ACh. **(B)** Histograms of fitted amplitudes from single-channel events from four separate patches show that ConA treatment had consistently smaller single-channel amplitudes than control treatment. **(C, D)** Histograms of single-channel amplitudes showing the combined data of all patches recorded for control (n = 4) and ConA (n = 4)

treated Jurkat cells showing that ConA treatment caused a significant reduction of the amplitudes of open single-channel events ($p < 0.0001$, Wilcoxon sum rank test). Only the amplitudes of open single-channel events are shown for clarity. **(E, F)** Histograms of open duration of single-channel events compiled from all patches show no difference in distributions between control and ConA treatment. **(G, H)** However, the histograms of closed duration of single-channel events show similar kinetics between ConA and control treated cells.

3.3.8 TCR activation decreases action potential firing frequency of layer 1 cortical neurons

We examined the physiological consequence of decreasing α7 nicotinic receptor currents following TCR activation by measuring action potential firing rate of layer 1 cortical interneurons. Since most cortical neurons in brain slices lack intrinsic ability to spontaneously fire action potentials due to severed afferent inputs, we performed current-clamp recordings in whole-cell configuration mode from layer 1 interneurons and applied depolarizing constant current steps (0 pA to 200 pA, 10 pA steps for 500 ms). To ascertain the excitability of the recorded neuron we plotted input-output curves of current injection vs action potential frequency.

To test whether α7 nicotinic receptors contribute to the firing rate of layer 1 prefrontal cortical interneurons, we bath applied 10 nM MLA (α7 nAChR competitive antagonist) ($n = 7$) and noticed a significant decrease in the action potential firing frequency as compared to baseline control ($n = 7$) ($p < 0.0001$, MLA factor, two-way ANOVA) **(Fig. 3.26 A-C)**. All the recorded neurons included in the analysis had stable resting membrane potentials (RMPs) that were more negative than -60 mV and overshooting action potentials. There was no significant difference in the mean RMP and R_{input} between control and MLA treated slices (data not shown). If an α7 antagonist decreased neuronal excitability then a specific α7 agonist, PHA543613, should increase neuronal excitability. Indeed, when PHA543613 (100 μM for 575 msec) was applied 75 msec preceding and during a 200 pA (500 msec) depolarization there was a significant

increase ($p = 0.03$, $n = 7$, paired t-test) in action potential firing frequency (30 ± 2 Hz) in the same neuron as compared when there was only 200 pA depolarization but no co-stimulation with PHA543613 (27 ± 2 Hz) **(Fig. 3.26 G,H).** Since, TCR activation results in the inhibition of α7 nicotinic receptor currents, to examine the involvement of TCRs in modulating the firing rate of layer 1 interneurons we compared whole-cell current-clamp recordings of control treated brain slices from WT mice ($n = 7$) with ConA treated brain slices from WT mice ($n = 9$). We found a significant decrease in the mean firing frequency of ConA treated WT brain slices (18 ± 4 Hz) as compared to control treated WT brain slices (26 ± 3 Hz) ($p < 0.0001$, treatment factor, two-way ANOVA) **(Fig. 3.26 A,D,F).** If ConA mediated activation of TCRs caused a decrease in neuronal firing rate due to decreased α7 nicotinic receptor currents then we would predict an increase in firing rate in TCR β subunit KO mice since baseline α7 nicotinic currents in TCR β KO mice have elevated α7 nicotinic currents in brain slices **(Fig. 3.19 C)**. A comparison of the mean action potential firing frequency showed a significant increase in neurons recorded from control treated brain slices of TCR β KO mice (40 ± 5 Hz, $n = 10$) as compared to neurons from control treated brain slices of WT mice (26 ± 3 Hz, $n = 7$) ($p < 0.0001$, genotype factor, two-way ANOVA) (**Fig. 3.26 A, E, F).**

We performed current-clamp experiments in layer 1 interneurons from brain slices of α7 nAChR knockout mice to determine whether TCR modulation of neuronal excitability was through α7 receptors. ConA incubation ($n = 6$) in α7 nAChR null slices showed similar levels of neuronal excitability as control treatment ($n = 11$) for much of the range of stimulation intensities ($p = 0.25$, ConA vs control treatment, two-way ANOVA) **(Fig. 3.26 I).** Indeed, when averaging over all current stimulation intensities

the ConA mediated decrease in frequency in neuronal firing from α7 nAChR null mice (n = 6) was significantly less than the ConA mediated decrease in neuronal firing frequency in wildtype mice (n = 9) ($p = 0.005$, Wilcoxon rank sum test) **(Fig. 3.26 J)**. This supports that TCR activation is attenuating neuronal excitability through modulation of α7 nAChRs.

This set of data shows that α7 nAChRs contribute to the excitability of layer 1 cortical neurons and that TCR mediated inhibition of α7 receptor function contributed to reduced neuronal excitability. The source of ACh to activate α7 nAChRs in the cortex may be from cut cholinergic terminals from neurons originating from the nucleus basalis magnocellularis. There has even been a recent report showing local cholinergic interneurons in the cerebral cortex (von Engelhardt et al., 2007).

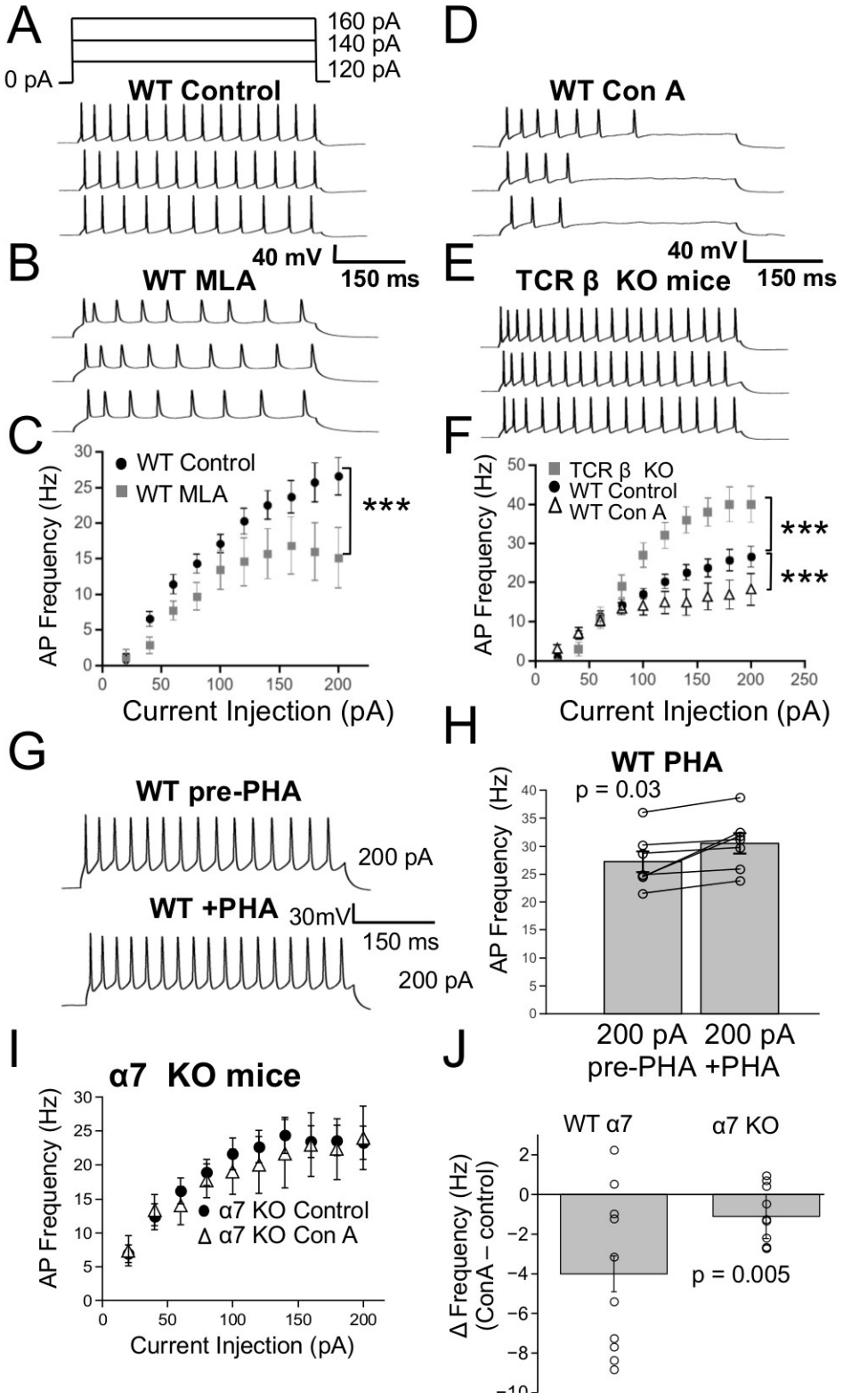

Figure 3.26 TCR activation modulates neuronal excitability of layer 1 cortical interneurons.

(A, B) Firing frequency of layer 1 cortical neurons is modulated by α7 nicotinic receptors as evidenced by the decrease in action potential firing in the presence of a specific α7 antagonist, MLA (10 nM) in brain slices from wildtype mice. Current-clamp recordings are shown for current steps (120, 140 and 160 pA). **(C)** The action potential firing rate of layer 1 interneurons in response to current steps (0 pA to 200 pA) was significantly lower with MLA treatment (n = 7) as compared to control treatment from wildtype mouse brain slices (n = 7) ($p < 0.0001$, MLA factor, two-way ANOVA). **(E, F)** A significant increase in the action potential firing rate was observed in layer 1 cortical neurons from control treated TCR β KO mice (n = 10) as compared to control treated wildtype mice (n = 7)($p < 0.0001$, genotype factor, two-way ANOVA) over current steps ranging between 0 and 200 pA. **(A, D, F)** Wildtype brain slices with ConA treatment (n = 9) resulted in a significant decrease in the action potential firing rate of layer 1 cortical interneurons as compared to control treated wildtype mouse brain slices (n = 7) ($p < 0.0001$, two-way ANOVA) (current steps ranged between 0 and 200 pA). **(G, H)** There was a significant increase ($p = 0.03$, n = 7, paired t-test) in action potential frequency upon PHA543613 (PHA, 100 μM) co-application with 200 pA than with 200 pA depolarizing stimulation alone from brain slice recordings obtained from wildtype mice. **(I)** Current-clamp recordings from layer 1 interneurons from α7 nAChR knockout mice show that ConA treatment (n = 6) displays similar neuronal excitability as compared to control treatment (n = 11) ($p = 0.25$, ConA vs control treatment factor, two-way ANOVA). Each connected pair of circles represent the frequency before and after PHA application for one cell. **(J)** In brain slices of wildtype mice there was a significantly greater attenuation in action potential firing frequency with ConA treatment (n = 9) as compared to ConA treatment of α7 nAChR knockout mice (n = 6)($p = 0.005$, Wilcoxon rank sum test). Each circle in **(J)** represents the mean ConA mediated decrease in firing frequency for one specific current stimulation.

3.4 Discussion

This study shows for the first time that the immune protein, the T cell receptor, can modulate nAChR function and neuronal activity in the brain. Activating TCRs decreases the function of α7 nAChRs in Jurkat cells and in layer 1 interneurons of the medial prefrontal cortex. The mechanism of TCR mediated dampening of α7 nicotinic currents was due to downstream activation of Src family tyrosine kinases, namely Fyn and Lck kinases. TCRs' effect of attenuating α7 nAChR responses is mediated through Y442 of α7 since mutating Y442 to alanine in the α7 nAChR blocked TCRs' negative modulation. TCR activation leads to a decrease in the number of surface α7 nAChRs. TCR activation

also decreases α7 single-channel conductance. Furthermore, TCRs and α7 nAChRs influence neuronal excitability. Inhibition of α7 receptors decreases the frequency of action potentials. Activation of TCRs also inhibited the neuronal firing frequency while neurons from TCR β KO mice exhibited enhanced firing rate of action potentials. Thus, the TCR mediated regulatory mechanism of α7 nAChR function illustrates a novel role of TCRs in the CNS affecting ligand-gated ion channel function and neuronal excitability.

3.4.1 TCRs modulate neural function and α7 nAChR activity

To our knowledge this is the first demonstration that TCRs in the CNS can modify neuronal activity and that one of the mechanisms is through modulation of α7 nAChR function. We have shown that TCRs can decrease α7 currents in prefrontal cortical interneurons **(Fig. 3.19)**. Our data also show that there is endogenous activation of TCR mediated decrease of α7 responses in the CNS since TCRβ subunit KO mice had significantly larger α7 currents than WT mice **(Fig. 3.19)**. We also observed that TCRs modulate neuronal excitability. TCR activation resulted in a significant decrease in current-evoked action potential firing, while in TCR β subunit KO mice neurons had a significantly enhanced action potential firing **(Fig. 3.26)**. In the displayed example of action potential waveforms during MLA application, it appears that the action potentials showed broader spike widths with no afterhyperpolarization as compared to cells recorded in control solution. An explanation could be that MLA may also nonspecifically target other ion channels, including potassium channels. This is unlikely since there is no published report of MLA blocking potassium channels and the low concentration that is used (10 nM) is likely not able to block channels. It may be possible that the effect of MLA on action potential broadening may be an indirect effect. A decrease in the calcium

influx due to inhibition of α7 receptors via MLA may inhibit calcium dependent potassium channels, which require the influx of calcium via α7 nAChRs to activate the potassium channels. Activation of calcium activated potassium channels due to calcium flux through α7 receptors has been demonstrated in chromaffin cells (Fuentealba et al., 2004). However, the effect of action potential broadening with MLA was not observed consistently in all the cells that we recorded.

The TCR is an octameric complex that includes the CD3ζ subunit. CD3ζ plays an important role in dendritic structure and development in cultured hippocampal and cortical neurons (Baudouin et al., 2008).

3.4.2 TCRs decrease α7 nAChR function through phosphorylation of tyrosine 442

Our Western blot and electrophysiology data support that TCRs have effect through phosphorylation of α7 receptors at tyrosine 442 **(Fig. 3.21)**, which is the only putative tyrosine phosphorylation site within the cytoplasmic loop of α7 recognized by ProSite analysis. We show that both Fyn and Lck kinases are involved in TCR mediated attenuation of α7 nicotinic responses since FKD or deletion of Lck both prevented ConA from decreasing α7 activity **(Fig. 3.20)**. Overexpressing FKD successfully competed with endogenously expressed Fyn kinase. Since genistein, a broad spectrum inhibitor of tyrosine kinase, and FKD both augmented α7 currents **(Fig. 3.20)**, our results are consistent with the results of Charpantier et al (2005) and Cho et al (2005). Furthermore, we were able to abolish the effect of ConA stimulated TCR mediated decrease in α7 responses by mutating tyrosine 442 to alanine. This is consistent with the results of Charpantier et al (2005) who also mutated tyrosine 386 and tyrosine 442 to alanines but did not distinguish the effect of each tyrosine. We propose that tyrosine 442 is the key

tyrosine that is phosphorylated and induces altered α7 nAChR function following TCR activation. However, our results are at odds with that of Cho et al (2005), who mutated either tyrosine 317, 386 or 442 to phenylalanine without any effect on genistein mediated potentiation of α7. One potential caveat of site directed mutagenesis is that mutating one amino acid into another may have more than the intended consequence. Mutating tyrosine, to another amino acid may alter the structure of the protein since the functional properties of amino acid side groups and their degree of hydrophobicity plays a role in stabilizing protein conformation (Yutani et al., 1987). In our study, as in those of Charpantier et al (2005), the mutation was made to alanine while Cho et al (2005) mutated the residue to phenylalanine, which may explain the discrepancy.

3.4.3 Mechanisms of TCR mediated decrease of α7 currents

Our exploration of the mechanisms of TCR mediated decrease in nAChR function indicate two contributing parallel steps: 1) a decrease in surface α7 receptors; and 2) a decrease in single-channel conductance. Our results showing a decrease in cell surface receptors upon TCR stimulation using Fl-BTx binding is consistent with the results of Cho et al (2005), who showed that inhibition of tyrosine kinase with genistein enhanced surface α7 receptors, while Charpantier et al (2005) showed no alterations in surface α7 receptors when inhibiting tyrosine kinase activity. This TCR mediated decrease in surface receptors is mediated by phosphorylation of tyrosine 442 since mutation of this residue to alanine in α7 completely abolished TCRs' effect of decreasing surface α7 receptors **(Fig. 3.22).**

Interestingly tyrosine 442 lies within the amphipathic helix. The amphipathic helix lines the cytoplasmic side portals of cys-loop receptors and forms part of the ion

permeation pathway (Hales et al., 2006). We found that TCR activation decreases the single-channel conductance of α7 receptors **(Figs. 3.23, 3.25)**. This allows a unique property of reversible modification of single-channel function through post-translational modification, namely tyrosine phosphorylation. This is consistent with the results of Charpantier et al (2005), who proposed that tyrosine phosphorylation of α7, which decreased macroscopic currents, was due to alterations in channel function. We further examined whether the gating kinetics of α7 were also affected by TCR activation. We analyzed the activation and desensitization kinetics and open and closed channel durations **(Figs. 3.24, 3.25)** and determined that α7 gating kinetics were unaffected by TCR activation. Thus, only single-channel conductance is decreased by TCR activation.

3.4.4 Physiological role of TCRs in the CNS

Our study demonstrates that an immune protein receptor complex, the TCR, has a neuronal function in the CNS. TCRs play an important role in modulating postsynaptic cholinergic neurotransmission by dampening α7 nicotinic currents **(Fig. 3.19)**. Although we used an exogenous compound ConA for stimulation of TCRs, we also have evidence that endogenous activation of TCRs already occur in the CNS, which dampen α7 currents. This is shown by significantly augmented α7 nAChR currents from layer 1 interneurons of TCR β KO mice as compared to WT **(Fig. 3.19)**. Furthermore, both TCR signaling and α7 mediated neurotransmission affect neuronal excitability since inhibition of α7 with MLA decreases action potential firing similar to TCR activation with ConA, while neurons from TCR β KO mice had elevated firing frequency **(Fig. 3.26)**.

TCR modulation of α7 receptors involve a unique form of cellular signaling in the CNS. Unlike the receptor tyrosine kinases, insulin receptor (Ahmadian et al., 2004; Cho

et al., 2005) and TrkB receptor (Zhou and Hablitz, 1996; Fernandes et al., 2008) signaling, which involve the release and binding of insulin and brain-derived neurotrophic factors to their respective receptors, the TCR is an octameric receptor complex, which binds to an antigen presented by either MHCI or MHCII found on the surface of the antigen presenting cell. MHCI molecules are widely distributed in the CNS (Huh et al., 2000) and reside on neurons and microglia (Tooyama et al., 1990; Neumann et al., 1997; Corriveau et al., 1998). We propose that TCR mediated tyrosine kinase signaling is based on cell-cell contacts and therefore senses neighboring cells by binding to MHCI of adjacent neurons or microglia. Interestingly, microglia are involved in the pruning of synaptic spines as evidenced by synaptic material engulfed by microglia (Paolicelli et al., 2011). A purely speculative function of TCR activation is the down-regulation of α7 receptors during microglial pruning of neuronal dendritic spines. This may be a protective mechanism to decrease calcium influx through the highly calcium permeable α7 receptors during the trauma of spine pruning.

TCR signaling through cell-cell contacts may also be necessary for the modulation of ion channel expression during formation of synapses. Cell-cell contact signaling may be formed when MHCI molecules from a presynaptic neuron binds to TCRs on the postsynaptic neuron. Evidence supporting the role of TCR-MHCI complex in modulating neurotransmission includes the fact that MHCI deficient mice display enhanced long-term potentiation in the hippocampus (Huh et al., 2000). Futhermore, CD3ζ subunits were shown to modulate AMPA glutamatergic neurotransmission and dendritic development (Xu et al., 2010) in neurons of the retina.

nAChRs play an important role in affecting not only neuronal excitability but also synaptic plasticity in many CNS areas (Fujii et al., 2000; Ji et al., 2001; Couey et al., 2007). Our results show that α7 nAChRs contribute to neuronal excitability of cortical interneurons. Therefore, TCR inhibition of nAChR activity can dynamically and precisely tune the excitability of neurons. Since other ligand-gated ion channels including $GABA_A$ (Wan et al., 1997), NMDA (Wang and Salter, 1994) and AMPA receptors (Ahmadian et al., 2004) can be functionally modulated by Src tyrosine kinases, this opens the possibility that TCRs can modulate neuronal excitability by impacting the activity of many other ion channels in the CNS.

Chapter 4 - cAMP-Dependent Protein Kinase Decreases α7 Nicotinic Receptor Activity in Layer 1 Prefrontal Cortical Interneurons

Abstract

Phosphorylation of ion channels in the brain plays a key role in the modification of the strength of synaptic transmission. Modulation of neuronal nicotinic acetylcholine receptors (nAChRs) in the brain by protein kinases targeting putative phosphorylation consensus sites in the long cytoplasmic domain may play a critical role in the regulation of the functional properties of the receptor and ultimately neuronal excitability. The homopentameric α7 nAChRs are the most prevalent nAChR subtype in the CNS after α4β2 nAChRs. Serine 365 residue in the M3-M4 cytoplasmic loop of α7 nAChR is a putative phosphorylation binding site for protein kinase A (PKA), making it a prime target for modulation by this kinase. In this study, we used the cell permeable second messenger 8-Br-cAMP to directly modulate the activity of α7 nicotinic receptors. We performed whole-cell voltage-clamp recordings in HEK 293T cells and in layer 1 interneurons of the prefrontal cortex in mouse brain slices. In both HEK 293T cells and layer 1 interneurons α7 nAChR mediated whole-cell currents were significantly decreased upon stimulation with 8-Br-cAMP. Next, we examined the role of PKA in the regulation of α7 nAChRs. Co-transfecting a dominant negative form of PKA (PKA-DN) abolished 8-Br-cAMP's effect of diminishing α7 nicotinic currents, while constitutively active catalytic subunit of PKA (PKA-Cα) decreased α7 currents relative to control. In brain slices, KT-5720, an inhibitor of PKA, nullified 8-Br-cAMP's effect on attenuating

α7 nicotinic currents, while applying a purified catalytic subunit of PKA in the pipette solution significantly decreased α7 currents. The decrease in α7 nicotinic currents was not due to decreases in single-channel conductance, as determined by current fluctuation analysis nor changes in gating kinetics. Using mutant α7 receptors, where serine 365 was mutated to alanine (α7(S365A)) in the M3-M4 cytoplasmic domain, there was no effect of 8-Br-cAMP on α7 receptor function indicating that PKA's effect was directly on α7 receptors. Furthermore, 8-Br-cAMP activation of PKA reduced surface expression of α7 nAChRs, as visualized by surface labelling with Alexa 647-conjugated α-bungarotoxin, but had no effect on the surface expression of the mutant form of the receptor, α7(S365A). These results demonstrate that the α7 nicotinic receptors constitute a major substrate for modulation via the cAMP/PKA pathway and suggest that factors which regulate physiological intracellular cAMP levels can modulate α7 responses within neurons.

Publication Information

This Chapter is based in part on the following manuscript "cAMP-Dependent Protein Kinase Decreases α7 Nicotinic Receptor Activity in Layer 1 Prefrontal Cortical Interneurons", **Pragya Komal**, Anthony Renda and Raad Nashmi (in preparation). P.K. and R.N. designed the research; P.K. and A.R. performed the experiments; P.K., A.R. and R.N. analyzed the data; P.K., A.R. and R.N. wrote the paper.

4.1 Introduction

Neuronal nicotinic acetylcholine receptors (nAChRs) have a widespread distribution throughout the brain and play a key role in mediating neurotransmission in the CNS. The homopentameric α7 nAChR receptor is the second most abundant nAChR subtype in the brain after α4β2 (Clarke et al., 1985; Gotti et al., 2006; Nashmi and Lester, 2006; Perry et al., 2002; Whiting et al., 1987) and is known to enhance cognitive behaviors such as attention (Levin, 2002; Simon Sydserff, 2009; Young et al., 2007) and memory (Castner et al., 2011; Thomsen et al., 2010; Yang et al., 2013). Dysfunction of α7 receptors have been implicated in various neurological disorders. Altered expression of α7 nAChRs have been found in the brains of smokers, people stricken with schizophrenia and Alzheimer's disease (AhnAllen, 2012; Freedman et al., 1995; Wevers et al., 1999). Therefore, understanding how modifications to α7 nAChRs alter their function and expression in neurons will further enhance our knowledge of the mechanisms that α7 nAChRs contribute to normal behaviors and pathological neural disorders. Protein kinases play a major role in modifying the activity of ion channels and ultimately neuronal excitability (Astman et al., 1998; Komal et al., 2014; Liu and Murray, 2012; Man et al., 2007; Porter et al., 1990). The two major subclasses of protein kinases are those that target tyrosine for phosphorylation (tyrosine kinases) and the serine/threonine kinases. Protein kinase A (PKA) was first discovered and isolated in 1968 from rabbit skeletal muscle (Walsh et al., 1968) and is an enzyme that phosphorylates serines of target proteins (Maller et al., 1978). PKA is a tetrameric complex consisting of two regulatory and two catalytic subunits (Naira et al., 1985). Upon binding to cAMP the regulatory subunits release the catalytic subunits, which are then activated. In neurons,

PKA has a wide range of substrates ranging from ion channels to transcription factors (Meyer and Shen, 2000; Zhong et al., 2009). For example, PKA mediated phosphorylation of glutamate receptors has been shown to affect multiple forms of synaptic plasticity (Esteban et al., 2003).

α7 nAChRs, like other nAChRs, are substrates of protein kinases (Komal et al., 2014; Moss et al., 1996; Vijayaraghavan et al., 1990). One major mechanism regulating the function of α7 nAChRs and other nAChR subtypes is the phosphorylation of the major cytoplasmic loop of the receptor, which contains putative phosphorylation sites for protein kinases including PKA and tyrosine kinase (Moss et al., 1996; Charpantier et al., 2005). Electrophysiological studies have shown that Src-family of tyrosine kinases can negatively regulate the function of α7 nAChRs(Charpantier et al., 2005; Cho et al., 2005; Komal et al., 2014) In addition to phosphotyrosine, there is a serine in the M3-M4 cytoplasmic loop of both chick and rat α7 nAChRs, which has been shown to be phosphorylated by PKA but not CaMKII, PKC nor PKG (Moss et al., 1996). There have been studies that have examined the impact of PKA on nAChR function mainly in the peripheral nervous system (Margiotta et al., 1987) and in the muscle (Green et al., 1991). Interestingly, activation of α7 nAChRs themselves results in a signal transduction, which activates PKA (Cheng and Yakel, 2014; Dajas-Bailador et al., 2002). However, to date there has been no report on the effect of PKA on modulating α7 nAChR activity in the CNS.

In this study, we show that PKA activation via 8-Br-cAMP reduces α7 nicotinic receptor currents expressed in transfected HEK 293T cells and in layer 1 interneurons of the mouse prefrontal cortex (PFC). The PKA mediated effect on receptor function was

absent in HEK 293T cells expressing an α7 nAChRs with a serine 365 to alanine mutation in the putative PKA phosphorylation site. Additionally, we show that the cAMP-PKA pathway mediates the attenuation of α7 nAChR function since a constitutively active form of PKA in HEK 293T cells also dampended α7 nAChR currents and conversely a dominant negative form of PKA prevented 8-Br-cAMP's negative modulation of α7 whole-cell currents. Using α-bungarotoxin labeling we found that 8-Br-cAMP stimulation decreased surface expression of α7 nAChRs in HEK 293T cells. Together, our results show that the PKA signaling decreases α7 nicotinic receptor mediated cholinergic neurotransmission in layer 1 interneurons of the prefrontal cortex due to a decrease in surface receptor expression.

4.2 Experimental Procedures

4.2.1 cDNA constructs

Mouse α7 cDNA were kindly provided by Jerry Stitzel (University of Michigan, Ann Arbor, MI). Venus fluorescent protein cDNA was provided by Atsushi Miyawaki (Riken Brain Science Institute, Tokyo, Japan) (Nagai et al., 2002). Human RIC-3 cDNA was provided by Neil Millar (The University College London, UK) (Lansdell et al., 2005). The cDNA for mouse α7 nAChR subunit tagged with Venus fluorescent protein (α7-V) in the M3-M4 cytoplasmic loop, was generated previously in the lab (Komal et al., 2014). In mutant α7(S365A) cDNA the serine 365 codon (AGC) was mutated to the alanine codon (GCA) by site directed mutagenesis (Bio Basic Inc.). A dominant negative mouse PKA plasmid M7 pdnPKA-GFP cDNA (Ungar and Moon, 1996) and a PKA catalytic

subunit C alpha (PKA-Cα) cDNA (Uhler and McKnight, 1987) were ordered from Addgene (cat # 16716 and 15310, respectively) .

4.2.2 HEK 293T cell culture and transfection

HEK293T cells were maintained in plating media consisting of Dulbecco's Modified Eagle medium (DMEM), supplemented with 10% fetal bovine serum (FBS), 2 mM L-glutamine, 100 U/ml penicillin and 100 μg/ml streptomycin. For electrophysiology 35 mm petri dishes were coated with 5 mm diameter round glass coverslips (cat # 64-0700, Warner) with 1% gelatin type B (cat# GX0048-1, EMD™) or 1 mg/ml poly-DL-lysine (cat# P9011, Sigma-Aldrich) for 2 hours. For confocal imaging, HEK293T cells were grown on glass coverslip bottom dishes (cat# P35G-1.0-14-C, MatTek Corporation) coated for 2 hrs with 1% gelatin. Cells were maintained in a 5% CO_2 incubator at 37°C. Cells were grown to 40-50% confluency and then transiently transfected with fugene transfection reagent (cat # PRE2311, Promega). To each 35 mm dish, 2 μg cDNA of either α7, α7-Venus or their S365A mutant versions, 2 μg cDNA of RIC-3 and 3 μl of Fugene Transfection Reagent (catalog #PRE2311, Promega) were mixed with 250 μl of warmed incomplete media, which is the plating media minus FBS. Venus cDNA (0.2 μg) was added to α7 to visually identify transfected HEK293 cells for whole-cell patch-clamp recordings.

4.2.3 Drugs

8-Bromo-cAMP, sodium salt (8 μM, cat# 1140), cAMPS-Rp, triethylammonium salt (100 μM, cat#1337), PHA543613 hydrochloride (100 μM, cat# 3092), CNQX disodium salt (10 μM, cat# 1065), KT-5720 (200 nM, cat# 1288) were all ordered from Tocris

Bioscience. Acetylcholine chloride was ordered from Sigma-Aldrich (1 mM, cat# A6625) while tetrodotoxin citrate (0.5 μM, Cat # T-550) was purchased from Alomone Labs. Protein kinase A catalytic subunit protein that was added to the pipette solution during slice electrophysiology was obtained from Sigma-Aldrich (200 U/ml, cat# P2645).

4.2.4 Whole-cell patch-clamp electrophysiology from cultured cells

HEK 293T cells were visualized with differential interference contrast illumination using an upright microscope (Nikon FN1) with a CFI APO 40X W NIR objective (0.80 numerical aperture, 3.5 mm working distance). We identified transfected cells with Venus fluorescent protein using fluorescence illumination with a mercury lamp. Whole-cell patch-clamp recordings were performed using a Multiclamp 700B amplifier (Molecular Devices), low passed filtered at 4 kHz, digitized at 10 kHz with a Digidata 1440A (Molecular Devices) and recorded using pClamp 10.2 acquisition software (Molecular Devices).

During recordings, cells were perfused continuously at 2 ml/min with extracellular solution comprised of the following (in mM): 150 NaCl, 4 KCl, 2 $CaCl_2$, 2 $MgCl_2$, 10 HEPES, and 10 D-glucose adjusted to pH 7.4. Extracellular recording solution was maintained at 31^{o}C using a temperature controller (TC-344B, Warner Instruments) and in-line heater (SH-27B, Warner Instruments). Standard whole-cell patch-clamp recordings were performed using patch pipettes pulled from borosilicate glass electrodes (1.5 mm OD and 1.0 mm ID, catalog #1B150F-4, WPI) on a P-97 Flaming/Brown micropipette puller (Sutter Instruments). Patch electrodes had tip resistances between 6 and 11 MΩ and were filled with (in mM): 108 KH_2PO_4, 4.5 $MgCl_2$, 0.9 EGTA, 9 HEPES, 0.4 $CaCl_2$, 14 creatine phosphate (Tris salt), 4 Mg-ATP, 0.3 GTP

(Tris salt), pH 7.4 with KOH. The membrane potential was held at -60 mV and corrected for liquid junction potential. Acetylcholine (ACh, 1 mM) was applied rapidly for 1 sec duration using the two-barrel glass θ-tube valve driven drug applicator (Komal et al., 2011) positioned 300 μm away from the recorded cell. Solution exchange rates were typically less than 500 μs (10-90% peak time) as measured from open tip junction potential changes using 10% extracellular solution.

4.2.5 Whole-cell patch-clamp electrophysiology from brain slices

All experiments on mice were performed in accordance of the Canadian Council of Animal Care and approved by the Animal Care Committee at the University of Victoria. Postnatal day 10-20 C57BL/6J mice (stock# 000664, The Jackson Laboratory) of either sex were used for all our electrophysiology experiments. Mice were deeply anesthetized with isofluorane and decapitated. Brains were removed and placed in ice-cold slicing solution containing the following (in millimolar): 250 sucrose, 2.5 KCl, 1.2 NaH_2PO_4, 1.3 $MgCl_2$, 2.4 $CaCl_2$, 26 $NaHCO_3$ and 11 D-glucose. Coronal slices (320 μm thick) were cut with a vibratome (Leica 1000S) from prefrontal and frontal cortices and transferred to an extracellular recording solution filled incubation chamber in a 32°C water bath for at least 45min, before being transferred to the recording chamber. During recordings, slices were perfused continuously at 2 ml/min with extracellular solution comprised of the following (in mM): 125 NaCl, 2.5 KCl, 1.2 NaH_2PO_4 , 1.3 $MgCl_2$, 2.4 $CaCl_2$, 26 $NaHCO_3$, and 11 D-glucose, aerated with 95% O_2 and 5% CO_2 during incubation and recording. Layer 1 interneurons of the medial prefrontal cortex were visualized and targeted for whole-cell recordings using an upright microscope (Nikon FN1) with a CFI APO 40X W NIR objective (0.80 numerical aperture, 3.5 mm working distance) and

equipped with infra-red video-assisted differential interference contrast illumination. Patch electrodes had tip resistances between 6 and 11 MΩ and were filled with pipette solution containing (in mM): 130 potassium gluconate, 5 EGTA, 0.5 $CaCl_2$, 2 $MgCl_2$, 10 HEPES, 3 Mg-ATP, 0.2 GTP, and 5 phosphocreatine Tris, pH adjusted to 7.4 with KOH, osmolarity adjusted to 300 mOsm with sucrose. Whole-cell voltage-clamp recordings were performed at 31°C using a temperature controller (TC-344B, Warner Instruments) and in-line heater (SH-27B, Warner Instruments), with a MultiClamp 700B amplifier (Molecular Devices) and pCLAMP 10.2 software (Molecular Devices). Data were low passed filtered at 4 kHz and sampled at 10 kHz with a Digidata 1440A data acquisition system (Molecular Devices). The membrane potential was corrected for liquid junction potential, and series resistance was monitored throughout the experiment. Neurons were held at -60 mV. A specific agonist for α7 nicotinic receptor, 100 μM PHA543613 hydrochloride was applied for 1 s duration, every 1 minute, using a valve driven θ-tube drug applicator system (Komal et al., 2011)

4.2.6 Current fluctuation analysis to estimate single-channel conductance

Single-channel conductance of α7 nicotinic receptors was determined by performing non-stationary fluctuation analysis on whole-cell mediated α7 nicotinic receptor responses from brain slices, elicited via application of 100 μM PHA543613 hydrochloride, at -60 mV. This technique has been previously described by (Brown et al., 1998; Komal et al., 2014; Sigworth, 1980). We used Clampfit 10.2 software (Molecular Devices) to conduct fluctuation analysis on the whole-cell current traces. In brief, an ensemble of α7 nAChR responses was aligned by the point of maximal rise and averaged. The mean responses was scaled to the peak and substracted from individual responses. The variance of the

current at each sample point of each trace was plotted against the mean current of the averaged traces at the same sample point in time. Then a linear fit was performed through the sampled points. The slope of the fit estimated the unitary current, i, of the nicotinic ion channel. The single-channel conductance was calculated using the equation $\gamma = i / (V_h - E_{rev})$ where, V_h is the holding potential (-60 mV) and E_{rev} is the reversal potential for α7 receptors, determined experimentally as (-0.7 mV).

4.2.7 Alexa Fluro-647 α-bungarotoxin labeling of surface α7 nAChRs

We utilized Venus fluorescent protein tagged α7 nicotinic receptor (α7-V) cDNA construct tagged with venus fluorophore (α7-V) and hemagglutinin epitope present in the long intracellular cytoplasmic loop spanning third and fourth transmembrane domains. HEK 293T cells plated on coverslip bottom 35 mm culture dishes were transiently transfected (per dish) with 2 μg each α7-V, RIC-3 and 3 μl of Fugene. On second day of post-transfection, cells were treated with sterile H_2O or 100 μM 8-Br-cAMP and incubated at 37ºC for 30 min. Cells were washed once with ice cold PBS (pH 7.4) and then labeled with Alexa Fluor 647 α-bungarotoxin (1mg/ml, Fl-BTx, Cat# B35450, Life Technologies) at 1:200 dilution for an hour at 4°C . Subsequently, cells were washed and fixed with 2% PFA for 10 min at 4°C and washed twice again before imaging. Surface expression of Fl-BTx labeled α7-Venus receptors vs mutant α7-Venus (α7(S365A)-V) receptors were examined with a Nikon C1si spectral confocal microscope system using a Plan Apo VC 60X 1.4 NA oil immersion objective (0.13 mm working distance). A lambda stack of X-Y images were collected simultaneously with each laser sweep onto an array of 32 photomultiplier tubes and averaged over four laser sweeps. Venus fluorophore intensity was imaged between 496.5 – 696.5 nm at 5 nm wavelength

intervals. Fl-BTx was excited with a 638 nm laser line at 20% maximal intensity and wavelength emissions were collected between 590 – 750 nm, averaged over four laser sweeps and Fl-BTx was analyzed at the peak emission of Alexa Fluor 647 (670 nm). Images were acquired over a 50 μm x 50 μm field of view at 512 pixels x 512 pixels digital resolution, and 12 bit intensity resolution. The pixel dwell time was set at 5.52 μsec and the pinhole was set to medium (60 μm diameter). Using ImageJ v1.43r software images were analyzed for mean signal intensity of Fl-BTx per cell and normalized to mean Venus intensity per cell to quantify surface expression of α7-V nicotinic receptors for both control and 8-Br-cAMP treated cells.

4.2.8 Statistics

All data are presented as mean ± standard error (S.E.). Significant difference ($p < 0.05$) between two groups of data were determined using a *t*-test for continuous data meeting parametric assumptions of equal variances and normality. Otherwise, a Wilcoxon rank sum test was performed for nonparametric data. Comparison between three or more groups were analyzed using an analysis of variance (ANOVA) for parametric data followed by *post hoc* multiple pairwise analysis using a Tukey's HSD tests. For nonparametric data involving comparison of three or more groups of data a Kruskal-Wallis rank sum test was performed followed by pairwise analyses using Wilcoxon rank sum tests. We also performed two-way ANOVAs on data with more than one treatment group that was repeated over time. All statistical analyses were performed using the R statistical computing language (www.R-project.org).

4.3 Results

4.3.1 8-Br-cAMP decreases α7 nicotinic receptor currents in HEK 293T cells

Catalytic PKA is activated when cAMP binds to the regulatory subunits of PKA. To test whether activation of PKA can modulate α7 nAChR function, we used 8-Br-cAMP, a cell membrane permeable analogue of cAMP. 8-Br-cAMP, rather than cAMP, was used because 8-Br-cAMP is resistant to hydrolysis by endogenous phosphodiesterases, which normally terminate cAMP signaling. The PKA signaling pathway was triggered by incorporating 8-Br-cAMP in the recording pippette. Since previous studies have shown a dose dependent (100 μM to 1 mM) effect of cAMP on other nicotinic receptor subtypes in insect ganglionic neurons (Courjaret and Lapied, 2001), in the present study we used 100 μM concentration of 8-Br-cAMP throughout our study to examine the effect of activated PKA on α7 naChRs. We examined the effect of 8-Br-cAMP on α7 nicotinic receptor function by performing whole-cell recordings from HEK 293T cells transiently transfected with α7 nicotinic receptors. Control α7 nAChR responses recorded from HEK 293T cells and elicited by 1 mM ACh application (for 1 sec) showed a mean current amplitude of 603 ± 100 pA (n = 21) that maintained a steady amplitude with repeated ACh applications (1 min intervals) **(Fig. 4.27 A, C, D)**. The α7 nAChR responses showed a significant and progressive attenuation in the peak current over repeated ACh applications when 8-Br-cAMP was present in the micropipette solution, with a mean current response of 269 ± 82 pA (n = 15) (p = 0.004, Wilcoxon rank sum test) **(Fig. 4.27 C)** (p = 0.0005, treatment factor, two-way ANOVA) **(Fig. 4.27 D)**. 8-Br-cAMP stimulation resulted in time dependent decrease in α7 nAChR mediated peak response amplitude over repeated ACh applications with a mean exponential decay time constant

of 5.4 ± 1.8 min, with the inset graph of **Fig. 4.27 B** showing an example of one cell with a decay time constant of 4 min. This indicated that the 8-Br-cAMP's effect on decreasing α7 nAChR responses was not instantaneous but occurred on the order of minutes timescale.

We next examined the effect of 8-Br-cAMP on α7 nAChR gating kinetics, by fitting the time course of α7 current decay during ACh application to the sum of two exponential functions. The time course of α7 nAChRs decay kinetics from HEK 293T cells showed no significant difference in either the fast (control: 54 ± 10 ms, n = 18 vs 8-Br-cAMP: 65 ± 19 ms, n = 21) (p = 0.9, Wilcoxon rank sum test) nor the slow time constants (control: 351 ± 92 ms, n = 18 vs 8-Br-cAMP: 238 ± 39 ms, n = 15) (p = 0.8, Wilcoxon rank sum test) between control and 8-Br-cAMP treated cells **(Fig. 4.27 E)**. We also found no significant difference in the percentage composition of the fast or slow decay components of the α7 nicotinic responses between control (amplitude co-efficient τ fast: 22 ± 5 %, n = 18; τ slow: 78 ± 5%, n = 18) and 8-Br-cAMP stimulated cells (amplitude co-efficient τ fast: 21 ± 3%, n = 15; τ slow: 79 ± 3%, n = 15) (p = 0.6, Wilcoxon rank sum test for both τ slow and τ fast) **(Fig. 4.27 F)**. These data indicate that PKA activation via 8-Br-cAMP decreases α7 nAChR function without affecting channel gating kinetics.

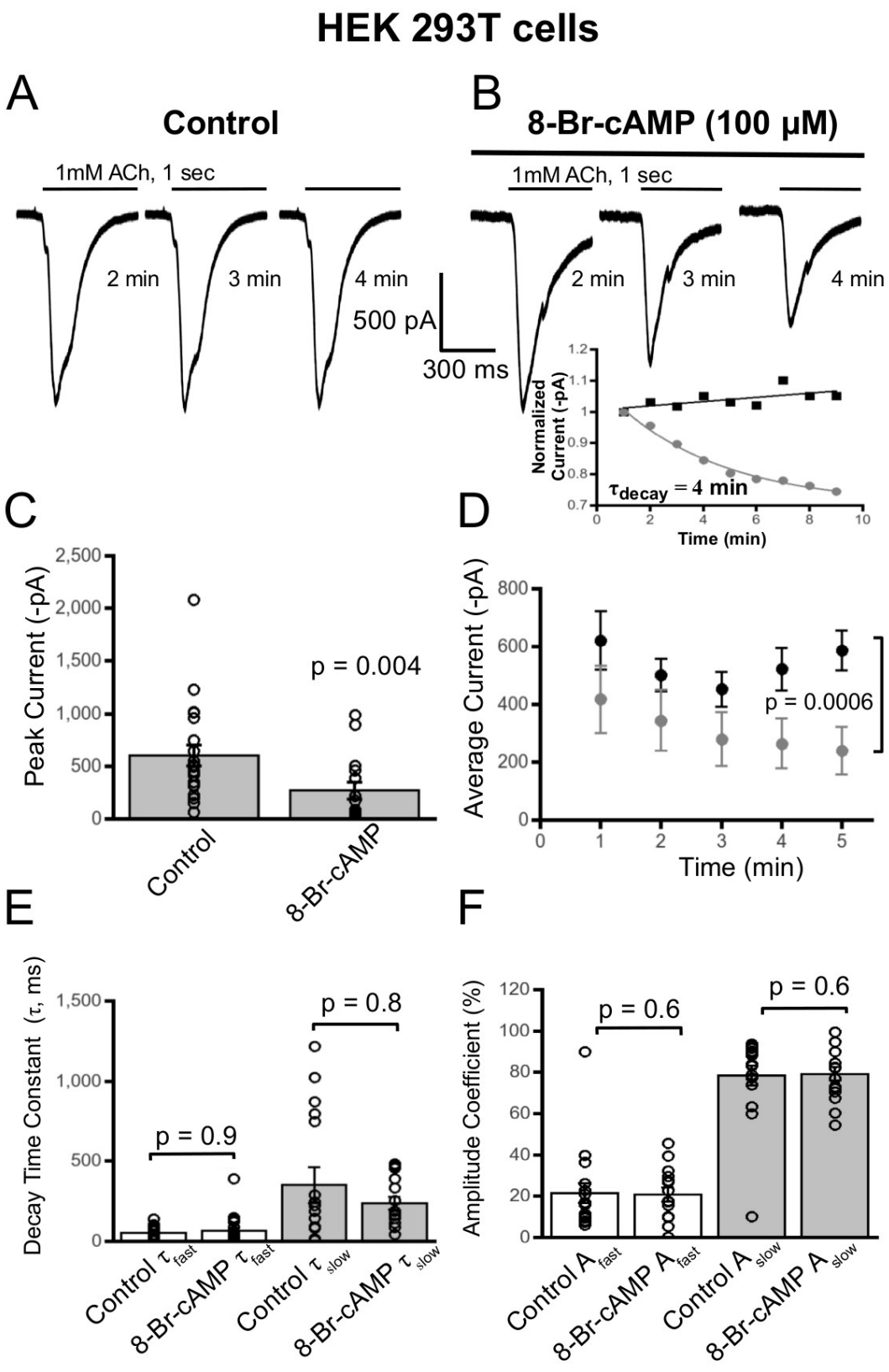
HEK 293T cells
A
Control
1mM ACh, 1 sec
2 min
3 min
4 min
500 pA
300 ms
B
8-Br-cAMP (100 µM)
1mM ACh, 1 sec
2 min
3 min
4 min
Normalized Current (-pA)
τdecay = 4 min
Time (min)
C
Peak Current (-pA)
p = 0.004
Control
8-Br-cAMP
D
Average Current (-pA)
p = 0.0006
Time (min)
E
Decay Time Constant (τ, ms)
p = 0.9
p = 0.8
Control τfast
8-Br-cAMP τfast
Control τslow
8-Br-cAMP τslow
F
Amplitude Coefficient (%)
p = 0.6
p = 0.6
Control Afast
8-Br-cAMP Afast
Control Aslow
8-Br-cAMP Aslow

Figure 4.27 8-Br-cAMP stimulation attenuates α7 nAChR currents upon repetitive ACh application in HEK 293T cells.
Acetylcholine (1mM) evoked α7 nAChR whole-cell currents traces for control **(A)** and 8-Br-cAMP (100 μM) treated cells showing a decline in α7 currents in the 8-Br-cAMP treated cells **(B)**. **(B)** Inset graph shows the quantification of the progressive decline in α7 response, which decayed with a time constant of 4 min. **(C)** The mean current amplitude of α7 nAChRs from control (n = 21) differed significantly from 8-Br-cAMP stimulated cells (n = 15) (p = 0.004, Wilcoxon rank sum test). For all the figures, bars represent mean ± SE of responses with each measured cell represented as a circle. **(D)** Mean current amplitude of ACh mediated α7 whole cell currents at 1 min time intervals for 8-Br-cAMP stimulated cells was significantly attenuated as compared to control (p = 0.0006, two-way ANOVA). **(E)** Decay kinetics of α7 nicotinic receptor currents during ACh application showed no change in fast and slow decay time constant for control (n = 18) and 8-Br-cAMP (n= 21) (p = 0.9 for τfast, p = 0.8 for τslow, Wilcoxon rank sum tests) stimulated cells. **(F)** No difference in the percentage composition of amplitude coefficients are observed for fast and slow decay time components of α7 nAChRs responses for control (n = 18) and 8-Br-cAMP stimulated neurons (n = 15) (p = 0.6, Wilcoxon rant sum tests for both τfast and τslow components).

4.3.2 8-Br-cAMP stimulation inhibits α7 nicotinic receptor currents in layer 1 cortical interneurons

Layer 1 neurons of the prefrontal cortex are predominantly GABAergic and the majority of these interneurons exhibit robust α7 nicotinic receptor currents (Charpantier et al., 2005; Christophe et al., 2002; Komal et al., 2014). Since we found that in cell lines 8-Br-cAMP activation of PKA attenuates α7 nicotinic receptor function we asked whether the same modulation occurs for α7 nAChRs endogenously expressed in CNS neurons. Therefore, we targeted layer 1 medial prefrontal cortical neurons for whole-cell recordings. Recordings were performed in the presence of TTX (0.5 μM) and CNQX (10 μM) to block action potential dependent release of neurotransmitters and α-amino-3-hydroxy-5-methyl-4-isoxazolepropionic acid (AMPA) receptors. We examined α7 nAChRs responses elicited by the rapid application of α7 nAChR selective agonist PHA543613 (100 μM for 1 sec duration, every 1 min) from control and 8-Br-cAMP

stimulated neurons, in which the intracellular pipette solution contained 100 μM 8-Br-cAMP. The average peak current of the α7 nAChR responses of the 8-Br-cAMP stimulated neurons (67 ± 4 pA, n = 26) was significantly reduced as compared to the α7 nAChR responses of control treated neurons (104 ± 9 pA, n = 18) (p = 0.008, t-test) **(Fig 4.28 A-C)**. Moreover, neurons stimulated with 8-Br-cAMP (100 μM) in the recording pipette showed a significantly greater progressive time-dependent decrease in α7 mediated whole-cell currents (n = 13) as compared to α7 nAChR currents recorded from control treated neurons (n = 27) (p = 0.03, treatment factor, two-way ANOVA), which showed no decrement in amplitude of α7 nAChR currents over time **(Fig. 4.28 D)**. The time course of the progressive inhibition of α7 nAChR current responses mediated by 8-Br-cAMP in layer 1 cortical neurons occurred with an exponential decay time constant of 2.2 ± 0.6 min. These results indicated that 8-Br-cAMP mediated negative modulation of α7 nicotinic receptor activity in neurons, just like in HEK cells, occurred on a timescale of minutes, which is more consistent with 8-Br-cAMP targeting PKA and eliciting signal transduction actions of PKA, rather than 8-Br-cAMP nonspecifically inhibiting α7 nAChRs directly, which would have occurred almost immediately.

To examine whether 8-Br-cAMP altered the gating kinetics of α7 nAChRs expressed in neurons, we analyzed the current decay of α7 during the 1 sec PHA543613 application by fitting the decay current to a function of two exponentials. There was no significant difference in the fast (control τ fast: 20 ± 4 ms, n = 20 vs 8-Br-cAMP τ fast: 26 ± 5 ms, n = 20) (p = 0.4, Wilcoxon rank sum test) nor slow decay kinetics (control τ slow: 165± 42 ms, n = 20 vs 8-Br-cAMP τ slow: 194 ± 36 ms, n = 20) (p = 0.1, Wilcoxon rank sum test) of α7 nicotinic responses recorded from brain slices **(Fig. 4.28**

E). Also, the percentage composition of the fast (control τ fast: 45 ± 6%, n = 20 vs 8-Br-cAMP τ fast: 44 ± 5%, n = 20) or slow decay components (control τ slow: 55 ± 6%, n = 20 vs 8-Br-cAMP τ slow: 57 ± 5%, n = 20) of the α7 nicotinic responses from layer 1 interneurons, calculated as amplitude coefficients, were not different between control and 8-Br-cAMP treated neurons ($p = 0.4$ and $p = 0.6$, t-tests for slow and fast τ components, respectively) **(Fig. 4.28 F)**. These observations indicate that 8-Br-cAMP stimulated decrease of α7 nicotinic currents in layer 1 interneurons was not due to alterations in receptor gating kinetics.

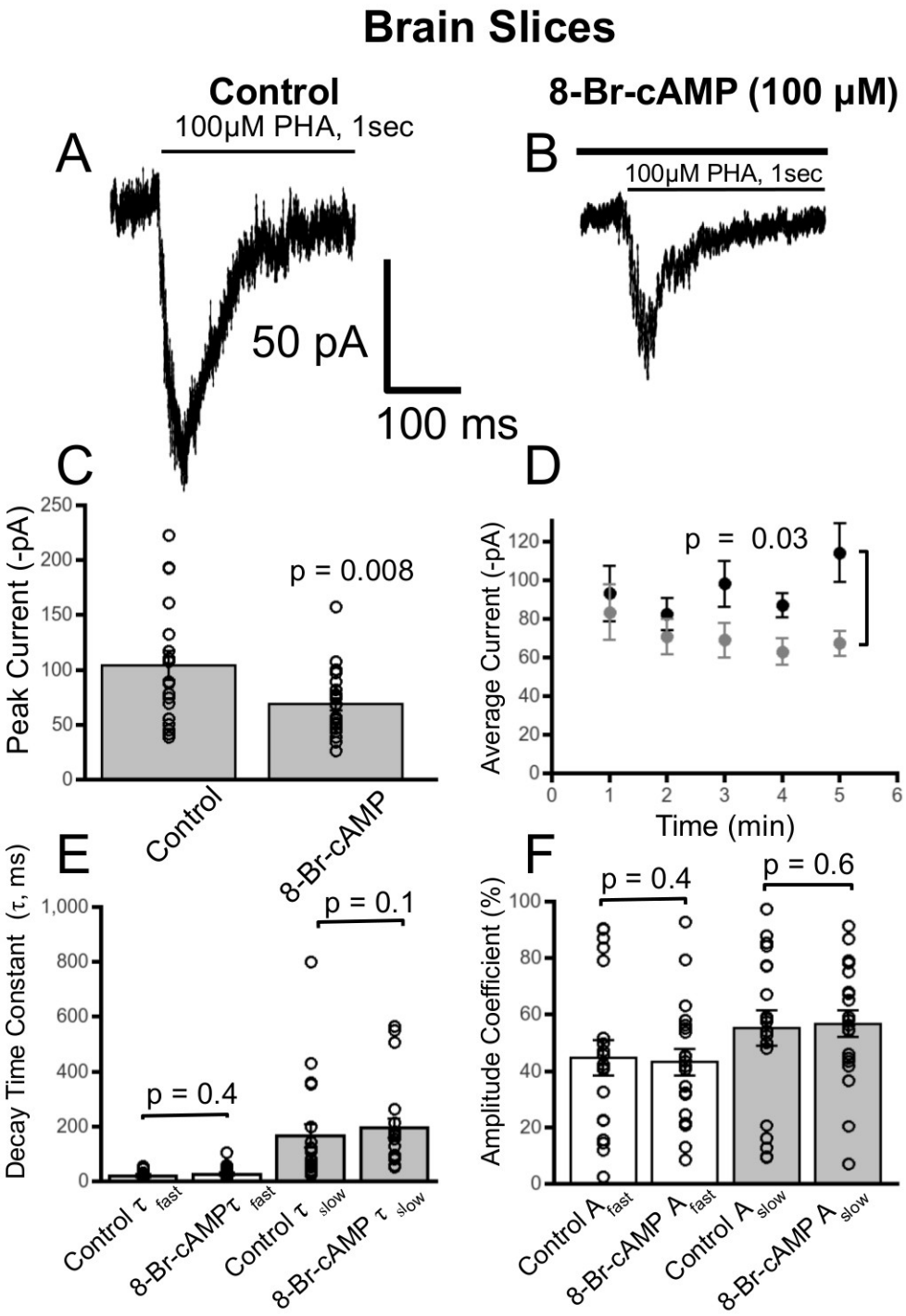

Figure 4.28 8-Br-cAMP mediated attenuation of α7 nAChR currents in layer 1 PFC interneurons.

(A,B) Exemplary traces of PHA543613 (100 µM) activated whole-cell α7 nicotinic responses for control and 8-Br-cAMP dialyzed layer 1 interneurons. **(C)** There was a significant decrease in the mean current amplitude of α7 nAChRs of 8-Br-cAMP (100

μM) (n = 26) treated interneurons as compared to control (n = 18) (p = 0.008, Wilcoxon rank sum test). **(D)** Time dependent reduction of α7 nAChR responses with 8-Br-cAMP (n = 13) as compared to control (n = 17) (p = 0.03, two-way ANOVA). **(E)** An illustration of desensitization decay kinetics of α7 nAChR currents showing no change in fast and slow decay time constants for control (n = 20) and 8-Br-cAMP (n= 20) p = 0.4 for τfast, p = 0.1 for τslow, Wilcoxon rank sum tests) administered interneurons. No difference in the percentage composition of amplitude coefficients are observed for fast and slow decay time components of α7 nAChRs responses for control (n = 20) and 8-Br-cAMP stimulated neurons (n = 20) (p = 0.4 and p = 0.6 , for τfast and τslow components, respectively, Wilcoxon rank sum tests).

4.3.3 In HEK 293T cells 8-Br-cAMP activates PKA to inhibit α7 nicotinic receptor function

We further investigated whether 8-Br-cAMP modified α7 nicotinic receptor currents through the activation of PKA by performing experiments using a dominant negative form of PKA (PKA-DN) and alternatively PKA catalytic subunit alpha (PKA-Cα), which would be a constitutively active form of PKA. The dominant negative form of PKA has a single mutation in one of the cAMP binding sites of the regulatory domain of the enzyme thus resulting in a loss of PKA function. In HEK 293T cells transfected with only α7 nAChRs and recorded using control patch pipette solution, application of ACh (1 mM) elicited an average α7 nAChR response of 484 ± 72 pA (n = 16). With 8-Br-cAMP (100 μM) in the micropipette, there was a significant attenuation of α7 receptor responses to 273 ± 39 pA (n = 11) (p = 0.01, Kruskal-Wallis rank sum test; p = 0.009, Wilcoxon rank sum test *post hoc* analysis) **(Fig. 4.29)**. In contrast, 8-Br-cAMP was unable to alter α7 nicotinic responses in HEK 293T cells in which α7 nAChRs were co-transfected with the dominant negative form of PKA (390 ± 36 pA, n = 11) as compared to control responses (p = 0.57, Wilcoxon rank sum test). However, the mean α7 nAChR whole-cell currents recorded from PKA-DN expressing cells that were treated with 8-Br-cAMP (390 ± 36

pA, n = 11) was significantly greater than cells only expressing α7 nAChRs and exposed to 8-Br-cAMP (273 ± 39 pA, n = 11) (p = 0.03, Wilcoxon rank sum test) **(Fig. 4.29)**. These results provide additional supporting evidence that 8-Br-cAMP inhibits α7 function through activation of PKA.

To further support that PKA is negatively modulating α7 nicotinic receptor function we had undertaken an alternative approach to the previous set of experiments. We utilized mouse PKA catalytic subunit alpha (PKA-Cα) cDNA and co-transfected it with α7 nAChRs in HEK 293T cells. By over-expressing PKA catalytic subunit-Cα via transient transfection, we are essentially creating a constitutively active form of PKA since the catalytic subunits would greatly outnumber the PKA regulatory subunits. ACh (1mM) mediated whole-cell currents for α7 nicotinic receptor responses co-transfected with PKA-Cα showed a significant decrease in the average peak current amplitude (416 ± 76 pA, n = 9) as compared to control cells having only α7 receptors (702 ± 73 pA, n = 12) (p = 0.01, t-test) **(Fig. 4.30 A-C)**. Unlike previous experiments in which 8-Br-cAMP in the recording pipette resulted in a α7 current amplitude that started equal to control but diminished progressively greater over time than the steady α7 current of the control cells, the PKA-Cα expressing cells (n = 9) consistently showed significantly smaller α7 nAChR current and remained steady at the same diminished current amplitude as compared to the control cells (n = 12) (p < 0.001, treatment factor, two-way ANOVA) **(Fig. 4.30)**. We also found no difference in channel gating kinetics (data not shown). These results strongly indicate that overstimulation of PKA activity in cells strongly attenuates α7 nicotinic receptor function.

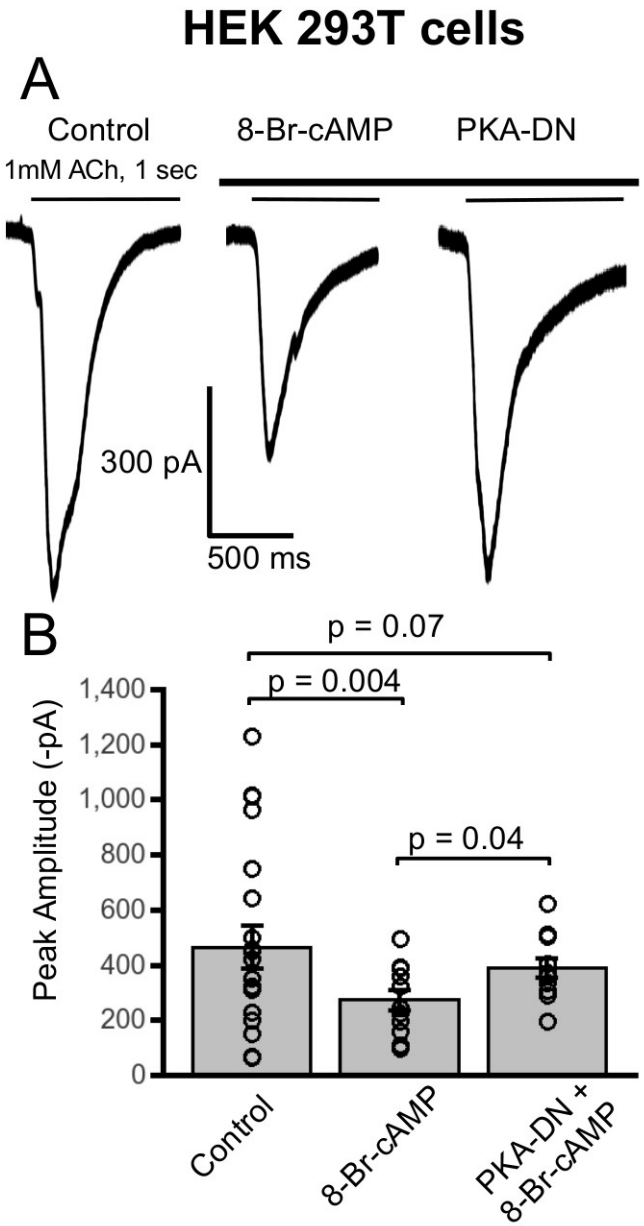

Figure 4.29. Dominant Negative PKA abolishes the effect of 8-Br-cAMP on α7 nAChR responses.

(A) Exemplary waveforms of ACh (1 mM) evoked α7 nAChR responses from HEK 293T cells under three conditions including: control treatment, 8-Br-cAMP treatment and 8-Br-cAMP treatment with co-transfected dominant negative PKA (PKA-DN). **(B)** 8-Br-cAMP (100 μM) (n = 11) stimulation resulted in a signficant attenuation of the mean α7 nicotinic receptor current as compared to control (n = 16) (p = 0.004, Welch t-test). This attenuation in nAChR current with 8-Br-cAMP was abolished when PKA-DN (n = 11) was co-transfected (p = 0.07, Welch t-test). However, 8-Br-cAMP stimulation in α7 only cells was significantly attenuated α7 receptor currents as compared to cells co-transfected

with PKA-DN (p = 0.04, Welch t-test). No effect of 8-Br-cAMP stimulation on cells co-tranfected with PKA-DN as compared to Control (p = 0.07, Welch t-test).

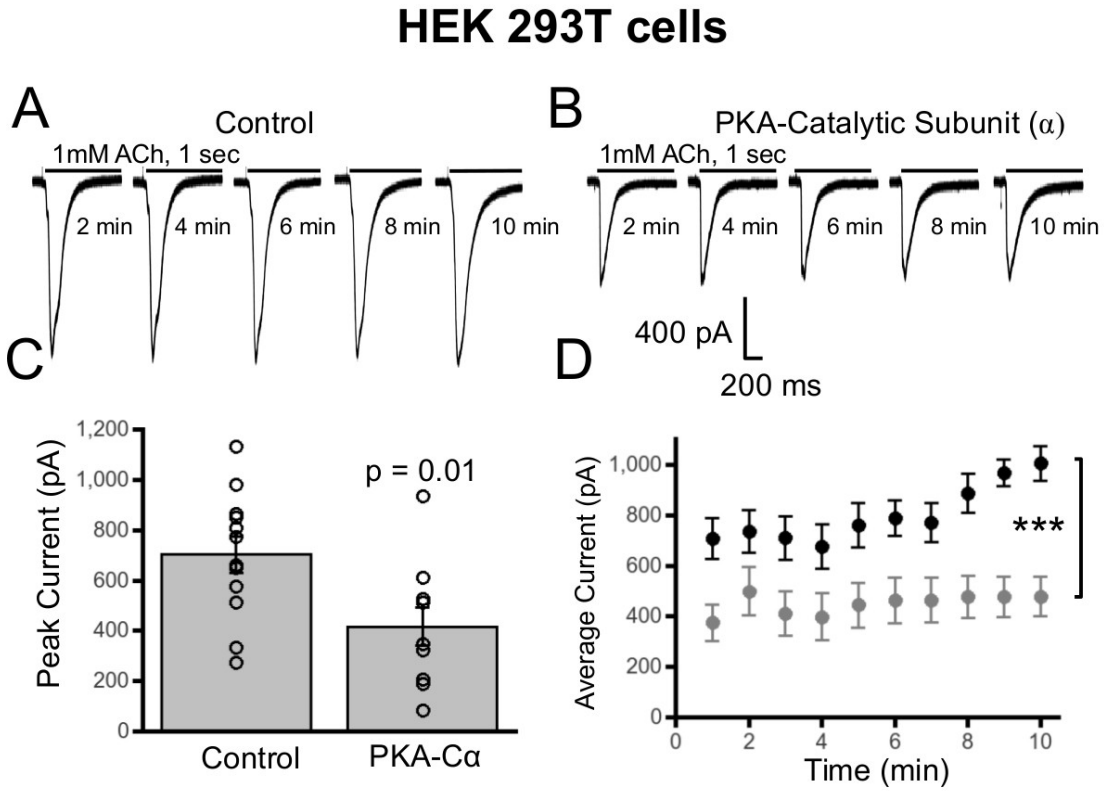

Figure 4.30. Protein kinase A catalytic subunit inhibits α7 nAChR responses in HEK 293T cells.

(A) Sample traces of ACh (1mM) evoked α7 nAChR responses from HEK 293T cells transiently expressing α7 nAChRs only and **(B)** α7 receptors co-expressed with PKA catalytic subunit-alpha (PKA-Cα)**. (C)** A significant decrease in the mean current amplitude of α7 nAChRs is observed from cells co-expressing PKA-Cα (n = 9) as compared to control (cells expressing only α7 nAChRs) (n = 12) (p = 0.01, t-test). **(D)** PKA-Cα and α7 nAChR co-transfected cells consistently showed steady and reduced α7 nicotinic responses with repeated ACh applications as compared to control (α7 nAChRs only) (***, p < 0.0001, two-way ANOVA).

4.3.4 PKA activation inhibits α7 nicotinic currents in layer 1 PFC neurons

To confirm that activation of PKA in neurons will also inhibit α7 nicotinic currents we performed whole-cell recordings from layer 1 PFC interneurons in brain slices. The PKA

catalytic subunit (200 U/ml) was included in the patch electrode solution during the recording of PHA543613 (100 μM) elicited α7 responses. We found that neurons dialized with the active form of the PKA catalytic subunit caused a significant decrease in the α7 nicotinic responses (56 ± 6.7 pA, n = 15) from layer 1 interneurons as compared to responses recorded with control patch electrode solutions (101 ± 9 pA, n = 30)(p = 0.003, Kruskal-Wallis rank sum test; p = 0.002, Wilcoxon rank sum test, *post hoc* analysis) **(Fig. 4.31)**. The decrease in α7 nAChR current responses with catalytic PKA (56 ± 7 pA, n = 15) (p = 0.002, Wilcoxon rank sum test) was similar to that of 8-Br-cAMP (100 μM) stimulation (62 ± 3 pA, n = 23). However, having the PKA blocker KT-5720 (200 nM) in the patch recording solution (111 ± 15 pA, n = 14, p = 0.7, Wilcoxon rank sum test) abrogated any decrease with 8-Br-cAMP application. These observations suggest that endogenous PKA in CNS neurons play an important role in regulating synaptic transmission by inhibiting α7 nicotinic responses in layer 1 cortical neurons.

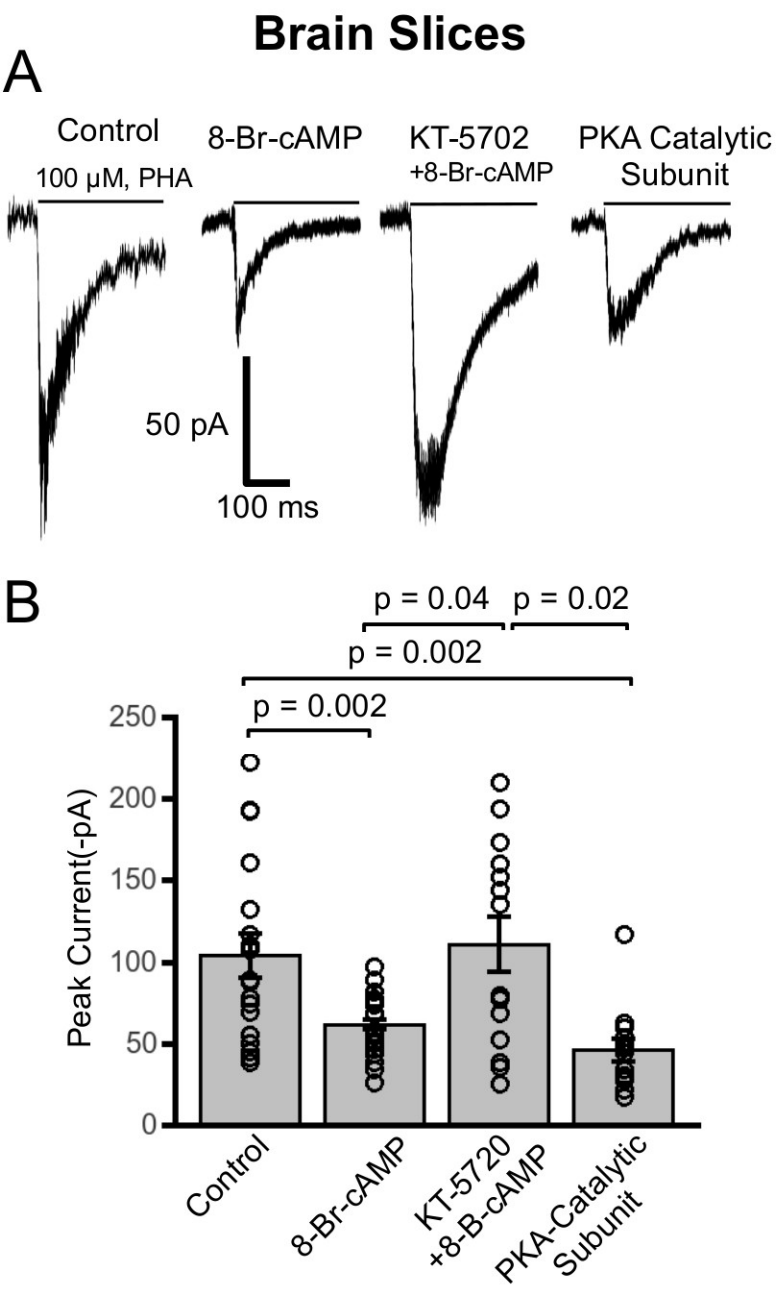

Figure 4.31. PKA activation and inhibition have opposing effects on modulating α7 nAChR currents in PFC interneurons.
(A) Exemplary traces of PHA543613 (100 µM) evoked α7 nAChRs whole-cell current responses from layer 1 interneurons for control, 8-Br-cAMP (100 µM), KT-5720 (200nM, PKA inhibitor) and PKA catalytic subunit (200 U/ml). **(B)** Plot illustrating differences in the mean current amplitude for the four test conditions. α7 receptor responses were significantly attenuated with 8-Br-cAMP (n = 23) as compared to control responses (n = 30) (p = 0.002, Wilcoxon rank sum test). Dialyzing neurons with PKA catalytic subunit in the patch pipette (n = 15) similarly diminished α7 current responses (p = 0.002, Wilcoxon rank sum test). The effect of 8-Br-cAMP in inhibiting α7 nAChRs responses

was abolished with the PKA inhibitor KT-5720 (n = 14), which showed α7 responses that were significantly greater than 8-Br-cAMP (p = 0.04, Wilcoxon rank sum test) and the PKA catalytic subunit activated neurons (p = 0.02, Wilcoxon rank sum test).

4.3.5 PKA activation does not alter α7 nicotinic receptor single-channel conductance

A possible mechanism for the PKA mediated inhibition of α7 nicotinic receptor responses could be decreased intrinsic channel function. To evaluate if 8-Br-cAMP affected α7 nAChR single-channel conductance, we performed ionic current fluctuation analysis on whole-cell recorded α7 nicotinic currents from HEK 293T cells and brain slices. Non-stationary current fluctuation analysis provides a good estimate of single-channel conductance of ion channels (Gill et al., 1995; Komal et al., 2014; Sigworth, 1980, 1981). We tested whether in HEK 293T cells and cortical interneurons 8-Br-cAMP mediated stimulation of PKA decreased α7 nAChR single-channel conductance. The variance of the current fluctuations of ACh (1mM) mediated α7 whole-current responses is plotted against the mean current of the whole-cell current at each time point. The slope of the relationship gives the unitary current and the single-channel conductance (γ) is calculated as the unitary current divided by the electrochemical driving force. Exemplar current fluctuation analyses are shown for control (γ = 57 pS) and 8-Br-cAMP (γ = 58 pS) treated PFC interneurons from brain slices **(Fig. 4.32 A, B)**. On average there was no significant difference in α7 nAChR single-channel conductance of control treated (43 ± 9 pS, n = 18) vs 8-Br-cAMP treated layer 1 interneurons (34 ± 10 pS, n = 11) (p = 0.6, Wilcoxon rank sum test) **(Fig. 4.32 C)**. Also we found no significant difference in the mean single-channel conductance of α7 receptor responses recorded from HEK 293T cells between control (63 ± 16 pS, n = 15) and 8-Br-cAMP (74 ± 16 pS, n = 15) (p = 0.6, Wilcoxon

rank sum test) **(Fig. 4.32 D)**. Therefore, the 8-Br-cAMP mediated decrease in α7 nAChR mediated whole-cell currents is not due to alterations in single-channel conductance.

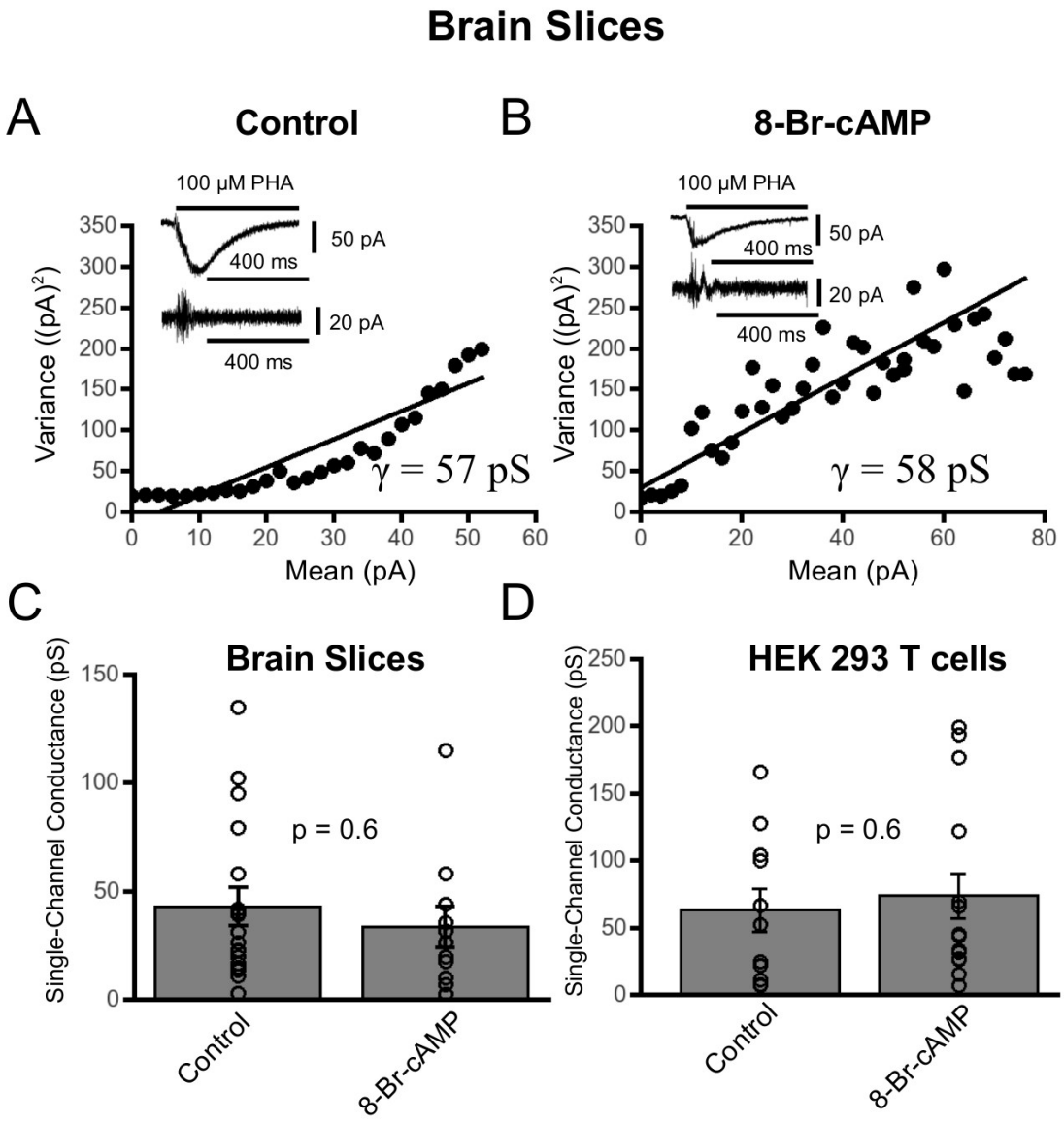

Figure 4.32 8-Br-cAMP stimulation does not alter α7 nAChR single-channel conductance.

(A) Nonstationary current fluctuation analysis depicting mean current-variance relationship performed with PHA543613 (100 µM) elicited α7 nAChR responses from layer 1 interneurons for control and **(B)** 8-Br-cAMP (100 µM, in the recording pipette) stimulated interneurons. Inset shows whole-cell recorded α7 nicotinic current waveforms and their respective AC filtered waveforms for both control and 8-Br-cAMP stimulation. **(C)** No significant change in the mean single-channel conductance is observed for α7

responses between control (n = 18) and 8-Br-cAMP treated cortical interneurons (n = 11) (p = 0.6, Wilcoxon rank sum test). **(D)** No significant difference in the mean single-channel conductance for α7 responses is observed between control (n = 11) and 8-Br-cAMP treated HEK 293T cells (n = 15) (p = 0.6, Wilcoxon rank sum test).

4.3.6 PKA targets serine 365 in the M3-M4 cytoplasmic loop of α7 nAChRs to modulate α7 nAChR function

A previous study showed that a serine residue located in the chick and rat neuronal α7 nAChR is phosphorylated only by protein kinase A and not by protein kinase C, cGMP-dependent protein kinase, or calcium/calmodulin-dependent protein kinase (Moss et al., 1996). Through Prosite analysis of the mouse α7 nAChR cDNA we found a single putative PKA phosphorylation site at serine 365. Therefore, in order to examine whether PKA targets serine 365 directly to modulate α7 nAChR function we produced a mutant form of the α7 nAChR cDNA, in which we mutated serine 365 to alanine α7(S365A). Therefore, in HEK293T cells expressing mutant α7(S365A) receptors we compared the effects of control solution vs 8-Br-cAMP on α7 nAChR mediated whole-cell currents elicited by 1 mM ACh application. Unlike previous results with wildtype α7 nAChRs, for the mutant α7(S365A) receptors there was no significant attenuation of the nicotinic currents from 8-Br-cAMP stimulated cells (809 ± 134 pA, n = 12) as compared to control treatment (826 ± 123 pA, n = 15) (p = 0.4, t-test) **(Fig. 4.33 A-C)**. Repeated application of ACh (every 1 min) showed a consistent amplitude of mutant α7(S365A) receptor currents over 10 min that were not significantly different between recordings performed with 8-Br-cAMP in the patch electrode solution and control patch solutions (p = 0.7, two-way ANOVA) **(Fig. 4.33 D)**. These results imply that serine 365 in the M3-

M4 cytoplasmic loop of α7 nAChRs forms a major regulatory site for PKA in modulating α7 receptor function.

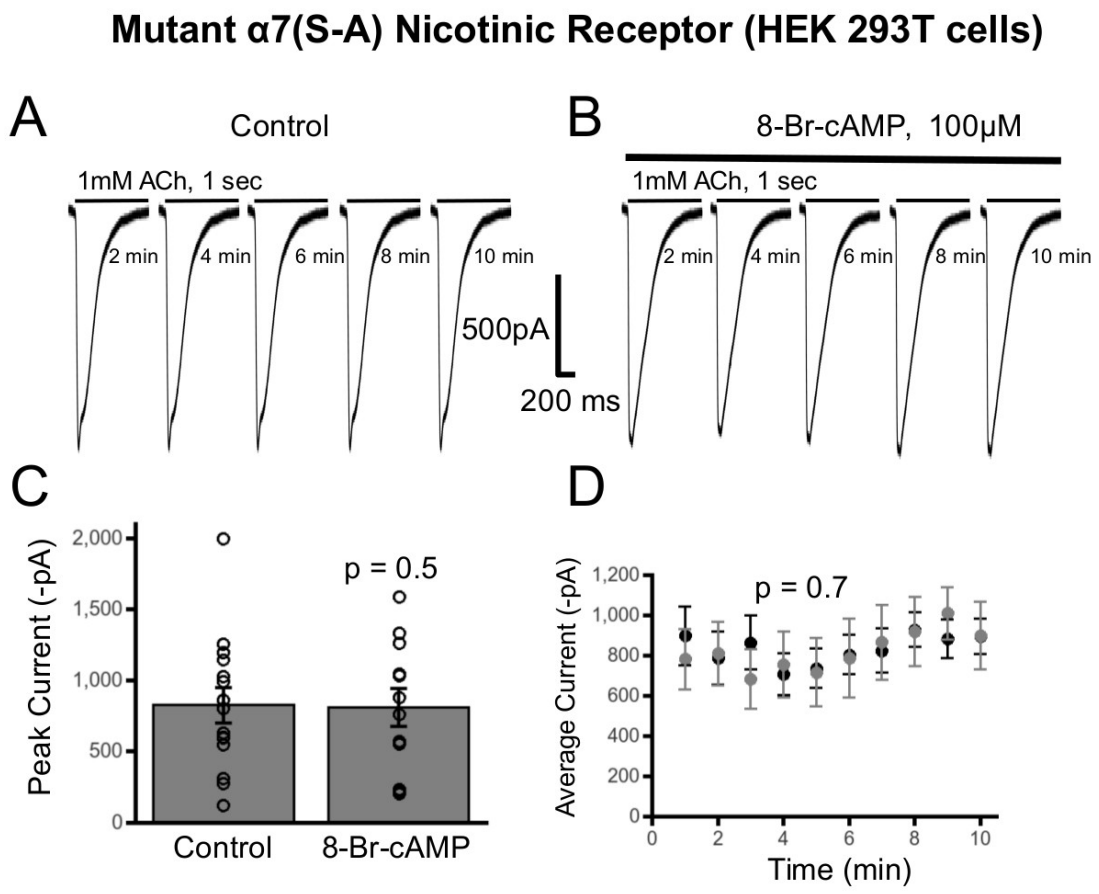

Figure 4.33 PKA targets serine 365 of α7 nAChRs to modulate channel function.

(A) Whole-cell current traces of α7 nAChRs with the serine 365 to alanine mutation (α7(S–A)), shows no alterations in the amplitude of the ACh (1 mM) elicited nicotinic currents with 8-Br-cAMP stimulation of HEK 293T cells **(B).** **(C)** There was no significant difference in ACh mediated mutant α7(S-A) responses between control (n = 15) and 8-Br-cAMP stimulated cells (n = 12) (p = 0.5, t-test). **(D)** Repeated applications of ACh with 1 min intervals showed no time dependent effect of 8-Br-cAMP stimulation on mutant α7(S–A) nAChR responses (n = 12) as compared to Control (n = 15) (p = 0.7, two-way ANOVA).

4.3.7 PKA targets serine 365 to decrease α7 nicotinic receptor surface expression

Since our results ruled out the possibility that PKA modulation of α7 was due to changes in single-channel conductance or gating kinetics, we explored whether a potential mechanism of the negative regulation of α7 nAChR function may be due to decreased surface receptor expression following PKA stimulation. We performed surface labeling of fluorescent protein tagged α7 nAChRs (α7-Venus) transfected in HEK293T cells using Alexa Fluor 647 α-bungarotoxin (Fl-BTx) labeling under nonpermeablized conditions. Spectral confocal images were obtained and the mean intensity of Fl-BTx labeling was normalized to the mean intensity of Venus fluorescence on a per cell basis to calculate the amount of surface expression of α7 nAChRs. We found that 8-Br-cAMP (100 μM for 30 min) stimulated HEK 293T cells transiently transfected with α7-Venus nAChRs, showed significantly less Fl-BTx labeling of surface α7 nAChRs (0.21 ± 0.03, n = 31) as compared to control (0.37 ± 0.05, n = 28) ($p = 0.01$, Wilcoxon rank sum test) **(Fig. 4.34 A-F, M)**. The total cellular Venus flurophore intensity remained the same for control and 8-Br-cAMP treated dishes (data not shown).

Next we tested whether PKA mediates its effect of diminishing surface receptor expression by targeting serine 365 of the α7 nAChR. Using the mutant receptor, α7(S365A)Venus transfected in HEK 293T cells we found no significant difference in the surface expression of mutant α7(S365A)Venus nAChRs with 30 min control treatment (0.06 ± 0.01, n = 25) and mutant α7(S365A)Venus nAChRs with 30 min of 100 μM 8-Br-cAMP incubation (0.07 ± 0.02, n = 13) ($p = 0.5$, Wilcoxon rank sum test) **(Fig. 4.34 G -L, N)**. These results indicate that PKA targets serine 365 of the M3-M4 cytoplasmic loop of α7 nAChRs to down-regulate expression of surface receptors.

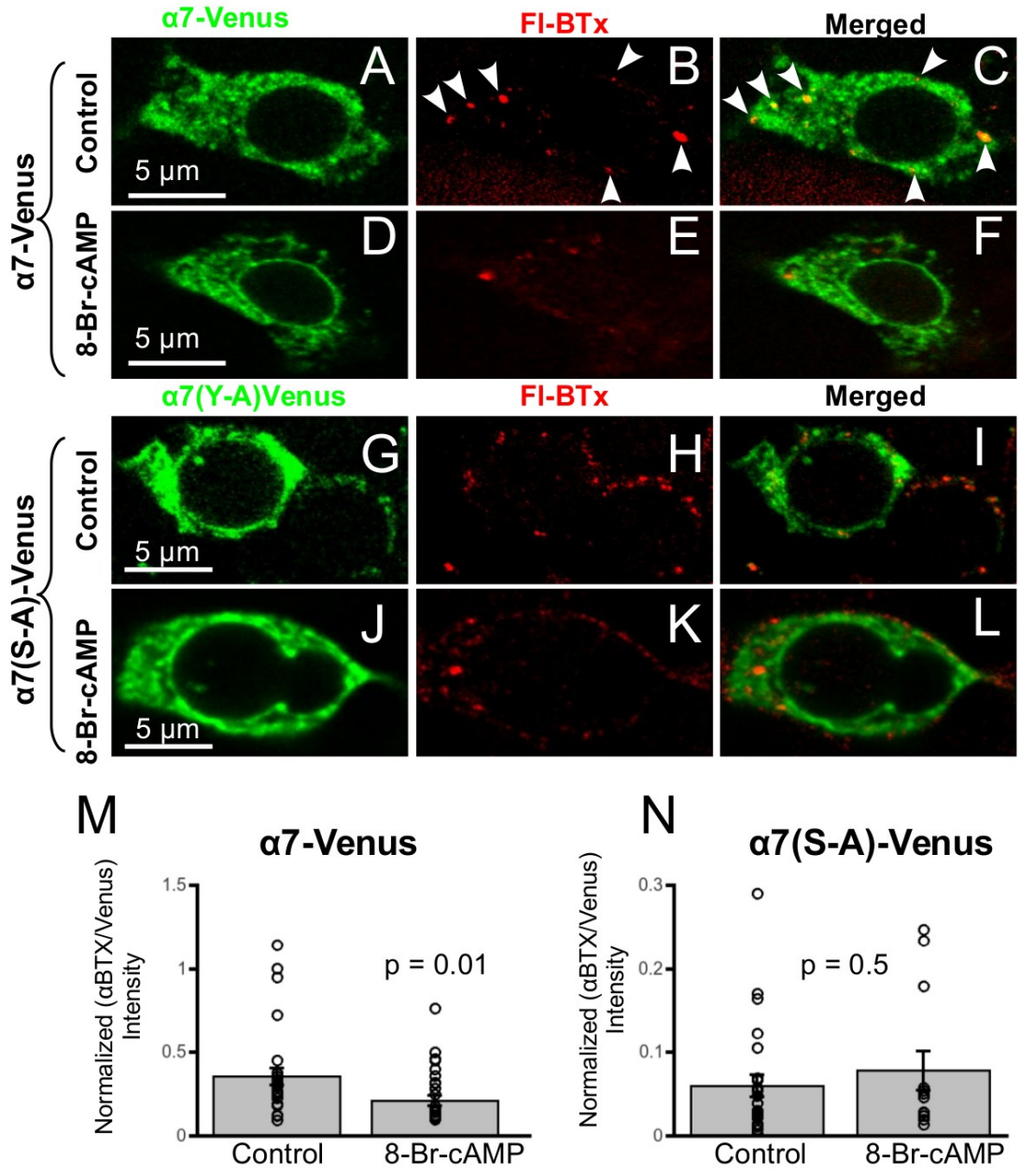

Figure 4.34. PKA stimulation decreases surface expression of α7 nAChRs.
(A-F) Confocal images of HEK 293T cells transfected with α7-Venus. Surface labeling of α7-Venus is performed with Alexa Fluor 647 α-bungarotoxin (Fl-BTx) under nonpermeabilizing conditions. **(M)** 8-Br-cAMP (100 μM for 30 min) stimulation (n = 31) resulted in a significant decrease in the amount of surface α7-Venus receptors as determined with Fl-BTx labeling as compared to control treatment (n = 28) (p = 0.01, Wilcoxon rank sum test). **(G-L)** Confocal images of HEK 293T cells transfected with mutant α7-Venus in which the putative PKA phophorylated site (S365) was mutated to alanine (α7(S-A)Venus). **(N)** 8-Br-cAMP (100 μM for 30 min) stimulation (n = 13)

showed no significant change in Fl-BTx bound surface mutant α7-Venus nAChRs as compared to control treatment (n = 25) (p = 0.5, Wilcoxon rank sum test).

4.4 Discussion

This study demonstrates that α7 nicotinic receptor function on CNS neurons is negatively modulated by cAMP dependent protein kinase A. 8-Br-cAMP attenuated α7 nicotinic receptor currents but did not change the desensitization kinetics nor single-channel conductance of α7 nAChRs in both HEK 293T cells and layer 1 PFC interneurons. Serine 365 in the cytoplasmic M3-M4 domain of α7 nAChRs appears to be the molecular substrate of protein kinase A, since 8-Br-cAMP treatment of HEK 293T cells expressing mutant α7(S365A) nAChRs no longer resulted in a decrease of nicotinic current as was the case with wildtype α7 nAChRs. We also showed that PKA activation inhibited α7 nicotinic receptor function in cell lines and in brain slices since co-transfecting dominant negative PKA or preincubating the brain slice with PKA antagonist, KT-5720 abrogated the effects of 8-Br-cAMP, while transfecting PKA-Cα in cells or including purified PKA catalytic subunit in the recording pipette attenuated α7 nicotinic receptor currents in cell lines and in cortical interneurons. Using Fl-αBTx labeling we found that the mechanism of the PKA mediated down-regulation of α7 nicotinic receptor currents was due to a decrease in the surface expression of α7 nAChRs from the direct action of PKA targeting serine 365 in the major cytoplasmic domain of α7 nAChRs.

4.4.1 Mechanism of attenuation of α7 nAChR function by PKA

To our knowledge this is the first study which has demonstrated a direct effect of the cAMP-PKA pathway in modulating nicotinic receptor function in CNS neurons. In a

study that examined the effects of PKA on $GABA_A$ receptors, which are also Cys-loop receptors, in spinal neurons, Porter and colleagues (Porter et al., 1990) similarly showed that PKA inhibited $GABA_A$ currents that were not due to changes in single-channel conductance nor gating kinetics. Although α7 nAChRs are different members of the Cys-loop family of receptors, they display similar attenuation in current response to PKA stimulation as $GABA_A$ receptors. Similarly, we found that PKA stimulation did not alter single-channel conductance nor gating kinetics of α7 nAChRs. One reason for the lack of effect of 8-Br-cAMP mediated PKA activation on single-channel conductance could be due to the fact that the putative PKA phosphorylation site, serine (S365) residue, lies close to the M3 transmembrane domain in the M3-M4 cytoplasmic loop of the channel, which is away from the pore-lining amphipathic helix situated close to the M4 transmembrane domain. The amphipathic helix lines the cytoplasmic side portals of Cys-loop receptors and forms part of the ion permeation pathway (Hales et al., 2006). Our previous study showed that tyrosine kinase phosphorylation of a conserved tyrosine (Y442) resulted in decreased whole-cell currents from α7 nAChRs that was contributed by attenuation of single-channel conductances (Komal et al., 2014) in addition to decreased surface receptor expression. Thus, it appears that PKA as well as tyrosine kinases can decrease α7 nicotinic receptor function in CNS neurons but through slightly different mechanisms. The differing mechanisms of effects of PKA and tyrosine kinase on single-channel conductance is likely due to the different locations of the target residues, with Y442 located close to the pore lining amphipathic helix while S365 is located away from the amphipathic helix. Our electrophysiology data **(Fig. 4.33)** and Fl-

αBTx labeling of surface receptors **(Fig. 4.34)** of mutant α7(S365A) nicotinic receptors clearly demonstrate that this serine residue forms the major target of PKA.

Previous studies have also monitored the effect of 8-Br-cAMP on nicotinic receptor function in bovine adrenal chromaffin cells and chick ganglionic neuronal culture (Dubin et al., 1992; Margiotta et al., 1987). Dubin et al found no effect of 8-Br-cAMP on nAChR responses. Margiotta et al (1987) found potentiation of nicotinic responses on 8-Br-cAMP treatment in chick ganglionic neurons. The discrepancy among the results could be due to the differences in the nAChR subunit composition or the concentration of 8-Br-cAMP. α3β4 nAChRs constitute the main nAChR subtype found in adrenal chromaffin cells and chick ganglionic neurons (Sala et al., 2008). Also it was shown that α7 nAChRs do not contribute to catecholamine secretion from chromaffin cells (Sala et al., 2008). Moreover, both of these studies used 20 fold higher concentration of 8-Br-cAMP (2 mM) and monitored nAChR responses on a longer time scale ranging from 6–48 hrs. Under physiological conditions the level of PKA activation determines the net effect on receptor function as demonstrated in the case of $GABA_A$ receptors (Cai et al., 2002). It can be argued that different concentrations of 8-Br-cAMP could have opposing effect on receptor function. In our studies, we monitored the functional modulation of α7 nAChRs directly in CNS neurons, using 100 μM 8-Br-cAMP at an acute time scale of 1-30 min. However, we found that the mechanism of attenuation of α7 peak responses with PKA activation was solely due to a loss of surface expression of α7 receptors, with no change in single-channel conductance. This is in contrast to the Margiotta and colleagues (1987) study, which showed an increase in nicotinic current in ganglionic neurons that was not due to alterations in expression of surface receptors,

single-channel conductance nor gating kinetics. The difference again is likely due to the difference in make-up of nAChR subunit composition and that they studied more prolonged effects of 8-Br-cAMP (3-48 hrs).

The question remains, what is the mechanism that PKA is activated in layer 1 cortical interneurons of the PFC? Neurotransmitters such as dopamine, norepinephrine and serotonin target G-protein coupled receptors and signal through cAMP mediated PKA pathways (Cai et al., 2002; Seamans and Yang, 2004; Seamans et al., 2001; Yan, 2002). These neuromodulators have been shown to regulate other ionotropic receptors like $GABA_A$ and glutamate ion channels, thereby, modulating neurotransmission (Flores-Hernandez et al., 2000; Wang and O'Donnell, 2001). In pyramidal neurons of the prefrontal cortex serotonin was shown to modulate post-synaptic $GABA_A$ receptors depending on the strength of PKA activation level (Cai et al., 2002). In addition, neuronal activity itself is considered one potent mechansim of PKA activation (Dunn et al., 2006). Based on these evidence, it is reasonable to speculate that neuromodulators such as dopamine, norepinephrine or serotonin would have a net impact on α7 nicotinic receptor function under physiological conditions.

4.4.2 Physiological relevance of PKA in synaptic plasticity and neurotransmission

Our study demonstrates the physiological importance of PKA regulation on α7 nicotinic receptor function in CNS neurons. Postsynaptic α7 nAChRs are involved in fast synaptic transmission where it modulates firing properties of neurons (Frazier et al., 1998; Jones and Wonnacott, 2004). Therefore, it is crucial to understand the cellular mechanisms ion channels are regulated in order to have a better understanding of neural function and excitability in the brain (Alkondon et al., 1998). It is well documented that protein kinase

A activation in neurons has been shown to contribute to long-term potentiation (LTP) in the dentate gyrus of the hippocampus. Since α7 nicotinic receptors have been shown to contribute towards LTP (Matsuyama et al., 2000; Ondrejcak et al., 2012), a cellular mechanism for learning and memory, PKA modulation of α7 nicotinic receptor function may influence synaptic plasticity and memory formation in different brain regions.

Layer 1 cortical interneurons can influence layer 2/3 pyramidal neuronal excitability by either inhibiting pyramidal neurons directly via GABAergic neurotransmission or conversely increase pyramidal neuronal excitability through disynaptic disinhibition (Arroyo et al., 2012; Christophe et al., 2002). If we assume a monosynaptic inhibition of pyramidal neurons, then the action of PKA on inhibiting α7 nicotinic receptor activity would putatively lead to an overall increase in pyramidal neuronal excitability. One mechanism that PKA would be stimulated is through activation of G protein coupled receptors that signal through the cAMP-adenylate cyclase pathway. One important neurotransmitter system that signals through this pathway is the dopamine neurotransmitter that acts on D1 or D5 dopamine receptors. Dopamine in the prefrontal cortex is known to play an important role in executive cognitive function such as enhancing motivation and working memory (Phillips et al., 2004, 2008). Thus if dopamine were to increase activation of PKA, we would predict that dopamine would attenuate α7 nAChRs on layer 1 cortical interneurons; thus providing less inhibitory input to pyramidal neurons and enhancing their excitability. It was shown that dopamine release through VTA afferents in the PFC results in “up states” of pyramidal neuronal excitability (Lewis and O’Donnell, 2000). These “up states” are plateau depolarizations of the membrane potential that results in burst firing. Perhaps PKA modulation of α7

nAChRs is a contributing mechanism of these "up states" of neuronal excitability. Through the actions of dopamine α7 nAChRs may be an important regulator of working memory and motivation. Although in our study we examined postsynaptic α7 nAChRs, α7 receptors are also located presynaptically, where they facilitate neurotransmitter release. The attenuation of α7 nAChR function by PKA activation could also potentially affect the release of neurotransmitters like dopamine and glutamate as shown in the rat prefrontal cortex (Livingstone et al., 2010) and modulate postsynaptic excitability. However, due to multiple isoforms of PKA expressed in neurons and the difference in their subcellular localization, it remains unclear which isoform combination of regulatory and catalytic subunits of PKA has the major effect of modulating α7 nAChRs as well as other ion channels (Meinkoth et al., 1990).

Chapter 5 - General discussion

The aim of the present study was to examine the effects of Fyn, Lck and protein kinase A activation directly on α7 nicotinic receptor function and trafficking. Three major findings arise from the study. Firstly, T cell receptor activation via downstream Fyn and Lck kinases attenuates α7 nicotinic receptor function, decreases surface expression and single-channel conductance but not the gating kinetics of the receptor. Secondly, the effect of tyrosine kinase in attenuating α7 currents is due to direct phosphorylation of α7 nicotinic receptors at a conserved tyrosine 442 located in the M3-M4 cytoplasmic loop. Thirdly, 8-Br-cAMP mediated PKA activation also negatively modulates α7 nicotinic receptor function directly by decreasing the expression of receptors at the surface but does not effect single-channel conductance or channel kinetics.

5.1 Ion-channel regulation by immune proteins

The results from chapter 3 from this thesis expand our current understanding of immune proteins role in neuronal function. There has been a significant progress ion our understanding of the regulation of nervous system by immune cell specific proteins expressed in the nervous system and their altered expression in neurodegenerative conditions (Rogers et al., 1988; Stubbs et al., 1985; Wolozin et al., 1986; Wong et al., 1984). Here, I will put my findings into broader context of immune receptor signaling and its regulation of ion channels.

5.1.1 Immune specific proteins have neuronal functions

One of the breakthroughs in the field of immune-neuronal interaction came 25 years ago when neuroscientists first formally discovered that the cytokine, interleukin-1 (IL-1), activated a subgroup of hypothalamic neurons (Berkenbosch et al., 1987; Dunn, 1988). There exists a complex interaction between the brain and the immune system via expression of proteins originally known to have a role in immune function and considered native only to immune cells. One of the specific immune gene families first discovered was the major histocompatibility complex class I (MHCI), whose expression contributed to activity dependent plasticity of synapses within the mammalian central nervous system (CNS) (Corriveau et al., 1998). Shatz et al ((Huh et al., 2000) examined the role and expression of MHC I in the retina. An unbiased differential gene screening was conducted to identify genes regulated by the blockade of endogenous action potential activity during eye-specific segregation. Unexpectedly, the most promising candidate found from this screening was the MHC I gene (Huh et al., 2000). Thereafter, the other components of MHC I molecules β2 microglobulin (a co-subunit of MHC I) and its potential binding partner CD3ζ (a protein complexed to receptors for MHC I) were found to be expressed in neurons. A neuronal function of MHC I in the CNS was then elucidated by the use of mice genetically deficient for cell surface MHC I (Fourgeaud et al., 2010). This study showed for the first time that in the hippocampus CA3–CA1 synapses, loss of MHC I caused a significant drop in the AMPA/NMDA receptor ratio. The increase in basal NMDAR-mediated responses in MHC I deficient neurons were associated with changes in the trafficking of AMPARs in response to NMDA. Thus, in

addition to its immune role, this was the first study which provided a neuronal function of MHC I in the regulation of ion channel function and trafficking in CNS neurons.

Despite these recent advances, many questions remained unresolved with regards to the signaling mechanism and the potential pathways of interaction between immune proteins and their neuronal targets. First, if MHC I regulates glutamate receptor trafficking, what is the potential mechanism of interaction and receptor regulation? Is it possible that MHC I utilizes the same signaling pathways in immune cells as it does in neurons but for specific neuronal functions? What are the different targets for MHC in neurons? Do they target specifically neuronal proteins or do they have broad specificity? What are the potential binding partners for MHC I in neurons for its proper function and expression? Does MHC I function autonomously or does it require additional immune proteins like TCRs for execution and function like that in immune cells?

5.1.2 T cell receptor - MHC I interaction

Chapter 3 of this thesis presents the first evidence for a nonclassical function of the T cell receptor in CNS neurons, specifically that TCRs can modulate neuronal excitability by dampening α7 nAChR physiology and surface expression. While it had been previously found that TCR β and CD3ζ subunits of TCR are expressed in the cortical neurons (Baudouin et al., 2008; Syken and Shatz, 2003) so far no study demonstrated their function in CNS neurons. The results of this thesis, utilizing a mouse line deficient in TCR β subunit (TCR β knockout mice) exclusively provided a systematic assessment of increased function and excitability of layer 1 interneurons of the PFC cortex by α7 nicotinic receptors. Though we used an exogenous ligand Concanavilin A (ConA) for TCR activation, we clearly show that downstream activation of Fyn and Lck kinases were

mandatory for TCR effect on α7 nAChR function and expression. Furthermore, we proved that the TCR effect on α7 channel function was due to the downstream activation of Src kinases.

Though a well described function of MHC I have been well elucidated by previous studies, we provide first evidence for the TCR, a potential binding partner of MHC I, in neuronal function. Despite being known that the source of MHC I can be in both neurons or microglia, it still remains unclear under what physiological condition MHC presents endogenous signal peptides to TCR signaling.

Given the central importance of the homomeric α7 receptor function in working memory and attention tasks, ample evidence of α7 receptor dysfunction and low expression have been observed in neurodegenerative conditions like schizophrenia (Martin-Ruiz et al., 2003; Thomsen et al., 2010; Wallace and Bertrand, 2013). Recently, the genetic linakge of MHC I gene in chromosome 6, containing a single-nucleotide polymorphism (SNPs) has been identified and associated with cognitive impairment performance in patients with schizophrenia and healthy comparison subjects (Walters et al., 2013). SNP rs6904071 showed an association with episodic memory and hippocampal volume, consistent with the studies focusing on the role of MHC I in synaptic plasticity and glutamate receptor function. This finding opens the question whether over-expression of MHC I with SNP rs6904071 would result in upregulation of TCR signaling and thus cause downregulation of α7 receptor function in schizophrenia. Neuronal MHC I upregulation have also been observed during inflammation (Foster et al., 2002), seizures (Corriveau et al., 1998), injury (Thams et al., 2008) and aging

(Edström et al., 2004). However, presently it is unknown if under these conditions there is a concomitant increase in TCR expression.

5.2 Protein kinase A mediated regulation of α7 nicotinic receptor function

In this dissertation, direct regulation of α7 nAChR function by PKA was studied in HEK293T cell line and layer 1 cortical interneurons. My research also investigated the effects of PKA activation on receptor trafficking. Patch-clamp electrophysiological techniques along with cortical neuronal cell culture were used to analyze the effect of 8-Br-cAMP stimulation on receptor function, surface expression and kinetics. Other studies have used a wide range of concentrations of cyclic AMP over longer time scale from minutes to days in cell lines (Madhok et al., 1995; Quik et al., 1997). One study showed enhancement of nicotonic responses in chick ciliary ganglion neurons with cAMP analogues using 0.2 mM concentration. The authors proposed that the enhancement in whole-cell currents were due to the conversion of surface non-functional receptors into functional ones (Margiotta et al., 1987). They showed that there was no change in mAb35 labelled surface nAChR expression nor in single-channel conductance. In our study, we monitored α7 nAChR modulation by PKA at an acute time scale of minutes. We showed that PKA can attenuate α7 nAChR currents in both HEK293T cells and in layer 1 interneurons of the frontal and prefrontal cortices. The modulation requires PKA and a conserved serine in the M3-M4 cytoplasmic loop of α7 (Ser 365). We also provide evidence of a loss of α7 nAChR expression on the cell surface upon PKA activation (Simonson et al., 2010).

Neuromodulators like dopamine, norepinephrine and serotonin target G-protein coupled receptors and signal through cAMP mediated PKA pathways (Cai et al., 2002; Seamans and Yang, 2004; Seamans et al., 2001; Yan, 2002). These neuromodulators have been shown to regulate other ionotropic receptors like $GABA_A$ and glutamate ion channels, thereby, modulating neurotransmission (Flores-Hernandez et al., 2000; Wang and O'Donnell, 2001). In pyramidal neurons of the prefrontal cortex serotonin was shown to modulate post-synaptic $GABA_A$ receptors depending on the strength of PKA activation level (Cai et al., 2002). In addition, neuronal activity itself is considered one potent mechansim of PKA activation (Dunn et al., 2006). Based on this evidence, it is reasonable to speculate that the electrical activity of the neuron in combination with these neuromodulators would have a net impact on α7 nicotinic receptor function under physiological conditions. The broad substrate targets of PKA and the variety of different PKA isoforms and their different subcellular localizations in neurons through association with anchoring proteins (AKAPs) further adds complexicity to PKA function in neurons. It is through the subcellular localizations of specific PKA isoforms that PKA achieves some degree of specificity in signal transduction (Francis and Corbin, 1994; Rosenmund et al., 1994; Zhong et al., 2009). The subcellular localization and therefore specificity in PKA signaling is believed to arise in part from compartmentalization of PKA itself through AKAPs (Buxton and Brunton, 1983; Wong and Scott, 2004). This gives another level of complexity in regulation of α7 nAChRs in neurons. In the future, it will be important to investigate how PKA activation changes subcellular translocation of α7 nicotinic receptors in neurons through its distinct PKA isoforms and whether such regulation differs in neurons of different brain regions. Any changes in receptor

translocation via distinct PKA isoforms would be critical to our understanding of the regulation of synaptic strength and plasticity. In our study, we provide evidence using brain slices and HEK293T cells that PKA activation targets Ser365 on α7 nAChRs to decrease α7 whole-cell currents. Mechanistically we determined that the attenuation of α7 currents was due to a reduction of cell surface receptors and not due to alterations in single-channel conductance. Overall, our results provide a molecular basis for understanding PKA signaling effect on homopentameric α7 nicotinic receptor in neurons .

Chapter 6 - Future directions

6.1 Role of TCR in CNS neurons

In this thesis, I provide the first evidence of direct regulation of α7 receptor function and subcellular trafficking by TCR mediated Src kinase and protein kinase A pathway. Future experiments for TCR mediated effects on α7 receptor function should investigate the subcellular expression of α7 nicotinic receptor in layer 1 of prefrontal cortex in wildtype and TCRβ knockout mice. Since, we showed that TCRβ KO mice displayed increased excitability in layer 1 interneurons, monitoring the level of receptor expression as well as the subcellular expression in neurons would increase our understanding towards TCR regulation of α7 nAChR expression and neuronal excitability. Also, increased excitability observed in these TCRβ KO mice begs the question what effect elevated neuronal TCR expression might have in neuronal function. Furthermore, although MHC I is known to play a critical role in the MHC I-TCR interacting complex in the immune system, it is unknown whether a similar complex is functional in the brain. Therefore, it will be important to examine whether MHC I deficient mice would experience similar upregulation of α7 nAChR currents as the TCRβ KO mice. In addition, it would be interesting to investigate the subcellular localization patterns in CNS neurons of both MHC I and TCR relative to α7 nAChRs using immunogold labelling and electron microscopy. Another point to examine is whether MHC I, α7 nAChRs and TCRs regulate each other's expression levels. MHC I molecules are the presenters of endogenous peptide needed for TCR activation (Ekeruche-Makinde et al., 2013). If the level of MHC I decreases in TCR β KO mice, it will strengthen our proposal that in the CNS MHC I

functions by presenting an endogenous peptide to the TCR. Also the peptides that are presented by MHC I on the surface of neurons are presently unknown and is an important issue that needs to be addressed. What are these endogenous peptides? Are they unique for different neuronal cell types and do they form a specific signal for specific interactions with other neurons is still unknown and are big questions to tackle for future research.

6.2 α7 nicotinic acetylcholine receptor modulation by PKA

In this thesis, we provide evidence of α7 nAChR modulation by the cAMP-PKA signaling pathway. However, a number of issues need attention. In all my experiments, I have used a direct activator of PKA, 8-Br-cAMP, and monitored α7 nicotinic receptor function by performing whole-cell patch-clamp recordings. Under physiological conditions the level of PKA activation determines the net effect on receptor function as demonstrated in the case of $GABA_A$ receptors (Cai et al., 2002). A dose response, using nM-mM concentrations of 8-Br-cAMP could be done in future to examine the effect on α7 receptor function and expression in HEK293T cells. This experiment would determine whether different concentrations of cAMP have similar or opposing effects on receptor modulation. An endogenous physiological activator of cAMP-PKA pathway like the neurotransmitter dopamine could be used to examine its effect on α7 mediated currents and neuronal excitability of layer 1 interneurons of the PFC in wildtype vs α7 knockout mice. It is known that layer 1 interneurons of the PFC receive dense dopaminergic projections from the midbrain (Livingstone et al., 2009). The latter study with dopamine would reflect if dopamine release alone in the PFC would be sufficient to impact α7 receptor function. It may be that co-release of other modulators are required to

have a significant impact on α7 receptor activity. Another issue which was not covered in the present study is to examine whether different isoforms of PKA, PKA I and II, have differential effects on α7 receptor activity. Since, these PKA isoforms differ in the level of expression and subcellular localization, it would be important to know if both isoforms have the same or differerent effects in their regulation of α7 function and trafficking. Nevertheless, I did show direct effect of PKA on α7 receptor function via mutation of the serine 365 residue in the M3-M4 cytoplasmic loop of α7. Using prosite analysis and from a published list of phosphorylation motifs for variety of kinases (Pearson and Kemp 1991), the M3-M4 cytoplasmic loop of the α7 nAChR also appears to contain putative serine/threonine protein kinase phosphorylation sites for calcium calmodulin dependent kinase and caesin kinase. However, one study clearly showed in an in vitro assay that out of the four serine/threonine kinases tested, which included calcium calmodulin dependent kinase II, cGMP dependent kinase, PKC and PKA, only PKA resulted in phosphorylation of a serine residue located in the cytoplasmic loop of the α7 receptor (Moss et al., 1996).

Since α7 nAChRs have a high degree of calcium permeability, calcium influx through the α7 nAChRs themselves could provide the calcium secondary messenger to activate other signaling pathways. Therefore, α7 nAChR activation along with PKA stimulation, could lead to cross-talk of multiple signal transduction pathways (Liu and Berg, 1999; Shen and Yakel, 2009b). In such a scenario, I propose that the association of a macromolecular complex with the intracellular loop of α7 nicotinic receptors could be regulated by PKA and involved in the regulation of receptor function. Altogether, based on numerous investigations and my own studies of protein modulation of α7 nAChRs, I revealed the diversity and complexity of the effects of an immune protein, namely TCR,

and different protein kinases, including PKA and tyrosine kinase, in modulating α7 nAChR function. Although these studies examined at a basic level how specific proteins may modulate the function of α7 nAChR function, these findings may increase our understanding of the role of nAChRs in cognitive performance such as attention and working memory and how dysfunctional alterations in modulation of α7 nAChR function may potentially contribute to the pathogenesis of neurological disorders such as schizophrenia or Alzheimer's disease.

Bibliography

Abel, T., Nguyen, P.V., Barad, M., Deuel, T.A., Kandel, E.R., and Bourtchouladze, R. (1997). Genetic demonstration of a role for PKA in the late phase of LTP and in hippocampus-based long-term memory. Cell *88*, 615–626.

Ahmadian, G., Ju, W., Liu, L., Wyszynski, M., Lee, S.H., Dunah, A.W., Taghibiglou, C., Wang, Y., Lu, J., Wong, T.P., et al. (2004). Tyrosine phosphorylation of GluR2 is required for insulin-stimulated AMPA receptor endocytosis and LTD. EMBO J *23*, 1040–1050.

AhnAllen, C.G. (2012). The role of the α7 nicotinic receptor in cognitive processing of persons with schizophrenia. Curr. Opin. Psychiatry *25*, 103–108.

Alitto, H.J., and Dan, Y. (2013). Cell-type-specific modulation of neocortical activity by basal forebrain input. Front. Syst. Neurosci. *6*, 79.

Alkondon, M., and Albuquerque, E.X. (2005). Nicotinic receptor subtypes in rat hippocampal slices are differentially sensitive to desensitization and early in vivo functional up-regulation by nicotine and to block by bupropion. J. Pharmacol. Exp. Ther. *313*, 740–750.

Alkondon, M., Pereira, E.F., Cortes, W.S., Maelicke, A., and Albuquerque, E.X. (1997). Choline is a selective agonist of alpha7 nicotinic acetylcholine receptors in the rat brain neurons. Eur. J. Neurosci. *9*, 2734–2742.

Alkondon, M., Pereira, E.F., and Albuquerque, E.X. (1998a). alpha-bungarotoxin- and methyllycaconitine-sensitive nicotinic receptors mediate fast synaptic transmission in interneurons of rat hippocampal slices. Brain Res. *810*, 257–263.

Alkondon, M., Pereira, E.F., and Albuquerque, E.X. (1998b). alpha-bungarotoxin- and methyllycaconitine-sensitive nicotinic receptors mediate fast synaptic transmission in interneurons of rat hippocampal slices. Brain Res. *810*, 257–263.

Arroyo, S., Bennett, C., Aziz, D., Brown, S.P., and Hestrin, S. (2012). Prolonged disynaptic inhibition in the cortex mediated by slow, non-α7 nicotinic excitation of a specific subset of cortical interneurons. J. Neurosci. Off. J. Soc. Neurosci. *32*, 3859–3864.

Artyomov, M.N., Lis, M., Devadas, S., Davis, M.M., and Chakraborty, A.K. (2010). CD4 and CD8 binding to MHC molecules primarily acts to enhance Lck delivery. Proc. Natl. Acad. Sci. U. S. A. *107*, 16916–16921.

Astman, N., Gutnick, M.J., and Fleidervish, I.A. (1998). Activation of protein kinase C increases neuronal excitability by regulating persistent Na+ current in mouse neocortical slices. J. Neurophysiol. *80*, 1547–1551.

Bailey, C.D.C., De Biasi, M., Fletcher, P.J., and Lambe, E.K. (2010). The nicotinic acetylcholine receptor alpha5 subunit plays a key role in attention circuitry and accuracy. J. Neurosci. Off. J. Soc. Neurosci. *30*, 9241–9252.

Baudouin, S.J., Angibaud, J., Loussouarn, G., Bonnamain, V., Matsuura, A., Kinebuchi, M., Naveilhan, P., and Boudin, H. (2008). The signaling adaptor protein CD3zeta is a negative regulator of dendrite development in young neurons. Mol Biol Cell *19*, 2444–2456.

Beaulieu, J.-M., and Gainetdinov, R.R. (2011). The Physiology, Signaling, and Pharmacology of Dopamine Receptors. Pharmacol. Rev. *63*, 182–217.

Berg, D.K., and Conroy, W.G. (2002). Nicotinic alpha 7 receptors: synaptic options and downstream signaling in neurons. J Neurobiol *53*, 512–523.

Berkenbosch, F., Oers, J. van, Rey, A. del, Tilders, F., and Besedovsky, H. (1987). Corticotropin-releasing factor-producing neurons in the rat activated by interleukin-1. Science *238*, 524–526.

Berridge, M.J. (2012). Cell Signalling Biology: Module 2 - Cell signalling pathways. Biochem. J.

Bertrand, D., Galzi, J.L., Devillers-Thiéry, A., Bertrand, S., and Changeux, J.P. (1993). Mutations at two distinct sites within the channel domain M2 alter calcium permeability of neuronal alpha 7 nicotinic receptor. Proc Natl Acad Sci U A *90*, 6971–6975.

Bibevski, S., Zhou, Y., McIntosh, J.M., Zigmond, R.E., and Dunlap, M.E. (2000). Functional Nicotinic Acetylcholine Receptors That Mediate Ganglionic Transmission in Cardiac Parasympathetic Neurons. J. Neurosci. *20*, 5076–5082.

Biton, B., Bergis, O.E., Galli, F., Nedelec, A., Lochead, A.W., Jegham, S., Godet, D., Lanneau, C., Santamaria, R., Chesney, F., et al. (2007). SSR180711, a novel selective alpha7 nicotinic receptor partial agonist: (1) binding and functional profile. Neuropsychopharmacol. Off. Publ. Am. Coll. Neuropsychopharmacol. *32*, 1–16.

Bloem, B., Poorthuis, R.B., and Mansvelder, H.D. (2014). Cholinergic modulation of the medial prefrontal cortex: the role of nicotinic receptors in attention and regulation of neuronal activity. Front. Neural Circuits *8*, 17.

Blom, N., Gammeltoft, S., and Brunak, S. (1999). Sequence and structure-based prediction of eukaryotic protein phosphorylation sites. J Mol Biol *294*, 1351–1362.

Boulanger, L.M. (2009). Immune proteins in brain development and synaptic plasticity. Neuron *64*, 93–109.

Boulanger, L.M., and Shatz, C.J. (2004). Immune signalling in neural development, synaptic plasticity and disease. Nat Rev Neurosci *5*, 521–531.

Boulanger, L.M., Huh, G.S., and Shatz, C.J. (2001a). Neuronal plasticity and cellular immunity: shared molecular mechanisms. Curr Opin Neurobiol *11*, 568–578.

Boulanger, L.M., Huh, G.S., and Shatz, C.J. (2001b). Neuronal plasticity and cellular immunity: shared molecular mechanisms. Curr. Opin. Neurobiol. *11*, 568–578.

Brandon, E.P., Zhuo, M., Huang, Y.Y., Qi, M., Gerhold, K.A., Burton, K.A., Kandel, E.R., McKnight, G.S., and Idzerda, R.L. (1995). Hippocampal long-term depression and depotentiation are defective in mice carrying a targeted disruption of the gene encoding the RI beta subunit of cAMP-dependent protein kinase. Proc. Natl. Acad. Sci. U. S. A. *92*, 8851–8855.

Brandon, E.P., Idzerda, R.L., and McKnight, G.S. (1997). PKA isoforms, neural pathways, and behaviour: making the connection. Curr. Opin. Neurobiol. *7*, 397–403.

Brandon, E.P., Logue, S.F., Adams, M.R., Qi, M., Sullivan, S.P., Matsumoto, A.M., Dorsa, D.M., Wehner, J.M., McKnight, G.S., and Idzerda, R.L. (1998). Defective motor behavior and neural gene expression in RIIbeta-protein kinase A mutant mice. J. Neurosci. Off. J. Soc. Neurosci. *18*, 3639–3649.

Breese, C.R., Adams, C., Logel, J., Drebing, C., Rollins, Y., Barnhart, M., Sullivan, B., Demasters, B.K., Freedman, R., and Leonard, S. (1997). Comparison of the regional expression of nicotinic acetylcholine receptor alpha7 mRNA and [125I]-alpha-bungarotoxin binding in human postmortem brain. J. Comp. Neurol. *387*, 385–398.

Broide, R.S., O'Connor, L.T., Smith, M.A., Smith, J.A.M., and Leslie, F.M. (1995). Developmental expression ofα7 neuronal nicotinic receptor messenger RNA in rat sensory cortex and thalamus. Neuroscience *67*, 83–94.

Brown, M.T., and Cooper, J.A. (1996). Regulation, substrates and functions of src. Biochim. Biophys. Acta *1287*, 121–149.

Brown, A.M., Hope, A.G., Lambert, J.J., and Peters, J.A. (1998). Ion permeation and conduction in a human recombinant 5-HT3 receptor subunit (h5-HT3A). J Physiol *507 (Pt 3)*, 653–665.

Brownlie, R.J., and Zamoyska, R. (2013). T cell receptor signalling networks: branched, diversified and bounded. Nat. Rev. Immunol. *13*, 257–269.

Brozoski, T.J., Brown, R.M., Rosvold, H.E., and Goldman, P.S. (1979). Cognitive deficit caused by regional depletion of dopamine in prefrontal cortex of rhesus monkey. Science *205*, 929–932.

Brugge, J.S., and Erikson, R.L. (1977). Identification of a transformation-specific antigen induced by an avian sarcoma virus. Nature *269*, 346–348.

Brusés, J.L., Chauvet, N., and Rutishauser, U. (2001). Membrane lipid rafts are necessary for the maintenance of the (alpha)7 nicotinic acetylcholine receptor in somatic spines of ciliary neurons. J Neurosci *21*, 504–512.

Buisson, B., and Bertrand, D. (1998). Open-channel blockers at the human alpha4beta2 neuronal nicotinic acetylcholine receptor. Mol. Pharmacol. *53*, 555–563.

Buxton, I.L., and Brunton, L.L. (1983). Compartments of cyclic AMP and protein kinase in mammalian cardiomyocytes. J. Biol. Chem. *258*, 10233–10239.

Byrne, J.H., and Kandel, E.R. (1996). Presynaptic facilitation revisited: state and time dependence. J. Neurosci. Off. J. Soc. Neurosci. *16*, 425–435.

Cai, X., Flores-Hernandez, J., Feng, J., and Yan, Z. (2002). Activity-dependent bidirectional regulation of GABA(A) receptor channels by the 5-HT(4) receptor-mediated signalling in rat prefrontal cortical pyramidal neurons. J. Physiol. *540*, 743–759.

Castner, S.A., Smagin, G.N., Piser, T.M., Wang, Y., Smith, J.S., Christian, E.P., Mrzljak, L., and Williams, G.V. (2011). Immediate and sustained improvements in working memory after selective stimulation of α7 nicotinic acetylcholine receptors. Biol. Psychiatry *69*, 12–18.

Castro, N.G., and Albuquerque, E.X. (1995). alpha-Bungarotoxin-sensitive hippocampal nicotinic receptor channel has a high calcium permeability. Biophys. J. *68*, 516–524.

Centonze, D., Picconi, B., Gubellini, P., Bernardi, G., and Calabresi, P. (2001). Dopaminergic control of synaptic plasticity in the dorsal striatum. Eur. J. Neurosci. *13*, 1071–1077.

Chan, W.K., Wong, P.T.-H., and Sheu, F.-S. (2007). Frontal cortical alpha7 and alpha4beta2 nicotinic acetylcholine receptors in working and reference memory. Neuropharmacology *52*, 1641–1649.

Changeux, J.P., Bertrand, D., Corringer, P.J., Dehaene, S., Edelstein, S., Léna, C., Le Novère, N., Marubio, L., Picciotto, M., and Zoli, M. (1998). Brain nicotinic receptors: structure and regulation, role in learning and reinforcement. Brain Res Brain Res Rev *26*, 198–216.

Charpantier, E., Wiesner, A., Huh, K.-H., Ogier, R., Hoda, J.-C., Allaman, G., Raggenbass, M., Feuerbach, D., Bertrand, D., and Fuhrer, C. (2005a). Alpha7 neuronal nicotinic acetylcholine receptors are negatively regulated by tyrosine phosphorylation and Src-family kinases. J Neurosci *25*, 9836–9849.

Charpantier, E., Wiesner, A., Huh, K.-H., Ogier, R., Hoda, J.-C., Allaman, G., Raggenbass, M., Feuerbach, D., Bertrand, D., and Fuhrer, C. (2005b). α7 Neuronal Nicotinic Acetylcholine Receptors Are Negatively Regulated by Tyrosine Phosphorylation and Src-Family Kinases. J. Neurosci. *25*, 9836–9849.

Charpantier, E., Wiesner, A., Huh, K.-H., Ogier, R., Hoda, J.-C., Allaman, G., Raggenbass, M., Feuerbach, D., Bertrand, D., and Fuhrer, C. (2005c). α7 Neuronal Nicotinic Acetylcholine Receptors Are Negatively Regulated by Tyrosine Phosphorylation and Src-Family Kinases. J. Neurosci. *25*, 9836–9849.

Chen, D., and Patrick, J.W. (1997). The alpha-bungarotoxin-binding nicotinic acetylcholine receptor from rat brain contains only the alpha7 subunit. J Biol Chem *272*, 24024–24029.

Chen, G., Greengard, P., and Yan, Z. (2004). Potentiation of NMDA receptor currents by dopamine D1 receptors in prefrontal cortex. Proc. Natl. Acad. Sci. U. S. A. *101*, 2596–2600.

Cheng, Q., and Yakel, J.L. (2014). Presynaptic α7 Nicotinic Acetylcholine Receptors Enhance Hippocampal Mossy Fiber Glutamatergic Transmission via PKA Activation. J Neurosci *34*, 124–133.

Cho, C.-H., Song, W., Leitzell, K., Teo, E., Meleth, A.D., Quick, M.W., and Lester, R.A.J. (2005a). Rapid upregulation of alpha7 nicotinic acetylcholine receptors by tyrosine dephosphorylation. J Neurosci *25*, 3712–3723.

Cho, C.-H., Song, W., Leitzell, K., Teo, E., Meleth, A.D., Quick, M.W., and Lester, R.A.J. (2005b). Rapid upregulation of alpha7 nicotinic acetylcholine receptors by tyrosine dephosphorylation. J. Neurosci. Off. J. Soc. Neurosci. *25*, 3712–3723.

Christophe, E., Roebuck, A., Staiger, J.F., Lavery, D.J., Charpak, S., and Audinat, E. (2002a). Two types of nicotinic receptors mediate an excitation of neocortical layer I interneurons. J Neurophysiol *88*, 1318–1327.

Christophe, E., Roebuck, A., Staiger, J.F., Lavery, D.J., Charpak, S., and Audinat, E. (2002b). Two types of nicotinic receptors mediate an excitation of neocortical layer I interneurons. J. Neurophysiol. *88*, 1318–1327.

Clarke, P.B., and Reuben, M. (1996). Release of [3H]-noradrenaline from rat hippocampal synaptosomes by nicotine: mediation by different nicotinic receptor subtypes from striatal [3H]-dopamine release. Br. J. Pharmacol. *117*, 595–606.

Clarke, P.B., Schwartz, R.D., Paul, S.M., Pert, C.B., and Pert, A. (1985). Nicotinic binding in rat brain: autoradiographic comparison of [3H]acetylcholine, [3H]nicotine, and [125I]-alpha-bungarotoxin. J. Neurosci. Off. J. Soc. Neurosci. *5*, 1307–1315.

Cohen, P. (2002). The origins of protein phosphorylation. Nat. Cell Biol. *4*, E127–E130.

Corringer, P.J., Le Novère, N., and Changeux, J.P. (2000). Nicotinic receptors at the amino acid level. Annu Rev Pharmacol Toxicol *40*, 431–458.

Corriveau, R.A., Huh, G.S., and Shatz, C.J. (1998). Regulation of class I MHC gene expression in the developing and mature CNS by neural activity. Neuron *21*, 505–520.

Couey, J.J., Meredith, R.M., Spijker, S., Poorthuis, R.B., Smit, A.B., Brussaard, A.B., and Mansvelder, H.D. (2007). Distributed network actions by nicotine increase the threshold for spike-timing-dependent plasticity in prefrontal cortex. Neuron *54*, 73–87.

Courjaret, R., and Lapied, B. (2001). Complex intracellular messenger pathways regulate one type of neuronal alpha-bungarotoxin-resistant nicotinic acetylcholine receptors expressed in insect neurosecretory cells (dorsal unpaired median neurons). Mol. Pharmacol. *60*, 80–91.

Cull-Candy, S., Brickley, S., and Farrant, M. (2001). NMDA receptor subunits: diversity, development and disease. Curr. Opin. Neurobiol. *11*, 327–335.

Dahan, D.S., Dibas, M.I., Petersson, E.J., Auyeung, V.C., Chanda, B., Bezanilla, F., Dougherty, D.A., and Lester, H.A. (2004). A fluorophore attached to nicotinic acetylcholine receptor beta M2 detects productive binding of agonist to the alpha delta site. Proc. Natl. Acad. Sci. U. S. A. *101*, 10195–10200.

Dajas-Bailador, F., and Wonnacott, S. (2004). Nicotinic acetylcholine receptors and the regulation of neuronal signalling. Trends Pharmacol Sci *25*, 317–324.

Dajas-Bailador, F.A., Mogg, A.J., and Wonnacott, S. (2002a). Intracellular Ca2+ signals evoked by stimulation of nicotinic acetylcholine receptors in SH-SY5Y cells: contribution of voltage-operated Ca2+ channels and Ca2+ stores. J. Neurochem. *81*, 606–614.

Dajas-Bailador, F.A., Soliakov, L., and Wonnacott, S. (2002b). Nicotine activates the extracellular signal-regulated kinase 1/2 via the alpha7 nicotinic acetylcholine receptor and protein kinase A, in SH-SY5Y cells and hippocampal neurones. J Neurochem *80*, 520–530.

Dani, J.A. (2001). Overview of nicotinic receptors and their roles in the central nervous system. Biol Psychiatry *49*, 166–174.

Dani, J.A., and Bertrand, D. (2006). Nicotinic Acetylcholine Receptors and Nicotinic Cholinergic Mechanisms of the Central Nervous System. Annu Rev Pharmacol Toxicol.

Dani, J.A., and Bertrand, D. (2007). Nicotinic acetylcholine receptors and nicotinic cholinergic mechanisms of the central nervous system. Annu Rev Pharmacol Toxicol *47*, 699–729.

Dau, A., Komal, P., Truong, M., Morris, G., Evans, G., and Nashmi, R. (2013). RIC-3 differentially modulates alpha4beta2 and alpha7 nicotinic receptor assembly, expression, and nicotine-induced receptor upregulation. BMC Neurosci. *14*, 47.

Davis, M.M., and Bjorkman, P.J. (1988). T-cell antigen receptor genes and T-cell recognition. Nature *334*, 395–402.

Dickinson, J.A., Kew, J.N.C., and Wonnacott, S. (2008). Presynaptic alpha 7- and beta 2-containing nicotinic acetylcholine receptors modulate excitatory amino acid release from rat prefrontal cortex nerve terminals via distinct cellular mechanisms. Mol. Pharmacol. *74*, 348–359.

Drenan, R.M., Grady, S.R., Whiteaker, P., McClure-Begley, T., McKinney, S., Miwa, J.M., Bupp, S., Heintz, N., McIntosh, J.M., Bencherif, M., et al. (2008). In vivo activation of midbrain dopamine neurons via sensitized, high-affinity alpha 6 nicotinic acetylcholine receptors. Neuron *60*, 123–136.

Dubin, A.E., Rathouz, M.M., Mapp, K.S., and Berg, D.K. (1992). Cyclic AMP and the nicotinic response of bovine adrenal chromaffin cells. Brain Res. *586*, 344–347.

Duffy, A.M., Zhou, P., Milner, T.A., and Pickel, V.M. (2009). Spatial and intracellular relationships between the α7 nicotinic acetylcholine receptor and the vesicular acetylcholine transporter in the prefrontal cortex of rat and mouse. Neuroscience *161*, 1091–1103.

Dunn, A.J. (1988). Systemic interleukin-1 administration stimulates hypothalamic norepinephrine metabolism parallelling the increased plasma corticosterone. Life Sci. *43*, 429–435.

Dunn, T.A., Wang, C.-T., Colicos, M.A., Zaccolo, M., DiPilato, L.M., Zhang, J., Tsien, R.Y., and Feller, M.B. (2006). Imaging of cAMP levels and protein kinase A activity reveals that retinal waves drive oscillations in second-messenger cascades. J. Neurosci. Off. J. Soc. Neurosci. *26*, 12807–12815.

Edelman, A.M., Blumenthal, D.K., and Krebs, E.G. (1987). Protein serine/threonine kinases. Annu. Rev. Biochem. *56*, 567–613.

Edström, E., Kullberg, S., Ming, Y., Zheng, H., and Ulfhake, B. (2004). MHC Class I, β2 microglobulin, and the INF-γ receptor are upregulated in aged motoneurons. J. Neurosci. Res. *78*, 892–900.

Ekeruche-Makinde, J., Miles, J.J., van den Berg, H.A., Skowera, A., Cole, D.K., Dolton, G., Schauenburg, A.J.A., Tan, M.P., Pentier, J.M., Llewellyn-Lacey, S., et al. (2013). Peptide length determines the outcome of TCR/peptide-MHCI engagement. Blood *121*, 1112–1123.

Escande-Beillard, N., Washburn, L., Zekzer, D., Wu, Z.-P., Eitan, S., Ivkovic, S., Lu, Y., Dang, H., Middleton, B., Bilousova, T.V., et al. (2010). Neurons preferentially respond to self-MHC class I allele products regardless of peptide presented. J Immunol *184*, 816–823.

Esteban, J.A., Shi, S.-H., Wilson, C., Nuriya, M., Huganir, R.L., and Malinow, R. (2003). PKA phosphorylation of AMPA receptor subunits controls synaptic trafficking underlying plasticity. Nat. Neurosci. *6*, 136–143.

Everitt, B.J., and Robbins, T.W. (1997). Central cholinergic systems and cognition. Annu. Rev. Psychol. *48*, 649–684.

Fayuk, D., and Yakel, J.L. (2005). Ca2+ permeability of nicotinic acetylcholine receptors in rat hippocampal CA1 interneurones. J Physiol *566*, 759–768.

Fenster, C.P., Beckman, M.L., Parker, J.C., Sheffield, E.B., Whitworth, T.L., Quick, M.W., and Lester, R.A. (1999). Regulation of alpha4beta2 nicotinic receptor desensitization by calcium and protein kinase C. Mol Pharmacol *55*, 432–443.

Fernandes, C.C., Pinto-Duarte, A., Ribeiro, J.A., and Sebastião, A.M. (2008). Postsynaptic Action of Brain-Derived Neurotrophic Factor Attenuates α7 Nicotinic Acetylcholine Receptor-Mediated Responses in Hippocampal Interneurons. J. Neurosci. *28*, 5611–5618.

Fischer, H., Liu, D.-M., Lee, A., Harries, J.C., and Adams, D.J. (2005). Selective modulation of neuronal nicotinic acetylcholine receptor channel subunits by Go-protein subunits. J. Neurosci. Off. J. Soc. Neurosci. *25*, 3571–3577.

Flores, C.M., DeCamp, R.M., Kilo, S., Rogers, S.W., and Hargreaves, K.M. (1996). Neuronal Nicotinic Receptor Expression in Sensory Neurons of the Rat Trigeminal Ganglion: Demonstration of α3β4, a Novel Subtype in the Mammalian Nervous System. J. Neurosci. *16*, 7892–7901.

Flores-Hernandez, J., Hernandez, S., Snyder, G.L., Yan, Z., Fienberg, A.A., Moss, S.J., Greengard, P., and Surmeier, D.J. (2000). D(1) dopamine receptor activation reduces GABA(A) receptor currents in neostriatal neurons through a PKA/DARPP-32/PP1 signaling cascade. J. Neurophysiol. *83*, 2996–3004.

Forster, I., and Bertrand, D. (1995). Inward rectification of neuronal nicotinic acetylcholine receptors investigated by using the homomeric alpha 7 receptor. Proc. Biol. Sci. *260*, 139–148.

Foster, J.A., Quan, N., Stern, E.L., Kristensson, K., and Herkenham, M. (2002). Induced neuronal expression of class I major histocompatibility complex mRNA in acute and chronic inflammation models. J. Neuroimmunol. *131*, 83–91.

Fourgeaud, L., Davenport, C.M., Tyler, C.M., Cheng, T.T., Spencer, M.B., and Boulanger, L.M. (2010). MHC class I modulates NMDA receptor function and AMPA receptor trafficking. Proc. Natl. Acad. Sci. U. S. A. *107*, 22278–22283.

Frahm, S., Slimak, M.A., Ferrarese, L., Santos-Torres, J., Antolin-Fontes, B., Auer, S., Filkin, S., Pons, S., Fontaine, J.-F., Tsetlin, V., et al. (2011). Aversion to nicotine is regulated by the balanced activity of β4 and α5 nicotinic receptor subunits in the medial habenula. Neuron *70*, 522–535.

Francis, S.H., and Corbin, J.D. (1994). Structure and function of cyclic nucleotide-dependent protein kinases. Annu. Rev. Physiol. *56*, 237–272.

Franke, C., Hatt, H., and Dudel, J. (1987). Liquid filament switch for ultra-fast exchanges of solutions at excised patches of synaptic membrane of crayfish muscle. Neurosci. Lett. *77*, 199–204.

Frazier, C.J., Rollins, Y.D., Breese, C.R., Leonard, S., Freedman, R., and Dunwiddie, T.V. (1998a). Acetylcholine activates an alpha-bungarotoxin-sensitive nicotinic current in rat hippocampal interneurons, but not pyramidal cells. J. Neurosci. Off. J. Soc. Neurosci. *18*, 1187–1195.

Frazier, C.J., Buhler, A.V., Weiner, J.L., and Dunwiddie, T.V. (1998b). Synaptic potentials mediated via alpha-bungarotoxin-sensitive nicotinic acetylcholine receptors in rat hippocampal interneurons. J. Neurosci. Off. J. Soc. Neurosci. *18*, 8228–8235.

Frazier, C.J., Strowbridge, B.W., and Papke, R.L. (2003). Nicotinic receptors on local circuit neurons in dentate gyrus: a potential role in regulation of granule cell excitability. J Neurophysiol *89*, 3018–3028.

Freedman, R., Wetmore, C., Strömberg, I., Leonard, S., and Olson, L. (1993). Alpha-bungarotoxin binding to hippocampal interneurons: immunocytochemical characterization and effects on growth factor expression. J Neurosci *13*, 1965–1975.

Freedman, R., Hall, M., Adler, L.E., and Leonard, S. (1995). Evidence in postmortem brain tissue for decreased numbers of hippocampal nicotinic receptors in schizophrenia. Biol. Psychiatry *38*, 22–33.

Fucile, S. (2004). Ca2+ permeability of nicotinic acetylcholine receptors. Cell Calcium *35*, 1–8.

Fuentealba, J., Olivares, R., Alés, E., Tapia, L., Rojo, J., Arroyo, G., Aldea, M., Criado, M., Gandía, L., and García, A.G. (2004). A choline-evoked [Ca2+]c signal causes catecholamine release and hyperpolarization of chromaffin cells. FASEB J. Off. Publ. Fed. Am. Soc. Exp. Biol. *18*, 1468–1470.

Fujii, S., Ji, Z., and Sumikawa, K. (2000). Inactivation of alpha7 ACh receptors and activation of non-alpha7 ACh receptors both contribute to long term potentiation induction in the hippocampal CA1 region. Neurosci Lett *286*, 134–138.

Ge, S., and Dani, J.A. (2005). Nicotinic Acetylcholine Receptors at Glutamate Synapses Facilitate Long-Term Depression or Potentiation. J. Neurosci. *25*, 6084–6091.

Germain, R.N. (1997). T-cell signaling: The importance of receptor clustering. Curr. Biol. *7*, R640–R644.

Germain, R.N. (2001). The art of the probable: system control in the adaptive immune system. Science *293*, 240–245.

Gill, C.H., Peters, J.A., and Lambert, J.J. (1995). An electrophysiological investigation of the properties of a murine recombinant 5-HT3 receptor stably expressed in HEK 293 cells. Br J Pharmacol *114*, 1211–1221.

Girod, R., Crabtree, G., Ernstrom, G., Ramirez-Latorre, J., McGehee, D., Turner, J., and Role, L. (1999). Heteromeric complexes of alpha 5 and/or alpha 7 subunits. Effects of calcium and potential role in nicotine-induced presynaptic facilitation. Ann. N. Y. Acad. Sci. *868*, 578–590.

Goddard, C.A., Butts, D.A., and Shatz, C.J. (2007). Regulation of CNS synapses by neuronal MHC class I. Proc Natl Acad Sci U A *104*, 6828–6833.

Gopalakrishnan, M., Molinari, E.J., and Sullivan, J.P. (1997). Regulation of human alpha4beta2 neuronal nicotinic acetylcholine receptors by cholinergic channel ligands and second messenger pathways. Mol Pharmacol *52*, 524–534.

Gotti, C., and Clementi, F. (2004). Neuronal nicotinic receptors: from structure to pathology. Prog Neurobiol *74*, 363–396.

Gotti, C., Zoli, M., and Clementi, F. (2006). Brain nicotinic acetylcholine receptors: native subtypes and their relevance. Trends Pharmacol. Sci. *27*, 482–491.

Gotti, C., Clementi, F., Fornari, A., Gaimarri, A., Guiducci, S., Manfredi, I., Moretti, M., Pedrazzi, P., Pucci, L., and Zoli, M. (2009). Structural and functional diversity of native brain neuronal nicotinic receptors. Biochem. Pharmacol. *78*, 703–711.

Grady, S., Marks, M.J., Wonnacott, S., and Collins, A.C. (1992). Characterization of nicotinic receptor-mediated [3H]dopamine release from synaptosomes prepared from mouse striatum. J. Neurochem. *59*, 848–856.

Green, W.N., Ross, A.F., and Claudio, T. (1991a). Acetylcholine receptor assembly is stimulated by phosphorylation of its gamma subunit. Neuron *7*, 659–666.

Green, W.N., Ross, A.F., and Claudio, T. (1991b). cAMP stimulation of acetylcholine receptor expression is mediated through posttranslational mechanisms. Proc. Natl. Acad. Sci. U. S. A. *88*, 854–858.

Guan, Z.Z., Zhang, X., Blennow, K., and Nordberg, A. (1999). Decreased protein level of nicotinic receptor alpha7 subunit in the frontal cortex from schizophrenic brain. Neuroreport *10*, 1779–1782.

Guillem, K., Bloem, B., Poorthuis, R.B., Loos, M., Smit, A.B., Maskos, U., Spijker, S., and Mansvelder, H.D. (2011). Nicotinic acetylcholine receptor β2 subunits in the medial prefrontal cortex control attention. Sci. 80- *333*, 888–891.

Haghighi, A.P., and Cooper, E. (1998). Neuronal nicotinic acetylcholine receptors are blocked by intracellular spermine in a voltage-dependent manner. J. Neurosci. Off. J. Soc. Neurosci. *18*, 4050–4062.

Hales, T.G., Dunlop, J.I., Deeb, T.Z., Carland, J.E., Kelley, S.P., Lambert, J.J., and Peters, J.A. (2006). Common Determinants of Single Channel Conductance within the Large Cytoplasmic Loop of 5-Hydroxytryptamine Type 3 and α4β2 Nicotinic Acetylcholine Receptors. J. Biol. Chem. *281*, 8062–8071.

Hemmings, H.C.J., Nairn, A.C., McGuinness, T.L., Huganir, R.L., and Greengard, P. (1989). Role of protein phosphorylation in neuronal signal transduction. FASEB J *3*, 1583–1592.

Hirano, A.A., Greengard, P., and Huganir, R.L. (1988). Protein Tyrosine Kinase Activity and Its Endogenous Substrates in Rat Brain: A Subcellular and Regional Survey. J. Neurochem. *50*, 1447–1455.

Hope, B.T., Nagarkar, D., Leonard, S., and Wise, R.A. (2007). Long-term upregulation of protein kinase A and adenylate cyclase levels in human smokers. J. Neurosci. Off. J. Soc. Neurosci. *27*, 1964–1972.

Hoyle, E., Genn, R.F., Fernandes, C., and Stolerman, I.P. (2006). Impaired performance of alpha7 nicotinic receptor knockout mice in the five-choice serial reaction time task. Psychopharmacology (Berl.) *189*, 211–223.

Huang, Y., and Wange, R.L. (2004). T cell receptor signaling: beyond complex complexes. J Biol Chem *279*, 28827–28830.

Huganir, R.L. (1987). Regulation of the nicotinic acetylcholine receptor by protein phosphorylation. J Recept Res *7*, 241–256.

Huganir, R.L., Miles, K., and Greengard, P. (1984). Phosphorylation of the nicotinic acetylcholine receptor by an endogenous tyrosine-specific protein kinase. Proc Natl Acad Sci U A *81*, 6968–6972.

Huh, G.S., Boulanger, L.M., Du, H., Riquelme, P.A., Brotz, T.M., and Shatz, C.J. (2000a). Functional Requirement for Class I MHC in CNS Development and Plasticity. Science *290*, 2155–2159.

Huh, G.S., Boulanger, L.M., Du, H., Riquelme, P.A., Brotz, T.M., and Shatz, C.J. (2000b). Functional requirement for class I MHC in CNS development and plasticity. Science *290*, 2155–2159.

Irvine, D.J., Purbhoo, M.A., Krogsgaard, M., and Davis, M.M. (2002). Direct observation of ligand recognition by T cells. Nature *419*, 845–849.

Janeway, C.A. (1992). The T Cell Receptor as a Multicomponent Signalling Machine: CD4/CD8 Coreceptors and CD45 in T Cell Activation. Annu. Rev. Immunol. *10*, 645–674.

Ji, D., Lape, R., and Dani, J.A. (2001a). Timing and location of nicotinic activity enhances or depresses hippocampal synaptic plasticity. Neuron *31*, 131–141.

Ji, D., Lape, R., and Dani, J.A. (2001b). Timing and location of nicotinic activity enhances or depresses hippocampal synaptic plasticity. Neuron *31*, 131–141.

Jiang, X., Wang, G., Lee, A.J., Stornetta, R.L., and Zhu, J.J. (2013). The organization of two new cortical interneuronal circuits. Nat. Neurosci. *16*, 210–218.

Jonas, P. (1995). Fast Application of Agonists to Isolated Membrane Patches. In Single-Channel Recording, B. Sakmann, and E. Neher, eds. (Springer US), pp. 231–243.

Jones, I.W., and Wonnacott, S. (2004). Precise localization of alpha7 nicotinic acetylcholine receptors on glutamatergic axon terminals in the rat ventral tegmental area. J Neurosci *24*, 11244–11252.

Jones, S., and Yakel, J.L. (1997). Functional nicotinic ACh receptors on interneurones in the rat hippocampus. J Physiol *504 (Pt 3)*, 603–610.

Kabbani, N., Nordman, J.C., Corgiat, B.A., Veltri, D.P., Shehu, A., Seymour, V.A., and Adams, D.J. (2013a). Are nicotinic acetylcholine receptors coupled to G proteins? BioEssays News Rev. Mol. Cell. Dev. Biol. *35*, 1025–1034.

Kabbani, N., Nordman, J.C., Corgiat, B.A., Veltri, D.P., Shehu, A., Seymour, V.A., and Adams, D.J. (2013b). Are nicotinic acetylcholine receptors coupled to G proteins? BioEssays *35*, 1025–1034.

Kadir, A., Almkvist, O., Wall, A., Långström, B., and Nordberg, A. (2006). PET imaging of cortical 11C-nicotine binding correlates with the cognitive function of attention in Alzheimer's disease. Psychopharmacology (Berl.) *188*, 509–520.

Kalia, L.V., Gingrich, J.R., and Salter, M.W. (2004). Src in synaptic transmission and plasticity. Oncogene *23*, 8007–8016.

Karczmar, A.G. (1993). Brief presentation of the story and present status of studies of the vertebrate cholinergic system. Neuropsychopharmacology *9*, 181–199.

Karlin, A. (2002). Emerging structure of the nicotinic acetylcholine receptors. Nat Rev Neurosci *3*, 102–114.

Kawaguchi, Y., and Kubota, Y. (1997). GABAergic cell subtypes and their synaptic connections in rat frontal cortex. Cereb. Cortex N. Y. N 1991 *7*, 476–486.

Kem, W.R. (2000). The brain alpha7 nicotinic receptor may be an important therapeutic target for the treatment of Alzheimer's disease: studies with DMXBA (GTS-21). Behav. Brain Res. *113*, 169–181.

Khiroug, L., Giniatullin, R., Klein, R.C., Fayuk, D., and Yakel, J.L. (2003). Functional mapping and Ca2+ regulation of nicotinic acetylcholine receptor channels in rat hippocampal CA1 neurons. J. Neurosci. Off. J. Soc. Neurosci. *23*, 9024–9031.

Khiroug, S.S., Harkness, P.C., Lamb, P.W., Sudweeks, S.N., Khiroug, L., Millar, N.S., and Yakel, J.L. (2002). Rat nicotinic ACh receptor alpha7 and beta2 subunits co-assemble to form functional heteromeric nicotinic receptor channels. J Physiol *540*, 425–434.

Kihara, T., Shimohama, S., Sawada, H., Honda, K., Nakamizo, T., Shibasaki, H., Kume, T., and Akaike, A. (2001). alpha 7 nicotinic receptor transduces signals to phosphatidylinositol 3-kinase to block A beta-amyloid-induced neurotoxicity. J. Biol. Chem. *276*, 13541–13546.

Kirschner, L.S., Yin, Z., Jones, G.N., and Mahoney, E. (2009). Mouse models of altered protein kinase A signaling. Endocr. Relat. Cancer *16*, 773–793.

Klink, R., de Kerchove d'Exaerde, A., Zoli, M., and Changeux, J.P. (2001). Molecular and physiological diversity of nicotinic acetylcholine receptors in the midbrain dopaminergic nuclei. J. Neurosci. Off. J. Soc. Neurosci. *21*, 1452–1463.

Komal, P., Evans, G., and Nashmi, R. (2011a). A rapid agonist application system for fast activation of ligand-gated ion channels. J Neurosci Methods *198*, 246–254.

Komal, P., Evans, G., and Nashmi, R. (2011b). A rapid agonist application system for fast activation of ligand-gated ion channels. J. Neurosci. Methods *198*, 246–254.

Komal, P., Gudavicius, G., Nelson, C.J., and Nashmi, R. (2014a). T-Cell Receptor Activation Decreases Excitability of Cortical Interneurons by Inhibiting α7 Nicotinic Receptors. J. Neurosci. Off. J. Soc. Neurosci. *34*, 22–35.

Komal, P., Gudavicius, G., Nelson, C.J., and Nashmi, R. (2014b). T-Cell Receptor Activation Decreases Excitability of Cortical Interneurons by Inhibiting α7 Nicotinic Receptors. J. Neurosci. *34*, 22–35.

Koval, L.M., Zverkova, A.S., Grailhe, R., Utkin, Y.N., Tsetlin, V.I., Komisarenko, S.V., and Skok, M.V. (2008). Nicotinic acetylcholine receptors alpha4beta2 and alpha7 regulate myelo- and erythropoiesis within the bone marrow. Int. J. Biochem. Cell Biol. *40*, 980–990.

Lambe, E.K., Picciotto, M.R., and Aghajanian, G.K. (2003). Nicotine induces glutamate release from thalamocortical terminals in prefrontal cortex. Neuropsychopharmacol. Off. Publ. Am. Coll. Neuropsychopharmacol. *28*, 216–225.

Lambert, J.J., Peters, J.A., Hales, T.G., and Dempster, J. (1989). The properties of 5-HT3 receptors in clonal cell lines studied by patch-clamp techniques. Br J Pharmacol *97*, 27–40.

Lansdell, S.J., Gee, V.J., Harkness, P.C., Doward, A.I., Baker, E.R., Gibb, A.J., and Millar, N.S. (2005). RIC-3 enhances functional expression of multiple nicotinic acetylcholine receptor subtypes in mammalian cells. Mol Pharmacol *68*, 1431–1438.

Latour, S., and Veillette, A. (2001). Proximal protein tyrosine kinases in immunoreceptor signaling. Curr. Opin. Immunol. *13*, 299–306.

Léna, C., de Kerchove D'Exaerde, A., Cordero-Erausquin, M., Le Novère, N., del Mar Arroyo-Jimenez, M., and Changeux, J.P. (1999). Diversity and distribution of nicotinic acetylcholine receptors in the locus ceruleus neurons. Proc. Natl. Acad. Sci. U. S. A. *96*, 12126–12131.

Lendvai, B., Kassai, F., Szájli, Á., and Némethy, Z. (2013). α7 Nicotinic acetylcholine receptors and their role in cognition. Brain Res. Bull. *93*, 86–96.

Leonard, S., Gault, J., Hopkins, J., Logel, J., Vianzon, R., Short, M., Drebing, C., Berger, R., Venn, D., Sirota, P., et al. (2002). Association of promoter variants in the alpha7 nicotinic acetylcholine receptor subunit gene with an inhibitory deficit found in schizophrenia. Arch Gen Psychiatry *59*, 1085–1096.

Lester, H.A., and Nerbonne, J.M. (1982). Physiological and pharmacological manipulations with light flashes. Annu. Rev. Biophys. Bioeng. *11*, 151–175.

Letzkus, J.J., Wolff, S.B.E., Meyer, E.M.M., Tovote, P., Courtin, J., Herry, C., and Lüthi, A. (2011). A disinhibitory microcircuit for associative fear learning in the auditory cortex. Nature *480*, 331–335.

Levin, E.D. (2002). Nicotinic receptor subtypes and cognitive function. J. Neurobiol. *53*, 633–640.

Levin, E.D., McClernon, F.J., and Rezvani, A.H. (2006). Nicotinic effects on cognitive function: behavioral characterization, pharmacological specification, and anatomic localization. Psychopharmacol. Berl *184*, 523–539.

Levin, E.D., Petro, A., Rezvani, A.H., Pollard, N., Christopher, N.C., Strauss, M., Avery, J., Nicholson, J., and Rose, J.E. (2009). Nicotinic alpha7- or beta2-containing receptor knockout: effects on radial-arm maze learning and long-term nicotine consumption in mice. Behav Brain Res *196*, 207–213.

Lewis, B.L., and O'Donnell, P. (2000). Ventral tegmental area afferents to the prefrontal cortex maintain membrane potential "up" states in pyramidal neurons via D(1) dopamine receptors. Cereb. Cortex N. Y. N 1991 *10*, 1168–1175.

Li, X.-W., and Wang, H. (2006). Non-neuronal nicotinic alpha 7 receptor, a new endothelial target for revascularization. Life Sci. *78*, 1863–1870.

Lin, H., Vicini, S., Hsu, F.-C., Doshi, S., Takano, H., Coulter, D.A., and Lynch, D.R. (2010). Axonal α7 nicotinic ACh receptors modulate presynaptic NMDA receptor expression and structural plasticity of glutamatergic presynaptic boutons. Proc. Natl. Acad. Sci. U. S. A. *107*, 16661–16666.

Lindstrom, J. (1996). Neuronal nicotinic acetylcholine receptors. Ion Channels *4*, 377–450.

Liu, Q., and Berg, D.K. (1999). Actin Filaments and the Opposing Actions of CaM Kinase II and Calcineurin in Regulating α7-Containing Nicotinic Receptors on Chick Ciliary Ganglion Neurons. J. Neurosci. *19*, 10280–10288.

Liu, X.-B., and Murray, K.D. (2012). Neuronal excitability and calcium/calmodulin-dependent protein kinase type II: Location, location, location. Epilepsia *53*, 45–52.

Liu, Y., and Dilger, J.P. (1991). Opening rate of acetylcholine receptor channels. Biophys. J. *60*, 424–432.

Liu, D.M., Cuevas, J., and Adams, D.J. (2000). VIP and PACAP potentiation of nicotinic ACh-evoked currents in rat parasympathetic neurons is mediated by G-protein activation. Eur. J. Neurosci. *12*, 2243–2251.

Liu, Q., Huang, Y., Xue, F., Simard, A., DeChon, J., Li, G., Zhang, J., Lucero, L., Wang, M., Sierks, M., et al. (2009). A Novel Nicotinic Acetylcholine Receptor Subtype in Basal Forebrain Cholinergic Neurons with High Sensitivity to Amyloid Peptides. J. Neurosci. *29*, 918–929.

Livingstone, P.D., Srinivasan, J., Kew, J.N.C., Dawson, L.A., Gotti, C., Moretti, M., Shoaib, M., and Wonnacott, S. (2009a). α7 and non-α7 nicotinic acetylcholine receptors modulate dopamine release *in vitro* and *in vivo* in the rat prefrontal cortex. Eur. J. Neurosci. *29*, 539–550.

Livingstone, P.D., Srinivasan, J., Kew, J.N.C., Dawson, L.A., Gotti, C., Moretti, M., Shoaib, M., and Wonnacott, S. (2009b). alpha7 and non-alpha7 nicotinic acetylcholine receptors modulate dopamine release in vitro and in vivo in the rat prefrontal cortex. Eur J Neurosci *29*, 539–550.

Livingstone, P.D., Dickinson, J.A., Srinivasan, J., Kew, J.N.C., and Wonnacott, S. (2010). Glutamate-dopamine crosstalk in the rat prefrontal cortex is modulated by Alpha7 nicotinic receptors and potentiated by PNU-120596. J Mol Neurosci *40*, 172–176.

Loewi, O. (1924). Über humorale Übertragbarkeit der Herznervenwirkung. Pflüg. Arch. Für Gesamte Physiol. Menschen Tiere *204*, 629–640.

Madhok, T.C., Matta, S.G., and Sharp, B.M. (1995). Nicotine regulates nicotinic cholinergic receptors and subunit mRNAs in PC 12 cells through protein kinase A. Brain Res. Mol. Brain Res. *32*, 143–150.

Maller, J.L., Kemp, B.E., and Krebs, E.G. (1978). In vivo phosphorylation of a synthetic peptide substrate of cyclic AMP-dependent protein kinase. Proc. Natl. Acad. Sci. U. S. A. *75*, 248–251.

Man, H.-Y., Sekine-Aizawa, Y., and Huganir, R.L. (2007). Regulation of α-amino-3-hydroxy-5-methyl-4-isoxazolepropionic acid receptor trafficking through PKA phosphorylation of the Glu receptor 1 subunit. Proc. Natl. Acad. Sci. *104*, 3579–3584.

Mansvelder, H.D., and McGehee, D.S. (2000). Long-term potentiation of excitatory inputs to brain reward areas by nicotine. Neuron *27*, 349–357.

Mansvelder, H.D., and McGehee, D.S. (2002). Cellular and synaptic mechanisms of nicotine addiction. J Neurobiol *53*, 606–617.

Margiotta, J.F., Berg, D.K., and Dionne, V.E. (1987a). Cyclic AMP regulates the proportion of functional acetylcholine receptors on chicken ciliary ganglion neurons. Proc. Natl. Acad. Sci. U. S. A. *84*, 8155–8159.

Margiotta, J.F., Berg, D.K., and Dionne, V.E. (1987b). Cyclic AMP regulates the proportion of functional acetylcholine receptors on chicken ciliary ganglion neurons. Proc. Natl. Acad. Sci. U. S. A. *84*, 8155–8159.

Martin-Ruiz, C.M., Haroutunian, V.H., Long, P., Young, A.H., Davis, K.L., Perry, E.K., and Court, J.A. (2003). Dementia rating and nicotinic receptor expression in the prefrontal cortex in schizophrenia. Biol. Psychiatry *54*, 1222–1233.

Maskos, U., Molles, B.E., Pons, S., Besson, M., Guiard, B.P., Guilloux, J.-P., Evrard, A., Cazala, P., Cormier, A., Mameli-Engvall, M., et al. (2005). Nicotine reinforcement and cognition restored by targeted expression of nicotinic receptors. Nature *436*, 103–107.

McGehee, D.S., and Role, L.W. (1995). Physiological diversity of nicotinic acetylcholine receptors expressed by vertebrate neurons. Annu Rev Physiol *57*, 521–546.

McKay, B.E., Placzek, A.N., and Dani, J.A. (2007). Regulation of synaptic transmission and plasticity by neuronal nicotinic acetylcholine receptors. Biochem Pharmacol *74*, 1120–1133.

Meinkoth, J.L., Ji, Y., Taylor, S.S., and Feramisco, J.R. (1990). Dynamics of the distribution of cyclic AMP-dependent protein kinase in living cells. Proc. Natl. Acad. Sci. U. S. A. *87*, 9595–9599.

Meyer, T., and Shen, K. (2000). In and out of the postsynaptic region: signalling proteins on the move. Trends Cell Biol. *10*, 238–244.

Millar, N.S., and Gotti, C. (2009). Diversity of vertebrate nicotinic acetylcholine receptors. Neuropharmacology *56*, 237–246.

Miller, E.K., and Cohen, J.D. (2001). An integrative theory of prefrontal cortex function. Annu. Rev. Neurosci. *24*, 167–202.

Mittaud, P., Camilleri, A.A., Willmann, R., Erb-Vögtli, S., Burden, S.J., and Fuhrer, C. (2004). A single pulse of agrin triggers a pathway that acts to cluster acetylcholine receptors. Mol. Cell. Biol. *24*, 7841–7854.

Moise, L., Piserchio, A., Basus, V.J., and Hawrot, E. (2002). NMR Structural Analysis of α-Bungarotoxin and Its Complex with the Principal α-Neurotoxin-binding Sequence on the α7 Subunit of a Neuronal Nicotinic Acetylcholine Receptor. J. Biol. Chem. *277*, 12406–12417.

Moss, S.J., McDonald, B.J., Rudhard, Y., and Schoepfer, R. (1996a). Phosphorylation of the predicted major intracellular domains of the rat and chick neuronal nicotinic acetylcholine receptor alpha 7 subunit by cAMP-dependent protein kinase. Neuropharmacology *35*, 1023–1028.

Moss, S.J., McDonald, B.J., Rudhard, Y., and Schoepfer, R. (1996b). Phosphorylation of the predicted major intracellular domains of the rat and chick neuronal nicotinic acetylcholine receptor alpha 7 subunit by cAMP-dependent protein kinase. Neuropharmacology *35*, 1023–1028.

Murphy, C.A., DiCamillo, A.M., Haun, F., and Murray, M. (1996). Lesion of the habenular efferent pathway produces anxiety and locomotor hyperactivity in rats: a comparison of the effects of neonatal and adult lesions. Behav. Brain Res. *81*, 43–52.

Murray, T.A., Liu, Q., Whiteaker, P., Wu, J., and Lukas, R.J. (2009). Nicotinic acetylcholine receptor alpha7 subunits with a C2 cytoplasmic loop yellow fluorescent protein insertion form functional receptors. Acta Pharmacol Sin *30*, 828–841.

Nagai, T., Ibata, K., Park, E.S., Kubota, M., Mikoshiba, K., and Miyawaki, A. (2002). A variant of yellow fluorescent protein with fast and efficient maturation for cell-biological applications. Nat. Biotechnol. *20*, 87–90.

Naira, A.C., Hemmings, H.C., and Greengard, P. (1985). Protein Kinases in the Brain. Annu. Rev. Biochem. *54*, 931–976.

Nashmi, R., and Lester, H.A. (2006). CNS localization of neuronal nicotinic receptors. J Mol Neurosci *30*, 181–184.

Nashmi, R., Dickinson, M.E., McKinney, S., Jareb, M., Labarca, C., Fraser, S.E., and Lester, H.A. (2003). Assembly of alpha4beta2 nicotinic acetylcholine receptors assessed with functional fluorescently labeled subunits: effects of localization, trafficking, and nicotine-induced upregulation in clonal mammalian cells and in cultured midbrain neurons. J Neurosci *23*, 11554–11567.

Nashmi, R., Xiao, C., Deshpande, P., McKinney, S., Grady, S.R., Whiteaker, P., Huang, Q., McClure-Begley, T., Lindstrom, J.M., Labarca, C., et al. (2007). Chronic nicotine cell specifically upregulates functional alpha 4* nicotinic receptors: basis for both tolerance in midbrain and enhanced long-term potentiation in perforant path. J Neurosci *27*, 8202–8218.

Natarajan, K., Li, H., Mariuzza, R.A., and Margulies, D.H. (1999). MHC class I molecules, structure and function. Rev. Immunogenet. *1*, 32–46.

Needleman, L.A., Liu, X.-B., El-Sabeawy, F., Jones, E.G., and McAllister, A.K. (2010). MHC class I molecules are present both pre- and postsynaptically in the visual cortex during postnatal development and in adulthood. Proc. Natl. Acad. Sci. U. S. A. *107*, 16999–17004.

Nestler, E.J., and Greengard, P. (1983). Protein phosphorylation in the brain. Nature *305*, 583–588.

Nestler, E.J., Walaas, S.I., and Greengard, P. (1984). Neuronal phosphoproteins: physiological and clinical implications. Sci. 80- *225*, 1357–1364.

Neumann, H., Schmidt, H., Cavalié, A., Jenne, D., and Wekerle, H. (1997). Major Histocompatibility Complex (MHC) Class I Gene Expression in Single Neurons of the Central Nervous System: Differential Regulation by Interferon (IFN)-γ and Tumor Necrosis Factor (TNF)-α. J. Exp. Med. *185*, 305–316.

Nitabach, M.N., Llamas, D.A., Thompson, I.J., Collins, K.A., and Holmes, T.C. (2002). Phosphorylation-dependent and phosphorylation-independent modes of modulation of shaker family voltage-gated potassium channels by SRC family protein tyrosine kinases. J. Neurosci. Off. J. Soc. Neurosci. *22*, 7913–7922.

Nivalda O Rodrigues-Pinguet, T.J.P. (2005). Mutations linked to autosomal dominant nocturnal frontal lobe epilepsy affect allosteric Ca2 activation of the alpha 4 beta 2 nicotinic acetylcholine receptor. Mol. Pharmacol. *68*, 487–501.

Ohashi, P.S., Mak, T.W., Van den Elsen, P., Yanagi, Y., Yoshikai, Y., Calman, A.F., Terhorst, C., Stobo, J.D., and Weiss, A. (1985). Reconstitution of an active surface T3/T-cell antigen receptor by DNA transfer. Nature *316*, 606–609.

Oshikawa, J., Toya, Y., Fujita, T., Egawa, M., Kawabe, J., Umemura, S., and Ishikawa, Y. (2003). Nicotinic acetylcholine receptor alpha 7 regulates cAMP signal within lipid rafts. Am J Physiol Cell Physiol *285*, C567–C574.

Palacios, R. (1982). Concanavalin A triggers T lymphocytes by directly interacting with their receptors for activation. J Immunol *128*, 337–342.

Paolicelli, R.C., Bolasco, G., Pagani, F., Maggi, L., Scianni, M., Panzanelli, P., Giustetto, M., Ferreira, T.A., Guiducci, E., Dumas, L., et al. (2011). Synaptic pruning by microglia is necessary for normal brain development. Science *333*, 1456–1458.

Papke, R.L., and Porter Papke, J.K. (2002). Comparative pharmacology of rat and human alpha7 nAChR conducted with net charge analysis. Br J Pharmacol *137*, 49–61.

Papke, R.L., and Thinschmidt, J.S. (1998). The correction of alpha7 nicotinic acetylcholine receptor concentration-response relationships in Xenopus oocytes. Neurosci. Lett. *256*, 163–166.

Parikh, V., Ji, J., Decker, M.W., and Sarter, M. (2010). Prefrontal beta2 subunit-containing and alpha7 nicotinic acetylcholine receptors differentially control glutamatergic and cholinergic signaling. J Neurosci *30*, 3518–3530.

Parsons, S.J., and Parsons, J.T. (2004a). Src family kinases, key regulators of signal transduction. Oncogene *23*, 7906–7909.

Parsons, S.J., and Parsons, J.T. (2004b). Src family kinases, key regulators of signal transduction. Oncogene *23*, 7906–7909.

Pearson, R.B., and Kemp, B.E. (1991). Protein kinase phosphorylation site sequences and consensus specificity motifs: tabulations. Methods Enzym. *200*, 62–81.

Perry, D.C., Xiao, Y., Nguyen, H.N., Musachio, J.L., Dávila-García, M.I., and Kellar, K.J. (2002a). Measuring nicotinic receptors with characteristics of alpha4beta2, alpha3beta2 and alpha3beta4 subtypes in rat tissues by autoradiography. J. Neurochem. *82*, 468–481.

Perry, D.C., Xiao, Y., Nguyen, H.N., Musachio, J.L., Dávila-García, M.I., and Kellar, K.J. (2002b). Measuring nicotinic receptors with characteristics of alpha4beta2, alpha3beta2 and alpha3beta4 subtypes in rat tissues by autoradiography. J. Neurochem. *82*, 468–481.

Phillips, A.G., Ahn, S., and Floresco, S.B. (2004). Magnitude of dopamine release in medial prefrontal cortex predicts accuracy of memory on a delayed response task. J. Neurosci. Off. J. Soc. Neurosci. *24*, 547–553.

Phillips, A.G., Vacca, G., and Ahn, S. (2008). A top-down perspective on dopamine, motivation and memory. Pharmacol. Biochem. Behav. *90*, 236–249.

Picciotto, M.R. (1998). Common aspects of the action of nicotine and other drugs of abuse. Drug Alcohol Depend *51*, 165–172.

Picciotto, M.R., Zoli, M., Rimondini, R., Léna, C., Marubio, L.M., Pich, E.M., Fuxe, K., and Changeux, J.P. (1998). Acetylcholine receptors containing the beta2 subunit are involved in the reinforcing properties of nicotine. Nature *391*, 173–177.

Pidoplichko, V.I., DeBiasi, M., Williams, J.T., and Dani, J.A. (1997). Nicotine activates and desensitizes midbrain dopamine neurons. Nature *390*, 401–404.

Pidoplichko, V.I., Prager, E.M., Aroniadou-Anderjaska, V., and Braga, M.F.M. (2013). α7-Containing Nicotinic Acetylcholine Receptors on Interneurons of the Basolateral Amygdala and their Role in the Regulation of the Network Excitability. J. Neurophysiol.

Poisik, O.V., Shen, J., Jones, S., and Yakel, J.L. (2008). Functional alpha7-containing nicotinic acetylcholine receptors localize to cell bodies and proximal dendrites in the rat substantia nigra pars reticulata. J. Physiol. *586*, 1365–1378.

Poorthuis, R.B., Bloem, B., Schak, B., Wester, J., de Kock, C.P.J., and Mansvelder, H.D. (2012). Layer-Specific Modulation of the Prefrontal Cortex by Nicotinic Acetylcholine Receptors. Cereb Cortex.

Porter, N.M., Twyman, R.E., Uhler, M.D., and Macdonald, R.L. (1990). Cyclic AMP-dependent protein kinase decreases GABAA receptor current in mouse spinal neurons. Neuron *5*, 789–796.

Poulter, L., Earnest, J.P., Stroud, R.M., and Burlingame, A.L. (1989). Structure, oligosaccharide structures, and posttranslationally modified sites of the nicotinic acetylcholine receptor. Proc Natl Acad Sci U A *86*, 6645–6649.

Quik, M., Philie, J., and Choremis, J. (1997). Modulation of α7 Nicotinic Receptor-Mediated Calcium Influx by Nicotinic Agonists. Mol. Pharmacol. *51*, 499–506.

Rapier, C., Lunt, G.G., and Wonnacott, S. (1990). Nicotinic modulation of [3H]dopamine release from striatal synaptosomes: pharmacological characterisation. J. Neurochem. *54*, 937–945.

Ribic, A., Zhang, M., Schlumbohm, C., Mätz-Rensing, K., Uchanska-Ziegler, B., Flügge, G., Zhang, W., Walter, L., and Fuchs, E. (2010). Neuronal MHC class I molecules are involved in excitatory synaptic transmission at the hippocampal mossy fiber synapses of marmoset monkeys. Cell. Mol. Neurobiol. *30*, 827–839.

Robbins, T.W. (2002). The 5-choice serial reaction time task: behavioural pharmacology and functional neurochemistry. Psychopharmacology (Berl.) *163*, 362–380.

Rogers, J., Luber-Narod, J., Styren, S.D., and Civin, W.H. (1988). Expression of immune system-associated antigens by cells of the human central nervous system: relationship to the pathology of Alzheimer's disease. Neurobiol. Aging *9*, 339–349.

Rosenmund, C., Carr, D.W., Bergeson, S.E., Nilaver, G., Scott, J.D., and Westbrook, G.L. (1994). Anchoring of protein kinase A is required for modulation of AMPA/kainate receptors on hippocampal neurons. Nature *368*, 853–856.

Roskoski, R., Jr (2004). Src protein-tyrosine kinase structure and regulation. Biochem. Biophys. Res. Commun. *324*, 1155–1164.

Russo, P., and Taly, A. (2012). α7-Nicotinic acetylcholine receptors: an old actor for new different roles. Curr. Drug Targets *13*, 574–578.

Rye, D.B., Wainer, B.H., Mesulam, M.M., Mufson, E.J., and Saper, C.B. (1984). Cortical projections arising from the basal forebrain: a study of cholinergic and noncholinergic

components employing combined retrograde tracing and immunohistochemical localization of choline acetyltransferase. Neuroscience *13*, 627–643.

Sala, F., Nistri, A., and Criado, M. (2008). Nicotinic acetylcholine receptors of adrenal chromaffin cells. Acta Physiol. Oxf. Engl. *192*, 203–212.

Sallusto, F., Impellizzieri, D., Basso, C., Laroni, A., Uccelli, A., Lanzavecchia, A., and Engelhardt, B. (2012). T-cell trafficking in the central nervous system. Immunol Rev *248*, 216–227.

Salter, M.W., and Kalia, L.V. (2004). Src kinases: a hub for NMDA receptor regulation. Nat. Rev. Neurosci. *5*, 317–328.

Samelson, L.E., Phillips, A.F., Luong, E.T., and Klausner, R.D. (1990). Association of the fyn protein-tyrosine kinase with the T-cell antigen receptor. Proc. Natl. Acad. Sci. U. S. A. *87*, 4358–4362.

Scott, J.D. (1991). Cyclic nucleotide-dependent protein kinases. Pharmacol. Ther. *50*, 123–145.

Seamans, J.K., and Yang, C.R. (2004). The principal features and mechanisms of dopamine modulation in the prefrontal cortex. Prog. Neurobiol. *74*, 1–58.

Seamans, J.K., Gorelova, N., Durstewitz, D., and Yang, C.R. (2001). Bidirectional Dopamine Modulation of GABAergic Inhibition in Prefrontal Cortical Pyramidal Neurons. J. Neurosci. *21*, 3628–3638.

Séguéla, P., Wadiche, J., Dineley-Miller, K., Dani, J.A., and Patrick, J.W. (1993). Molecular cloning, functional properties, and distribution of rat brain alpha 7: a nicotinic cation channel highly permeable to calcium. J Neurosci *13*, 596–604.

Seguela, P., Wadiche, J., Dineley-Miller, K., Dani, J.A., and Patrick, J.W. (1993). Molecular cloning, functional properties, and distribution of rat brain alpha 7: a nicotinic cation channel highly permeable to calcium. J. Neurosci. *13*, 596–604.

Shatz, C.J. (2009). MHC class I: an unexpected role in neuronal plasticity. Neuron *64*, 40–45.

Shen, J., and Yakel, J.L. (2009a). Nicotinic acetylcholine receptor-mediated calcium signaling in the nervous system. Acta Pharmacol Sin *30*, 673–680.

Shen, J., and Yakel, J.L. (2009b). Nicotinic acetylcholine receptor-mediated calcium signaling in the nervous system. Acta Pharmacol. Sin. *30*, 673–680.

Sigworth, F.J. (1980). The variance of sodium current fluctuations at the node of Ranvier. J Physiol *307*, 97–129.

Sigworth, F.J. (1981). Interpreting power spectra from nonstationary membrane current fluctuations. Biophys J *35*, 289–300.

Simons, K., and Toomre, D. (2000). Lipid rafts and signal transduction. Nat. Rev. Mol. Cell Biol. *1*, 31–39.

Simonson, P.D., Deberg, H.A., Ge, P., Alexander, J.K., Jeyifous, O., Green, W.N., and Selvin, P.R. (2010). Counting bungarotoxin binding sites of nicotinic acetylcholine receptors in mammalian cells with high signal/noise ratios. Biophys. J. *99*, L81–L83.

Simon Sydserff, E.J.S. (2009). Selective alpha7 nicotinic receptor activation by AZD0328 enhances cortical dopamine release and improves learning and attentional processes. Biochem. Pharmacol. *78*, 880–888.

Smith, C.L., Mittaud, P., Prescott, E.D., Fuhrer, C., and Burden, S.J. (2001). Src, Fyn, and Yes are not required for neuromuscular synapse formation but are necessary for stabilization of agrin-induced clusters of acetylcholine receptors. J. Neurosci. Off. J. Soc. Neurosci. *21*, 3151–3160.

Snyder, G.L., Fienberg, A.A., Huganir, R.L., and Greengard, P. (1998). A Dopamine/D1 Receptor/Protein Kinase A/Dopamine- and cAMP-Regulated Phosphoprotein (M r 32 kDa)/Protein Phosphatase-1 Pathway Regulates Dephosphorylation of the NMDA Receptor. J. Neurosci. *18*, 10297–10303.

Soderling, S.H., and Beavo, J.A. (2000). Regulation of cAMP and cGMP signaling: new phosphodiesterases and new functions. Curr. Opin. Cell Biol. *12*, 174–179.

Songyang, Z., Shoelson, S.E., Chaudhuri, M., Gish, G., Pawson, T., Haser, W.G., King, F., Roberts, T., Ratnofsky, S., and Lechleider, R.J. (1993). SH2 domains recognize specific phosphopeptide sequences. Cell *72*, 767–778.

Sterner, K.N., Weckle, A., Chugani, H.T., Tarca, A.L., Sherwood, C.C., Hof, P.R., Kuzawa, C.W., Boddy, A.M., Abbas, A., Raaum, R.L., et al. (2012). Dynamic Gene Expression in the Human Cerebral Cortex Distinguishes Children from Adults. PLoS ONE *7*, e37714.

STUBBS, E.G., RITVO, E.R., and MASON-BROTHERS, A. (1985). Autism and Shared Parental HLA Antigens. J. Am. Acad. Child Psychiatry *24*, 182–185.

Sutherland, E.W., and Rall, T.W. (1958). Fractionation and characterization of a cyclic adenine ribonucleotide formed by tissue particles. J. Biol. Chem. *232*, 1077–1091.

Swope, S.L., Moss, S.J., Blackstone, C.D., and Huganir, R.L. (1992). Phosphorylation of ligand-gated ion channels: a possible mode of synaptic plasticity. FASEB J *6*, 2514–2523.

Syken, J., and Shatz, C.J. (2003a). Expression of T cell receptor beta locus in central nervous system neurons. Proc Natl Acad Sci U A *100*, 13048–13053.

Syken, J., and Shatz, C.J. (2003b). Expression of T cell receptor beta locus in central nervous system neurons. Proc. Natl. Acad. Sci. U. S. A. *100*, 13048–13053.

Syken, J., Grandpre, T., Kanold, P.O., and Shatz, C.J. (2006). PirB restricts ocular-dominance plasticity in visual cortex. Science *313*, 1795–1800.

Taiwo, Y.O., and Levine, J.D. (1991). Further confirmation of the role of adenyl cyclase and of cAMP-dependent protein kinase in primary afferent hyperalgesia. Neuroscience *44*, 131–135.

Takagi, N., Cheung, H.H., Bissoon, N., Teves, L., Wallace, M.C., and Gurd, J.W. (1999). The Effect of Transient Global Ischemia on the Interaction of Src and Fyn With the N-Methyl-D-Aspartate Receptor and Postsynaptic Densities: Possible Involvement of Src Homology 2 Domains. J. Cereb. Blood Flow Metab. *19*, 880–888.

Tapia, L., Kuryatov, A., and Lindstrom, J. (2007a). Ca2+ permeability of the (alpha4)3(beta2)2 stoichiometry greatly exceeds that of (alpha4)2(beta2)3 human acetylcholine receptors. Mol. Pharmacol. *71*, 769–776.

Tapia, L., Kuryatov, A., and Lindstrom, J. (2007b). Ca2+ permeability of the (alpha4)3(beta2)2 stoichiometry greatly exceeds that of (alpha4)2(beta2)3 human acetylcholine receptors. Mol. Pharmacol. *71*, 769–776.

Tapper, A.R., McKinney, S.L., Nashmi, R., Schwarz, J., Deshpande, P., Labarca, C., Whiteaker, P., Marks, M.J., Collins, A.C., and Lester, H.A. (2004). Nicotine activation of alpha4* receptors: sufficient for reward, tolerance, and sensitization. Science *306*, 1029–1032.

Taskén, K., and Aandahl, E.M. (2004). Localized effects of cAMP mediated by distinct routes of protein kinase A. Physiol. Rev. *84*, 137–167.

Thams, S., Oliveira, A., and Cullheim, S. (2008). MHC class I expression and synaptic plasticity after nerve lesion. Brain Res. Rev. *57*, 265–269.

Thomas, S.M., and Brugge, J.S. (1997). Cellular functions regulated by Src family kinases. Annu. Rev. Cell Dev. Biol. *13*, 513–609.

Thomsen, M.S., Hay-Schmidt, A., Hansen, H.H., and Mikkelsen, J.D. (2010a). Distinct Neural Pathways Mediate α7 Nicotinic Acetylcholine Receptor–Dependent Activation of the Forebrain. Cereb. Cortex *20*, 2092–2102.

Thomsen, M.S., Hansen, H.H., Timmerman, D.B., and Mikkelsen, J.D. (2010b). Cognitive improvement by activation of alpha7 nicotinic acetylcholine receptors: from animal models to human pathophysiology. Curr. Pharm. Des. *16*, 323–343.

Tietje, K.R., Anderson, D.J., Bitner, R.S., Blomme, E.A., Brackemeyer, P.J., Briggs, C.A., Browman, K.E., Bury, D., Curzon, P., Drescher, K.U., et al. (2008). Preclinical

characterization of A-582941: a novel alpha7 neuronal nicotinic receptor agonist with broad spectrum cognition-enhancing properties. CNS Neurosci. Ther. *14*, 65–82.

Tooyama, I., Kimura, H., Akiyama, H., and McGeer, P.L. (1990). Reactive microglia express class I and class II major histocompatibility complex antigens in Alzheimer's disease. Brain Res. *523*, 273–280.

Triana-Baltzer, G.B., Liu, Z., Gounko, N.V., and Berg, D.K. (2008). Multiple cell adhesion molecules shaping a complex nicotinic synapse on neurons. Mol. Cell. Neurosci. *39*, 74–82.

Tribollet, E., Bertrand, D., Marguerat, A., and Raggenbass, M. (2004). Comparative distribution of nicotinic receptor subtypes during development, adulthood and aging: an autoradiographic study in the rat brain. Neuroscience *124*, 405–420.

Uhler, M.D., and McKnight, G.S. (1987). Expression of cDNAs for two isoforms of the catalytic subunit of cAMP-dependent protein kinase. J. Biol. Chem. *262*, 15202–15207.

Uhler, M.D., Carmichael, D.F., Lee, D.C., Chrivia, J.C., Krebs, E.G., and McKnight, G.S. (1986). Isolation of cDNA clones coding for the catalytic subunit of mouse cAMP-dependent protein kinase. Proc. Natl. Acad. Sci. U. S. A. *83*, 1300–1304.

Ungar, A.R., and Moon, R.T. (1996). Inhibition of protein kinase A phenocopies ectopic expression of hedgehog in the CNS of wild-type and cyclops mutant embryos. Dev. Biol. *178*, 186–191.

Unwin, N. (1995). Acetylcholine receptor channel imaged in the open state. Nature *373*, 37–43.

Unwin, N. (2005). Refined structure of the nicotinic acetylcholine receptor at 4A resolution. J Mol Biol *346*, 967–989.

Veillette, A., Bookman, M.A., Horak, E.M., and Bolen, J.B. (1988). The CD4 and CD8 T cell surface antigens are associated with the internal membrane tyrosine-protein kinase p56lck. Cell *55*, 301–308.

Vernino, S., Amador, M., Luetje, C.W., Patrick, J., and Dani, J.A. (1992). Calcium modulation and high calcium permeability of neuronal nicotinic acetylcholine receptors. Neuron *8*, 127–134.

Vijayaraghavan, S., Schmid, H.A., Halvorsen, S.W., and Berg, D.K. (1990). Cyclic AMP-dependent phosphorylation of a neuronal acetylcholine receptor alpha-type subunit. J Neurosci *10*, 3255–3262.

Wagner, K.R., Mei, L., and Huganir, R.L. (1991). Protein tyrosine kinases and phosphatases in the nervous system. Curr Opin Neurobiol *1*, 65–73.

Walaas, S.I., and Greengard, P. (1991). Protein phosphorylation and neuronal function. Pharmacol. Rev. *43*, 299–349.

Wallace, T.L., and Bertrand, D. (2013). Alpha7 neuronal nicotinic receptors as a drug target in schizophrenia. Expert Opin. Ther. Targets *17*, 139–155.

Wallace, T.L., and Porter, R.H.P. (2011). Targeting the nicotinic alpha7 acetylcholine receptor to enhance cognition in disease. Biochem Pharmacol *82*, 891–903.

Walsh, D.A., Perkins, J.P., and Krebs, E.G. (1968). An adenosine 3',5'-monophosphate-dependant protein kinase from rabbit skeletal muscle. J. Biol. Chem. *243*, 3763–3765.

Walters, J.T.R., Rujescu, D., Franke, B., Giegling, I., Vásquez, A.A., Hargreaves, A., Russo, G., Morris, D.W., Hoogman, M., Da Costa, A., et al. (2013). The role of the major histocompatibility complex region in cognition and brain structure: a schizophrenia GWAS follow-up. Am. J. Psychiatry *170*, 877–885.

Wan, Q., Man, H.Y., Braunton, J., Wang, W., Salter, M.W., Becker, L., and Wang, Y.T. (1997). Modulation of GABAA receptor function by tyrosine phosphorylation of beta subunits. J Neurosci *17*, 5062–5069.

Wang, J., and O'Donnell, P. (2001). D1 Dopamine Receptors Potentiate NMDA-mediated Excitability Increase in Layer V Prefrontal Cortical Pyramidal Neurons. Cereb. Cortex *11*, 452–462.

Wang, Y.T., and Salter, M.W. (1994). Regulation of NMDA receptors by tyrosine kinases and phosphatases. Nature *369*, 233–235.

Wang, H., Yu, M., Ochani, M., Amella, C.A., Tanovic, M., Susarla, S., Li, J.H., Wang, H., Yang, H., Ulloa, L., et al. (2003). Nicotinic acetylcholine receptor alpha7 subunit is an essential regulator of inflammation. Nature *421*, 384–388.

Wang, Q., Ting, W.L., Yang, H., and Wong, P.T.-H. (2005). High doses of simvastatin upregulate dopamine D1 and D2 receptor expression in the rat prefrontal cortex: possible involvement of endothelial nitric oxide synthase. Br. J. Pharmacol. *144*, 933–939.

Wecker, L., Guo, X., Rycerz, A.M., and Edwards, S.C. (2001). Cyclic AMP-dependent protein kinase (PKA) and protein kinase C phosphorylate sites in the amino acid sequence corresponding to the M3/M4 cytoplasmic domain of alpha4 neuronal nicotinic receptor subunits. J Neurochem *76*, 711–720.

Weiss, A., and Littman, D.R. (1994). Signal transduction by lymphocyte antigen receptors. Cell *76*, 263–274.

Weisskopf, M.G., Castillo, P.E., Zalutsky, R.A., and Nicoll, R.A. (1994). Mediation of hippocampal mossy fiber long-term potentiation by cyclic AMP. Science *265*, 1878–1882.

Weng, Z., Thomas, S.M., Rickles, R.J., Taylor, J.A., Brauer, A.W., Seidel-Dugan, C., Michael, W.M., Dreyfuss, G., and Brugge, J.S. (1994). Identification of Src, Fyn, and Lyn SH3-binding proteins: implications for a function of SH3 domains. Mol. Cell. Biol. *14*, 4509–4521.

Wevers, A., Monteggia, L., Nowacki, S., Bloch, W., Schütz, U., Lindstrom, J., Pereira, E.F., Eisenberg, H., Giacobini, E., de Vos, R.A., et al. (1999). Expression of nicotinic acetylcholine receptor subunits in the cerebral cortex in Alzheimer's disease: histotopographical correlation with amyloid plaques and hyperphosphorylated-tau protein. Eur. J. Neurosci. *11*, 2551–2565.

Whiting, P.J., and Lindstrom, J.M. (1988). Characterization of bovine and human neuronal nicotinic acetylcholine receptors using monoclonal antibodies. J. Neurosci. Off. J. Soc. Neurosci. *8*, 3395–3404.

Whiting, P.J., Liu, R., Morley, B.J., and Lindstrom, J.M. (1987). Structurally different neuronal nicotinic acetylcholine receptor subtypes purified and characterized using monoclonal antibodies. J Neurosci *7*, 4005–4016.

Wilkie, G.I., Hutson, P.H., Stephens, M.W., Whiting, P., and Wonnacott, S. (1993). Hippocampal nicotinic autoreceptors modulate acetylcholine release. Biochem. Soc. Trans. *21*, 429–431.

Williams, M.E., Burton, B., Urrutia, A., Shcherbatko, A., Chavez-Noriega, L.E., Cohen, C.J., and Aiyar, J. (2005). Ric-3 promotes functional expression of the nicotinic acetylcholine receptor alpha7 subunit in mammalian cells. J. Biol. Chem. *280*, 1257–1263.

Winer, J.A., and Larue, D.T. (1989). Populations of GABAergic neurons and axons in layer I of rat auditory cortex. Neuroscience *33*, 499–515.

Wolozin, B.L., Pruchnicki, A., Dickson, D.W., and Davies, P. (1986). A neuronal antigen in the brains of Alzheimer patients. Science *232*, 648–650.

Wong, W., and Scott, J.D. (2004). AKAP signalling complexes: focal points in space and time. Nat. Rev. Mol. Cell Biol. *5*, 959–970.

Wong, G.H.W., Bartlett, P.F., Clark-Lewis, I., Battye, F., and Schrader, J.W. (1984). Inducible expression of H–2 and Ia antigens on brain cells. Nature *310*, 688–691.

Wonnacott, S. (1997). Presynaptic nicotinic ACh receptors. Trends Neurosci. *20*, 92–98.

Woodford, T.A., Correll, L.A., McKnight, G.S., and Corbin, J.D. (1989). Expression and characterization of mutant forms of the type I regulatory subunit of cAMP-dependent protein kinase. The effect of defective cAMP binding on holoenzyme activation. J. Biol. Chem. *264*, 13321–13328.

Woolf, N.J. (1991). Cholinergic systems in mammalian brain and spinal cord. Prog Neurobiol *37*, 475–524.

Wooltorton, J.R.A., Pidoplichko, V.I., Broide, R.S., and Dani, J.A. (2003). Differential desensitization and distribution of nicotinic acetylcholine receptor subtypes in midbrain dopamine areas. J. Neurosci. Off. J. Soc. Neurosci. *23*, 3176–3185.

Xiao, C., Nashmi, R., McKinney, S., Cai, H., McIntosh, J.M., and Lester, H.A. (2009). Chronic nicotine selectively enhances alpha4beta2* nicotinic acetylcholine receptors in the nigrostriatal dopamine pathway. J Neurosci *29*, 12428–12439.

Xu, H., Chen, H., Ding, Q., Xie, Z.-H., Chen, L., Diao, L., Wang, P., Gan, L., Crair, M.C., and Tian, N. (2010). The immune protein CD3zeta is required for normal development of neural circuits in the retina. Neuron *65*, 503–515.

Xu, W., Doshi, A., Lei, M., Eck, M.J., and Harrison, S.C. (1999). Crystal structures of c-Src reveal features of its autoinhibitory mechanism. Mol. Cell *3*, 629–638.

Yan, Z. (2002). Regulation of GABAergic inhibition by serotonin signaling in prefrontal cortex: molecular mechanisms and functional implications. Mol. Neurobiol. *26*, 203–216.

Yang, X., Criswell, H.E., and Breese, G.R. (1996). Nicotine-induced inhibition in medial septum involves activation of presynaptic nicotinic cholinergic receptors on gamma-aminobutyric acid-containing neurons. J. Pharmacol. Exp. Ther. *276*, 482–489.

Yang, Y., Paspalas, C.D., Jin, L.E., Picciotto, M.R., Arnsten, A.F.T., and Wang, M. (2013). Nicotinic α7 receptors enhance NMDA cognitive circuits in dorsolateral prefrontal cortex. Proc. Natl. Acad. Sci. *110*, 12078–12083.

Young, J.W., Crawford, N., Kelly, J.S., Kerr, L.E., Marston, H.M., Spratt, C., Finlayson, K., and Sharkey, J. (2007a). Impaired attention is central to the cognitive deficits observed in alpha 7 deficient mice. Eur. Neuropsychopharmacol. J. Eur. Coll. Neuropsychopharmacol. *17*, 145–155.

Young, J.W., Crawford, N., Kelly, J.S., Kerr, L.E., Marston, H.M., Spratt, C., Finlayson, K., and Sharkey, J. (2007b). Impaired attention is central to the cognitive deficits observed in alpha 7 deficient mice. Eur Neuropsychopharmacol *17*, 145–155.

Young, J.W., Crawford, N., Kelly, J.S., Kerr, L.E., Marston, H.M., Spratt, C., Finlayson, K., and Sharkey, J. (2007c). Impaired attention is central to the cognitive deficits observed in alpha 7 deficient mice. Eur. Neuropsychopharmacol. J. Eur. Coll. Neuropsychopharmacol. *17*, 145–155.

Yutani, K., Ogasahara, K., Tsujita, T., and Sugino, Y. (1987). Dependence of conformational stability on hydrophobicity of the amino acid residue in a series of variant proteins substituted at a unique position of tryptophan synthase alpha subunit. Proc. Natl. Acad. Sci. *84*, 4441–4444.

Zhang, H., Garlichs, C.D., Mügge, A., and Daniel, W.G. (1998). Involvement of tyrosine kinases, Ca2+ and PKC in activation of mitogen-activated protein (MAP) kinase in human polymorphonuclear neutrophils. J. Physiol. *513*, 359–367.

Zhao, L., Kuo, Y.-P., George, A.A., Peng, J.-H., Purandare, M.S., Schroeder, K.M., Lukas, R.J., and Wu, J. (2003). Functional properties of homomeric, human alpha 7-nicotinic acetylcholine receptors heterologously expressed in the SH-EP1 human epithelial cell line. J. Pharmacol. Exp. Ther. *305*, 1132–1141.

Zhong, H., Sia, G.-M., Sato, T.R., Gray, N.W., Mao, T., Khuchua, Z., Huganir, R.L., and Svoboda, K. (2009). Subcellular Dynamics of Type II PKA in Neurons. Neuron *62*, 363–374.

Zhou, F.M., and Hablitz, J.J. (1996). Postnatal development of membrane properties of layer I neurons in rat neocortex. J. Neurosci. Off. J. Soc. Neurosci. *16*, 1131–1139.

(1989). Protein phosphorylation and the regulation of neuronal function. In In Basics Neurochemistry: Molecular, Cellular and Medical Asprects, (New York: Raven Press), pp. 373–398.